

DTIC FILE COPY

1

AGARD-LS-169

AGARD-LS-169

AD-A224 601

RESEARCH & DEVELOPMENT

AGARD LECTURE SERIES No. 169

# Comparative Engine Performance Measurements

(Mesures Comparatives des Performances des Moteurs)

**DISTRIBUTION STATEMENT A**  
Approved for public release  
Distribution Unlimited

DTIC  
ELECTE  
JUL 13 1990  
S D

DISTRIBUTION AND AVAILABILITY  
ON BACK COVER

90 07 12 201

NORTH ATLANTIC TREATY ORGANIZATION  
ADVISORY GROUP FOR AEROSPACE RESEARCH AND DEVELOPMENT  
(ORGANISATION DU TRAITE DE L'ATLANTIQUE NORD)

AGARD Lecture Series No.169

## Comparative Engine Performance Measurements

(Mesures Comparatives des Performances des Moteurs)

*This Lecture Series Note should be read in conjunction with Advisory Report 248  
"Propulsion and Energetics Panel Working Group 15 on The Uniform Engine Test Programme"  
and AGARDograph 307 "Measurement Uncertainty Within the Uniform Engine Test Programme".*



Accession	
NTIS	DTIC
URANT	JUSTICE
By	
Dist	
A-1	

This material in this publication was assembled to support a Lecture Series under the sponsorship of the Propulsion and Energetics Panel and the Consultant and Exchange Programme of AGARD presented on 14th—15th May 1990 in Torino, Italy, 17th—18th May 1990 in London, United Kingdom, 4th—5th June 1990 in Montreal, Canada and 7th—8th June 1990 in Monterey, United States.

# The Mission of AGARD

According to its Charter, the mission of AGARD is to bring together the leading personalities of the NATO nations in the fields of science and technology relating to aerospace for the following purposes:

- Recommending effective ways for the member nations to use their research and development capabilities for the common benefit of the NATO community;
- Providing scientific and technical advice and assistance to the Military Committee in the field of aerospace research and development (with particular regard to its military application);
- Continuously stimulating advances in the aerospace sciences relevant to strengthening the common defence posture;
- Improving the co-operation among member nations in aerospace research and development;
- Exchange of scientific and technical information;
- Providing assistance to member nations for the purpose of increasing their scientific and technical potential;
- Rendering scientific and technical assistance, as requested, to other NATO bodies and to member nations in connection with research and development problems in the aerospace field.

The highest authority within AGARD is the National Delegates Board consisting of officially appointed senior representatives from each member nation. The mission of AGARD is carried out through the Panels which are composed of experts appointed by the National Delegates, the Consultant and Exchange Programme and the Aerospace Applications Studies Programme. The results of AGARD work are reported to the member nations and the NATO Authorities through the AGARD series of publications of which this is one.

Participation in AGARD activities is by invitation only and is normally limited to citizens of the NATO nations.

The content of this publication has been reproduced directly from material supplied by AGARD or the authors.

Published May 1990

Copyright © AGARD 1990  
All Rights Reserved

ISBN 92-835-0565-4



Printed by Specialised Printing Services Limited  
40 Chigwell Lane, Loughton, Essex IG10 3TZ

## Abstract

The AGARD Propulsion and Energetics Panel has sponsored an international, inter-facility comparison programme for turbine engine test facilities over the past nine years. The effort was driven by the critical nature of engine test measurements and their influence on aircraft performance predictions, as well as the need for a sound understanding of test-related factors which may influence such measurements. The basic idea was that a nominated engine would be tested in several facilities, both ground-level and altitude, the results then compared, and explanations sought for any observed differences. This Lecture Series presents the information obtained from this comprehensive program. Emphasis is given to the definition and explanation of differences in test facility measurements and to the lessons learned from this unique experiment.

This Lecture Series, sponsored by the Propulsion and Energetics Panel of AGARD, has been implemented by the Consultant and Exchange Programme.

## Résumé

Ces neuf dernières années le Panel AGARD de Propulsion et d'Energétique a cautionné un programme international de comparaison sur les installations de test des turbomachines. Le projet doit son existence au caractère critique des mesures effectuées lors des essais en raison de leur incidence sur les prévisions des performances des aéronefs, ainsi qu'au besoin des bien comprendre tous les facteurs liés aux essais qui auraient pu influencer sur de telles mesures.

La notion de base du programme a été de choisir un moteur pour ensuite le tester dans un certain nombre d'installations, tant au sol qu'en altitude; de comparer les résultats et de tenter d'expliquer toute différence constatée d'une installation à l'autre.

Ce cycle de conférences présente les informations issues de ce programme très complet. Les communications mettent l'accent sur la définition et l'explication des écarts constatés dans les mesures obtenues des différentes installations de test et sur les enseignements retirés de cette expérience unique.

Ce cycle de conférences est présenté dans le cadre du Programme des Consultants et des Echanges, sous l'égide du Panel AGARD de Propulsion et d'Energétique.

## List of Authors/Speakers

**Lecture Series Director:** Dr J.G.Mitchell  
Micro Craft Inc.  
Corporate Headquarters  
207 Big Springs Avenue  
P.O. Box 370  
Tullahoma, TN 37388-0370  
United States

### AUTHORS/SPEAKERS

Mr A.R.Osborn  
Head of Trials Section  
Royal Aerospace Est.  
Propulsion Dept.  
Pyestock, Hants GU14 0LS  
United Kingdom

Mr D.M.Rudnitski  
Head, Engine Laboratory  
Div. of Mech. Engineering  
National Research Council  
Ottawa, Ontario K1A 0R6  
Canada

Mr R.E.Smith, Jr.  
Vice President & Chief Scientist  
Sverdrup Technology Inc.  
AEDC Div.  
Arnold Air Force Station  
TN 37389  
United States

Ir. J.P.K.Vlegheert  
Parkiepraat 36  
1171 HV Badhoevedorp  
The Netherlands

# Contents

	Page
<b>Abstract/Résumé</b>	iii
<b>List of Speakers</b>	iv
	Reference
<b>Preface</b> by J.G.Mitchell	1
<b>Design of the UETP Experiment</b> by R.E.Smith, Jr.	2
<b>The Basis for Facility Comparison</b> by A.R.Osborn	3
<b>Investigation of Factors Affecting Data Comparison</b> by D.M.Rudnitski	4
<b>Comparison of Altitude</b> by R.E.Smith, Jr.	5
<b>Comparison of Ground-Level Test Cells and Ground-Level to Altitude Test Cells</b> by D.M.Rudnitski	6
<b>Measurement Uncertainty in Gas Turbine Performance Determination</b> by J.P.K.Vleghert	7
<b>Experience in Developing an Improved Design of Experiment (Lessons Learned)</b> by R.E.Smith, Jr.	8
<b>Conclusions about Facility Capabilities &amp; Practices</b> by A.R.Osborn	9
<b>Experience in Developing an Improved Ground-Level Test Capability</b> by D.M.Rudnitski	10
<b>Appendices: General Test Plan</b> by R.E.Smith, Jr.	A
<b>Bibliography</b>	B

**PREFACE**

by

**Dr J.G.Mitchell**  
Micro Craft Inc.  
Corporate Headquarters  
207 Big Springs Avenue  
P.O. Box 370  
Tullahoma, TN 37388-0370  
United States

It has been well known that test techniques, test facilities and test instrumentation for ground testing of turbojet engines vary between countries and even within the same country. The impact of these differences on the reported measurements and performance has remained speculation since no controlled test program has evolved to address the issues. With an increase in the international development of new turbojet engines and international engine purchases, the need to define and resolve these testing inconsistencies has increased.

The Propulsion and Energetics Panel (PEP) of AGARD recognized this growing problem and sponsored an ambitious program to resolve it. Working Group 15, entitled the Uniform Engine Testing Program, was formed over ten years ago to organize and direct an international turbojet engine testing program and to analyze the test results. Tests were conducted in five countries (eight test facilities) in both altitude simulation facilities and ground test beds. A program which was initially expected to be lengthy by AGARD Working Group standards, grew even longer as the various test centers were caused to delay testing as a result of pressing national needs. The tenacity of Working Group 15 members and the continued support of the PEP membership and AGARD National Delegates permitted the program to reach a successful conclusion.

It is the purpose of this Lecture Series to present the results of this lengthy and unprecedented investigation to the aerospace community. Two documents have been published by Working Group 15, i.e., AGARD-AR-248 (The Uniform Engine Test Programme) and AGARDograph 307 (Measurement Uncertainty). These two documents contain the basic content of this Lecture Series. However, there were many additional investigations and much rationale that was not published. These Lecture Series notes contain selected portions of that additional information and are intended as a supplement to the documents already published.

- The Lecture Series emphasizes four main topics:
- Design and Conduct of the Test Program
  - Comparison of Test Results
  - Data Uncertainty Analyses
  - Lessons Learned from the Program Analysis

The AGARD PEP extends its sincere gratitude to the dedicated members and consultants of Working Group 15 and to the participating test centers which supported the test and analyses with excellent people and which bore the heavy expenses of the testing program.

## DESIGN OF THE UETP EXPERIMENT

By  
 Robert E. Smith, Jr.  
 Vice President and Chief Scientist  
 Sverdrup Technology, Inc./AEDC Group  
 Arnold Engineering Development Center  
 Arnold Air Force Base, TN USA

### SUMMARY

An experiment was successfully designed to meet the objectives of the Uniform Engine Test Program (UETP) as defined by the Propulsion and Energetics Panel (PEP) of AGARD. The experiment was based on the use of two specially modified J57-PW-19W turbine engines. The experiment was compatible with the capability and availability of eight different engine test facilities located within five NATO countries. Four of these test facilities are ground-level engine test facilities, and four are altitude engine test facilities. The experiment as designed was consistent with the test resources available at each test site.

The design of the experiment included the specification of the test article, the matrix of variables, the experimental measurements, and the formats of the test reports. In addition, the design of the experiment included the definition of three key methodologies, i.e., test, data processing, and measurement uncertainty, to the minimum extent necessary to meet the objectives of the UETP, and to maximize the level of confidence in the comparative engine performance measurements from each facility. This approach was consistent with a basic requirement of the UETP, which was to utilize local test facility practices to the maximum extent possible.

The experiment as designed was defined in a General Test Plan which was coordinated with and approved by all participants in the Uniform Engine Test Program. The General Test Plan was published and made available to all program participants. A literature search did not identify any existing publications which defined experiments of the scope required for the UETP.

The successful design of the UETP experiment was a major technical and management accomplishment and was a key contributor to the success of the UETP. The General Test Plan should serve as a baseline for the design of future experiments having the scope and complexity of the AGARD Uniform Engine Test Program.

### LIST OF SYMBOLS

TC      Test Condition  
 UETP    AGARD-PEP Uniform Engine Test Program

### 1.0 INTRODUCTION

The overall rationale and objectives for the Uniform Engine Test Program (UETP) were given in Lecture 1. One of the very first requirements of the UETP was the design of an experiment which would fulfill the program objectives within the constraints that were imposed. The experiment was required to provide information which could be used to quantify the similarities and differences in turbine engine performance measurement capabilities of various jet engine test facilities located within the NATO countries. The primary constraints imposed were as follows:

1. Steady-state engine performance only was to be measured.
2. The experiment was to be compatible with the capabilities of both ground-level test facilities and altitude test facilities which were operational in the NATO countries.
3. The scope and duration of the program were to be the minimum consistent with the test facility resources and engine operating times available at each of the participating test facilities.
4. Local practices for the design of test equipment, installation of the test article, and operation of the test facility were to be utilized to the maximum extent possible.
5. The experiment was to be designed to provide the highest levels of confidence in the comparative results.

The seven major elements or building blocks of the UETP experiment are:

1. Selection of Test Articles
2. Specification of Matrix of Variables
3. Identification of Experimental Measurements
4. Definition of Test Methodology
5. Specification of Test Data Processing
6. Definition of Measurement Uncertainty
7. Content of Reports

Each of these elements will be discussed, and the requirements for each will be identified. Some of the design alternatives that were considered will be presented, and the final design chosen for the UETP will be described.

The details of the UETP experiment were documented in the General Test Plan (GTP) (see Ref. 1). The contents of the GTP and some of the management and administrative practices followed in the preparation and maintenance of the GTP will be described.

## 2.0 DESIGN OF EXPERIMENT

The seven major elements of the UETP experiment are discussed. Some of the alternatives considered are presented. The final designs chosen for each element are described.

### 2.1 Selection of Test Article

This first element relates basically to the selection of an optimum jet engine. The primary considerations in the selection of the engine relate to the "ilities": availability, reliability, and supportability.

The most basic engine requirement was that two engines be available for the duration of the experimental portion of the program. The primary reason for two engines was to provide redundancy in the event that one engine should be damaged during the course of the test program. A secondary requirement for the second engine was to provide insight into the variability of facility test data to the extent that both engines survived the total test program.

The engines also had to be extremely reliable. The test program was expected to require hundreds of hours of engine operation over a period of several years. To minimize the cost and calendar time required to complete the program, it was essential that the engines withstand these operating requirements with little or no maintenance and repair and that only normal servicing be required. It was also a requirement that the engine have little or no performance change during the hundreds of hours of operation so that engine performance variation would not be a major factor in the comparison of the facility performance.

It was essential that the engine have a high level of field supportability. These supportability requirements included spare parts, maintenance and repair tooling and resources, and mature engine documentation. This required documentation included engine operating instructions and engine service instructions so that the engines could be effectively operated by the normally assigned personnel in each of the facilities without the necessity for additional specialized training.

Finally, to ensure applicability of the UETP results to current and future programs, it was desired that the engines contain at least contemporary technology levels in the aerodynamic, thermodynamic, and structural design. Ultra-modern, state-of-the-art technology was not desired.

To ensure the widest possible participation in the UETP it was required that the engine size (measured primarily in terms of airflow capacity) be compatible with a large number of NATO facilities. Further, as a test cost containment feature, and to simplify the test program, it was required that a non-afterburning engine configuration be chosen. Finally, to provide maximum confidence in the test results, it was required that the test engines have only minimum or no variable geometry so that small variations in geometric schedules as a function of operating time and set-up and adjustment would have no effect or an absolutely minimum effect on the consistency of the test data.

Initially, nine candidate engines were considered ranging in size from the 12.7 kN thrust GE J85 turbojet to the 97.8 kN thrust GE/SNECMA CFM-56 turbofan. Three candidate engines were identified which met most or all of these requirements.

CANDIDATES		57-PW-19W	J85-GE-17	TF41-A-1
Ratings (Sea-Level- Static at military power)	Thrust, kN	46.7	12.7	64.5
	Airflow, kg/sec	74.8	20.0	117.9

Each of the three candidates was carefully evaluated relative to the requirements listed above. Based on these evaluations, the J57-PW-19W engine was selected as the engine which best fulfilled the several requirements of the UETP.

The chairman of AGARD-PEP WG15, Dr. J. G. Mitchell, made a request to the United States Air Force for the loan of two J57-PW-19W engines to PEP WG15 for an indefinite period of time. The U.S. Air Force Logistics Command assigned two newly overhauled engines, serial numbers P607594 and F615037, to the UETP.

#### 2.1.1 Modifications to Production J57 Engine Configuration

Four minor modifications and/or additions were made to the production engine configuration to tailor the engine to the specific needs of the UETP (Fig. 1).

An inlet extension and bullet nose were added to the production engine configuration as shown schematically in Fig. 1a. These additions permitted installation of a standard set of referee instrumentation at the engine inlet as will be discussed in Section 2.3.

The engine compressor bleed system was modified to improve engine control system repeatability and expand the engine operating range with the bleeds closed. The compressor acceleration bleed system was modified from a bomber configuration, which utilized two bleed valves, to a fighter configuration, which utilized only a single bleed valve. In addition, the compressor anti-icing bleed port and the customer service bleed port were

capped because neither of these services was required for UETP. These compressor bleed modifications are summarized in Fig. 1a.

A tailpipe and reference exhaust nozzle were added to the engine as shown in Fig. 1b. These additions served two purposes. First, the addition of the tailpipe provided a simple, convergent exhaust nozzle rather than the aerodynamically complex plug nozzle configuration used on the production engine. Second, the cylindrical tailpipe provided a platform for the installation of extensive nozzle inlet referee instrumentation as will be discussed in Section 2.3.

Finally, an air-oil cooler is normally utilized with this engine in the aircraft installation. For the UETP, an auxiliary water-oil cooler was added to the lubrication system as noted in Fig. 1b.

To facilitate handling and installation of the test article in each of the test facilities, the engine as modified along with the referee instrumentation was installed in a mounting frame as shown in Fig. 2. This test article package included standard interfaces for all mechanical, electrical, and instrumentation connections. All engine modifications, the inlet extension, tailpipe, nozzle, and the engine mounting frame were provided by NASA Lewis. Only one inlet extension, bullet nose, tailpipe, and reference exhaust nozzle was provided for UETP. Therefore, the same set of hardware was used on both engines.

The referee exhaust nozzle was "trimmed" to provide the rated engine pressure ratio at the military power lever setting as a part of the first test entry at NASA Lewis. At some of the higher altitude test conditions, military power for the J57 is limited by the maximum observed turbine discharge temperature rather than this as-trimmed power lever setting. This maximum temperature limit was derated 10 K (from 893 to 883 K) to reduce the thermal wear on the engine hot section and, hence, reduce engine performance variation during UETP.

## 2.2 Matrix of Variables

Eleven sets of environmental conditions, i.e., inlet pressure, inlet temperature, and exhaust nozzle ambient pressure, were selected to allow systematic evaluation of the effects of altitude, Mach number, and Reynolds number on test facility performance. Test condition 11 was identified for the ground-level test facilities, and, of course, the specific values of inlet pressure, inlet temperature, and ambient pressure depend on the specific geographic site and the specific atmospheric conditions existing at the time of test.

Test conditions 1 through 10 were defined for the altitude test facilities as shown in Fig. 3. In the altitude-ram pressure ratio (Mach No.) plane, (Fig. 3) the altitude ranged from 1,700 m at a ram pressure ratio of 1 (Mach No. 0) up to an altitude of 5,800 m at a ram pressure ratio 1.7 (Mach No. 0.91). At a constant ram pressure ratio of 1.3 (Mach No. 0.63) the altitude was systematically varied from 3,800 m up to a maximum of 13,200 m.

In the inlet pressure-inlet temperature plane (Fig. 3) at a constant inlet pressure of 82.7 kPa, the inlet temperature was varied from a minimum of 253 K up to a maximum of 308 K. At a constant inlet temperature of 288 K, inlet pressure was systematically varied from a maximum of 82.7 kPa, down to a minimum of 20.7 kPa.

When these environmental conditions are converted to compressor inlet Reynolds No. indices (Fig. 3), the test conditions ranged from a maximum Reynolds No. index of 0.96, down to a minimum Reynolds No. index of 0.20.

The other key independent variable is engine power setting which, for the J57 engine, is best expressed as the high rotor speed. For the altitude facilities, nine rotor speed settings were identified ranging from just above the compressor-bleed closing speed to the high rotor speed corresponding to military power setting (see Fig. 3). For the ground-level facilities, a total of 18 high rotor speed settings were identified—nine in the range from idle to the maximum speed at which the compressor bleed valve is open, and nine additional speeds between bleed valve just closed and military power (see Fig. 3).

## 2.3 Experimental Measurements

The design of the experimental measurements portion of the experiment required attention in three specific areas. First, measurements were required to determine the overall engine performance as needed to provide comparative test facility performance and thus meet the primary program objective. Second, the experimental measurements were required to ensure that the test operations were under control and were conducted in a safe, reliable, and consistent manner. Third, experimental measurements were required for control of the experiment and to support diagnosis of observed differences between facilities and allow the health of the test article to be monitored. It was necessary that the five major functions of measurement methodology, that is, sense, calibrate, acquire, record, and process, be addressed in the test plan on an individual basis for each of these three areas to derive maximum benefit from the UETP.

The experimentally-measured parameters required and the measurement methodology chosen for each parameter are shown in Fig. 4. For the overall engine performance determination the entire experimental measurement methodology was designed to be based on the local practice at each test agency for each individual test unit (Fig. 4a).

For the control of test operations, the sensing and calibration of all measurements within the engine were provided as part of the test article referee instrumentation (Fig. 4a). The acquire and record functions used local practice, and the data processing methods were defined in the UETP General Test Plan (Ref. 1). The test cell environment (e.g., cell cooling air temperatures and cell wall temperatures) was measured and controlled in accordance with local practice.

For the control of the experiment the sense and calibrate functions were a part of the test article referee instrumentation (Fig. 4b). The acquire and record functions were based on local practice. The decision to use local practice for these two functions was a compromise based on cost and schedule containment. Obviously, it would have been desirable to use a referee set of instrumentation to acquire and record these control parameters. Such referee instrumentation would have introduced the smallest bias and precision errors into the data, and thus would have maximized the confidence in the diagnosis of difference between facilities. However, this use of referee

equipment would have been extremely costly and time consuming compared to the resources available in the UETP budgets. All of the control of experiment parameters were processed in accord with the UETP General Test Plan (Fig 4b.)

#### 2.4 Test Methodology

The two key elements in the design of the test methodology were the test installation and the test operation. As discussed in Section 2.1, the test article was packaged in a mounting frame which provided for standardized electrical and mechanical interfaces. Local installation practices at each agency/test unit were utilized up to the test article interface. Again, this was an essential part of the design of the experiment. Not only were local practices utilized for the design and implementation of the mechanical, aerodynamic, hydraulic, and electrical interfaces between the test cell and the test article, but also the set-up and alignment of the test facility and the test article were in accord with local practice.

A description of the installation at each of the eight test facilities is contained in Ref. 2. However, it is useful for the purposes of this lecture to examine the essential features of a typical ground-level test facility and a typical altitude test facility. The elevation and plan views of the engine installation in test cell No. 5 at the Engine Laboratory at NRCC are shown in Fig. 5. The essential features are the air inlet system, the engine test room, and the exhaust gas collection and silencer system. The engine and the engine inlet protective screen (anti-personnel screen) are shown installed on this engine test bed.

In a similar manner, the installation of the UETP engine in test cell T-2 in the Engine Test Facility at AEDC is shown in Fig. 6. Again the essential elements are the airflow measurement system, the air supply ducting, the engine inlet bellmouth, the labyrinth seal assembly, the engine support system, and the exhaust diffuser system.

A photograph of the UETP engine installed in test cell PSL-3 at NASA Lewis is shown in Fig. 7.

The second major element of the test methodology is the design of the test operation. This portion of the experiment was designed to maximize the use of local practice at each test agency and at each test unit. Several specific exceptions were included in the design to improve the confidence level and reliability of the test data. The six exceptions are as follows:

1. Engine trim rechecks only were authorized at each test unit. No re-trim of the engine control system was permitted without specific approval of the Chairman of Working Group 15. No engine trim was authorized during UETP.
2. Two data scans were required at each engine power setting.
3. Fixed time intervals were estimated for engine thermal stabilization before each data scan. A fixed time interval of 5 min was specified before the initial data scan. An additional time interval of 2 min for the repeat data scan was also specified. The validity of these time intervals was determined experimentally during the first test entry at NASA Lewis. Rechecks of these time interval requirements were also made at RAE(P) and NRCC.
4. No testing of the engines was to be conducted at "high" levels of relative humidity at the engine inlet. However, no specification of "high" was included in the General Test Plan.
5. As was discussed in Section 2.2 a predetermined, inter-mixed ascending and descending set of engine high rotor speed settings was defined for the program (Ref. 1). The matrix of engine speed settings was chosen to minimize the effects of control hysteresis, engine thermal effects, and bleed valve control variability on the results of the test program (Ref. 2).
6. Engine performance retention/deterioration throughout the total test duration of the UETP was to be determined from the observed differences between the engine performance during the initial test entry at NASA Lewis and a second test entry at NASA Lewis at the conclusion of all of the UETP testing. As will be discussed in later portions of this lecture series this portion of the experimental design was inadequate to meet the needs of the program. Further schedule conflicts at NASA Lewis and at NAPC did not allow this portion of the experiment to be conducted as designed. Specifically, the second entry test at NASA Lewis was accomplished prior to the engine testing at NAPC and was conducted in a test unit different from that used for the first entry. Therefore, it was not possible to determine the engine performance variation with the desired measurement uncertainty. This design approach to determine engine performance variation for the UETP was inadequate. The analysis of engine performance retention/deterioration will be addressed in Lecture 4.

#### 2.5 TEST DATA PROCESSING

The test data processing portion of the experiment was designed to utilize local practices at each test agency as applicable to each test unit to the maximum extent possible. Some of the specific functions of local data processing which were to be utilized included data editing and data validation with emphasis on the deletion of outlier data samples and the "fill-in" of missing data samples. Second, the thermodynamic properties of air and combustion gases were to be based on the properties defined at each test agency.

Three minor exceptions to the use of the local practice were implemented to simplify communication of test results between the test agencies and to simplify analysis of the results by WG15. The specific exceptions were defined in the General Test Plan (Ref. 1) and included (1) a uniform nomenclature and units of measurements, (2) uniform equations for the as-tested and "referred" engine performance parameters, and (3) a uniform format of the digital magnetic tapes which were used for data communications and data exchange between the several test agencies and the working group.

## 2.6 MEASUREMENT UNCERTAINTY

A uniform method to assess and communicate the uncertainty of all of the experimental measurements was adopted as a part of the design of the UETP experiment. The Abernethy and Thompson Method was adopted (Ref. 3). The GTP required each participant to prepare pretest estimates of the measurement uncertainty of the key parameters of engine air flow, net thrust, and specific fuel consumption at the target speed. These estimates were to be prepared for operation at test condition 3, test condition 9, and test condition 11 (see Fig. 3). The GTP also required that the elemental source errors be estimated at the conclusion of the testing in each test unit for all inputs into the four key parameters listed above, in addition to a posttest assessment of the measurement uncertainty for the four key parameters at the target speeds at the same three test conditions as identified for the pretest estimates.

This approach for the assessment of measurement uncertainty was inadequate and required substantial modification during the analysis phase of the effort (Ref. 4). These modifications will be addressed in Lecture 7.

## 2.7 REPORTING

The design of the experiment included four specific reports which were to be prepared as a part of the UETP program. First, each test agency was required to prepare a test plan tailored to each specific test unit that was scheduled for use. This test plan was to be based on the GTP and was to be prepared before the initiation of testing at each individual test unit. The format for this facility test plan was specified in the GTP.

Second, each facility was required to submit a final data package to the chairman of WG15 within 60 days after the completion of testing. This data package was to include digital magnetic data tapes in specified format and a test summary report containing at least the minimum information as specified in the GTP.

The final data packages were interchanged between facilities only after each had completed its test program and had transmitted the final test report to the chairman of Working Group 15. This approach ensured that each facility was "blind" during the conduct of the testing and had no prior knowledge of the test results from the other facilities. This "blind" approach was adopted to maximize the confidence in the results of the inter-facility comparisons.

Third, a facility final test report was required to be submitted to the chairman of the WG within 140 days after the release of the final data package. The format for this final test report was specified in the GTP. The same release restrictions that were applicable to the final data package discussed above were also applicable to the final test report.

Finally, AGARD reports which presented the results of the UETP were to be prepared on an as-required basis. As is now known, two AGARD reports were prepared for the UETP by WG15. The first of these reports presents the overall results of the test program (Ref. 2). The second report addresses in detail the results of the measurement uncertainty analysis portion of the program (Ref. 4).

## 3.0 GENERAL TEST PLAN

The design of the experiment for the UETP was reported in the GTP (Ref. 1). The designers of the format of the GTP properly anticipated that the test plan needed to be a living document. As such the plan would be responsive in a timely manner to a significant number of revisions identified throughout the course of the program. The format chosen met these requirements in an excellent manner.

The test plan included the management, technical, and logistic guidelines and associated controls which were necessary for the proper conduct of the UETP. The Table of Contents of the GTP (Ref. 1) is included in Appendix I to demonstrate the breadth and depth of this pioneering document.

The initial draft of the GTP was prepared by representatives of AEDC. This draft was reviewed and reworked by the full membership of PEP Working Group 15 to create the initial version of this general test plan. The initial test plan and subsequent revisions were coordinated with and approved by all participants in the UETP.

## LIST OF REFERENCES

1. Subcommittee 01, AGARD Propulsion and Energetics Panel, Working Group 15, "Uniform Engine Testing Program General Test Plan," June 1983. (Revised Edition).
2. Ashwood, P. F., principal author, and Mitchell, J. G., editor, "The Uniform Engine Test Programme-Report of PEP WG15," AGARD Advisory Report No. 248, February 1990.
3. Abernethy, R. B., and Thompson, J. W. "Handbook-Uncertainty in Gas Turbine Measurements," AEDC-TR-73-5 (AD-755-356), February 1973.
4. Vleght, J. P. K., editor, "Measurement Uncertainty Within the Uniform Engine Test Program," AGARDograph 307, May, 1989.

**APPENDIX I****UNIFORM ENGINE TESTING PROGRAM GENERAL TEST PLAN****TABLE OF CONTENTS (From Ref. 1)**Page

1.0	INTRODUCTION .....	
2.0	AGARD-UETP MEMBERSHIP .....	
3.0	AGARD-UETP OBJECTIVES AND MEMBERSHIP RESPONSIBILITIES .....	
3.1	Program Objectives .....	
3.2	AGARD Working Group 15 Authority/ Responsibilities .....	
4.0	AGARD-UETP TEST PARTICIPANTS .....	
5.0	PARTICIPANT TEST OBJECTIVES AND RESPONSIBILITIES	
5.1	Facility Test Objectives .....	
5.2	Participant Responsibilities .....	
5.3	Participant Test Schedule .....	
6.0	ENGINE DESCRIPTION .....	
6.1	General Description .....	
6.2	Compressor Bleeds .....	
6.3	Oil Cooler .....	
6.4	Engine Exhaust Nozzle .....	
6.5	Engine Instrumentation .....	
6.5.1	General .....	
6.5.2	Station Designation and Nomenclature .....	
6.5.3	Instrumentation Connections and Identification .....	
6.5.4	Referee Instrumentation Requirements .....	
6.5.5	Dynamic Pressure Transducers .....	
6.6	Spare Parts .....	
7.0	TEST INSTALLATION REQUIREMENTS	
7.1	General .....	
7.2	Engine Inlet Hardware .....	
7.3	Test Cell Cooling and Flow Gradients .....	
7.4	Engine Mount System .....	
7.5	Engine Installation Interface Definitions .....	
7.6	Engine Fuel System .....	
7.7	Power Lever Shaft Schedule and Rigging .....	
7.8	Electrical System Requirements .....	
7.9	Lubricating Oil System .....	
7.10	Hardware Items Available to UETP Participants .....	
7.11	Available Drawings for UETP .....	
8.0	TEST PROCEDURES .....	
8.1	Operating Procedures .....	
8.1.1	Engine .....	
8.1.2	Trim .....	
8.2	Pretest Checks .....	
8.2.1	Ignition Checks .....	
8.2.2	Fuel System Leak Checks .....	
8.2.3	Windmilling Check .....	
8.2.4	Engine Oil Service .....	
8.2.5	Engine Inspection .....	
8.3	Engine Posttest Inspection .....	
8.4	Test Condition .....	
8.4.1	Altitude Testing .....	
8.4.2	Sea-Level Testing .....	
8.5	Log Requirements .....	
9.0	TEST DATA REQUIREMENTS	
9.1	Acquisition .....	
9.2	Editing and Validation .....	
9.3	Standard Equations for UETP .....	
9.4	Nomenclature .....	

9.5	Data Presentation Format	.....
9.6	Format for Data Transmittal	.....
9.7	Suggested Performance Parameters	.....
9.8	Performance Plots	.....
9.9	Data and Report Transmittal	.....
10.0	ERROR ASSESSMENT	
11.0	REPORTING	
11.1	Facility Test Plan Format	.....
11.2	Facility Test Report	.....
12.0	ENGINE PRESERVATION AND SHIPPING	
12.1	Engine Preservation (Altitude Facilities)	.....
12.2	Engine Preservation (Sea-Level Test Facilities)	.....
12.3	Engine Waterwash	.....
12.4	Shipping	.....

#### TABLES

I.	Referee Instrumentation Recommendations	.....
II.	Mil Power Settings for Trim Check	.....
III.	Test Conditions	.....
	A. Engine No. 1, S/N 607594	.....
	B. Engine No. 2, S/N F615037	.....
	C. Sea-Level Facilities-Bleed Closed Settings	.....
	D. Sea-Level Facilities-Bleed Open Settings	.....
IV.	Test Summary Sheet	.....
V.	Description of Data Measurement Systems	.....
	A. Pressure	.....
	B. Temperatures	.....
VI.	Identification of Elemental Error Sources	.....
VII.	Estimated Measurement Uncertainties	.....
VIII.	Estimated Performance Parameter Uncertainties	.....

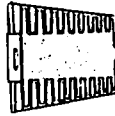
#### FIGURES

1.	Pratt & Whitney Aircraft J57-P-19W Turbojet Engine	.....
2.	Modified Tailpipe and Reference Nozzle Assy	.....
3.	UETP Engine Instrumentation Station Locations	.....
4.	Engine Internal Aerodynamic Pressure & Temperature Instrumentation	.....
5.	Engine Installation in NASA Supplied Test Stand	.....
6.	Engine Inlet Bulletnose	.....
7.	NASA Bulletnose and Engine Inlet Instrumentation Spool Piece Design	.....
8.	Engine Lubricating Oil System Schematic	.....
9.	J57 Installation at NASA LeRc	.....
10.	Standard AGARD Engine Performance Plots	.....

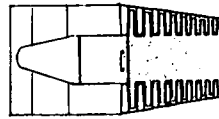
#### APPENDICES

I.	Recommended Spare Parts for J57 Unified Engine Test Program	.....
II.	Spectrometric Oil Analysis Program Sample (SOAP) Limits for J57-P-19W Engine	.....
III.	Engine Operating Procedures	.....
IV.	Engine Operational Limits	.....
V.	Calculation of Kinematic Viscosity Constants	.....

• INLET EXTENSION AND BULLETHOSE



PRODUCTION CONFIGURATION



AS MODIFIED FOR UETP

• COMPRESSOR BLEEDS -

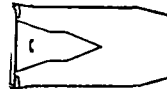
- COMPRESSOR ACCELERATION BLEEDS MODIFIED FROM BOMBER CONFIGURATION (2 VALVES) TO FIGHTER CONFIGURATION (1 VALVE)
- ANTI-ICING BLEED
- CUSTOMER SERVICE BLEED } ENGINE PORTS CAPPED

a. Engine inlet and compressor

• TAILPIPE AND REFERENCE EXHAUST NOZZLE



PRODUCTION CONFIGURATION



AS MODIFIED FOR UETP

• ENGINE SERVICE SYSTEMS

AUXILIARY WATER-TO-OIL COOLER ADDED TO LUBRICATION SYSTEM

b. Tailpipe, nozzle, and service systems  
 Figure 1. Modifications to production J-57 engine.

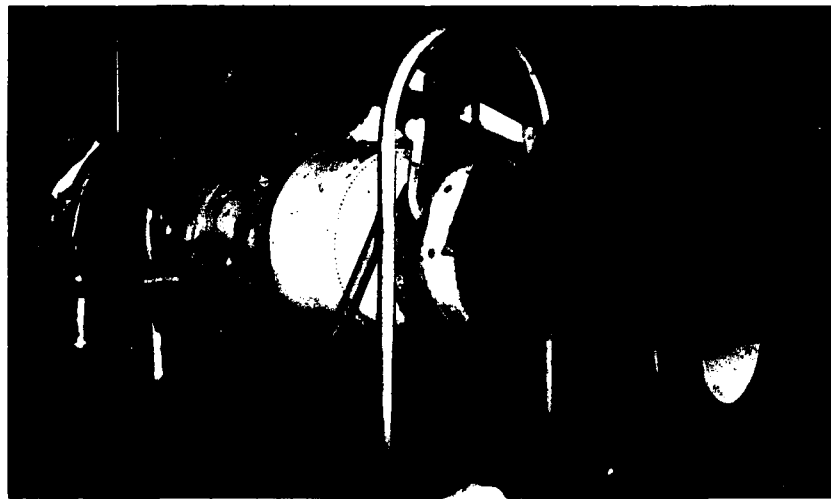
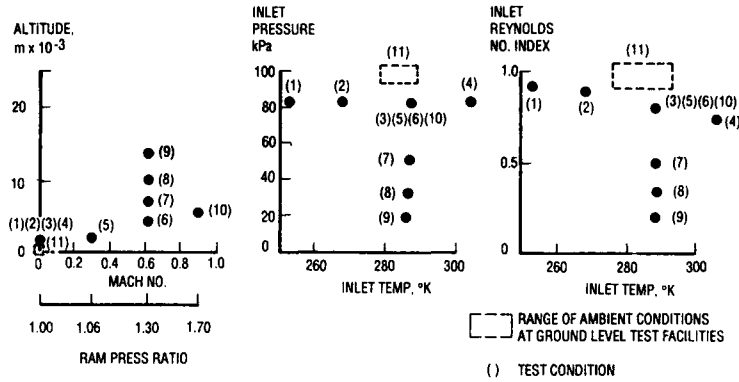


Figure 2. Test article for Uniform Engine Test Program (UETP).

• ENVIRONMENTAL PARAMETERS



• ENGINE POWER PARAMETERS

- ALTITUDE FACILITIES - 9 HIGH ROTOR SPEEDS - BLEED "JUST CLOSED" TO MIL
- GROUND LEVEL FACILITIES - 18 HIGH ROTOR SPEEDS - IDLE TO MIL

Figure 3. Matrix of UETP test variables.

• OVERALL ENGINE PERFORMANCE (PRIMARY PROGRAM OBJECTIVE)

PARAMETER	MEASUREMENT	METHODOLOGY
	AIRFLOW FUEL FLOW NET THRUST SPECIFIC FUEL CONSUMPTION	SENSE, CALIBRATE
LOCAL PRACTICE AT EACH TEST AGENCY/TEST UNIT		LOCAL PRACTICE AT EACH TEST AGENCY/TEST UNIT

• CONTROL OF TEST OPERATIONS (SAFE, RELIABLE, CONSISTENT OPERATIONS)

PARAMETER	MEASUREMENT	METHODOLOGY	
	ENGINE INLET PRESS. & TEMP. ENGINE EXHAUST AMBIENT PRESS. ROTOR SPEEDS POWER LEVEL ANGLE ENGINE VIBRATION ENGINE FUEL PRESS. & TEMP. ENGINE OIL PRESS. & TEMP. ENGINE BLEED VALVE POSITION	SENSE, CALIBRATE	ACQUIRE, RECORD
TEST ARTICLE REFEREE INSTRUMENTATION		LOCAL PRACTICE	UETP GENERAL TEST PLAN
TEST CELL ENVIRONMENT	LOCAL PRACTICE	.	.

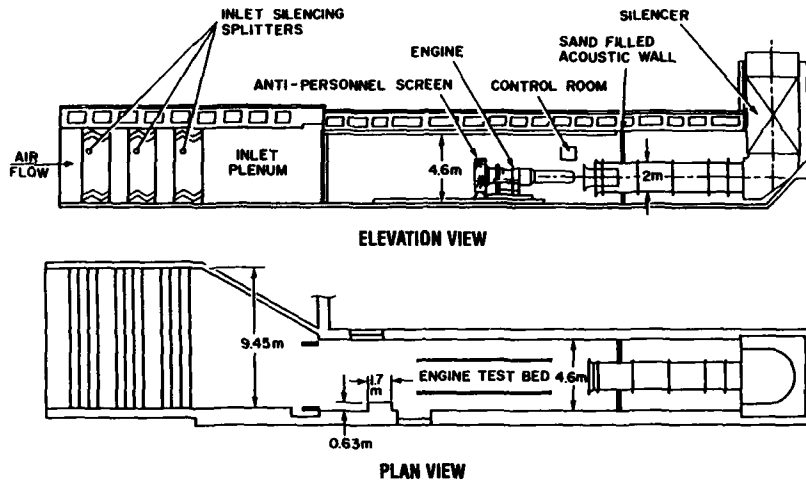
a. Engine performance and control of test

• CONTROL OF EXPERIMENT (DIAGNOSIS OF OBSERVED DIFFERENCES, ENGINE HEALTH MONITORING)

PARAMETER	MEASUREMENT	METHODOLOGY	
	COMPRESSOR AIRFLOW COMPRESSOR INLET DYNAMIC PRESS. COMPRESSOR BLEED PRESS. & TEMP. COMPRESSOR DISCH. PRESS. & TEMP. TURBINE DISCHARGE PRESS. & TEMP. EXH. NOZZLE INLET PRESS. & TEMP. EXH. NOZZLE GAS FLOW ENGINE FUEL FLOW	SENSE, CALIBRATE	ACQUIRE, RECORD
TEST ARTICLE REFEREE INSTRUMENTATION		LOCAL PRACTICE (COST AND SCHEDULE CONTAINMENT- COMPROMISE)	UETP GENERAL TEST PLAN

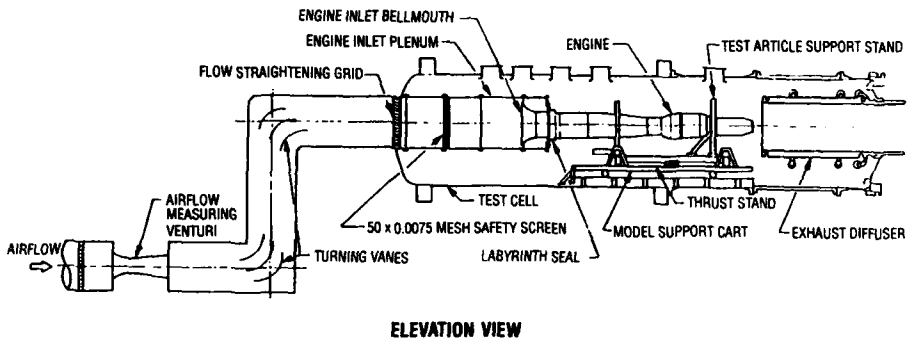
b. Control of experiment

Figure 4. Experimental Measurements for UETP.



**NO.5 TEST CELL - ENGINE LABORATORY - NRCC**

Figure 5. Typical UETP installation, ground-level test facility.



**TEST CELL T-2 - ENGINE TEST FACILITY - AEDC**

Figure 6. Typical UETP installation, altitude test facility.



**TEST CELL PSL-3 - NASA LEWIS**

Figure 7. Typical UETP test installation.

**THE BASIS FOR FACILITY COMPARISON**

A. R. Osborn  
Propulsion Department  
Royal Aerospace Establishment  
Pyestock, Farnborough, Hants GU14 0LS, England

Copyright (C) Controller HMSO London 1990

**SUMMARY**

One of the main objectives of the UETP was an engine facility comparison to identify the bias measurement performance differences between test sites. This Paper identifies the methods used to present these comparisons in the final report and the alternative presentations considered in the Working Group 15 discussions, but not published elsewhere. In addition, many other factors affecting engine performance determination are discussed and the planned methodology adopted by the UETP to determine these elemental differences. Finally, some examples of UETP engine performance measurement anomalies are highlighted and an attempt made to identify the reason for them with a recommendation on how they should be treated.

**1 INTRODUCTION**

During the meetings and discussions of Working Group 15 to analyse and report<sup>1</sup> the UETP, the basis for facility comparisons was covered by many techniques, some based on facility measurements, others by engine internal performance measurements and finally some based on a combination of plant and engine measurements. To illustrate the specific methodologies employed and those agencies, or in some cases individuals, who performed the major part of these investigations, the following list identifies each in turn:-

(a)	Overall engine performance	: P.F. Ashwood (UK), AEDC
(b)	Measurement uncertainty	: WG15 Sub group
(c)	Performance retention	: AEDC
(d)	Inlet total pressure calculation methods	: NRCC
(e)	Inlet total pressure distortion	: NASA
(f)	Engine settling time	: NASA, RAE, NRCC
(g)	Secondary airflow in ground-level facilities	: NRCC
(h)	Nozzle thrust and airflow functions	: RAE
(j)	Engine internal air flow using flow functions	: Professor Jacques (Belgium)
(k)	Fuel flow analysis	: NRCC
(l)	Temperature lapse rate	: AEDC, RAE
(m)	Nozzle area change	: NASA

Although certain organisations are identified for each task in the list, there was considerable debate within Working Group 15 itself and other personnel and agencies not listed often contributed to the work. Nevertheless, those listed provided the main effort for each item and should take the appropriate credit.

This lecture will now examine more closely some of the items in the above list, but will exclude others. Those considered will only be reported on from the point of view of method and procedure rather than a detailed analysis of the results. The major items excluded are the measurement uncertainty, the nozzle coefficients, flow coefficients and fuel-flow analyses, all of which will be covered by my colleagues in other sections of the lecture series.

**2 DATA ANALYSIS PROCEDURE**

**2.1 The main choice of presentation of overall performance**

The measured engine test data gathered at each test site were converted into turbine engine performance parameters, utilizing a set of standard equations specified in the General Test Plan which was drawn up prior to the first engine test (Ref 2). However, test plant data were analysed by each test facility using the local equations they normally applied in an engine test. After the data for each test facility were declared satisfactory by that test site, a copy was provided to each participant, both in tabular form and on magnetic tape, in a format specified in the General Test Plan. An example of the tabular form is shown in Fig 1. The test results were released only to those facilities that had completed their testing and to nominated members of the Working Group. Facilities testing later in the programme therefore had to wait for data from previous tests until after completing their own tests and declaring their own results satisfactory. It was impractical to publish the complete set of test results in the final report because of the enormous quantity involved and therefore a condensed format was sought to display inter-facility differences.

A set of six parameter pairs were chosen for the main inter-facility performance comparison. These six parameter pairs were:

(a)	NLONH vs NHRD	shaft speed ratio versus HP rotor speed
(b)	T702 vs P702	nozzle inlet temperature versus nozzle inlet pressure

(c)	WAIRD vs NLRD	airflow versus LP rotor speed
(d)	WFRD vs NHRD	fuel flow versus HP rotor speed
(e)	FNRD vs P7Q2	net thrust versus nozzle inlet pressure
(f)	SFCRD vs FNRD	fuel consumption versus net thrust

The letters RD in these nomenclature indicate the parameter has been normalized to the desired conditions using non-dimensional pressure and temperature relationships. For the altitude test conditions all parameters have been corrected to the nominated flight conditions, eliminating small differences between the as-tested values and the nominal values. The ground-level test conditions have been corrected to standard sea-level conditions of 101.3 kPa pressure, 288 K temperature and a ram ratio of 1.0, eliminating differences due to varying ambient conditions between test sites and day-to-day fluctuations. The six parameter pairs listed above enable inter-facility comparisons to be made for the following primary checks.

PLOT (a)	: speed matching check
PLOT (b)	: nozzle conditions and hence secondary thrust and airflow check
PLOT (c)	: primary airflow check
PLOT (d)	: primary fuel flow check
PLOT (e)	: thrust derivation check
PLOT (f)	: overall performance check

Since the altitude testing was configured so that performance curves were carried out at four separate inlet temperatures, four separate inlet pressures and four different ram ratios, whilst keeping the remaining two parameters constant, the main results have been presented in these three groupings so that trends could be established. The reason for the testing to be configured this way is because altitude test facilities generally control test conditions by adjusting these primary variables to achieve true flight conditions. To illustrate the difference in these chosen test variables and a typical engine flight envelope they can be seen plotted in Fig 2. The change in  $T_1$  is at constant Mach number and altitude. The change in  $P_1$  gives a constant Mach number and changing altitude and the change in ram ratio leads to both change in Mach number and altitude. Using this format it was possible to detect if any one test site had measurement problems with any one primary variable.

Since only one of the pair of engines was tested at all four altitude test sites, results for this engine, serial number 607594, were presented in the final report. In addition, the other engine, serial number 615037, was tested at all four sea-level test sites and so these were presented separately for the ground-level comparisons. For the altitude-to-ground level comparisons, the data from engine 607594 was used where four altitude and two ground-level facilities provided data. Fig 3 summarises the order of testing of the two engines at the various test facilities that participated in the plan.

The condensed set of performance data were published such that four graphs were displayed on each page and the total number of pages totalled 18. Fig 4 shows a typical display of data on one page and in fact shows the sfc curves for the four altitude test facilities at varying inlet pressures with inlet temperature constant at 288 K and ram ratio held at 1.30.

## 2.2 Sensitivity indicators

To quantify the inter-facility differences for the purpose of comparison, the maximum spread of each parameter (expressed as a percentage of the median value) was calculated at approximately the mid-thrust point. These spreads have been indicated on the performance curves and were derived from the equations fitted to the data points calculated for each facilities results. In addition, each graph has 1 percent bandwidths added for both the x and y variables to assist in assessing the effects of real variations or errors in these parameters relative to the scales chosen for the presentation, see Figure 4.

## 2.3 The method of accounting deterioration

The test procedure included precautions to identify performance degradation, firstly, by each test site testing at a set condition at the beginning of their tests and at the same condition at the end of their tests. Secondly, the engines were tested on two occasions at NASA, being the first test site and the last test site in the sequence, (excepting MAPC, Trenton, who did not test the engine until after the main analysis had been completed because of higher priority work). None of the results presented in the facility comparisons have been corrected for deterioration which were detected as being very small, and within uncertainty limits. This topic nevertheless attracted a great deal of discussion in the WG meetings and justifies more detailed treatment in a companion lecture.

## 2.4 The choice of curve-fit

Engine performance curves are generally presented as a correlation of one parameter against another for example  $y = \text{sfc}$  correlated against  $x = \text{FN}$ . The graphs for any one test site will always show a certain amount of scatter about some central curve, see Fig 5, and there will be some doubt as to the correct position of the curve if drawn by hand. Fitting a polynomial equation eliminates that uncertainty; the form it can take being:-

$$\begin{aligned} \text{either a straight line} & \quad y = b_0 + b_1x \\ \text{or a quadratic} & \quad y = b_0 + b_1x + b_2x^2 \\ \text{or a cubic} & \quad y = b_0 + b_1x + b_2x^2 + b_3x^3 \end{aligned}$$

or perhaps even some higher degree.

The numerical value of the coefficients  $b_0, b_1, b_2, b_3$  are calculated from the data by the method of 'least squares'. That is, the values are found such that the sum of the squares of all the deviations from the curve are minimised.

A typical deviation is,  $e_i = (y_i - \hat{y}_i)$

where  $\hat{y}$  is the value of  $y$  on the curve

so that  $\sum e_i^2$  is a minimum for calculated values of  $b_0, b_1, b_2, b_3, \dots$

The detailed procedure for doing these calculations can be found in all standard statistical text books.

The UETP test plan specified that all curve fitting would take the form of a quadratic so that each test site would carry out a uniform process. Although in general this policy was justifiable, since the main area of interest for comparisons was at a mid-thrust point, it does have some weaknesses. Quadratics are inherently symmetrical curves and it can be demonstrated that in the case of some variables this order of polynomial fit is not necessarily the best when judged on statistical significance tests. The complex nature of a gas turbine does not always lead to parameters correlating in convenient symmetrical relationships, particularly at points at either end of the range of measurement. This can be demonstrated by examining an SFCRD versus FNRD curve obtained with data measured at RAE(P) at test condition 9, Fig 6. A measure of the significance of the curve fit can be obtained by the value of the Relative Error Limit of Curve Fit (RELFCF) for each polynomial, the 0.18 for the cubic being superior to the 0.27 for the quadratic. Table 1 summarises the differences in SFCRD for three power level levels at all the 10 test conditions for the RAE(P) data. It indicates that in about half the cases a slightly better result would have been obtained for low and high engine power comparisons if cubics had been adopted. However, as stated earlier, since mid-thrust levels were the target levels for performance comparisons the quadratics specified were more than satisfactory.

## 2.5 Alternative presentations

Other forms of presentation of overall performance were considered by the Working Group and a bargraph presentation was seriously put forward as the prime method in the early stages of discussion. However, as testing proceeded and more participants joined the discussion team, it became apparent that a bargraph presentation was not favoured by the majority of participants, who argued it would only show differences at a single or limited number of power settings. In addition, there was some uncertainty as to how to choose the datum for such a presentation. Some participants thought it should be based on an average value of all facilities, others considered the datum should be the results of the first test facility. An example of a proposed format is shown in Fig 7. It was finally agreed that the main overall results should take the graphical form, outlined earlier, so that differences would be displayed over the complete measurement range. However, a limited form of bargraph presentation was included in the final report, but only showed the overall spread of results from the altitude facilities for the primary parameters of FNRD versus P702, MA1RD versus MLRD and SFCRD versus FNRD, see Fig 8. These results were included at all test conditions and the datum was taken as the facility with the lowest value, not always the same facility in all cases, ie the bar showed the percentage spread in the parameter for all test facilities at a mid-thrust point. Two sets of bars were included, one for all four altitude facilities and a second set excluding the CEPr result because some of their results exhibited large scatter. This was considered to adversely influence the presentation, particularly the thrust versus nozzle inlet pressure bargraph. This exclusion of the CEPr results in some presentations will be explained in other lectures in this series.

One further method of presentation was used which took the form of a tabulation of differences. Table 2 shows the format used for the altitude test site comparison and consists of a list of the selected parameters together with the independent variables, basically the same six parameter pairs selected for the graphical presentation. The overall percentage spread at a mid-thrust point was chosen together with the percentage of data points which fell within a fixed 2 percent bandwidth. Additionally, the estimated uncertainty bandwidth spread was added to the table for each parameter to help make a judgement on the quality of the measured data. The table of differences again include values with and without CEPr results included because of the reasons given earlier.

This form of presentation was also adopted for the sea-level test bed comparison and the altitude/sea-level test bed comparison, tables 3 and 4. In the case of the sea-level bed comparison, the percentage spread values in the table for the four test sites have been quoted with and without the Turkish test site results. Again the reason for this policy was based on the fact that the Turkish test site results displayed a large scatter in the measurements compared with the remaining three facilities. For the altitude to sea-level comparison, five test facility results were used, NASA, AEDC, RAE(P), CEPr and NRCC and these were based on data obtained using engine 607594. The results obtained in the altitude facilities were measured at an inlet pressure of 82.7 kPa and then referred to standard pressure of 101.3 kPa using the specified equations in the General Test Plan. These adjustments did not introduce discrepancies, since it was judged that these would be negligible at the high pressure condition where Reynolds number remains high enough to prevent changes in flow conditions affecting turbomachinery characteristics.

## 2.6 Other factors considered in the performance analysis

### 2.6.1 Humidity

All the altitude test facilities had plant which was capable of supplying dry air to the engine and therefore humidity effects on engine performance were negligible (humidity never exceeded 0.1 percent water by weight). In the case of the sea-level beds, the humidity on the actual test dates at all those facilities taking part remained sufficiently low to ensure the effects were negligible or very small.

### 2.6.2 Inlet total pressure

The effect of inlet total pressure on engine performance was approached from two fronts. Firstly, the effect of changing the method of calculation of inlet pressure given a certain engine face pressure distribution and secondly, the effect of changes in inlet pressure profile, ie inlet pressure distortion.

The effect of the way inlet pressure was calculated was investigated by NRCC<sup>3</sup> by applying five different methods of calculation to a particular inlet distribution obtained at NRCC in their tests. Fig 9 shows the circumferential location of all the probes used in the analysis.

Method 1 used the simple arithmetic average of the 20 mainstream pressure readings assuming the probes were located at the centroids of five equal areas and was the method recommended in the General Test Plan.

$$P_T \text{ average} = \frac{1}{N} \sum_{n=1}^N P_n$$

Method 2 was similar to Method 1, but used weighting factors determined from the actual measured probe locations

$$P_T \text{ average} = \frac{1}{A} \sum_{n=1}^N P_n dA_n$$

Method 3 was similar to Method 2, but only used those probes in the inviscid flow regime. This was determined by comparing the total pressure at each probe with the value for the centre line probe. If the difference was greater than the pressure measurement uncertainty for the facility, then the value for that probe was discarded, the probe being assumed to be in viscous flow.

Method 4 calculated the average pressure by considering the measurements from two rakes in an inner and outer boundary layer ring sector, combined with four main ring sectors. Appropriate weighting factors were determined for each annular sector.

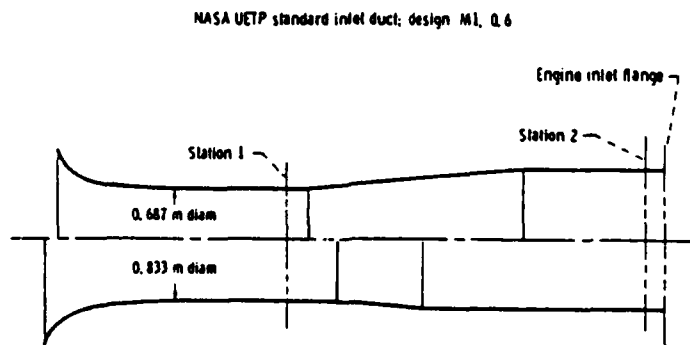
Finally, Method 5 further increased the weighting afforded the boundary layer probes.

Table 5 summarises the results of all five methods using NASA data, which gave the most pronounced inlet pressure profile and would therefore demonstrate the differences in calculation techniques.

The conclusion drawn in the UETP tests was that the GTP method, Method 1, produced a value of  $P_T$  average within 0.07 percent of that obtained if all the probes, including those in the boundary layer, were used to obtain an integrated mean inlet total pressure. However, it must be noted that this solution will not necessarily suit all engine inlet rake geometries and pressure profiles. Where boundary layers are thin, but significant, and the main pressure rake does not capture the pressure decay at the duct wall, then simple averaging may produce a significant error. This will then carry forward an error bias in those important parameters that depend on an accurate inlet pressure measurement, in particular thrust determination.

### 2.6.3 Inlet total pressure distortion

The effect of inlet pressure distortion on performance measurements was examined by comparing the results from the two NASA tests, the first and second entry tests. Between these tests the inlet ducting at NASA was changed from a duct with 0.687m diameter throat to a geometry with a significantly larger throat, 0.833m diameter, see diagram below.



Larger inlet duct: design M1. Q.36

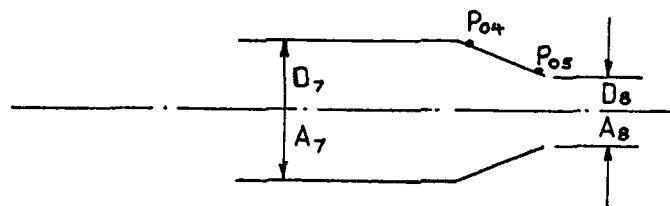
Schematics of inlet ducting used for inlet total-pressure profile investigation.

Using data selected from test conditions 6, see Fig 10, it is obvious that the duct with the small throat venturi gives a poor inlet pressure profile. The larger throated duct gave a dramatic improvement in inlet pressure profile. Despite the marked change in  $P_T$  profile the effect on most performance parameters of the engine to changes in inlet duct geometry was found to be generally small. The change in shaft speed ratio,  $N_{LWH}$ , was negligible, 0.02 percent, but the change in airflow versus LP compressor pressure ratio was more

significant, 0.6 percent. However, the engine did not contain a great deal of diagnostic instrumentation and therefore it is impossible to detect precisely what happened internally within the compressor components. It is postulated that this engine was insensitive to the maldistribution in pressure in the first few stages of the low pressure compressor and therefore the effect on overall engine performance was negligible. The early design of this engine with relatively low loading of components means that it is very tolerant to distorted inlet flow. More modern engine designs might be more sensitive to inlet pressure distortion and might show differences in overall engine performance.

#### 2.6.4 Boattail force

During the analysis of the UETP thrust data it became apparent that the method of accounting the boattail force differed between test sites. Some sites ignored this force assuming from past experience that it was relatively small, whilst others accounted for it as part of their normal procedure. The engine was fitted with surface pressure tappings at the rear of the nozzle and the boattail force was estimated using these measurements, see diagram below. Figure 11 shows the results for conditions 6 and 9 for the altitude facilities and a value for each sea-level test site. It can be seen that generally the force is insignificant when compared with the level of net thrust, never exceeding 0.07 percent in the case of the altitude facilities justifying the decision of those sites which did not account for it.



$$F_{BT} = (P_{04} - P_{05})(A_7 - A_8)/2$$

#### 2.6.5 Change in exhaust nozzle area

There was some concern that the exhaust nozzle might be damaged, dented or ovalised changing the effective area,  $A_8$ , during the course of the UETP. This was not borne out by exit area measurements made at each test site during the course of tests. The average area measured at some of the test sites from a series of measurements is shown below.

	$A_8$ sq.m	Diff from average per cent
NASA	0.2376	0.04
AEDC	0.2378	0.13
NRCC	0.2372	-0.13
RAE(P)	0.2374	-0.04
Average	0.2375	

It can be seen that the area remained constant for all practical purposes and the correlations of shaft speeds also confirmed that effective nozzle area remained constant at all test sites.

#### 2.6.6 Nozzle inlet, Station 7, rake alignment

During the first NASA test it became apparent that the Station 7 total pressure rakes did not adequately measure a true mean pressure. The pressure profile at Station 7 was strongly influenced by the large upstream turbine exit struts and the attendant swirl in the flow. In an effort to understand the nozzle entry total pressure profile, the tailpipe, and hence rake, was rotated at increments of 10 degrees over an arc  $\pm 20$  degrees either side of the datum UETP position. Measurements of pressure were taken at test conditions 6 and 9. Figure 12 shows a plot of the average total pressure derived from the rake, a static pressure and turbine exit total pressure for the 5 angular positions at test condition 6 at a high rotor speed of 8900 rpm. Whereas the static pressure and turbine exit pressure remain fairly constant, the derived total pressure from the rake varies over a bandwidth of 2.5 percent at this flight condition. The corresponding effect on calculated nozzle coefficients at test condition 6, thrust CG8 and flow CG8, can be seen in Fig 13. The difference in thrust coefficient is of the order of 4 percent for a rotation of 20 degrees in either direction from the datum position. For the flow coefficient there are not only changes in level, but the shapes of the curves are also altered. Although at high engine power the coefficient is comparable for all three angular positions, at lower engine powers the coefficients are 1.5 to 2.5 percent lower for the extreme angles of  $\pm 20$  degrees. Some of the differences in observed nozzle coefficients can be accounted for by small changes in other measured parameters, for example, airflow, fuel flow, thrust and ambient pressure. In summary therefore, and taking into account the other measured differences in influential parameters, a 3.5 percent decrease in P7 gave a 1.9 increase in CG8 and a 4.3 percent increase in CG8 resulting from a 10 degree rotation of the tailpipe.

This investigation on nozzle instrumentation serves to indicate that:-

- (a) It is difficult to provide an array of pressure instrumentation that will give a true integrated average total pressure in the jet pipe.
- (b) If total pressure instrumentation is provided, then it must remain consistent throughout all development and flight testing if coefficients are to be used to derive thrust and airflow from facility measurements.
- (c) Static pressure measurements in the jet pipe are less sensitive to local flow disturbances and are a far more rugged measurement. Therefore, provided care is taken in the geometry and manufacture of the tapping a reliable total pressure can be derived and used to calculate nozzle coefficients.

#### 2.6.7 Engine settling time

The UETP General Test Plan specified an engine thermodynamic settling time of 5 minutes before the data capture scan sequence was initiated. A repeat scan was to be initiated a further two minutes later. The recommendation for the settling time was reached after exploratory tests at NASA showed stable operation would be reached within the five minutes.

Further investigations both at RAE, an altitude test facility, and NRCC, a ground-level test facility, confirmed that five minutes settling time was sufficient to enable the engine to reach stable thermodynamic conditions prior to a data scan being initiated.

In any test of a new type of engine in a test facility, a period should be set aside to investigate thermodynamic settling time in the test programme at the earliest opportunity so that when steady-state performance measurements are being collected sufficient time can be left to enable thermodynamic stabilization to have taken place.

#### 2.7 An enhanced method of presenting performance differences

It has been shown earlier that the standard performance graphs for the inter-facility comparisons make it difficult for the reader to distinguish the results for each individual test site. This was because the 'y' scale had to cover such a large range to encompass the range of measurements that individual differences were not large enough for the eye to see. The presentation could be improved by enlarging the 'y' scale such that differences are magnified.

##### 2.7.1 Enlarging the 'y' scale

Fig 14 shows a typical selected UETP graphical presentation of FNRD versus P702 at an inlet pressure of 51.7 kPa, an inlet temperature of 288 K and a ram ratio of 1:30. It is difficult to detect the differences in performance of some test sites in this presentation. Only in the case of CEPr, where the difference is 5 percent, is it apparent. The technique of enlarging the 'y' scale consists of constructing a datum line so that it lies a little below all the actual results. In this case the datum line has been chosen to be:-

$$y = 12.804x - 11.850$$

The difference of every measured point from the datum line,  $\Delta FNRD$ , is calculated and these values re-plotted, see Fig 15. It is now possible to see all the detailed features which were not apparent in Fig 14.

Separate polynomial curves can now be fitted to the data from each facility. In the case of CEPr, a curve of degree 3 was selected, by statistical significance tests, as the best fit. For the other facilities, curves of degree 2 were found to be appropriate.

The range of  $\Delta FNRD$  between facilities is now shown to be 5.1 percent of FNRD or 0.70 kW. This is slightly different from the 5.4 percent originally quoted in the UETP report, probably due to alternative curve fitting (ie the cubic chosen here for the CEPr result).

Values of random error limit of curve fit (RELCF) have also been calculated for each curve fit and give an indication of the scatter of the results about the curve that has been fitted. More will be said about RELCF in the lecture on statistical techniques. The scatter of points about the fitted curves gives a guide to the precision errors for each test facility, typically very small. The differences between the fitted curves give an indication of the bias errors between test sites which are much larger than the precision errors.

In conclusion, where comparisons are to be made between test results which are expected to give differences which are only a small percentage of the overall range of measurement, then it is recommended that not only should the full graphical presentation be shown, but also the enlarged 'y' scale method should be adopted. By presenting both displays, the shapes of the overall curves can be interrogated and the differences accurately identified.

#### 2.8 Examples of observed anomalies

##### 2.8.1 The measurement of P7 and T7 at CEPr

A detailed examination of the main altitude results reveals the observed anomaly that the CEPr data for FNRD versus P702 at all test conditions gave higher curves when compared with the other three facilities, AEDC, NASA and RAE(P). The differences between the CEPr data and the data obtained at the other facilities is quite marked, for example see Fig 16. However, the plots of T702 versus P702 do not show the same large differences between CEPr and other facility data.

In section 2.6.6 it was shown that the P7 static pressure measurement was a rugged measurement and insensitive to changes in nozzle hardware geometry, rotation, etc. Using this measurement, a total pressure can be calculated assuming a jet pipe area and a value for gamma, the ratio of specific heats. This process was applied to all the altitude facility data for P87 to calculate a P7CALC at all ten test conditions. A difference analysis was then carried out using the principles outlined in section 2.7. Plots were produced of P7 measured versus P7CALC for the data from all four facilities and a straight line fitted to this data. Percentage difference graphs were then plotted for the difference of each point from the straight line plotted against the P7CALC value. This analysis enlarged the 'y' scale and highlighted the difference in measurements between each facility for P7. An example of these plots can be seen in Fig 17, where the data for each facility are plotted with a different symbol and Fig 17A is for Test Condition 4 and Fig 17B is for Test Condition 9.

In this analysis the P7 measured values for CEPr were consistently below those for the other test sites. At all ten test conditions P7 differences between RAE(P) and AEDC were never greater than approximately 0.5 percent. In six out of ten conditions NASA P7 also agreed well with RAE(P) and AEDC never being more than 1 percent different. At Test Condition 3, no NASA data were available, leaving three Test Conditions, 5, 6 and 10 where large differences occurred, greater than 3 percent. However, NASA identified these test conditions as those where tailpipe rotation was present and P7 measured has already been shown to be affected by this change in geometry (see section 2.6.6). Therefore, the large observed differences in P7 at these three test conditions are not unexpected. The large differences in P7 between the CEPr data and other test facilities must therefore be due to either a mis-aligned tailpipe assembly or some other bias in the pressure measurements collected from the rake assembly. It is therefore recommended that the results of FNRD versus P7Q2 for CEPr be discounted from the facility comparison.

If the T7Q2 versus P7Q2 results are now examined it will be found that similar differences are found in the CEPr data when compared with the other facilities. However, the differences in these plots are not always consistent with those of the FNRD versus P7Q2 figures. Flow distortions due to wakes from turbine struts are not so dominant in creating total temperature distortion and therefore this result is probably not unusual. Nevertheless, since CEPr P7 data has already been shown to be unsatisfactory it must therefore be recommended that the T7Q2 plots against P7Q2 should also be disregarded.

#### 2.8.2 The Turkey sea-level test bed results

The ground-level test facility comparisons showed the Turkey sea-level test bed (TUAF) results, although having approximately the same curve slope as the other three test facilities, departed rather more from the mean than expected, for example see Fig 18. The most probable reason for this departure is due to a lack of empirical corrections for this type of engine in the TUAF facility. The TUAF test stand was designed for pre and post engine overhaul testing of those engines in the Turkish Airforce inventory. The J57-19 engine is not one of these engines and therefore cell correction factors are not available. In addition, manual recording of data at this facility increased both the measurement bias and precision uncertainties. The TUAF published results for the UETP are therefore considered unrepresentative for their particular test stand. In view of this the, TUAF data have not been included when calculating the percentage spreads between facilities.

#### 2.8.3 The NASA results for the ground-level/altitude facility comparison

In the altitude/ground-level test site comparisons, with the exception of NASA, all the altitude facility data related to an inlet temperature of 288 K. Because Test Condition 3 for engine 607594 was omitted by NASA due to a restricted test window, Test Condition 4 (T1 = 308 K) was substituted instead. The uncertain magnitude of the effect of inlet temperature change on the levels of performance parameters in the comparison meant that although the NASA curves are shown on the figures, their data have been excluded from the calculation of spreads at the mid-thrust point.

### 3 CONCLUDING REMARKS

This Paper has provided an insight into the various methods considered for the process of test facility comparisons during the UETP. It must be emphasised that this Paper must be considered in conjunction with the main UETP report, AGARD AR 248 in which a comprehensive picture of all aspects is provided. The Lecture Series will now continue with detailed considerations of the results obtained from the testing and the statistical techniques applied to the results. It should be noted that this unique exercise provided the first opportunity for all the test sites to determine the actual bias in their measurements. The importance of this event is that it enabled the estimates of bias, which could previously only be based on subjective judgements, to be compared with reality. In fact, as a later lecture will show, the agreement was good which gives confidence in the use of these subjective methods for different engines or when major changes to facilities are made.

### 4 REFERENCES

1. Ashwood, P.F., 'The Uniform Engine Test Programme. Report of the Propulsion and Energetics Panel Working Group 15. AGARD AR 248, February 1990.
2. Mitchell, J.G., 'Uniform Test Engine Testing Programme. General Test Plan, January 1983. Revised June 1983.
3. Algun, F., Bird, J.W., Rudnitski, D.M., 'The Effect of Inlet Pressure on Gas Turbine Engine Performance. NRCC Report CTR-ENG-003, August 1985.

TABLE 1

UETP - Percent  $\Delta$  SFCRD between cubic and quadratic curve fitting for RAE(P) data

UETP Test Cond.	Power Level		
	Low $\Delta$ SFCRD %	Medium $\Delta$ SFCRD %	High $\Delta$ SFCRD %
1	-0.05	0	+0.05
2	+0.05	0	-0.05
3	+0.05	0	0
4	+0.05	0	-0.05
5	+0.11	+0.08	-0.15
6	+0.16	+0.07	-0.21
7	+0.16	0	-0.17
8	+0.10	+0.13	-0.13
9	+0.26	+0.09	-0.27
10	+0.19	-0.05	-0.23

$$\Delta \text{ SFCRD} = \frac{\text{Quadratic} - \text{Cubic}}{\text{Quadratic}} \% \text{ Percent}$$

Table 2  
Altitude facility comparison (altitude conditions) (NASA\*, AEDC, CEPr, RAE(P))

Engine Parameter (Independent Variable)	Overall percentage spread at mid thrust (Without CEPr)	Data within two per cent band (per cent)	Percentage spread of estimated uncertainty	Comments
NLQNH (NHRD)	0.4 to 0.8 (0.04 to 0.6)	99	0.04 to 1.4	1 Smallest variation of any data set. 2 Cycle re-match with time accounts for 0.3 per cent variation.
T7Q2 (P7Q2)	0.6 to 2.0 (0.3 to 1.3)	98	0.6 to 1.2	1 Several temperature and pressure sensors replaced. 2 Possible variation of flow pattern in tailpipe. 3 Cycle re-match with time accounts for up to 0.3 per cent variation.
WA1RD (NLRD)	1.3 to 3.6 (1.3 to 2.9)	88	0.8 to 5.2	Sonic venturi appears to offer measurement accuracy benefits.
WFRD (NHRD)	3.8 to 5.5. (1.0 to 3.0)	63†	0.8 to 3.4	Volumetric positive displacement meter appears to offer measurement accuracy benefits.
FNRD (P7Q2)	3.4 to 5.4 (0.3 to 3.3)	69†	0.8 to 6.4	1 Some variation due to thermal non-equilibrium effects. 2 P7 measurement effects.
SFCRD (FNRD)	0.9 to 2.4 (0.9 to 2.4)	89	1.2 to 7.0	

\*No NASA data for Test Condition 3.

†CEPr results consistently displaced from other three facilities. If deleted, figures become 85 (WFRD) and 92 (FNRD).

Table 3  
Ground-level bed comparison (SLS conditions) (NRCC, CEPr, TUAF, AEDC\*)

Engine parameter (Independent Variable)	Overall percentage spread at mid-thrust (with TUAF)	Percentage spread of estimated uncertainty	Comments
NLONH (NHR)	0.5 (1.5)	0.2 to 1.6	Spread similar to that in altitude facilities.
T7Q2 (P7Q2)	1.1 (2.5)	0.9 to 1.8	Spread affected by failure of T7 thermocouples at NRCC.
WA1R (NLR)	1.9 (4.8)	0.6 to 1.5	NRCC airflow low by 1-1.5 per cent
WFR (NHR)	3.5 (8.0)	0.9 to 2.5	Spread reduced to 1.8 per cent when CEPr values removed
FNR (P7Q2)	0.7 (2.5)	1.0 to 2.3	
SFCR (FNR)	1.8 (3.5)	1.5 to 3.5	

\*Tests in AEDC altitude cell at standard sea-level static conditions included for comparison.

Table 4  
Ground level bed/altitude cell comparison. Sea-Level Static Conditions. Engine 607594

Engine parameter (Independent Variable)	Overall spread at mid-thrust (Percent)	Comments
NLONH (NHRD)	0.5	
T7Q2 (P7Q2)	2.3	Spread affected by failure of T7 thermocouples at NRCC
WA1R (NLRD)	2.5	NRCC airflow low by 1.0 - 1.5 percent.
WFR (NHR)	3.6	
FNR (P7Q2)	5.0	Spread reduced to 3.0 percent if CEPr (Alt) non-equilibrium values removed.
SFCR (FNR)	2.7	Max spread is between NRCC (GL) highest and AEDC (Alt) lowest

TABLE 5

Differences in engine inlet total pressure using  
different calculation methods.

NASA Condition 3 Test Point 746	Number of pressure values considered	Percentage contribution of the main rake to P2AV	Percentage contribution of the boundary layer rake to P2AV	Total area assigned to all probes ( Physical area 836.892 in )	Average Pressure Calculated [ kPa ]
Method 1 (GTP Baseline)	20 (main)	100 % (Simple arithmetic average)	-	Total Area	83.246
Method 2	20 (main)	100 %	-	837.720	83.246
Method 3	8 (main)	100 %	-	333.544 (40% of area)	84.048
Method 4	46 (main + boundary layer)	90 %	10 %	697.406	83.186
Method 5	58 (main + boundary layer)	67 %	33 %	837.672	83.206

Specimen Test Summary Sheet

UNIFORM ENGINE TESTING PROGRAM  
 LOCATION: RAE, PYESTOCK, ENGLAND FACILITY: CELL 3 RECORDED: 84-18- 2 11-49-56 POINT: 101  
 PROCESSED: 84-18- 8 13-55-55

SUMMARY OF TEST CONDITIONS

ALT 1041. M WAI 69.398 KG/S  
 RMI 0.3565 WAF 100.42 G/S  
 TAV 253.02 KPA FM 42.2478 KN  
 PCV 81.581 KPA NLPER 181.434 X  
 PCELL 81.581 KPA NHPR 95.882 X  
 M 81.4723 SFC 23.775 G/KN.S

STA	STATION AVERAGES			AIRFLOW (KG/S)			THRUST (KN)		
	T(K)	P (KPA)	PS (KPA)	WAI	WAIRO	WAV	FC	FCLS	FN
00	253.02	81.051	81.051	69.398	88.199	69.887	45.5869	45.5869	45.5869
2	253.02	82.291	73.549	78.248	8.39635	8.37238	55.057	55.057	55.057
13			251.527	71.369	1.88288	1.88288	42.2478	42.2478	42.2478
3	504.07	1069.06		72.341			47.3883	47.3883	47.3883
31			1021.27				3.2599	3.2599	3.2599
5	834.02	230.620							
7	828.66	220.372	200.156						
04			81.231						
05			81.051						
08			80.931						

ENGINE PRES.  
 & TEMP. RATIOS  
 P502 2.0826  
 T502 3.2891  
 P70AMB 1.0153  
 P70AMB 2.7189  
 T702 2.6788  
 T702 3.2648

COMPRESSOR  
 PERFORMANCE  
 P302 13.0011  
 T302 2.3043  
 EC 0.92454

FIG.1 TYPICAL TABULATED DATA SHEET

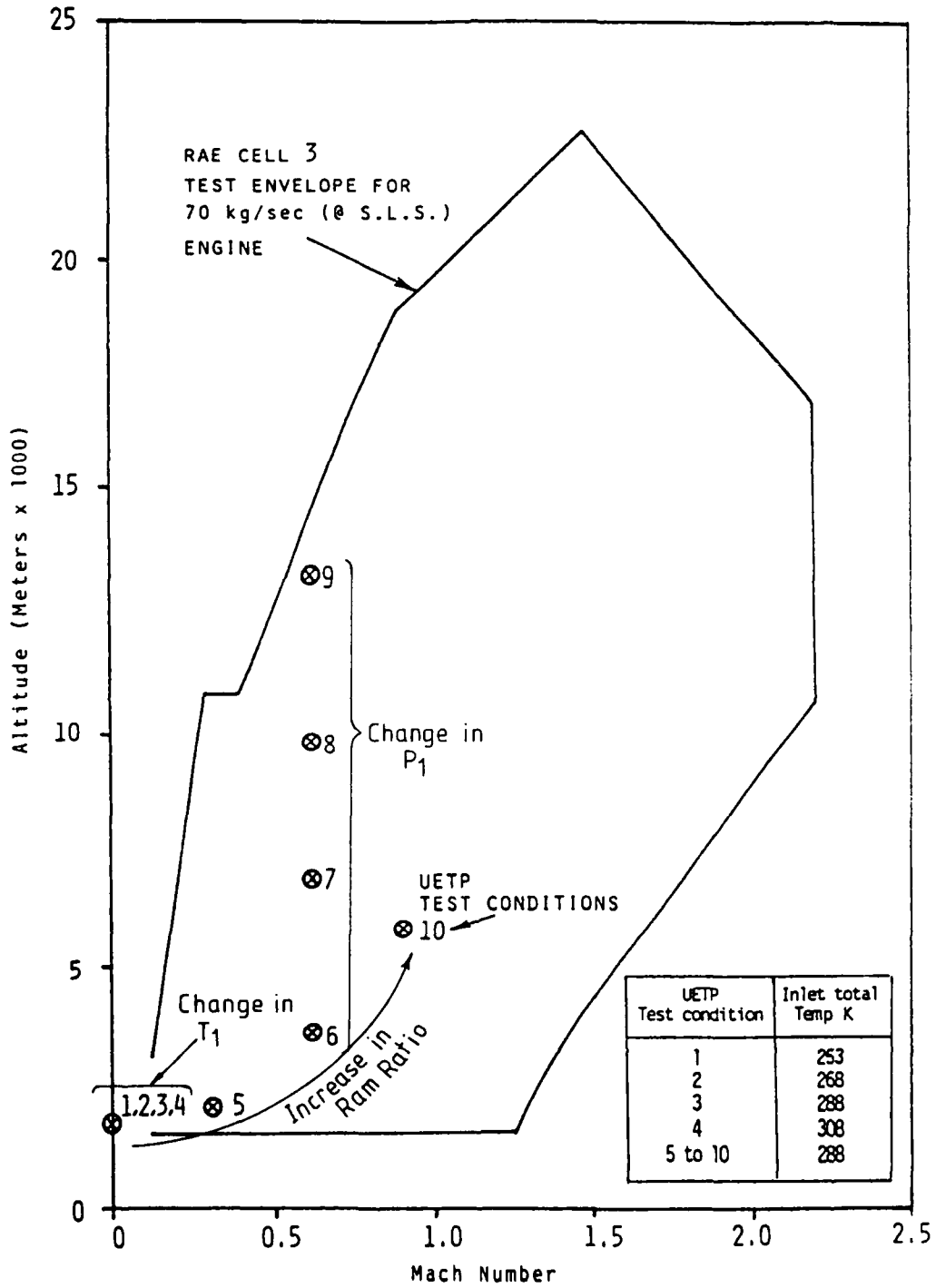


FIG 2 TEST ENVELOPE FOR RAE (P) CELL 3

UETP TEST CHRONOLOGY

FACILITY Engine Serial No.	ALTITUDE		SEA LEVEL	
	607594	615037	607594	615037
NASA (1)	✓	✓		
AEDC	✓	✓		
NRCC (1)			✓	✓
CEPr	✓		✓	✓
RAE(P)	✓ *			
TUAF				✓
RAE(P)	✓			
NASA (2)	✓	✓		
NRCC (2)			✓	✓
NAPC				✓

## Notes:-

1. \* Test aborted

2. Numbers in brackets denote FIRST and SECOND Test Series at same site.

FIG. 3 GEOGRAPHICAL AND CHRONOLOGICAL ORDER OF ENGINE TESTS

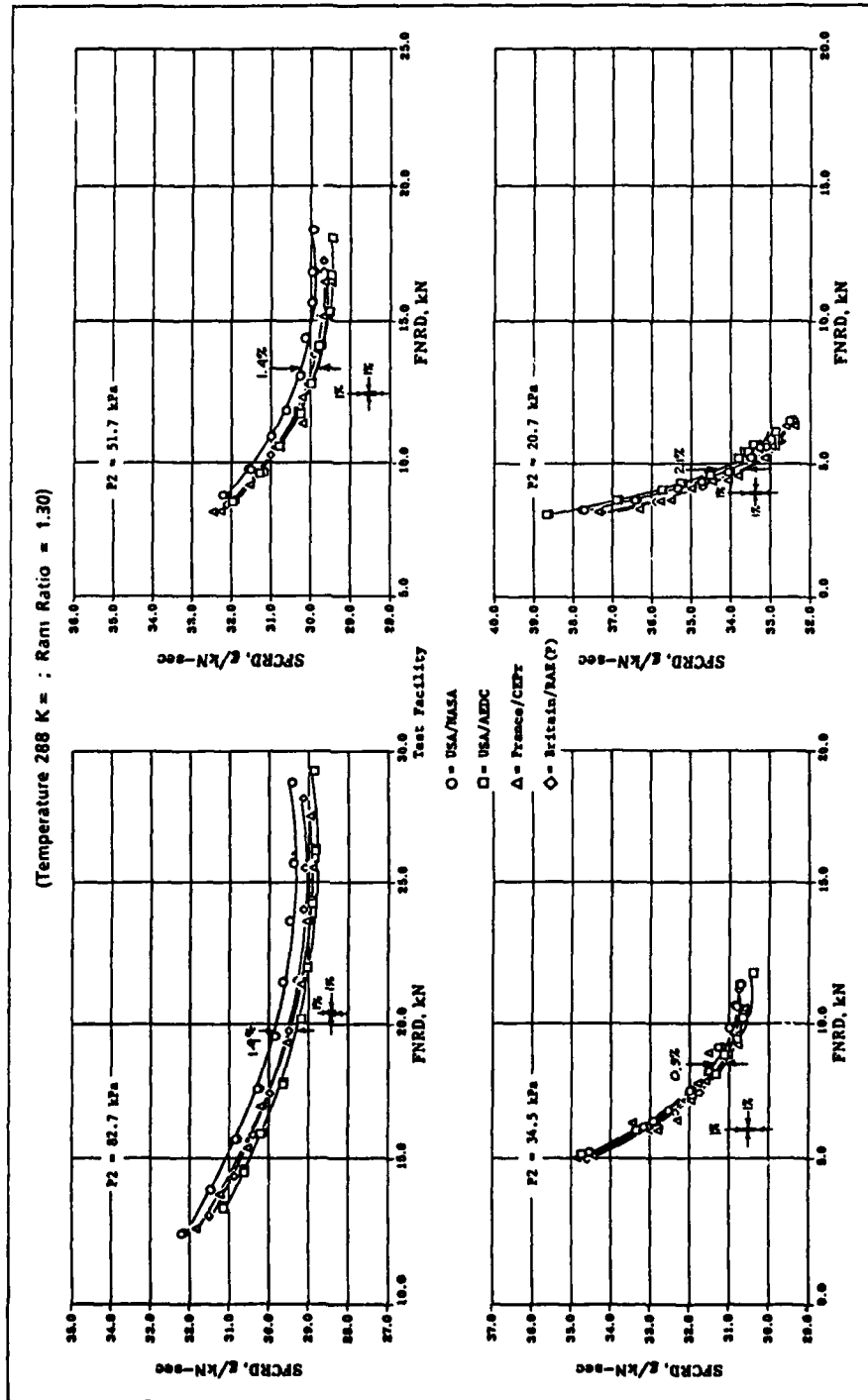


FIG. 4 TYPICAL GRAPHICAL DATA PRESENTATION

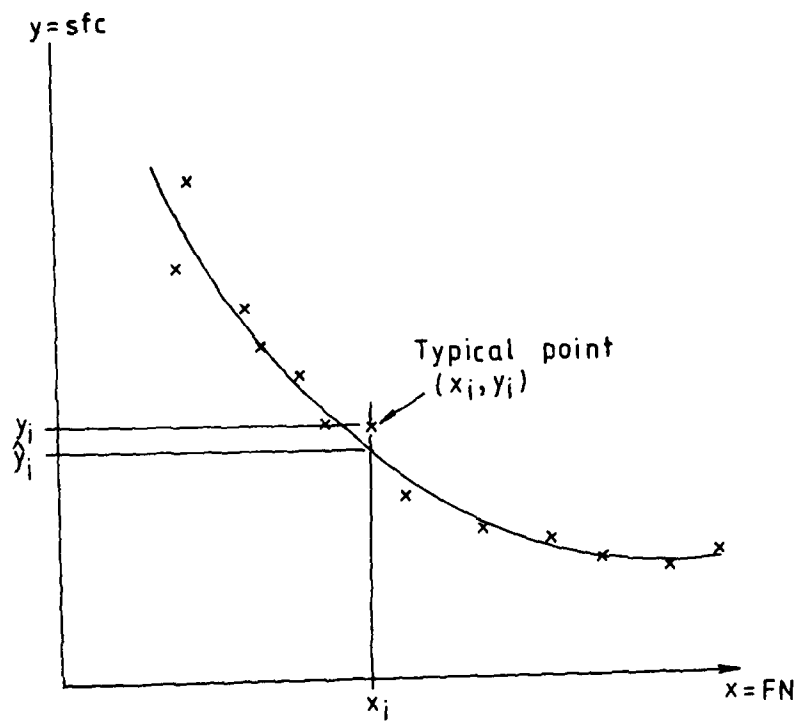


FIG.5 TYPICAL ENGINE PERFORMANCE CURVE

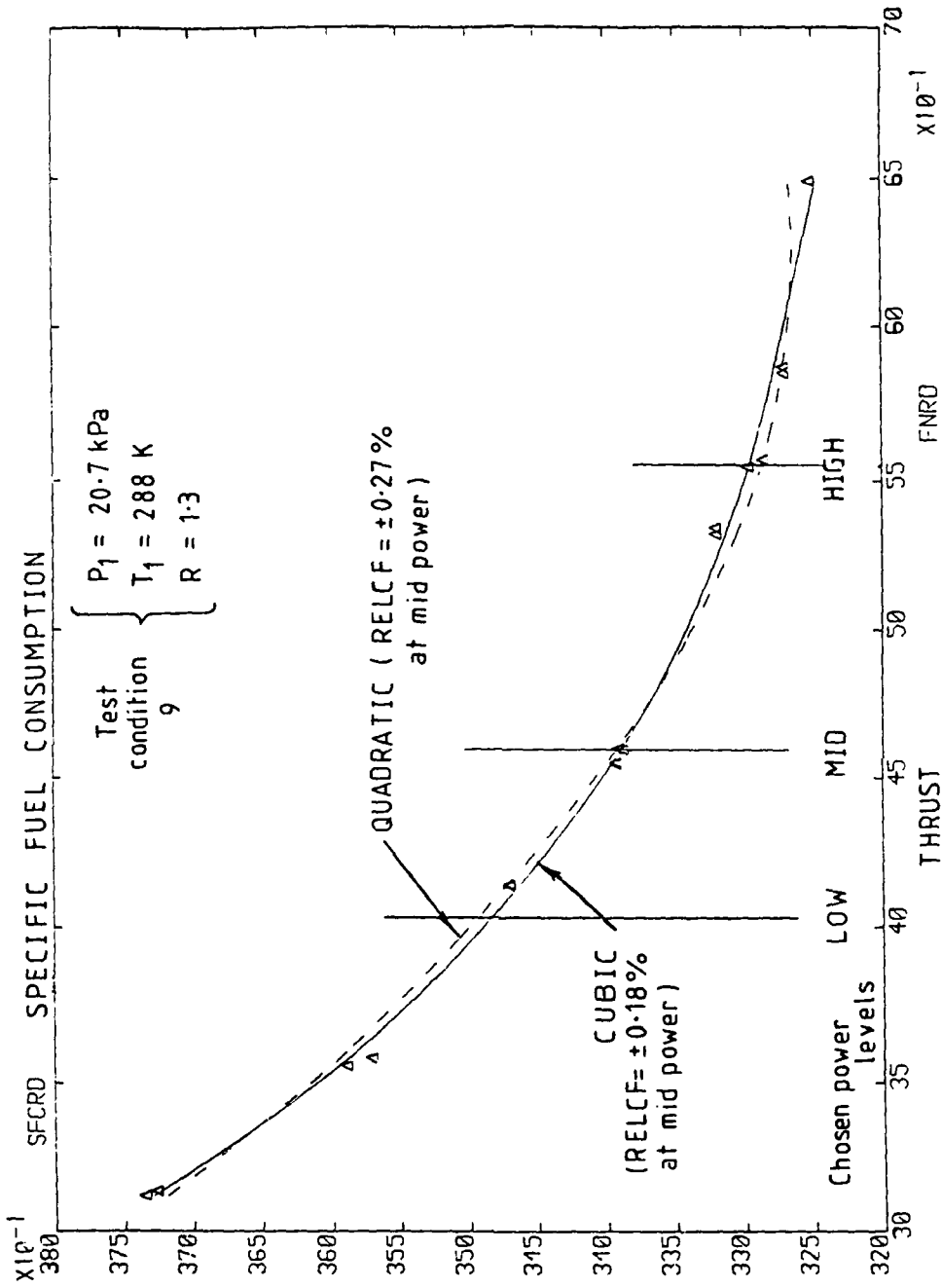
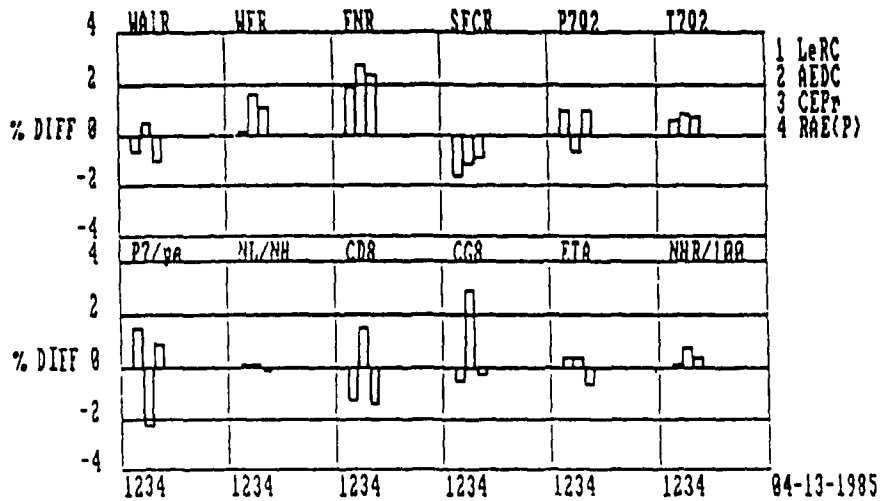


FIG. 6

A COMPARISON OF CUBIC AND QUADRATIC CURVE FITS AT UETP CONDITION 9 FOR THE R.A.E. DATA

UETP ALTITUDE FACILITY COMPARISON  
 Eng- P-687594 Const. Parameter Ps7/P2= 1.735 Ref = LeRC  
 TC=6(82.7-1.3-288)



UETP ALTITUDE FACILITY COMPARISON  
 Eng- P-687594 Const. Parameter Ps7/P2= 1.735 Ref = LeRC  
 TC=9(20.7-1.3-288)

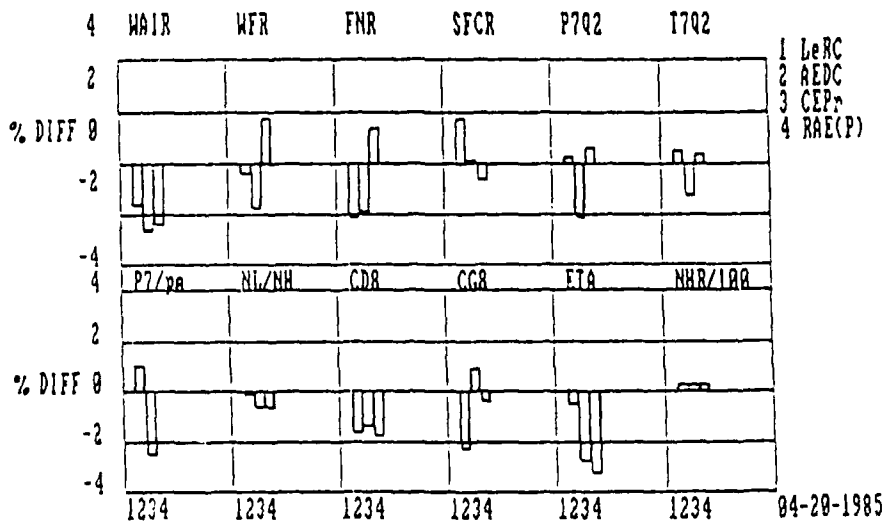


FIG. 7 EXAMPLE OF PROPOSED BARGRAPH PRESENTATION

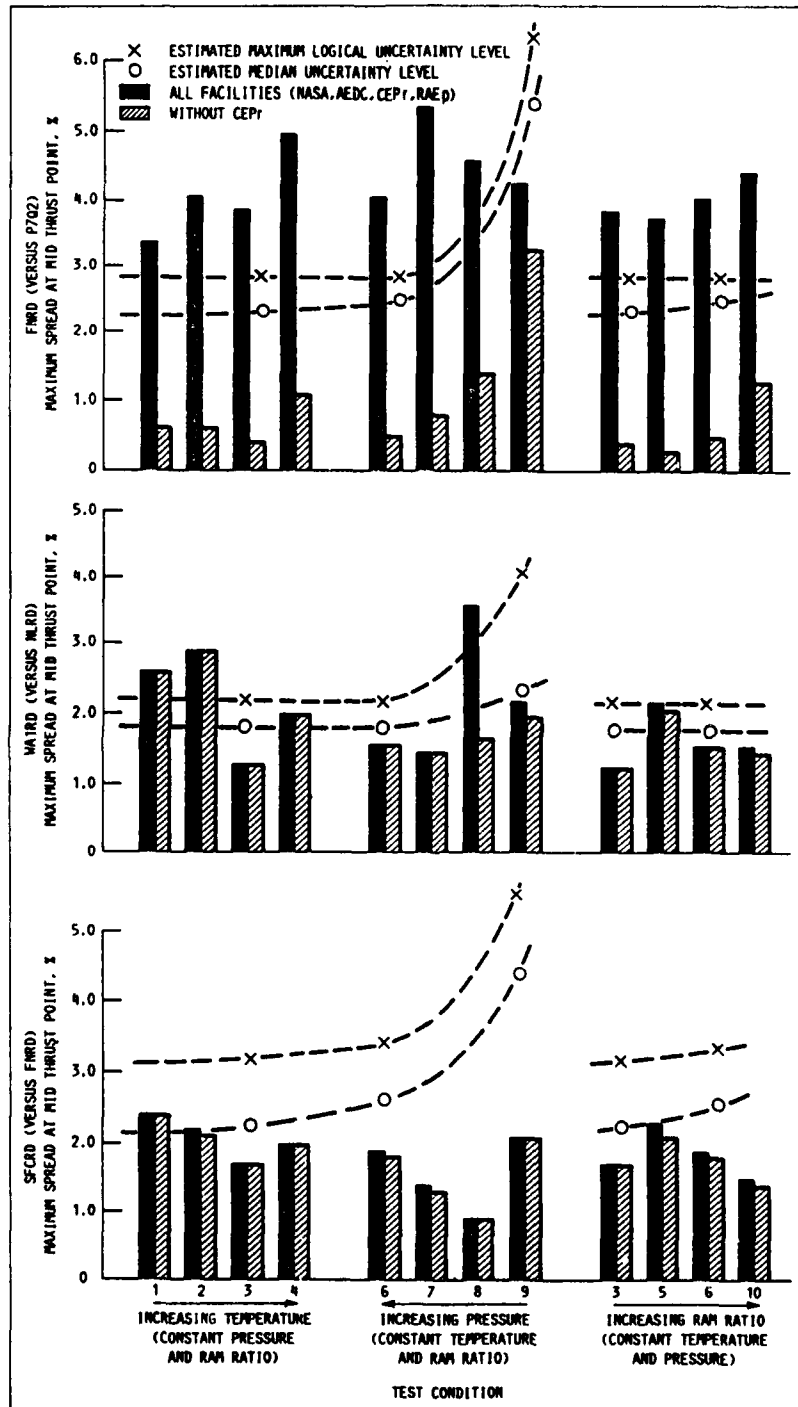


Fig. 8 Spreads in net thrust, airflow, and SFC — altitude facilities

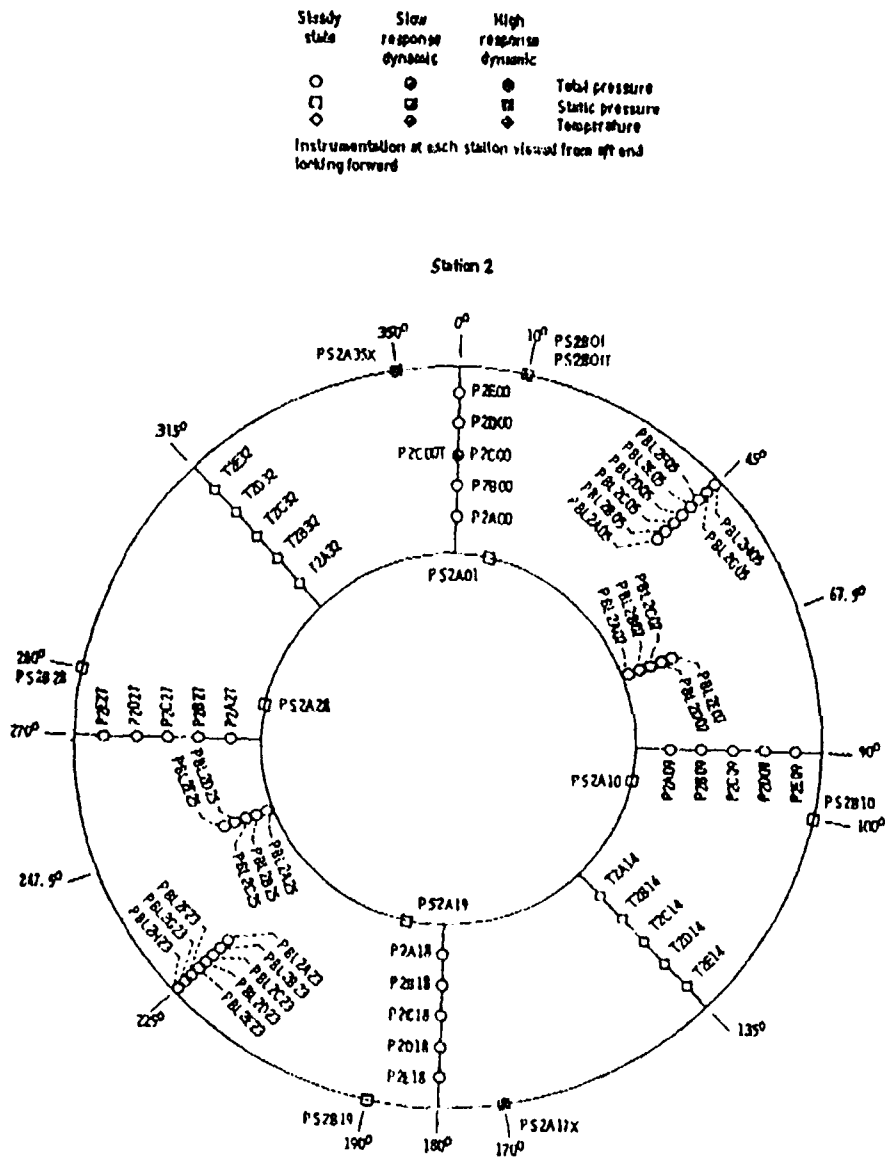


Figure 9: Circumferential Location of Probes

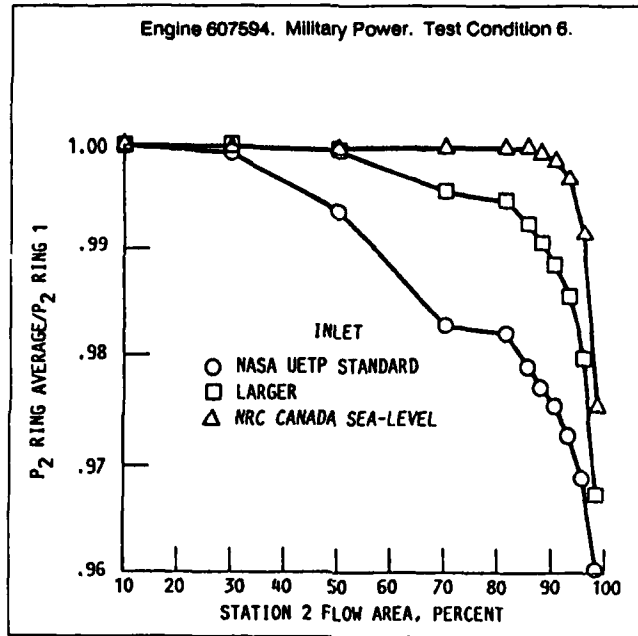


Fig.10 Effect of inlet duct on station 2 total pressure profile

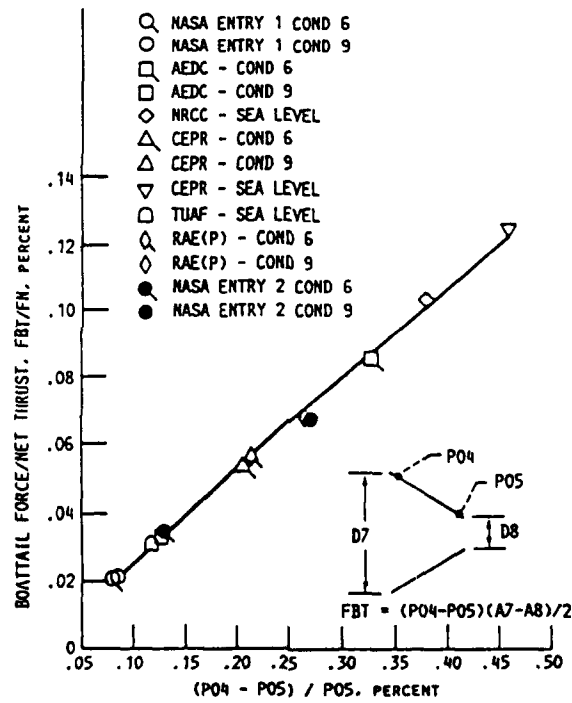


FIG.11 BOATTAIL FORCE

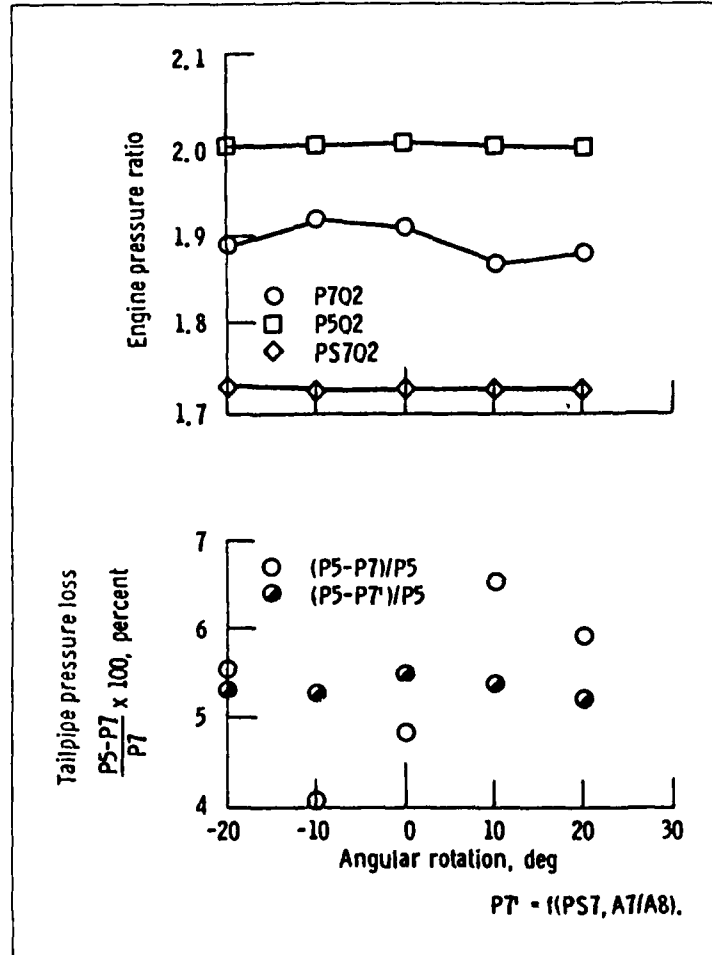


Fig.12 Total and static pressure variation with tailpipe rotation (TC6-607594 NHR = 8900 rev/min)

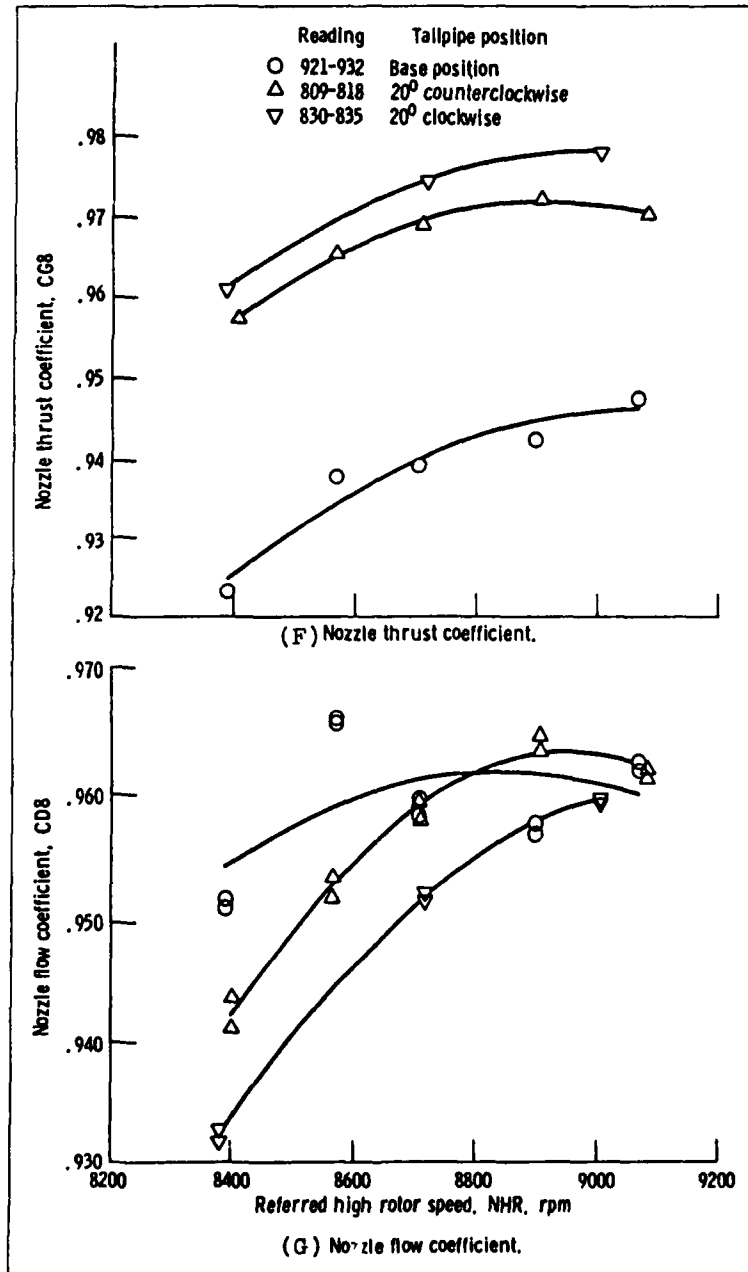


Fig.13 Effect of tailpipe rotation on thrust and flow (TC9-607594)

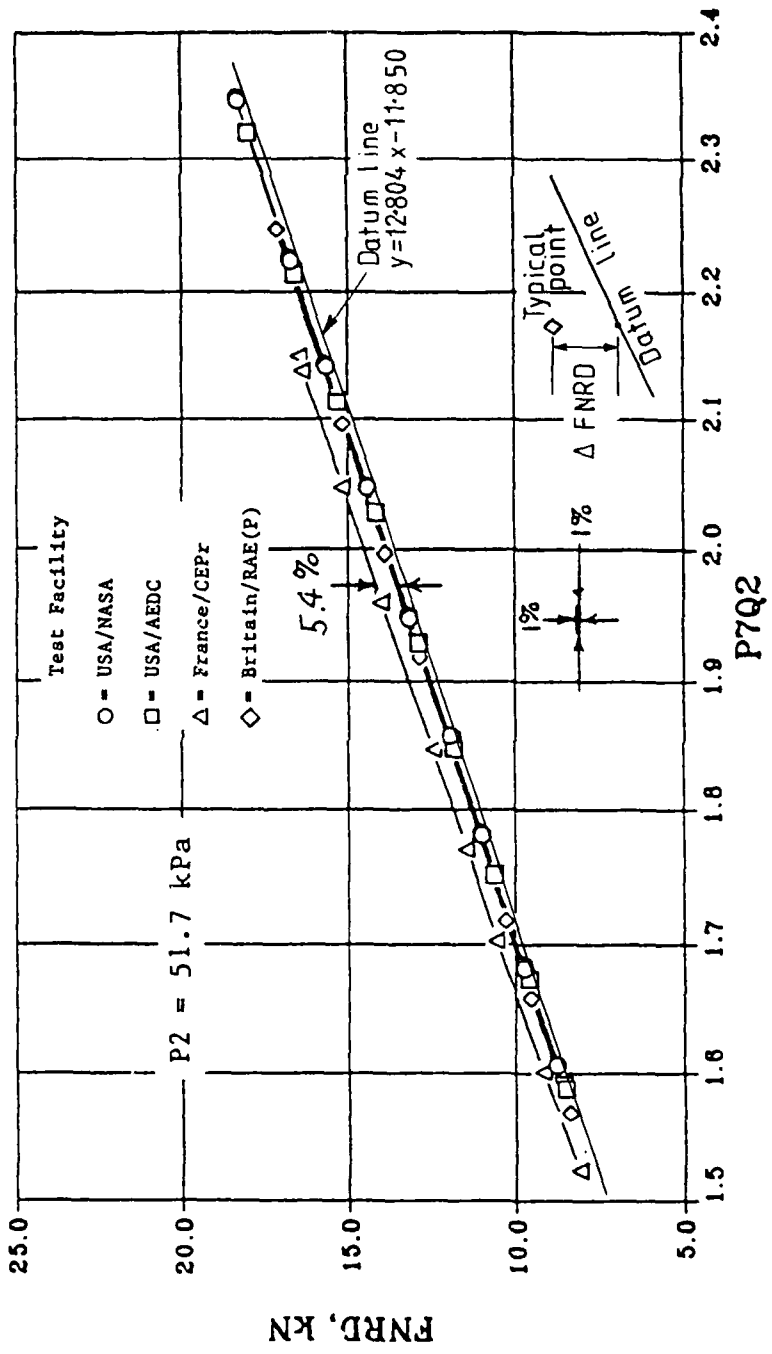


FIG.14 EXAMPLE OF STANDARD UETP GRAPHICAL PRESENTATION

Facility	Degree of curve	%
○ NASA	2	0.15
□ AEDC	2	0.18
△ CEPr	3	0.49
◇ RAE(P)	2	0.12

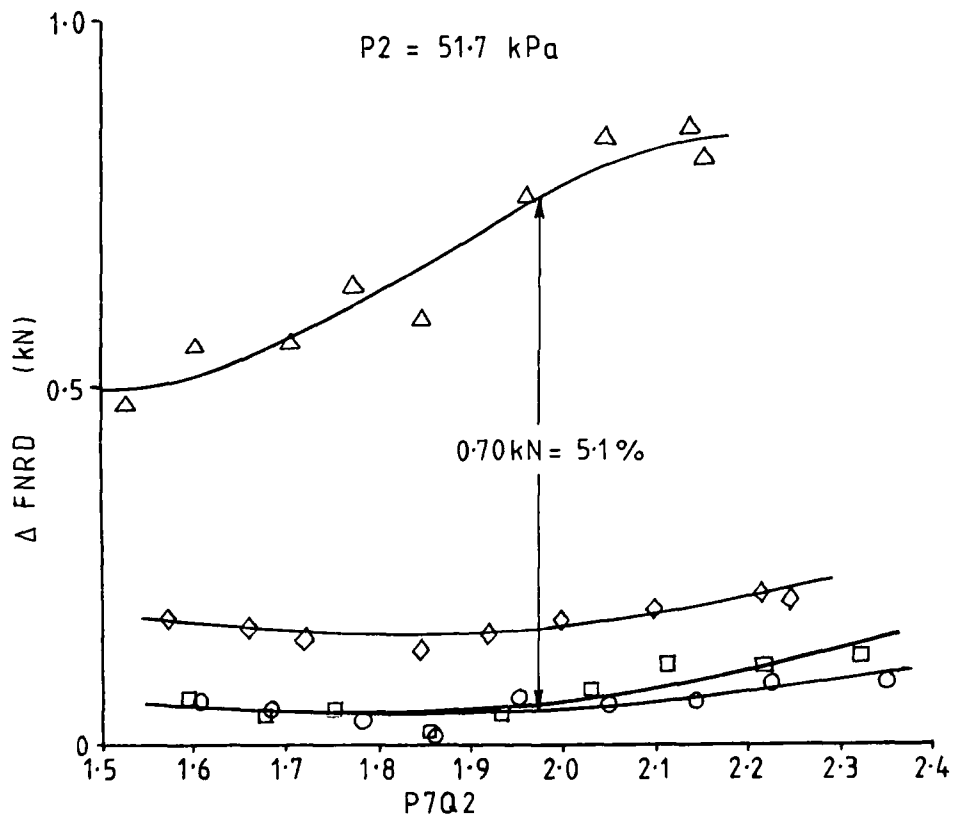


FIG.15 EXAMPLE OF REVISED GRAPHICAL  
PRESENTATION

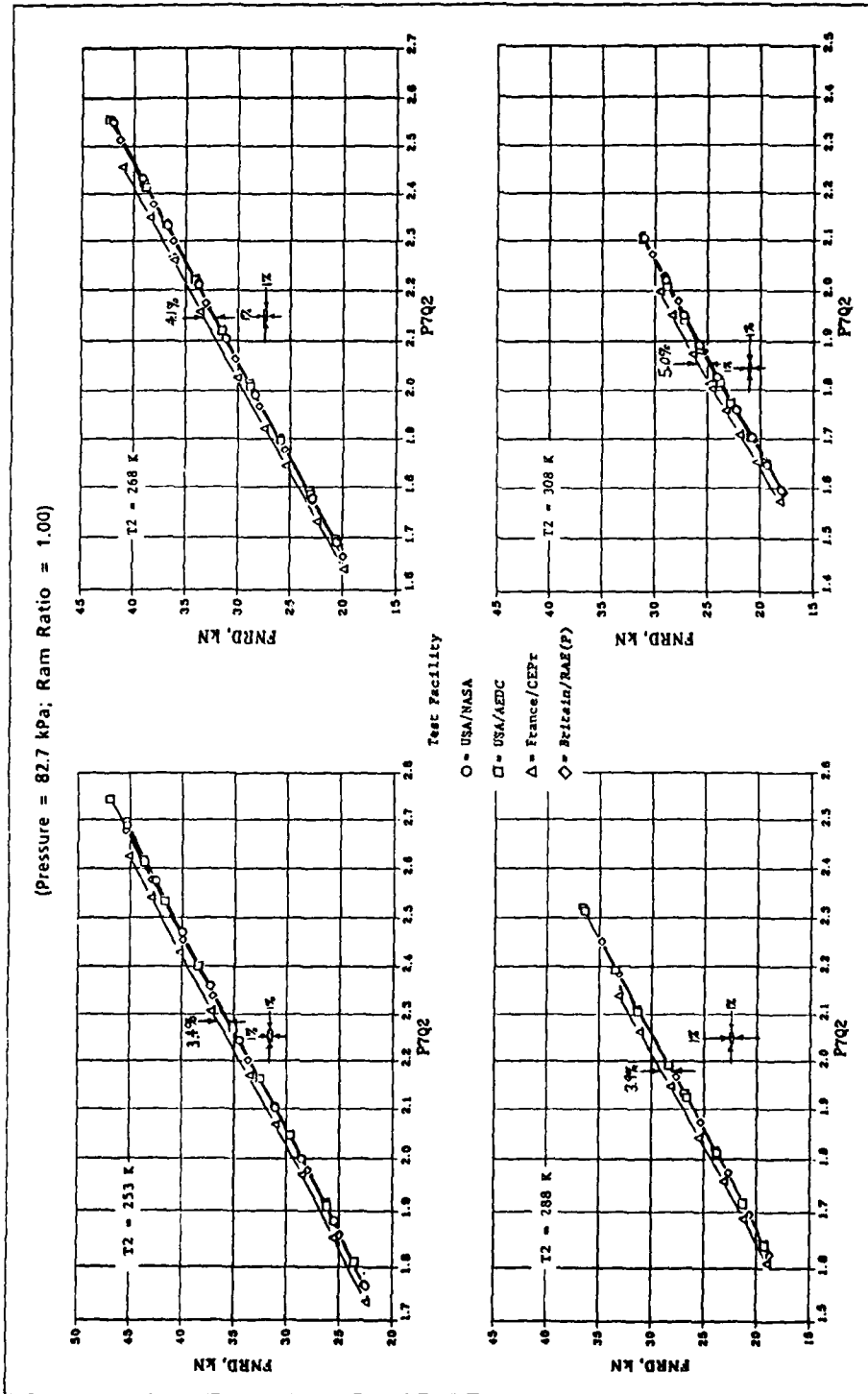


Fig. 16 Altitude facility net thrust comparison with variable inlet temperature (engine 607954)

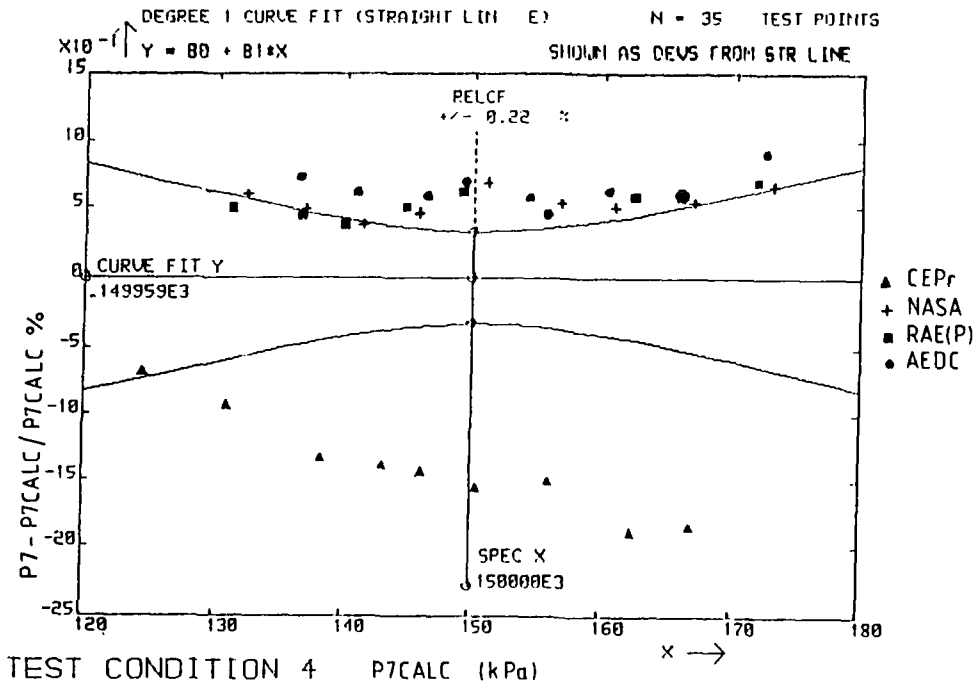


FIG.17A

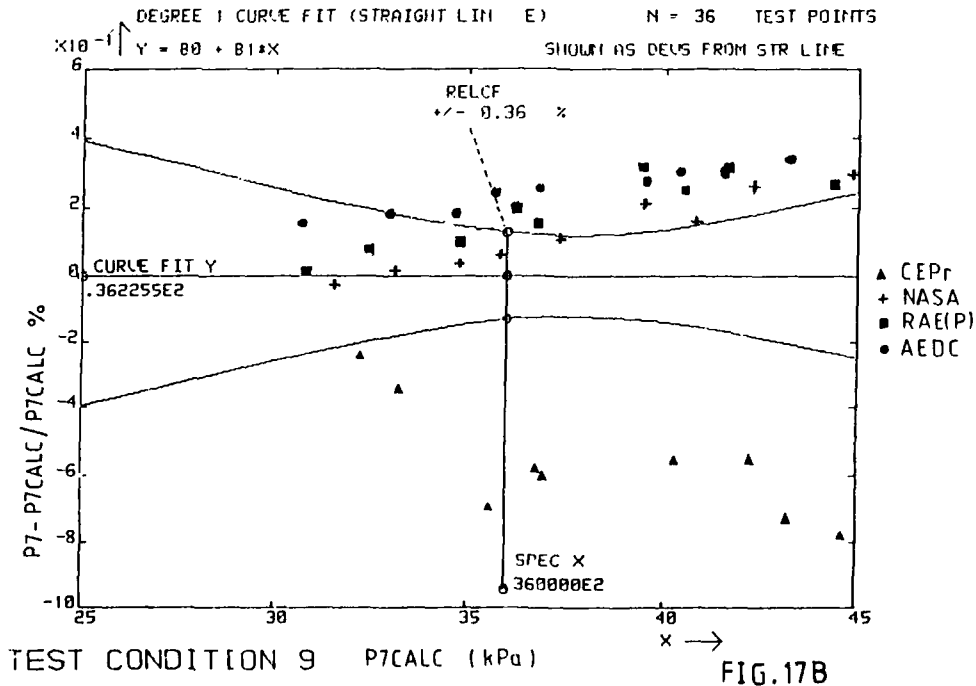


FIG.17B

FIG.17 P7 PRESSURE MEASUREMENT ANALYSIS

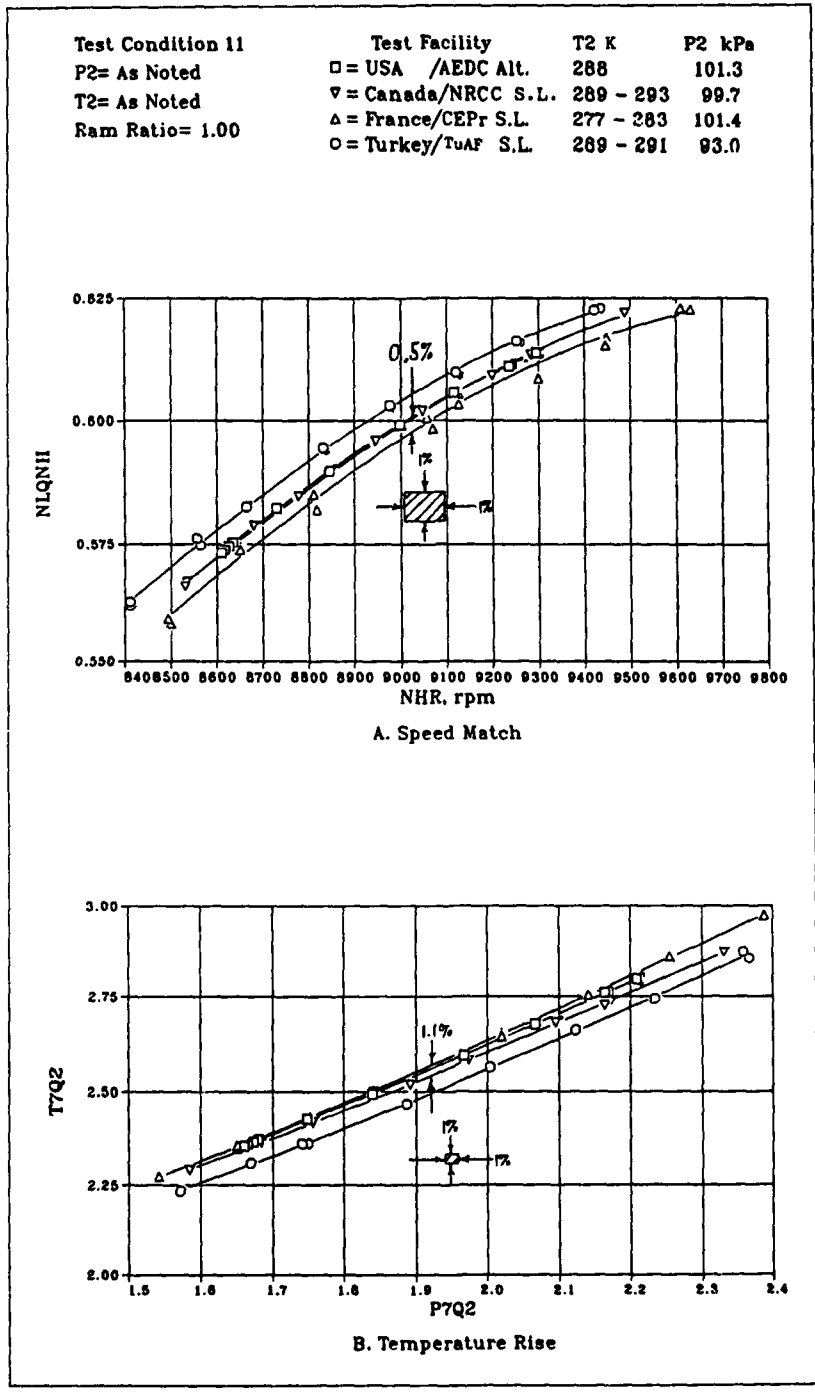


Fig. 18 Ground level test facility comparison (engine 615037)

## INVESTIGATION OF FACTORS AFFECTING DATA COMPARISON

by  
 D.M. Rudnitski  
 Section Head  
 Engine Laboratory  
 National Research Council Canada  
 Ottawa, Ont. K1A 0R6  
 CANADA

### SUMMARY

In evaluating engine performance in test facilities, ground-level test beds or altitude tanks, facility influences on performance measurements must be quantified. Of the three main engine parameters, only fuel flow measurement is facility type independent, whereas thrust and airflow calculation procedures tend to be facility type specific. Data consistency checks for thrust and airflow using the method of flow coefficient, has been demonstrated to be quite a useful tool for inter-facility comparisons, whereas for fuel flow, sensor redundancy is most common.

The possibility of engine deterioration occurring during an extended test program required close monitoring of basic engine parameters using facility independent sensors. Although some long-term changes in engine behaviour did occur, the magnitude of these shifts did not warrant data correction.

### LIST OF SYMBOLS

A8	Area at Exhaust Nozzle Inlet
AEDC	Arnold Engineering Development Center
AEDC	Arnold Engineering Development Centre
CDS	Flow Coefficient
CEPr	Centre d'Essais des Propulseurs
CG8	Gross Thrust Coefficient
FG	Gross Thrust
GTP	General Test Plan
LHV	Lower Heating Value
NASA	National Aeronautics and Space Administration
NHR	High Rotor Speed
NLQNH	Ratio of Rotor Speeds
NLR	Low Rotor Speed
NRCC	National Research Council of Canada
P2AV	Average Pressure at Compressor Inlet Plane
P3	Compressor Discharge Pressure
P7	Exhaust Nozzle Inlet Total Pressure
P7QAMB	Nozzle Pressure Ratio
PAMB	Static Pressure at Exhaust Nozzle Plane
PS7	Exhaust Nozzle Inlet Static Pressure
RAE(P)	Royal Aerospace Establishment Pyestock
RAMSPC	Specified Ram Ratio
SFC	Specific Fuel Consumption
T3	Compressor Discharge Temperature
T4	Combustor Exit Temperature
T7	Exhaust Nozzle Inlet Total Temperature
TUAF	Turkish Air Force Supply and Maintenance Centre
UETP	Uniform Engine Test Program
WA1	Facility Measured Engine Airflow
WA2	Reference Engine Airflow
WF	Facility Fuel Flow
WFE	Engine Reference Fuel Flow

### 1 INTRODUCTION

The previous lectures have provided some appreciation of the complexity of the UETP, as not only was this project conducted over a period of several years, but the variety of test installations and lack of environmental control in certain facilities made direct data comparison more challenging than originally envisaged. This lecture will deal with a number of factors affecting data comparison, pointing out the differences between altitude and ground-level test beds regarding thrust and airflow measurement. Another consideration was that the ambient corrections for temperature, pressure, and to a lesser extent humidity, using the data reduction equations included in the General Test Plan (GTP), (Ref. 1), were valid over a limited excursion range, introducing additional deviations in the calculated performance parameters. These corrections are of greater significance for ground-level test beds, which have no capability for environmental control.

The three main performance parameters, airflow, thrust and fuel flow were critically evaluated using a system of cross checks and consistency checks to quantify any facility or interfacility bias. In cases where the values exceeded declared uncertainty limits, reasons for

variations were sought. Of course, in an engine test program involving considerable engine running time, the question of engine performance retention must be addressed. There was considerable debate on whether there was any engine deterioration, and if so, how could it be accounted for in the data comparison.

In this lecture, the following subject areas will be discussed, with typical examples excerpted from Ref. 2 as appropriate.

1. Facility test configuration, altitude vs. ground-level
2. Thrust definition, altitude vs. ground-level
3. Ambient corrections
4. Measurement consistency checks for airflow, thrust and fuel flow
5. Engine rematching, with concentration on performance retention

A number of facility effects were already covered in the previous lecture, but it is worth briefly recapping some of the more significant ones.

## 2 FACILITY EFFECTS

### 2.1 Test Configurations

Prior to the discussion of engine performance measurements, it is necessary to examine the test configuration and the requirements imposed by the basic physics of the engine and engine operating environment.

There were two classes of test facilities in the UETP, the ground-level test bed, and the direct-connect or altitude test configuration. For a ground-level test bed, the engine directly takes in atmospheric air, and exhausts directly back into the atmosphere. The direct-connect configuration derives its name from the fact that the engine inlet is directly connected to a controlled air supply system, and the exhaust exits into a separately controlled environment. The essential features of the different types of turbine engine test configurations are shown in Figure 1 (Ref. 3 and 4).

#### 2.1.1 Ground-level Test Bed

The ground-level test beds differed from one another in two major respects: the size of the cell cross section and the layout of the flow path. The outdoor test stand at NAPC represented one extreme, the engine being in a free field environment with no inlet silencing splitters or exhaust defuser. The other beds were enclosed cells with the inlet arranged either horizontally (NRCC and CEP) or vertically (TUAF) and with the exhaust discharging vertically upwards. In ground-level test cells, the diffuser size and placement have a marked effect on the test cell secondary flow rates and windage drag on the engine installation. It is preferable to use an augmentor tube which can be moved relative to the engine exhaust plane, and a variety of collector inserts to modify the flow area. The engine nozzle/collector diameter ratio, the entrance configuration and spacing between the engine nozzle and collector are key design elements in determining the entrained secondary airflow and the static pressure field around the nozzle. In general, the nozzle/collector diameter ratio determines the secondary airflow, and hence inlet momentum and windage drag, while the nozzle/collector spacing strongly influences the local static pressure field around the nozzle. Of course, there is an interaction between these two effects, thus each installation should be specifically tuned. Detailed descriptions of the individual beds are given in Appendix II A of Ref. 2.

#### 2.1.2 Altitude Test Cells

The altitude cells were all of the same basic, direct connect type; the main differences were the size of the cell, the design of the joint between the fixed inlet ducting and the moveable portion attached to the thrust frame, the method of measuring the inlet airflow, and the geometry of the exhaust collector and its positioning in relation to the engine nozzle.

Although there are a number of hardware options available to implement each of the key functions in a direct-connect test configuration, it is nevertheless essential that each of the following functions be successfully implemented.

First, the flow of air through the engine must be known very accurately. A venturi or an inlet bellmouth represent two of the devices used to accomplish this measurement. After the flow of working fluid is carefully measured, it may be necessary to condition the flow profiles of the air entering the engine.

If thrust is to be determined from the sum of all body forces acting through the engine mounting trunnions, then a key element in the direct-connect test installation is the interface between the test cell structural ground plane and the metered plane on the engine thrust stand. It is a challenging problem to provide an interface plane that is free of mechanical forces and, at the same time, has zero leakage for those cases where the airflow measurement system is located off the engine thrust measurement system. Perhaps the most essential element in the entire thrust measurement system is the thrust stand which supports the test engine during operation. The force measurement subsystem within the thrust stand provides a direct measurement of the forces applied to the thrust stand.

Finally, for control of the engine exit environment in enclosed test installations, it is necessary to utilize some type of exhaust diffuser to collect the engine exhaust gases and direct them away from the test cell. If adverse test cell flow recirculations are to be avoided in altitude test cells, it is necessary to match the exhaust diffuser to the test cell exhauster equipment and the test article mass flow. Test cell flow recirculations stem from the viscous mixing of the engine exhaust jet with the ambient air and the resulting flow impingement of the exhaust jet with the diffuser walls. Detailed descriptions of the individual cells are given in Appendix II B of Ref. 2.

### 2.1.3 Comparison of Installation Geometries

In view of the possible influence of the test installation on the performance of the engine - at the inlet by virtue of the effect on inlet total pressure profile, particularly in the boundary layer, and at the exhaust through the influence of static pressure gradients resulting from the entrained air - it was thought desirable to record the major features of each installation geometry.

The inlet and exhaust geometries of the ground-level beds are compared in Figure 2 and the geometries of the altitude cells in Figure 3. The main dimensions of the exhaust collectors are summarized in Table 1.

### 2.2 Gross Thrust Definition

Reference instrumentation was provided for all practicable measurements, with the stated purpose of setting test conditions, monitoring engine health and recording engine performance retention. Of the main performance parameters, two of the three, facility airflow and fuel flow, could be compared against the reference measurements, leaving thrust as a facility parameter only. Thrust, gross or net, is a derived parameter, made up of scale-force, pressure-area and inlet momentum terms. In general, the scale-force term is dominant, particularly for ground-level beds, however, at high Mach numbers achievable in altitude facilities the scale-force is only a small component.

Special attention was directed to the measurement of the total pressure and temperature at the compressor inlet (Station 2) and the static pressure at the nozzle outlet (Station 0.5) as these parameters have a critical influence on engine performance.

One of the difficulties in the UETP was in the definition of PAMB, and how this pressure differed in each installation type. In an outdoor facility, the engine operates in a uniform static pressure field; thus the pressure in the plane of the nozzle exit is the same as that surrounding the engine. For this situation, with still-air conditions, the measured thrust on the load cell is equal to the engine gross thrust. In an indoor facility, an exhaust collector is generally placed in close proximity to the nozzle exit, creating an ejector effect, thereby inducing secondary airflow through the test cell. This placement, combined with the secondary airflow entering the collector, locally modifies the static pressure field at the nozzle exit.

For this situation, the engine static pressure environment is different from that measured by the trailing edge static taps (Station 0.5), the value of which was defined as PAMB in the GTP. To overcome this difficulty, all pressure forces were referred to a plane upstream of the engine inlet, which when added to the scale force and momentum terms, yielded a value for gross thrust (Ref. 5). See Figure 4 for the defined control volume. Correction to standard day conditions in ground-level beds is then simply:

$$FGRC = FG/(P2AV/101.325)$$

rather than:

$$FGR = (FG/\delta) + (AS/\delta)(PAMB - P2AV)$$

as defined for ground-level test beds in the GTP.

Additionally, for ground-level facilities,  $FGRC = FNRC$ , i.e., *net thrust = gross thrust*.

Section 9 of Ref. 2 pointed out the inadequacy of the thrust equations when applied to an outdoor stand or a ground-level test bed.

Referring back to Figure 1C, in an altitude chamber the PAMB term is essentially cell pressure, PSO, as the cooling airflow is small enough to limit the variation in static pressure around the nozzle.

Since the data comparisons using thrust were based on the equations in the GTP, Ref. 1, there will be differences on the ground-level bed comparisons that are artificial. The magnitude of these differences will be dealt with in a later lecture.

### 2.3 Ambient Corrections

#### 2.3.1 Introduction

When setting up test conditions it is impossible to achieve the required values precisely, even in altitude facilities where a high degree of control can be exercised. On ground-level test beds no control is possible over inlet conditions and significant variations from the desired values have to be accepted, particularly with respect to inlet temperature.

For the UETP programme, the engine performance parameters obtained at the "as set" test conditions were corrected to the desired conditions using the conventional equations given in Appendix IV of Ref. 2. Similar equations were used when referring altitude test data to standard ground-level conditions.

In the course of detailed analysis of NRCC Second Entry (SE) tests which were run at conditions well removed from standard sea-level conditions, discrepancies were seen between fuel flow data referred to standard sea-level conditions using the GTP formulae, and those from tests run at or close to the standard conditions. Also, RAE(P) in their post-test data report, observed that fuel flows measured at RAE(P) did not relate using the normal reference method with change in engine inlet air temperature. See Figure 16.1 from Ref. 2 for an example.

As a result of the observed discrepancies in the UETP data adjustment parameters, a more detailed investigation was made of the relationships used to adjust data for a mismatch of inlet temperature from standard day conditions and engine ram pressure ratio effects.

#### 2.3.2 Analysis Methodology

The adjustment parameters used in the UETP to correct airflow, fuel flow and thrust for a mismatch in temperature and/or pressure are presented in the following equations which were obtained from Appendix IV of Ref. 2.

**Airflow**

$$WA1R = WA1\sqrt{W}/s$$

**Fuel Flow**

$$WFR = (WF/6/7)(LHV/42960)$$

**Thrust**

$$FGR = (FG/s) + (A8/s)[PAMB - (P2AV/RAMSPC)]$$

To evaluate the deviations in the UETP data comparisons which resulted from the use of the UETP referred equations, a comparison was made of adjusted data using output from the UETP equations and output from a J57 engine model simulation. The engine model simulation was compiled by AEDC using J57 component maps supplied by the US Air Force, Wright-Patterson AFB. The engine model was trimmed to the UETP engine using UETP Test Condition 3 data (92.7/1.0/288).

After validation of the J57 engine model simulation, output from the model was compared with the UETP inlet temperature and engine ram pressure ratio correction predictions and differences noted.

**2.3.3 Temperature Lapse Rate**

The variation of engine performance with inlet temperature is referred to as temperature lapse rate. The differences between the lapse rates that result from using the UETP correction factors and the J57 model simulation are presented in Figure 5. The comparisons were accomplished using low rotor speed settings that bracketed the range of interest for the UETP sea-level and near sea-level test data. Figure 5 also presents the ground-level facilities inlet temperature excursions.

Because of the ability of altitude test facilities to set inlet temperature within a few degrees, the imperfections in the UETP temperature referred equations have no impact on the UETP altitude facility data comparisons. Except for the NRCC (SE) data, the error in the ground-level facility data comparisons using the UETP referred equations is about 0.2 per cent.

**2.3.4 Ram Ratio Effects**

The UETP data adjustments for engine ram pressure ratio variations are basically correct for a choked exhaust nozzle; however, most of the UETP sea-level and near sea-level test data were obtained with an unchoked exhaust nozzle. The differences in engine performance as a result of using the UETP ram ratio correction factors and the J57 model simulation are presented in Figure 6. The comparisons were again made at a corrected low rotor speed of 5806 rev/min which corresponds to an exhaust nozzle pressure ratio of about 2.1 at sea-level and a speed of 5277 rev/min which corresponds to an exhaust nozzle pressure ratio of about 1.7 at sea-level. Figure 6 also presents the overall UETP ground-level and altitude facility engine ram pressure excursions for the sea-level and near sea-level test conditions.

Based on the differences shown in Figure 6, there is no significant impact of the UETP facilities variations in engine ram pressure ratio on the data comparisons.

**2.4 Treatment of Failed Instrumentation**

During the course of the test series, a number of sensors travelling with the engines as the reference instrumentation suffered from physical deterioration. Particularly susceptible were the hot end sensors, T7 and P7, necessitating a change-out at CEPr, the fourth stop in the test sequence. As these measurements were rather critical in evaluating nozzle flow and thrust coefficients, some level of confidence had to be placed in the quality of measurements. Of particular importance was the treatment and/or synthesis of missing information when one or more of these sensors went unserviceable. In the case of P7, it was necessary to base comparisons on a measured PS7, and computing a P7 using a tailpipe area ratio and gamma. Temperature, T7, could not be synthesized. Instead, each facility had to declare their methods of probe substitution, but no quantitative analysis of facility methods was done. Thus, there is some additional uncertainty cast in data comparisons using T7.

**3 MEASUREMENT CONSISTENCY CHECKS**

Each facility employed their own in-house techniques for ensuring the integrity of their data, using various error checking techniques as part of the measurement evaluation process.

Maximum confidence in a measurement is only achieved when multiple sampling of two or more independent methods are employed and compared simultaneously, and when data comparisons are made with other facilities. Data outside the measurement uncertainty bands of comparative methods indicates the presence of an anomaly, an unaudited or poorly estimated error source.

In this section, we will review the methods employed for examining facility reported values for thrust, airflow and fuel flow.

**3.1 Comparison of Gross Thrust**

Gross thrust is the sum of the exhaust gas momentum and the static pressure force across the nozzle exit plane. The actual thrust measured in a test cell depends upon other terms such as inlet flow momentum, external static pressure distribution on the engine structure, and other forces acting on the engine test frame. The accurate derivation of gross thrust therefore relies on an accurate measurement of the actual thrust acting on the test frame as well as inlet airflow and velocity, cell static pressure measurement and the elimination of, or accounting for stray forces.

There are two types of measurement checks commonly used to validate engine scale-force thrust: tailpipe momentum checks and nozzle thrust coefficient checks. The tailpipe momentum check refers to the comparison of scale-force gross thrust with the value of gross

thrust computed from pressure and temperature traverses at the nozzle throat (Ref. 3). The nozzle coefficient checks consist of comparing the measured nozzle thrust coefficients with the predicted coefficient values from test rig and model data.

The analysis used in the UETP was to compare the gross thrust coefficient CG8 determined at each facility.

$$CG8 = \frac{\text{Gross thrust derived from measurement}}{\text{Isentropic gross thrust for same nozzle area and pressure ratio}}$$

The isentropic or ideal value is a function only of nozzle pressure ratio, nozzle area and gamma. CG8 has a well established relationship with pressure ratio, increasing up to a peak value at a nozzle pressure ratio of around 2.5 at which point it levels off and remains constant over a modest pressure ratio range, i.e., until under-expansion begins to have a marked effect.

In Figure 7, an envelope was drawn around the CG8 plots derived for all 10 test conditions at each altitude facility. Each envelope is made up of a series of curves, one for each altitude condition, that departs from the single curve for an ideal nozzle. This bandwidth is due to a combination of engine related effects such as Reynolds number, swirl angle, and boundary layers, and measurement errors.

All results in Figure 7 show the typical nozzle characteristic shape with choking pressure ratios occurring above 2.5, but NASA and CEPPr have a considerably broader range and higher maximum values than RAE(P) and AEDC.

The measurement of total pressure in the nozzle was suspected as being the main reason for this disparity, and in Sections 17.2 and 18.2.2 of Ref. 2, it is shown that total pressure was a function of exit swirl. This suspicion was confirmed when an alternative thrust function, defined below, was used as the basis of the comparison; one that is independent of nozzle total pressure.

Fortunately, the nozzle inlet static pressure was found to be a more accurate measurement from which an isentropic value of nozzle total pressure could be calculated. Assuming an area ratio of jet pipe to nozzle exit area of 1.7293 and a value of  $\gamma = 1.35$ , CG8 was recalculated (as CG8C) based on the calculated value of nozzle total pressure. These results are plotted in Figure 8. As can be seen, this not only reduces the width of each envelope within which the test points are contained, but also reduces the difference in the value of CG8C at which the envelopes flatten out. CEPPr results are 1 to 1¼ per cent higher than the mean of the other three facilities, except for Test Condition 9 where the values are two per cent lower than the others.

A comparison between the altitude test results and those from two of the ground-level test beds is given in Figure 9 using the results from Engine 607594. The altitude test condition selected for this comparison is that which corresponded nearest to the sea-level static condition. This again shows the CEPPr altitude test cell to be measuring the highest values of CG8C while the NRCC ground-level bed gives the lowest, the difference between them being approximately two per cent.

Differences of less than one per cent in CG8C between the various test centres are judged to be a good result, but values greater than this give increasing cause for concern. A three per cent difference is viewed as casting doubt on the validity of gross thrust derivation. With these criteria in mind, and acknowledging that there is no absolute standard against which to compare, it seems that RAE(P), NASA and AEDC altitude results are in good agreement at choked nozzle conditions while CEPPr measure a higher level of gross thrust. The ground-level test bed at NRCC measures gross thrust lower than the altitude facilities.

It has not been possible to identify solely from CG8C parametric studies which of the many measurements are the major contributors to the differences. As far as frame load is concerned, stray forces are usually of a low order and can be calibrated out unless they result from some altitude effect. Static pressure distribution within the test cell can be important in some facilities as subsequent analysis using data obtained from the outdoor test bed at NAPC has shown. The definition of PAMB is a critical item, and as shown in Part 2.2 of this lecture, the thrust accounting must refer to a well defined upstream momentum plane. In Ref. 2, Appendix VIII, it is shown that gross thrust FG for the NRCC facility was low by approximately 0.8% using the GTP equations. Taking this variation into account, the gross thrust coefficient for NRCC would fall on top of the data from RAE(P), CEPPr (SL) and NASA in Figure 9.

### 3.2 Comparison of Airflow

There are several types of measurement checks that may be performed for engine airflow: inlet duct, tailpipe, turbine nozzle, and nozzle coefficient checks.

Duct checks consist of comparing engine airflow from the facility primary airflow measurement system with calculated airflow using the engine bellmouth and/or measurements at the engine inlet (face) station. Tailpipe checks refer to comparison of the primary airflow measurement value with the value obtained using a tailpipe continuity balance. Turbine nozzle checks are based on a comparison of the high-pressure turbine nozzle flow function over the engine operating envelope. For choked turbine flow, the turbine nozzle flow function should be relatively constant, and independent of test conditions. The final check, nozzle coefficients, consists of comparing the as-tested nozzle discharge coefficients with the engine manufacturer's predicted values from test-rig and scale-model tests.

In the UETP, facility airflow, WA1, was compared using a combination of these methods, and as reported in Ref. 2, the comparison methods were roughly grouped into tailpipe momentum/nozzle coefficients and nozzle flow functions. Each of these comparisons will be discussed in turn.

#### 3.2.1 Exhaust Nozzle Flow Coefficients

This comparison technique compares the facility airflow, WA1, to the ideal airflow calculated in the engine tailpipe based on measured values of pressure, temperature, fuel flow and area. A flow coefficient, CD8 was defined as:

$$CD8 = \frac{\text{Facility measured airflow}}{\text{Isentropic airflow in exhaust nozzle}}$$

In the previous section, the reader was apprised of the measurement difficulties experienced with total pressure and temperature due to inoperative sensors and swirl. Total pressure was similarly synthesized from measured static pressure, but unfortunately the as-measured temperature had to be used. This recomputed flow coefficient was called CD8C.

As with CG8C, a convergent nozzle of fixed geometry produces a similar characteristic shape for CD8C. Figure 10 shows the envelope of results for all the four altitude test facilities obtained from Engine 607594. RAE(P) and AEDC appear to be in close agreement on airflow measurement with NASA one per cent higher and CEPr a further one per cent higher still.

A high value of CD8C is consistent with a high value of measured airflow and, because of its influence on inlet momentum, a high value of airflow leads to a high value of gross thrust. It can be seen therefore that as both CEPr nozzle coefficients are high, it is most likely that the source of difference is in the measurement of airflow rather than of scale force.

The comparisons between altitude and ground-level test beds, for Engine 607594 are given in Figure 11. Compared to CG8C, the spread of results is of the same order, about 2½ per cent.

The previous comments about the absolute accuracy of nozzle coefficient values at different altitude test facilities and the reasons for any variation are just as true for CD8. It should be remembered also that the main aim of the UETP however, was not to calibrate test facilities against each other. The emphasis was to evaluate various methods of analysis which can highlight any discrepancies in measurements and procedures, to benefit future testing. On this basis, it can be seen that nozzle coefficients CD8 and CG8 do provide a powerful means of checking the validity of thrust and airflow measurement. These coefficients are particularly useful if a facility has tested engines of a similar type before, or if a reference sea-level test result is available to provide a datum.

### 3.2.2 Turbine and Exhaust Nozzle Flow Functions

Another technique for assessing the quality of facility airflow is through the use of nozzle flow functions. As a reminder, each facility measured airflow, WA1, with a flow measuring system normally used by that facility. The reference airflow at the engine face, WA2, was deduced from basic pressure, temperature and area measurements.

Thus the measured values of WA1 and WA2 are independent, albeit using the same data system, and provide a good basis for comparison of the relative quality of the airflow data obtained at the various facilities.

In addition, other independent comparisons of flow data are possible because of the unique behaviour of selected gas flow functions at the first stage turbine nozzle and exhaust nozzle when critical flow (choked flow) exists at these stations. The flow function is defined as:

$$K = \frac{W\sqrt{T}}{P} = \text{Constant}$$

(when flow is choked and effective flow areas and gas properties remain constant)

The limited instrumentation available in the engines required some approximations to compute the gas flow functions. To minimise the effect of these approximations, the gas flow functions are presented only for conditions when critical flow simultaneously existed at these stations.

#### 3.2.2.1 Turbine Nozzle Flow Function

Two flow functions for the first stage turbine nozzle were defined as follows:

$$K1 = \frac{(WA1 + WF)\sqrt{T4}}{P3}$$

$$K2 = \frac{(WA2 + WF)\sqrt{T4}}{P3}$$

The use of P3 in these equations is based on the assumption that the combustor pressure drop is assumed to be the same for each facility and test condition. The values of WA1, WA2, WF, and P3 were measured directly. The turbine temperature T4 was calculated from the combustor equation using the measured values of T3, WA1 and WF. The combustor efficiency was assumed to be 100 per cent. The common value of T4 was used in each of the two flow functions; this has a negligible effect on K2.

These flow functions were evaluated over a wide range of test conditions for those data points which satisfied the requirement that both the first-stage turbine nozzle and the exhaust nozzle were choked. For this analysis, the exhaust nozzle was considered choked for those data points in which P7QAMB was greater than 2.4. Cycle analysis confirmed that the turbine nozzle was choked whenever the exhaust nozzle was choked. The complete evaluation was performed only for data obtained with Engine 607594.

The mean values of K1 and K2 at Test Conditions 6, 7, 8, 9 and 10 are shown in Figure 12.

### 3.2.2.2 Exhaust Nozzle Flow Function

One flow function for the exhaust nozzle was defined as follows:

$$KES = \frac{(WA1 + WF)\sqrt{T}}{PS7}$$

where WA1, WF, T and PS7 were measured directly.

This flow function was evaluated for most of the test conditions used when determining K1 and K2. Again, KES was evaluated only for those data points for which P7QAMB was greater than 2.4. The mean values of KES for the selected test conditions are also shown in Figure 12.

### 3.2.2.3 Data Analysis - Area, Pressure and Temperature

Variations in the values of the flow functions K1, K2 and KES as a function of test facility and/or test condition could be the result of real changes in the values of the flow functions and/or of measurement errors in the individual parameters (W, P and T) which enter into the calculations. The mean values of the flow functions for each test facility were arranged in order of testing so that engine operating time increased from left to right (Figure 12).

An initial examination of the flow functions was made to determine if there were long-term changes which occurred as a result of mechanical or aerodynamic changes in either the first stage turbine stator or the exhaust nozzle. Examples of potential changes include erosion, bowing and bending, which could affect the flow area, the flow coefficients, or the leakage paths. Physical inspection and measurement of the exhaust nozzle was possible and was carried out, but no change was evident. Physical inspection and measurement of the turbine stator was not possible because the engines were not disassembled.

To assess the condition of the turbine stator at the beginning and end of the UETP, a comparison was made of the values of K1 and K2 for NASA (FE) and NASA (SE) at Test Conditions 6 and 9. These data confirm that there was no significant change in the aerodynamic characteristics of the first stage turbine stator and associated instrumentation from the beginning to the end of the UETP. A decrease in the exhaust nozzle flow function KES of about two per cent between NASA (FE) and NASA (SE) is shown in Figure 12. Since there was no physical change to the nozzle, it is reasoned that the change in KES resulted from differences in the flow parameter measurements.

The design of the UETP and the analysis method chosen make possible an independent examination of two groups of parameters (WA + WF) and  $\sqrt{T/P}$ . The individual effects of P and T were not examined. Analysis of the consistency of the  $\sqrt{T/P}$  group is possible by comparing K1 and KES at the various test facilities and test conditions. This comparison is significant because identical values of (WA + WF) appear in each pair (K1 and KES) of flow functions and independent values of P and T appear in each flow function. As can be seen in Figure 12, the difference of levels of K1 among test facilities is essentially the same as the difference of levels of KES. For example, the values of K1 and KES from RAE and AEDC are similar and both are about one per cent lower than NASA (FE). The only significant exception to this result is the values of KES for NASA (SE), as was discussed above.

Based on this analysis, the accuracy of the measurements of  $\sqrt{T/P}$  in all facilities made an insignificant contribution to the observed variation in flow functions.

### 3.2.2.4 Data Analysis - Airflow

The previous analysis has just demonstrated that 1) changes in turbine stator and exhaust nozzle area and 2) measurement uncertainty of  $\sqrt{T/P}$  to observed variations of K1 and KES were insignificant. Thus essentially all the observed variations in these flow functions result from variation in the measured values of (WA1 + WF). Further, because the only difference between K1 and K2 is the substitution of WA2 for WA1, direct evaluation of the consistency of these two measurements is possible. Fortunately, the contribution of WF to the quantity (WA + WF) is very small (generally less than two per cent). Therefore, for purposes of this analysis, variations in K1 and K2 can be assumed to reflect directly the variation in the measurement of WA1 and WA2.

In the case of the ground-level facilities the values for K1 and K2, hence WA1 and WA2, agreed to within 2.0 per cent at NRCC and 1.3 per cent at CEPr. However, at NRCC the value of WA2 was greater than WA1. This was due to a known airflow measurement problem which resulted in K1 being about 1.0 - 1.5 per cent low. At CEPr, the value of WA2 was less than WA1. For the equivalent sea-level condition at AEDC the values of WA1 and WA2 agreed to less than 0.5 per cent and WA2 was the larger.

The analysis confirmed that the measured values of WA1 at RAE(P) and AEDC were very nearly identical and were about 1.0 per cent lower than the values measured at NASA. The values measured at CEPr were generally slightly higher than NASA although at Test Condition 9 the CEPr value was the same as at RAE(P) and AEDC. The values of K2 for Test Condition 11 from NRCC, CEPr and AEDC are not included in this comparison because they do not satisfy the condition of simultaneous choking of the turbine stator and the exhaust nozzle.

## 3.2.3 Fuel Flow Measurement

Fuel flow comparison techniques are generally limited to comparison against engine meters, pressure drop characteristics across fuel injectors, and burner efficiency. In the UETP, fuel flow was analyzed by first comparing the facility measured fuel flow with that measured by the reference meters on the engine. Second, to assess any possible biases in lower heating value and relative density, the values determined and used by each facility were compared with those obtained at a common reference facility. Finally, facility measured fuel flow was evaluated against independent engine parameters.

Subsequent to the analysis for the UETP, an analysis of fuel calorimeters was carried out under the auspices of the National Institute of Standards and Technology (NIST), formerly NBS, in which NRCC was one of the participants. A summary of these results will also be included.

### 3.2.3.1 Data Quality

Fuel flow data were compared between the facility and the reference (engine) systems. AEDC showed excellent agreement between facility and reference data under virtually all test conditions, i.e., differences did not exceed  $\pm 0.5$  per cent (Table 2).

The NASA data presented conflicting pictures in that during the first entry (FE) there was very good agreement, comparable to AEDC, while the second entry (SE) data were characterised by considerable scatter. This scatter, traced by NASA to facility problems, ranged between  $\pm 3.5$  per cent, exceeding the maximum declared uncertainty for fuel flow of  $\pm 1.7$  per cent (Test Condition 9).

RAE(P) declared its WFER values as invalid because of fuel temperature measurement problems and therefore a comparison between the two fuel flow measuring systems was not made. Any assessment in this report will be restricted to facility flow measurements.

The CEPr data were perhaps the least consistent. Differences ranged from very good (Engine 607594 Test Conditions 1, 3, 6, 10), 0 to -0.8 per cent, to very large at Test Condition 9.

Data from NRCC displayed very good agreement for the two fuel flow measurements, i.e., 0.6 to 0.8 per cent, sea-level static tests only.

The TUAF tests used only the engine fuel flow measuring system, so no comparisons were possible.

As a result of the above study and from participants' indications, all or part of the following data were suspect: RAE(P), all WFE; NASA (SE), Engine 607594, possibly both fuel measuring systems; CEPr, fuel flow measurements at Test Condition 9 measurements.

### 3.2.3.2 Examination of Differences in Fuel Analysis Between Facilities and NRCC

The fuels used by the program participants were analyzed by each facility to obtain the properties needed for fuel flow calculations. In addition, samples were sent to NRCC for an independent analysis. Of primary importance were specific gravity (relative density) and lower heating value (net heat of combustion). Since both appear as direct multipliers in the fuel flow calculation, differences were combined to indicate the total effect they might have on the calculation. The resultant differences were small and ranged from 0.04 to 0.35 per cent (Appendix VII) of Ref. 2. When referenced to the one per cent combined reproducibility, a measure of precision for the methods used by NRCC in the analysis, these differences are not significant.

### 3.2.3.3 Evaluation of Fuel Flow Measurement and Engine Performance

Subject to the above-mentioned reservations about some of the data, comparisons of fuel flow and engine performance were made for the participating facilities. Significant differences could appear depending on the basis for comparison. Small shifts in NHR at a given nozzle pressure ratio, attributed to engine rematching or facility effects, suggest that nozzle pressure ratio should be favoured as a basis of comparison.

For Engine 607594, plots of facility measured fuel flow (WFR) against nozzle pressure ratio (PS7QAMB) at each test condition show overall spreads of between two and three per cent at altitude test conditions, and three per cent at SLS conditions (Figures 15-1 and 15-2 in Ref. 2). With declared uncertainties of 1.0 to 1.5 per cent, the spread in the data indicates agreement, i.e.,  $\pm 1.5$  per cent about a mean value. Outlier curves of NASA (SE) at some altitude tests, and CEPr at SLS conditions, were disregarded because of previously identified problems.

Plots of WFR against high rotor speed (NHR) showed that with the exception of CEPr, the spread of altitude test curves of Engine 607594 was between two and three per cent. CEPr curves were consistently lower than the mean of the others and were not considered. At SLS conditions, excellent agreement existed between NRCC and AEDC; the CEPr curve was again low. Figure 13 is a typical example.

In conclusion, discounting known measurement errors, comparison among all facilities for fuel flow showed spreads of  $\pm 1.0$  - 1.5% about a mean value. Falling within the declared uncertainties, this agreement was judged to be very good.

### 3.2.3.4 Calibration Facility Comparison

Although not directly related to the specific participants in the UETP, the question of traceability to National Standards of fuel calibration facilities must be addressed. Each test facility has access to a calibration laboratory for fuel meters, which generally fall into two classes, volume and mass devices. Procedures are defined in their use to ensure that the specified accuracy is maintained. At the NRCC, a careful calibration of the volume type ballistic flow calibrator against Canadian Standards produced a calibration factor (K) that agreed within 0.0018% of the original one provided by the manufacturer.

In fall of 1987, an opportunity arose to participate in a round robin flow measurement testing program, conducted by the National Institute of Standards and Technology (NIST), formerly NBS. The program was initiated by the US Department of Defense, with some participation from industry and other agencies. NRCC was the only non-US participant. Without going into detail, the test results contained two major surprises. The bias differences, among participating facilities, ranged over 0.8% (Ref. 8). All calibrators were of the highest integrity, secondary in the traceability chain only to NIST. A spread of perhaps 0.3% ( $\pm 0.15\%$ ) was generally expected. The other discovery was even more startling. On inspection, it was noted that test points from calibrating devices based on mass establishment ("weighers") and those based on volume flow determination ("volumers") formed distinct islands among themselves, see Figure 14. This plot was derived from the NIST report and gives the results of one test configuration in simplified form. Even though each group had an outlier, the pattern was too conspicuous to be disregarded. No explanation has been found yet for this phenomenon. Should a fundamental bias of this magnitude exist between these two widely-used flowmeter calibrator systems, it would seriously compromise measurements from meters calibrated through them.

## 4 ENGINE 'REMATCHING'

### 4.1 Introduction

The intention of the UETP was to provide an "identical" test article to each test facility that would operate in a respectable consistent fashion throughout the round-robin. Although the engine and procedures were chosen to minimize time dependent performance variations or rematching, it had to be accepted that variations were possible over the long test program. Additional studies were also conducted to ensure that any apparent "rematching" was not the result of facility influences, such as:

1. *non-uniform inlet flow conditions and boundary layer thickness*
2. *secondary flow effects*
3. *cell heating and flow recirculation*
4. *instrument sampling rates*

All these effects were encountered in one form or another and attempts were made to quantify them, using back-to-back tests or special studies. The effect of long term performance retention is more subtle, as real changes had to be extracted from facility effects and measurement errors. The program was planned and the test vehicle chosen to minimize any changes of engine performance with time, but nevertheless, procedures were adapted to quantify them. They were:

1. *book-keeping engine performance changes that occurred at each test facility*
2. *conducting the first and last engine tests in the same test facility and measuring the overall change in engine performance*
3. *monitoring data from the engine internal instrumentation throughout the test program*

Item 1 was accomplished by having each facility conduct a repeat test at the completion of testing at the same conditions as were used at the start of its test program. The results of using this approach, however, were not conclusive. The difficulty was that the measured engine performance changes for the relatively short engine time involved appeared to be much smaller than the day-to-day random error values of the facility measurement system. As a result, it was not possible to discern consistent short term changes in the engine performance parameters.

Item 2 consisted of returning the engines to those facilities which first tested the engines, NASA for the altitude and NRCC for the ground-level tests. Re-testing at NRCC also included an engine water wash test to examine the effects of possible compressor fouling on engine performance. As was the case for Item 1 the determination of changes in engine performance was not entirely successful. The difficulty was that during the long elapsed times between the initial and repeat tests (4 years for the NASA tests and 3 years for the NRCC tests), facility equipment, measurement systems and procedure changes had taken place which resulted in changes to measured values which could not be distinguished from the measured engine performance changes. However, this was not the case for the water wash tests which were accomplished on a back-to-back basis using identical facility hardware, measurement systems and procedures.

A further complication at NRCC, was that the repeat tests were conducted at inlet temperatures considerably different from the first entry, the effects of which added a further 0.5% uncertainty in fuel flow and thrust (see Section 2.3).

The approach that provided the most consistent results was the monitoring of the engine internal instrumentation (Item 3). This consisted of using internal engine instrumentation to estimate changes with time in engine airflow, engine pressure/temperature ratios and engine thrust, along with the use of the engine fuel flow meter to estimate changes in engine specific fuel consumption. Considerable detail is given in Section 11 of Ref. 2, but the highlights will be outlined in this lecture.

### 4.2 Performance Retention Analysis Methodology

The analysis procedure for monitoring time-dependent performance changes was based on six criteria:

1. *use data from identical engine configurations*
2. *use data from identical instrumentation sensor configurations to minimize bias errors*
3. *use data with minimum precision error*
4. *use identical data calculation methods*
5. *use indicators representative of engine performance*
6. *present engine performance parameters in a manner that quantifies an engine change with operating time*

Selection of the engine tested at all altitude facilities, having a larger database and longer running hours, satisfied criterion 1. Engine (reference) instrumentation sensors, eight in total, were only used, satisfying criterion 2. Criterion 3 was satisfied by only using data with the engine nozzle choked ( $P7QAMB > 2.4$ ), minimizing ambient effects. Two test conditions and two engine power settings were chosen ( $NLR = \text{constant}$ ). The use of UETP standard equations satisfied criterion 4. Engine performance indicators (criterion 5) were a mix of directly measured parameters and those calculated from them. Direct measurements were available for:

1. *rotor speed ratio (NLQNH)*
2. *engine airflow (WA2R)*
3. *engine fuel flow (WFER)*
4. *engine temperature ratio (T5Q2)*
5. *engine pressure ratio (P5Q2)*

Calculated parameters were:

1. *gross thrust (FG)*
2. *turbine inlet temperature (T4)*
3. *specific fuel consumption (SPC)*

all for a constant value of low rotor speed (NLR)

Gross thrust (FG) had to be calculated from WA2, WFE, T5 and P5 assuming a convergent choked nozzle and a fixed value for nozzle thrust coefficient. Turbine inlet temperature (T4) was calculated assuming choked turbine nozzle flow and fixed values for combustor efficiency and flow area.

Selected engine performance indicators from each facility were evaluated in terms of percentage change from a common reference, NASA (FE) test results.

$$\% \text{ difference} = \frac{\text{Test Facility} - \text{NASA (FE)}}{\text{NASA (FE)}} \times 100\%$$

The differences were plotted as a function of accumulated engine time (criterion 6), using the mid-point of facility reported engine time for the evaluation.

#### 4.3 Data Analysis

Each performance parameter was plotted using as measured data for two test conditions and two values of NLR. The shaded lines in the figures indicate the assessed trends, the width reflecting the magnitude of the uncertainty estimates. All eight parameters are listed in Ref. 2, but only two, NLQNH and SFC are included here for illustrative purposes.

Speed ratio, Figure 15, shows an overall decrease of about 0.3% with engine time, and while not monotonic, the shape is well defined. Airflow variation (not shown here), WA2R, follows the same trend as the speed ratio data. The roll-off in speed ratio is accompanied by an overall decrease of 0.4% in engine airflow.

Gross thrust specific fuel consumption (SFC), Figure 16, and combustor temperature (T4) both indicate an increase with time, and are consistent with each other. While the uncertainty band in SFC is quite large, nevertheless a trend is visible. The overall increase in SFC is about 0.6%, while T4 rose between 8-16 K.

In general, since the analysis had to be based on limited data which exhibited appreciable scatter it was difficult to quantify the extent of any deterioration that may have occurred. It was concluded that engine performance remained essentially constant from beginning to end of the UETP, as shown below:

Rotor Speed Ratio:	minus 0.1 to 0.3 per cent
Airflow:	minus 0.4 to 0.7 per cent
Fuel Flow:	plus 0.5 per cent
Thrust:	minus 0.1 to 0.7 per cent
Specific Fuel Consumption:	plus 0.6 to 1.2 per cent
Combustor Temperature:	plus 8 to 16 K

#### 4.4 Engine Water Wash

NRCC performed a water wash on Engine 607594 in order to evaluate the effect of compressor fouling on engine performance. Washing was qualitatively assessed as 95 per cent effective for the low pressure compressor with some deposit left near the rotor blade tips. Retesting after the water wash disclosed no significant effect on engine performance for fuel flow, SFC, thrust, engine or compressor characteristics (T5/T2 vs. P5/T2, T3/T2 vs. P3/P2) when compared to the NRCC facility measurement repeatability (0.1 to 0.3 per cent). Component degradation recoverable by water wash was concluded to be a maximum of 0.1 per cent in rotor speed and 0.5 per cent in airflow.

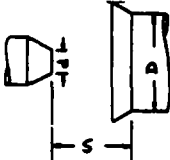
#### CONCLUDING REMARKS

This lecture has shown some of the differences between the ground-level test beds and altitude facilities, especially in the method of thrust accounting. The use of flow coefficients is a powerful tool to ensure consistency of facility thrust and airflow, and can effectively be used for inter-facility comparison providing choked nozzle conditions exist. Careful planning for monitoring performance retention is essential as engine deterioration could compromise the sought-after facility effects.

#### REFERENCES

- 1) Subcommittee 01, AGARD Propulsion and Energetics Panel, Working Group 15, "Uniform Engine Test Program - General Test Plan", June 1983 (Revised Edition).
- 2) Ashwood, P.F., principal author, and Mitchell, J.G., editor, "The Uniform Engine Test Programme - Report of PEP - WG15", AGARD Advisory Report No. 248, February 1980.
- 3) Covert, E.E., editor, James, C.R., et al., "Thrust and Drag - Its Prediction and Verification", Progress in Astronautics and Aeronautics, Vol. 98, 1985.
- 4) MIDAP Study Group, "Guide to In-Flight Thrust Measurement of Turbojets and Fan Engines", AGARDograph No. 237, January 1979.
- 5) MacLeod, J.D., "A Derivation of Gross Thrust for a Sea-Level Jet Engine Test Cell", National Research Council of Canada, DM-009, September 1988.
- 6) Mattingly, G.E. "A Round Robin Flow Measurement Testing Program Using Hydrocarbon Liquids: Results for First Phase Testing", US Department of Commerce, National Institute for Standards and Technology (Formerly National Bureau of Standards), Gaithersburg, MD, 20899, NISTIR 88-4013, 1988.

$d = 550 \text{ mm (nominal)}$



	D mm	S mm	$\frac{D}{d}$	$\frac{S}{d}$
NASA PSL3	1016	660	1.85	1.20
AEDC T2	1700	250	3.09	0.45
CEPr R6	1800	580	3.27	1.05
RAE(P) Cell 3	2134	1412	3.88	2.57
NRCC Cell 5	838	457	1.52	0.83
CEPr TO	1930	650	3.51	1.18
TUAF	1830	1500	3.33	2.73

Table 1 Comparison of exhaust geometries

FACILITY	ENG	(WFR - WFE2R)/WFE2R × 100 [%]					
		TEST CONDITION					
		1	3	6	9	10	11
NASA FE	594	0.3	0.4	0.5	-0.5	0.5	
	037	0.2	0.2	0.3	0.6 → 1.2	0.5	
NASA SE	594	0.5 → 3.0	0.5 → 2.5	0.5 → 3.5	-2.5 → -3.5	1.0 → 2.5	
	037	-0.4 → 1.1	-0.3 → -0.9	0.0 → 1.4	-0.7 → 2.7	0.2 → 1.0	
AEDC	594	0.1	-0.3	-0.6	-0.7	0.6	-0.3
	037	0.2	0.1	-0.1	0.3	0.0	0.1
NRCC	594						0.8
	037						0.6
CEPr	594	-0.7 → 0.2	-0.5	-0.3	-7.0 → -3.0	-0.2	-1.8
	037						-1.0 → 0.0
RAE (P)	594	-1.0 → 0.3	0.0 → 3.0	-2.0 → -0.7	-8.0 → -4.5	-1.5 → 0.0	
	037						

\*11 points of 18 had a % difference greater than -10%; some WFE2R values were beyond range

Table 2 Differences between facility and reference fuel flows

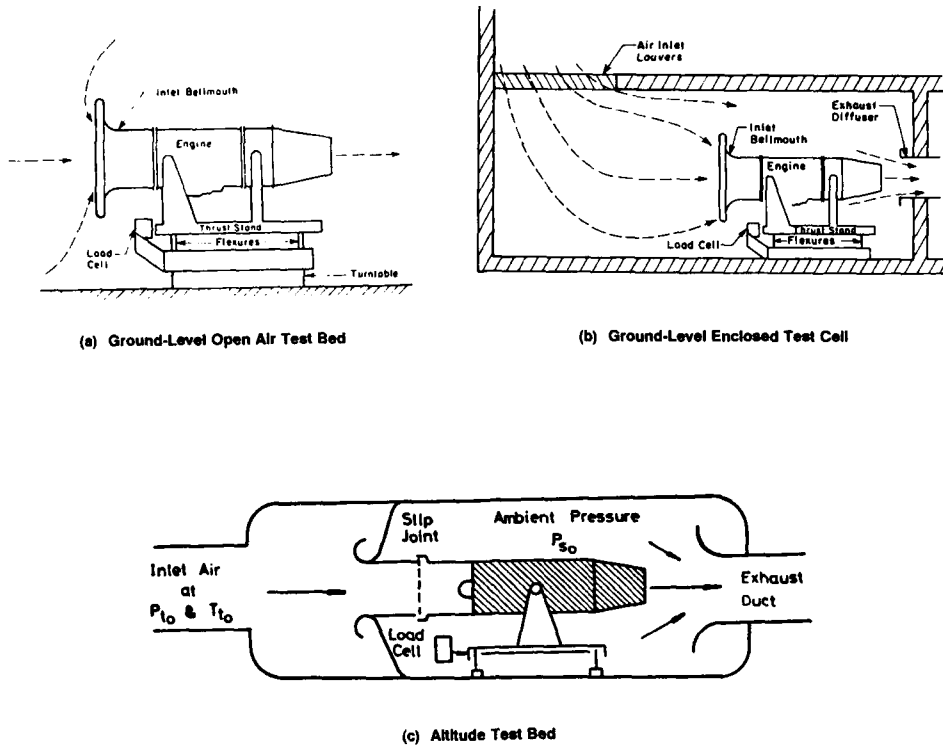


Figure 1 Engine test cell arrangements

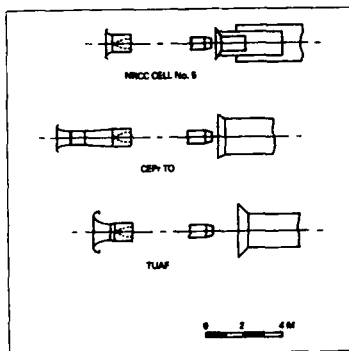


Figure 2 Comparison of inlet and exhaust geometries - ground-level beds

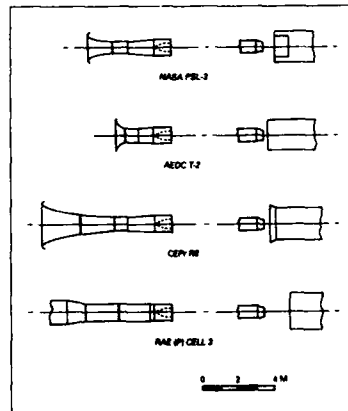


Figure 3 Comparison of inlet and exhaust geometries - altitude cells

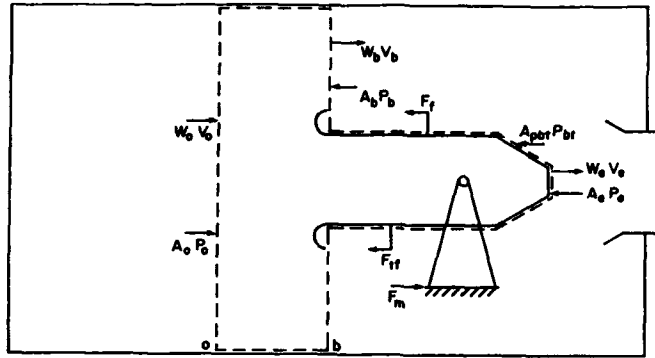


Figure 4 Engine and test cell control volume

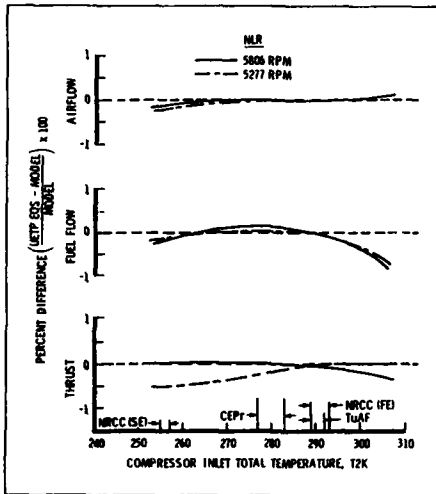


Figure 5 Comparison of UETP and engine model sea-level temperature correction factors

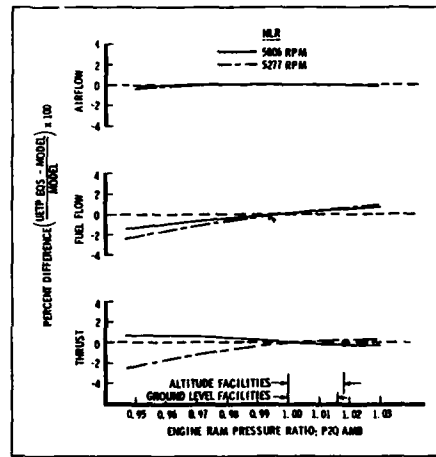


Figure 6 Comparison of UETP and engine model sea-level RAM ratio correction factors

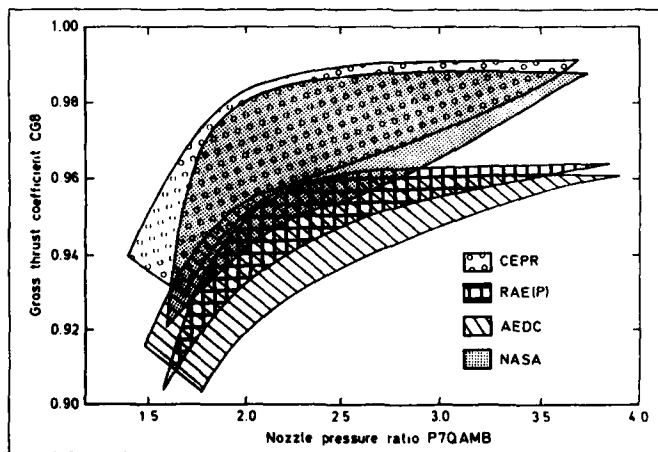


Figure 7 Gross thrust coefficient envelopes for all facilities (engine 607594)

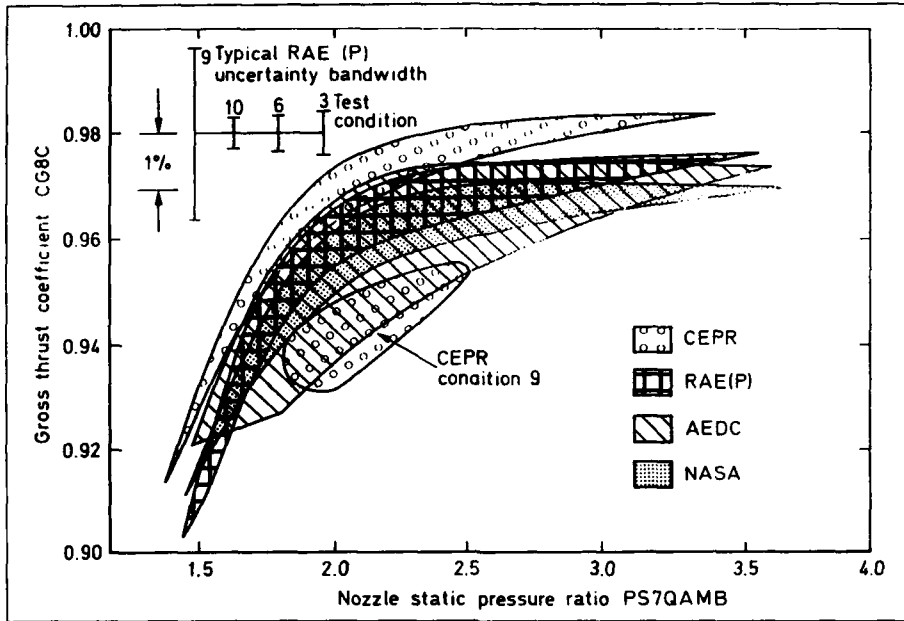


Figure 8 Revised thrust coefficient envelopes for all altitude facilities (engine 607594)

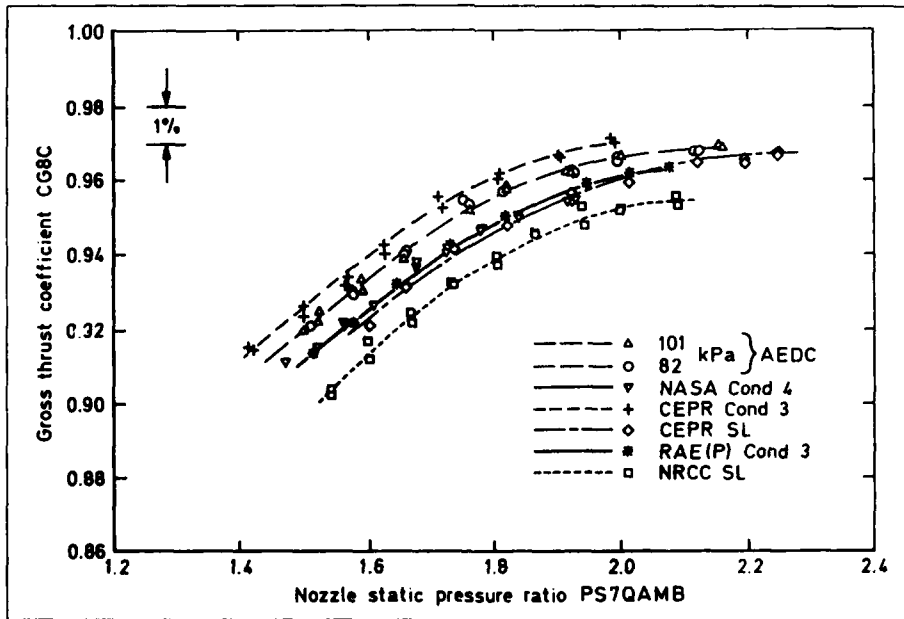


Figure 9 Revised thrust coefficient for altitude cells and ground-level test beds (engine 607594)

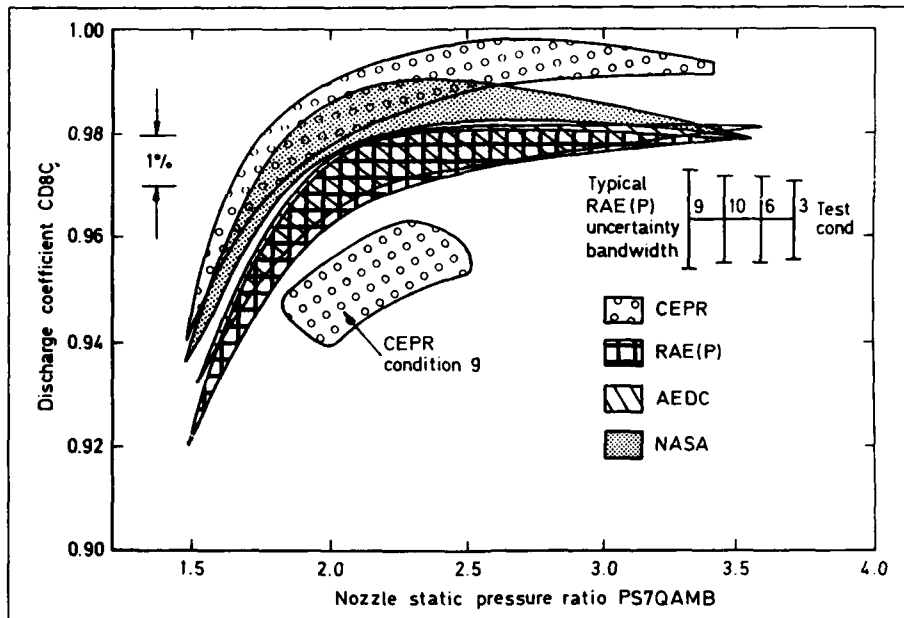


Figure 10 Revised discharge coefficient envelopes for all altitude facilities (engine 607594)

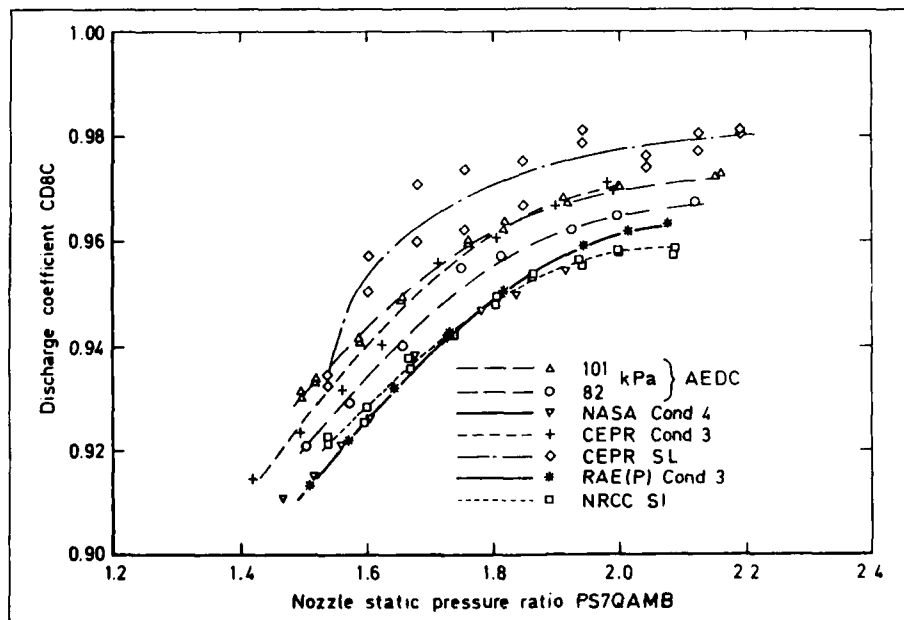


Figure 11 Revised discharge coefficient. Altitude cells and ground-level beds (engine 607594)

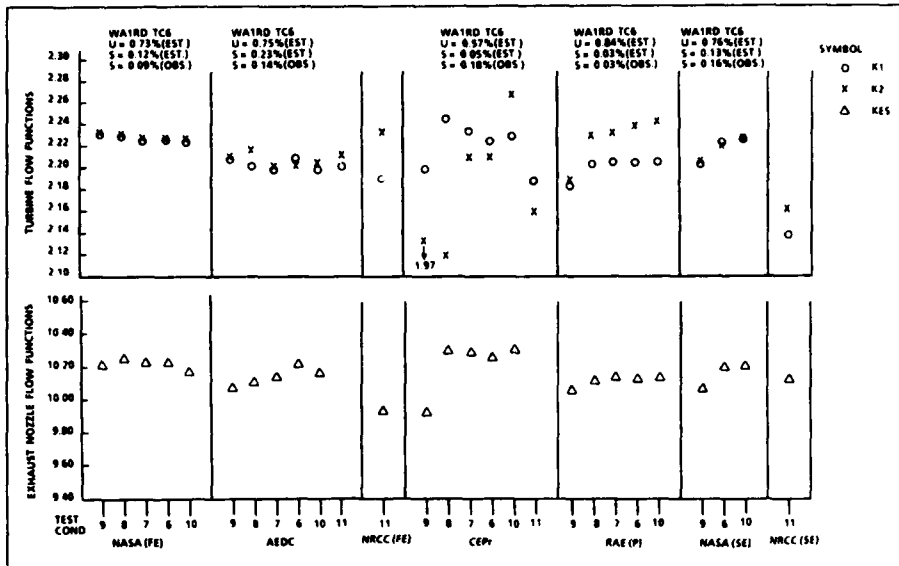


Figure 12 Variation of turbine and exhaust nozzle flow coefficients (engine 607594)

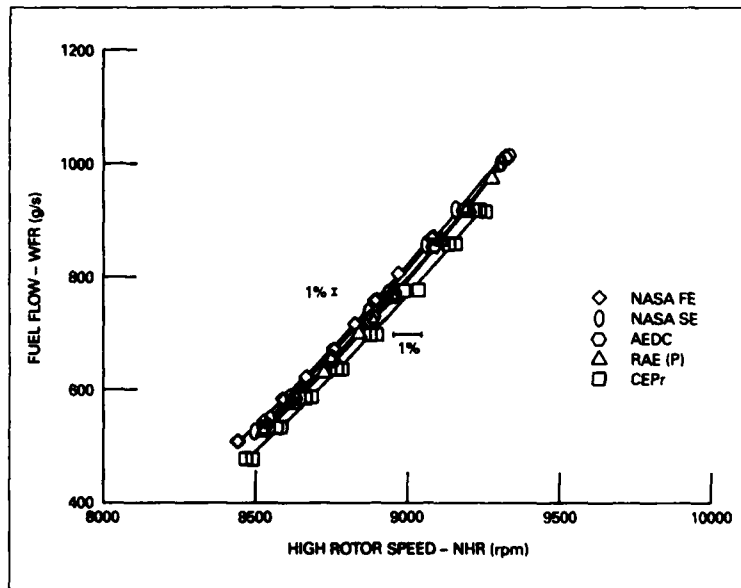


Figure 13 Fuel flow comparison based on high rotor speed (TC3 - 607594)

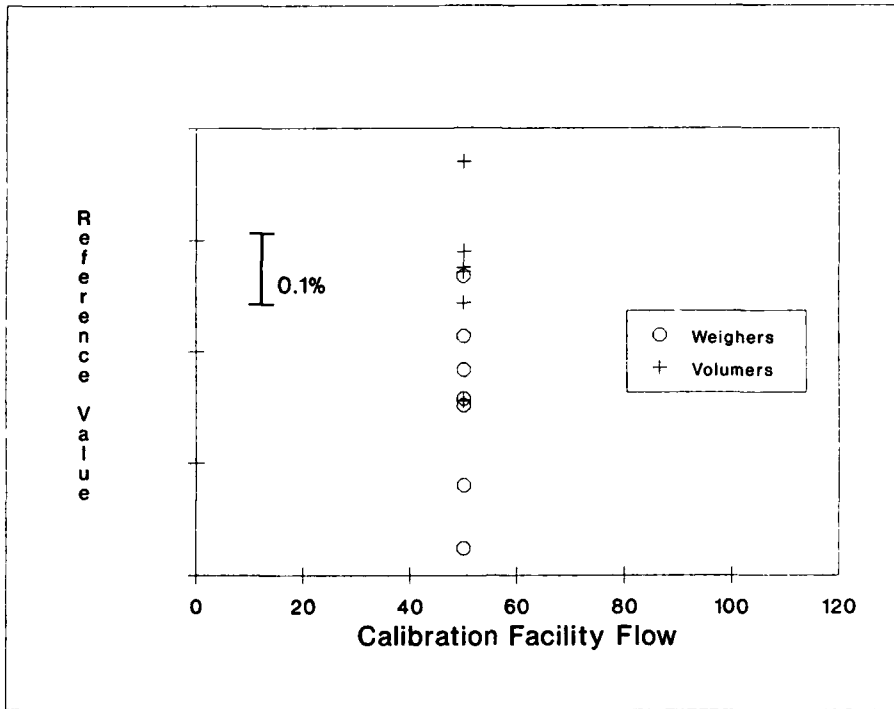


Figure 14 NIST Round-Robin calibration results

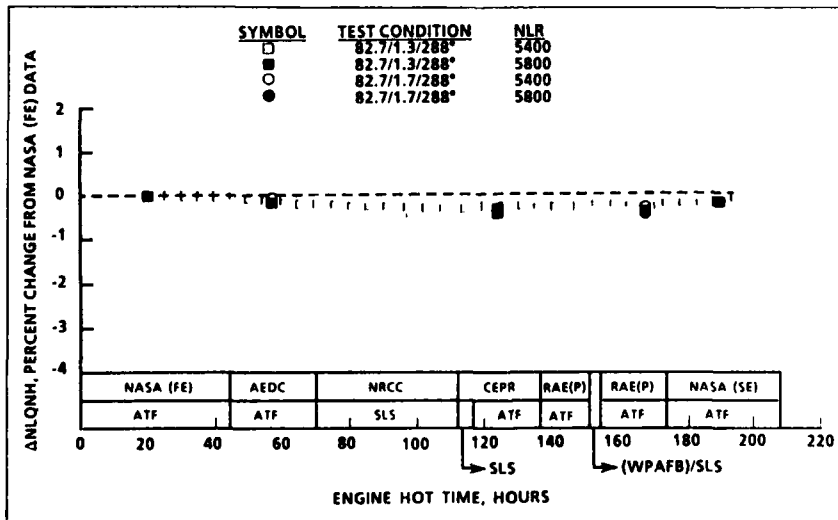


Figure 15 Rotor speed ratio change as a function of engine operating time

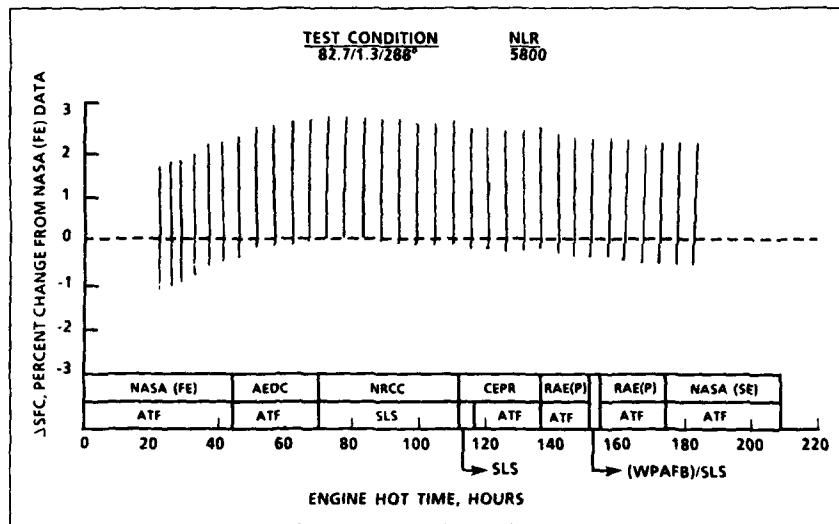


Figure 16 Gross thrust specific fuel consumption change as a function of engine operating time

## COMPARISON OF ALTITUDE TEST CELL RESULTS

By  
 Robert E. Smith, Jr.  
 Vice President and Chief Scientist  
 Sverdrup Technology, Inc./AEDC Group  
 Arnold Engineering Development Center  
 Arnold Air Force Base, TN USA

### SUMMARY

The steady-state performance of the J57-PW-19W engine as measured in four altitude test facilities located at NASA (Lewis), AEDC, RAE(P), and CEPr was compared and analyzed at each of ten simulated flight conditions. All of the performance comparisons were based on six pairs of fundamentally related parameters, which included combinations of engine rotor speeds, temperature ratio, pressure ratio, airflow, fuel flow, net thrust, and specific fuel consumption.

Two different methods were used to make the facility comparisons. First, the facility performance was compared using all engine data over the full range of test conditions and power settings tested. The comparison between the four altitude facilities was based on the fraction of test data which are within a 2-percent band, i.e.,  $\pm 1$  percent of the mean performance curves at each of the ten environmental test conditions. Second, facility performance was compared using the overall percentage spread of the characteristic curves fit to the six pairs of key engine performance parameters for all of the simulated flight conditions at one engine power setting.

Facility comparisons based on the first method showed approximately 90 percent or more of all the data was within a 2-percent bandwidth for four of the six parameter sets, i.e., engine speed ratio, engine temperature ratio, airflow, and specific fuel consumption. Only about 65 percent of the fuel flow and net thrust data was within the 2-percent band. The fuel flow and thrust data from CEPr were significantly different from the other three test facilities and contained confirmed anomalies. Omitting the CEPr data for these two parameters increased the fraction of data points within the 2-percent band to 85 percent for fuel flow and 92 percent for net thrust.

The ranges of overall engine performance spreads based on the second method are shown below for three of the key pairs of engine performance parameters. The differences were evaluated at approximately the mid-thrust level of the engine power range at each of the test conditions.

Engine Parameter	Independent Variable	Interfacility Spread (Max - Min.) %
Net Thrust	Engine Pressure Ratio	3.4 - 5.4 (0.3 - 3.3)*
Specific Fuel Consumption	Net Thrust	0.9 - 2.4 (0.9 - 2.4)*
Airflow	Low Rotor Speed	1.3 - 3.6 (1.3 - 2.9)*

\* The values in parenthesis show the spread excluding the CEPr results, which contained confirmed anomalies.

Extensive and in-depth analyses of all of the observed interfacility differences were performed. These analyses identified five primary factors which contributed to these interfacility differences as follows: thermal nonequilibrium of the engine, differences in measurement systems hardware and software, unreliable measurements of nozzle inlet total pressure, inlet flow distortion, and long-term performance non-repeatability within the engine. During the planning for the UETP, it was anticipated that different levels of engine inlet turbulence and variations of the magnitude of boattail force, i.e., force acting on the external surface of the engine exhaust, could significantly affect the performance measurements in the altitude facilities. With the limited inlet turbulence data obtained, it was not possible to determine if turbulence did or did not affect measured performance. On the other hand, the substantial amounts of boattail force data which were obtained showed that the levels of boattail force for the several UETP test installations were insignificant when compared to net thrust.

### LIST OF SYMBOLS

AEDC	Arnold Engineering Development Center
CEPr	Centre d'Essais des Propulseurs
FNRD	Net Thrust Corrected to Specified Conditions
IC	Influence Coefficient
NASA	National Aeronautics and Space Administration
NHRD	High-Pressure Compressor Rotor Speed Corrected to Specified Conditions, rpm
NLQNH	Ratio of Low Pressure Compressor to High Pressure Compressor Rotor Speed
NLRD	Low-Pressure Compressor Rotor Speed Corrected to Specified Conditions, rpm
NRCC	National Research Council of Canada
P2	Engine Inlet Total Pressure, kPa
P7	Exhaust Nozzle Inlet Total Press., kPa
P7Q2	Ratio of Exhaust Nozzle Inlet to Engine Inlet Total Pressure
RAE(P)	Royal Aerospace Establishment Pyestock

RPR	Ram Pressure Ratio
SFCRD	Specific Fuel Consumption Corrected to Specified Conditions, g/kN-sec
TC	Test Condition
T2	Engine Inlet Total Temperature, K
T7Q2	Ratio of Exhaust Nozzle Inlet to Engine Inlet Total Temperature
UETP	AGARD-PEP Uniform Engine Test Program
WAIRD	Facility Airflow Rate Corrected to Specified Conditions, kg/sec
WFERD	Referee Fuel Mass Flow Rate Corrected to Specified Conditions, g/sec
WFRD	Facility Fuel Mass Flow Rate Corrected to Specified Conditions g/sec

## 1.0 INTRODUCTION

One of the basic objectives of the AGARD Uniform Engine Test Program was to identify, analyze, and interpret facility-to-facility differences in steady-state engine performance as measured in four different altitude test facilities within the NATO countries. The test facilities are: Test Cell PSL3 at NASA (Lewis), Test Cell T-2 at AEDC, Altitude Cell 3 at RAE(P), and Altitude Test Cell R-6 at CEPr.

Six sets of engine performance parameters were selected to assess the differences in the performance of the four facilities. The selected parameter sets are:

NLQNH vs NHRD	WA1RD vs NLRD	FNRD vs P7Q2
T7Q2 vs P7Q2	WFRD vs NHRD	SFCRD vs FNRD

All comparisons of the performance of the altitude test facilities are based on data from only one J57-PW-19W engine (serial no. P607594). Although both engines were tested at NASA (Lewis) and AEDC, the second engine was not tested in the altitude test facilities at RAE(P) or CEPr.

Engine tests were conducted at ten different sets of environmental conditions. These test conditions included four different inlet temperatures (253, 268, 288, and 308 K) at constant inlet pressure (82.7 kPa) and ram ratio (1.00); four different inlet pressure conditions (82.7, 51.7, 34.7, and 20.7 kPa) at constant inlet temperature (288 K) and ram ratio (1.30); and four different ram ratio conditions (1.00, 1.06, 1.30, and 1.70) at constant inlet temperature (288 K) and inlet pressure (82.7 kPa).

The facility-to-facility differences in the six sets of engine performance parameters are addressed. Indicated differences in engine performance are a manifestation of differences in facility performance and are a summation of differences in five categories, i.e., test environment, test installation, test operation, test measurement, and the engine performance at each of the altitude test facilities.

Factors included in the test environment which could affect engine performance and, hence, facility performance are air quality parameters, e.g., specific humidity and fuel properties. Factors in the test installation which could affect engine performance include the pressure and temperature profiles at the facility/engine inlet and engine exit/facility interfaces. Factors in test operations which could affect engine performance include the time allowed after the specified test conditions are established for the engine to stabilize and reach thermal equilibrium. Factors in test measurement which could affect engine performance include the bias and precision errors of the individual measuring systems. Finally, the short-term (day-to-day) and long-term (duration of the UETP) repeatability of the engine performance itself would also affect the observed differences in measured engine performance between the facilities.

The data from all facilities is compared in two very different ways. First, the population distribution of all data values was analyzed over the entire range of engine power settings to determine the fraction of the values which are within a 2-percent band, i.e.,  $\pm 1$  percent of the mean performance curve. Second, the overall spreads of the engine performance parameters for all of the simulated flight conditions at one engine power setting were determined.

All of the altitude test data were processed in accord with the General Test Plan (Ref. 1). The engine performance data were corrected (referred) to the specified environmental test conditions to remove the effect of small differences between the as-tested inlet pressure, inlet temperature, and ram ratio and the specified environmental test conditions. The UETP General Test Plan (Ref. 1) specified repeat data scans be obtained at each test condition in the test matrix. These repeat data scans were obtained at NASA (Lewis), AEDC, and CEPr. In general, the repeat data scans were not obtained at RAE(P). Specifically, repeat data scans were obtained at RAE(P) at only two of the ten test conditions (conditions 4 and 9 - Section 6.2, Ref. 2).

In subsequent sections of the lecture, the facility-to-facility differences for each of the engine performance parameter sets are examined. Then, the effects of individual factors on the interfacility differences are examined. Finally, the interfacility differences are summarized, and the primary factors which lead to these differences are identified.

All of the material presented in this lecture is taken from sections 9, 11, 12, 14, 15, 17, and 18 of Ref. 2.

## 2.0 FACILITY-TO-FACILITY DIFFERENCES

The interfacility differences for each of the six chosen performance parameter sets are examined in the following sections. The characteristics of the measured performance at a typical test condition are identified, and the fraction of all the data within a 2-percent band is determined. Then the interfacility differences at each of the ten test conditions are grouped to display the effects of varying inlet temperature, inlet pressure, and ram pressure ratio on a parametric basis.

In a very few cases, data were not available from all four test facilities for all ten test conditions. The unavailability of these data may, in some few cases, reduce slightly the observed facility-to-facility differences. This effect on the UETP results is judged to be negligible.

## 2.1 Rotor Speed Ratio

Typical rotor speed ratio results from the four altitude facilities are presented in Fig. 1. Four characteristics of the rotor speed ratio data are visible. First, the rotor speed ratio decreases in the order of tests at NASA, AEDC, and RAE(P). The repeat scan data are indistinguishable or they lie along the characteristic curve for the NASA and AEDC data. The repeat scan data are significantly separated from the initial scan data and do not lie along the engine characteristic for the CEPr data. As noted earlier, only the initial data scans were generally obtained at RAE(P). The consistency in the measured rotor speed ratio characteristic at each facility suggests that the differences between facilities are probably caused by biases.

A total of 99 percent of the rotor speed data is within a 2-percent band. The 2-percent band is defined as  $\pm 1$  percent from the mean performance characteristic at each test condition.

A summary of the facility-to-facility differences in rotor speed ratio at the mid-thrust value is shown in Fig. 2. No systematic effect of the variation in test environment on rotor speed ratio is observed. Observed differences in rotor speed ratio for the four facilities range from a minimum of 0.4 percent to a maximum of 0.8 percent for the ten flight conditions. These interfacility differences are the smallest differences of any of the six parameter sets chosen. The analysis of the test data from CEPr confirmed that sufficient time was not allowed for the engine to reach thermal stabilization before some of the initial and repeat data scans were initiated. These thermal nonequilibrium effects at CEPr contributed randomly 0 to 0.3 percent to the observed interfacility differences. The engine cycle rematch contributed up to 0.3 percent to the interfacility differences in a systematic manner (Section 11, Ref. 2). The facility-to-facility differences vary from a minimum of 0.04 percent to a maximum of 0.6 percent when the data from CEPr are not included.

The detailed analysis and interpretation of the facility-to-facility differences in rotor speed ratio are presented in Sections 9.2.1, 11.3.1, and 18.2.1 of Ref. 2.

## 2.2 Temperature Ratio

The typical variation of engine temperature ratio T7Q2 as a function of engine pressure ratio P7Q2 is shown in Fig. 3. In a manner consistent with the characteristic of rotor speed ratio, the engine temperature ratio is neutral or increasing in the order of testing conducted at NASA, AEDC, and RAE(P). Detailed analysis of the test data identified a probable error of about 2 percent (low) in the nozzle inlet total pressure P7 measurements at CEPr. (Sections 13.1 and 18.2.2 - Ref. 2) The probable cause for this error could not be established. At these test conditions the influence coefficient  $\Delta T7Q2/\Delta P7Q2$  is approximately 0.6. Thus, the probable error in P7 at CEPr accounts for a displacement of engine temperature ratio of about 1.2 percent. Note that, in general, the repeat scan data are not displaced from the initial scan data for this parameter set at either NASA, AEDC or CEPr. A total of 98 percent of the engine temperature ratio data is within a 2-percent band.

The facility-to-facility differences in engine temperature ratio at the mid-thrust value are summarized in Fig. 4. A detailed examination of the differences in each of the three test environmental groupings shows a possible systematic effect of increasing T2 and decreasing P2. Observed differences in engine temperature ratio range from a minimum of 0.6 percent to a maximum of 2.0 percent for the ten test conditions. The engine cycle rematch contributed up to 0.3 percent in a systematic manner (Section 11, Ref. 2). The probable error in nozzle inlet total pressure P7 measurements at CEPr contributes approximately 1.2 percent to the observed differences. The facility-to-facility differences range from a minimum of 0.3 percent to a maximum of 1.3 percent when the data from CEPr are not included.

The detailed analysis and interpretation of the facility-to-facility differences in engine temperature ratio are presented in Sections 9.2.2, 11.3.3, and 18.2.2 of Ref. 2.

## 2.3 Airflow

Typical engine airflow results from the four altitude facilities are shown in Fig. 5. The airflow measured at NASA is the highest and that measured at RAE(P) is the lowest. The repeat scan data are not distinguishable from the initial scan data, or they lie along the airflow characteristic for the NASA (Lewis), AEDC, and CEPr data. A total of 88 percent of the air flow data is within a 2-percent band.

The facility-to-facility differences in engine airflow are summarized in Fig. 6. An examination of the grouping of the differences by the test environmental parameters indicates a probable systematic effect of decreasing inlet pressure. The observed differences in airflow at the mid-thrust value range from a minimum of 1.3 percent to a maximum of 3.6 percent. An anomaly in engine airflow and/or corrected low rotor speed was identified for test condition 8 at CEPr; however, probable cause could not be established. Differences in the test installations at the four facilities created significant differences in the total pressure profile at the engine inlet. A special analysis of the effects of variations in inlet flow distortion at the tip of the low-pressure compressor (tip radial distortion) was completed by representatives from NASA. The results of this analysis indicated that the distortion contribution to airflow difference is probably in the range from +0.5 to +1.0 percent. The engine airflow at RAE(P) is less than the airflow measured by the referee instrumentation by about 1 percent; however, a probable cause for this difference could not be established. The facility-to-facility differences in engine airflow range from a minimum of 1.3 percent to maximum of 2.9 percent when the data from CEPr test condition 8 are not included.

The detailed analysis and interpretation of the facility-to-facility differences in engine airflow are presented in Sections 9.2.3, 11.3.1, 12.1, 13.2, 14, 17.3, and 18.2.3 of Ref. 2.

## 2.4 Fuel Flow

The typical variation of engine fuel flow WFRD as a function of corrected high rotor speed is shown in Fig. 7. The fuel flow decreases in the order of testing at NASA, AEDC, and RAE(P). The repeat scan data are not

distinguishable from the initial scan data or lie along the fuel flow characteristic for the NASA and AEDC results. The repeat scan data are separate from the initial scan data and do not lie along the fuel flow characteristic for the CEPr data. Again, it should be noted that only initial scan data are generally available from RAE(P).

A total of 63 percent of the fuel flow data is within the 2-percent band. The fuel flow measurements at CEPr are consistently displaced from the measurements from the other three facilities. Further, the CEPr data contain significant effects of thermal nonequilibrium as discussed in the paragraph below. A total of 85 percent of the fuel flow data is within the 2-percent band when the data from CEPr are not included.

A summary of the facility-to-facility differences in engine fuel flow at the mid-thrust value is shown in Fig. 8. There is no systematic effect of changes in the test environment. The observed differences in fuel flow range from a minimum of 3.8 percent to a maximum of 5.5 percent. In a manner similar to that discussed for rotor speed ratio in Section 2.1, the thermal nonequilibrium of the engine operating conditions at CEPr contributed from 0 to 2.5 percent to the facility-to-facility differences in a random manner. The engine cycle rematch contributed up to 0.5 percent to the interfacility differences in a systematic manner. The engine inlet total pressure distortion at the tip of the low-pressure compressor affected engine air flow as discussed in Section 2.3. This distortion effect is propagated into the facility-to-facility differences of fuel flow and would probably contribute between 0.5 and 1 percent. The reference engine fuel flow measurements were not obtained at RAE(P); therefore, this diagnostic parameter was not available for inclusion in the analysis. A special study was completed by representatives from NRCC to determine the effect of variations in the chemical analysis of the fuels on the observed interfacility differences in fuel flow. The fuel property analyses contributed from 0.04 percent to 0.35 percent. The facility-to-facility differences in fuel flow range from a minimum of 1.0 percent to a maximum of 3.0 percent when the CEPr data are not included.

The detailed analysis and interpretation of the facility-to-facility differences in engine fuel flow are presented in Sections 9.2.4, 11.3.2, 15, 18.2.4 of Ref. 2.

## 2.5 Net Thrust

The typical variation of engine net thrust versus engine pressure ratio is shown in Fig. 9. The net thrust measurements at NASA, AEDC, and RAE(P) are very tightly clustered. As was discussed in Section 2.2, the nozzle inlet total pressure measurements at CEPr were probably 2 percent low. The influence coefficient  $\Delta FNRD/\Delta P7Q2$  is approximately 2. Thus, the probable error in P7 at CEPr accounts for a displacement of net thrust of approximately 4 percent. The repeat scan data are not distinguishable from the initial scan data at NASA, AEDC, or CEPr. A total of 69 percent of the net thrust data is within the 2-percent band. The net thrust measurements at CEPr are consistently displaced from the measurements from the other three facilities. A total of 92 percent of the net thrust data is within the 2-percent band when the data from CEPr are not included.

The facility-to-facility differences in engine net thrust at the mid-thrust value are summarized in Fig. 10. An examination of the differences in each of the test environmental groupings shows a possible systematic effect of increasing engine inlet temperature and increasing ram pressure ratio. Observed differences in engine net thrust range from a minimum of 3.4 percent to a maximum of 5.4 percent. As discussed in Section 2.2, the measured values of nozzle inlet total pressure P7 were probably 2 percent low at CEPr. This probable error contributes approximately 4 percent to the observed differences in net thrust. Engine cycle rematch contribution ranges from 0 to -1.0 to 0 percent in a systematic manner. Unlike the discussion in Section 2.3 and 2.4 for airflow and fuel flow, respectively, the engine inlet flow distortion at the tip of the low-pressure compressor probably has little or no effect on the net thrust versus engine pressure ratio characteristic. The net thrust at AEDC was approximately 3 percent lower than at the other three facilities at test condition 9; however, the probable cause of this difference could not be determined. The interfacility differences in engine net thrust range from a minimum of 0.3 percent to a maximum of 3.3 percent when the CEPr data are not included. The maximum difference of 3.3 percent is reduced to only 1.4 percent when the AEDC data at test condition 9 are not included.

The detailed analysis and interpretation of the facility-to-facility differences in net thrust as a function of engine pressure ratio are included in Sections 9.2.5, 11.3.3, 12.3, 13.1, and 18.2.5 of Ref. 2.

## 2.6 Specific Fuel Consumption

Typical engine specific fuel consumption results from the four altitude facilities are shown in Fig. 11. The specific fuel consumption (SFCRD) was highest at NASA and lowest at AEDC. The repeat scan values are distinguishable from the initial scan values in many cases. The parameter set of SFCRD and FNRD was chosen to display this key performance parameter because of the basic relationships of these two variables. This choice, however, is unique when compared to the other five sets of parameters because net thrust appears in both the dependent and independent variables. The appearance of a common variable in both the independent and dependent parameters required special attention during the detailed analysis. A total of 89 percent of the specific fuel consumption data is within a 2-percent band.

The facility-to-facility differences in engine specific fuel consumption at the mid-thrust value are summarized in Fig. 12. No systematic effect of test environment is noted. Observed differences in SFC at the four facilities range from a minimum of 0.9 percent to a maximum of 2.4 percent. The engine rematch contribution probably ranged from 0 to 1 percent. The effect of inlet flow distortion at the engine inlet is probably negligible because of the offsetting effects in both fuel flow and net thrust. The SFC was higher at AEDC than at the other facilities for test condition 9; however, the probable cause of this difference could not be determined. The contribution of the thermal nonequilibrium of the engine at CEPr is negligible. This insensitivity to thermal nonequilibrium is judged to be fortuitous and is related to the specific design features of the J57 engines used in the UETP. It is highly unlikely that this insensitivity would exist on other engines having different aerodynamic and thermodynamic designs and different control logic. The range of facility-to-facility differences in SFC of 0.9 percent to 2.4 percent did not change as a result of the analysis.

The detailed analysis and interpretation of the facility-to-facility differences in specific fuel consumption are contained in Sections 9.2.6, 11.3.4, and 18.2.6 of Ref. 2.

### 3.0 ASSESSMENT OF INTERFACILITY DIFFERENCES

The effects of a total of 17 individual factors (see Fig. 13) on the UETP results were carefully assessed during the detailed analysis and interpretation of the observed performance differences between the four altitude test facilities. In the vast majority of these assessments, it was possible to establish with a high level of confidence the reason for and the magnitude of the contribution to the interfacility differences on a factor-by-factor basis. Two of these factors were of sufficient size and could be established with sufficiently high confidence that both were included in the final assessment of the interfacility differences. These two factors are (1) the engine thermal nonequilibrium during the data scans at CEPr and (2) the anomaly in the measurement of nozzle inlet total pressure at CEPr. The magnitude of each of these factors and the engine parameters affected are shown in Fig. 13. These two relatively large factors were included in the final assessment of interfacility differences by the removal of the CEPr data because no correction of the data to account for either effect was possible.

The remainder of the factors investigated were not incorporated in the final assessment of interfacility differences as shown in Fig. 13. The results of each assessment were judged on the basis of the magnitude of their effect on the interfacility differences and on the level of confidence which could be placed on the analysis and interpretation. Three of these factors, specifically the effects of engine cycle rematch on the rotor speed ratio and on engine temperature ratio and the effect of fuel properties analysis on fuel flow were not incorporated in the final assessment because they were judged to be too small to significantly affect UETP results, even though the magnitudes of the effects were known with sufficient confidence. Alternatively, a number of the factors such as the effect of engine cycle rematch on fuel flow, thrust, and SFC, the effect of inlet flow distortion on airflow and fuel flow, and the difference between the facility airflow measurement and the referee airflow measurement at RAE(P) were not incorporated in the final assessment because while the magnitudes were large enough to affect the assessment of interfacility differences, the confidence which the values could be established was judged to be too low. Remaining factors, e.g., the undefined anomalies at test condition 8 at CEPr and test condition 9 at AEDC, and the fuel system difficulties encountered at several facilities could not be resolved by analysis.

Two additional factors, engine inlet turbulence and boattail force, were carefully assessed during the detailed analysis and interpretation of the facility-to-facility differences. However, neither of these factors is listed in Fig. 13 for two very different reasons.

In the case of the engine inlet turbulence, the measurement approach defined in the General Test Plan (Ref. 1) did not permit sufficient characterization of turbulence levels between facilities to determine if the different turbulence levels created a change in performance (Section 12.2-Ref 2.)

On the other hand, the boattail force measurements prescribed in the General Test Plan provided high-quality measurements of these forces. These measurements showed that the boattail force for the UETP test configurations was less than 0.1 percent of the net thrust level and was, therefore, insignificant (Section 12.3-Ref. 2).

A compilation of the performance of all four altitude test facilities is shown in Fig. 14. The results of both methods of facility performance determination, i.e., (1) the fraction of the population of all data which was within a 2-percent band and (2) the minimum and maximum facility-to-facility differences for all test conditions at one power setting are shown for each of the six sets of engine performance parameters. The final analysis of the population distribution of all the data showed that 85 to 95 percent was within the 2-percent band. The maximum facility-to-facility performance differences at the mid-thrust range of the engine were generally 3 percent or less.

#### LIST OF REFERENCES

1. Subcommittee 01, AGARD Propulsion and Energetics Panel, Working Group 15, "Uniform Engine Testing Program General Test Plan," June 1983, (Revised edition).
2. Ashwood, P. F., principal author, and Mitchell, J. G., editor, "The Uniform Engine Test Programme-Report of PEP WG15," AGARD Advisory Report No. 248, February 1990.

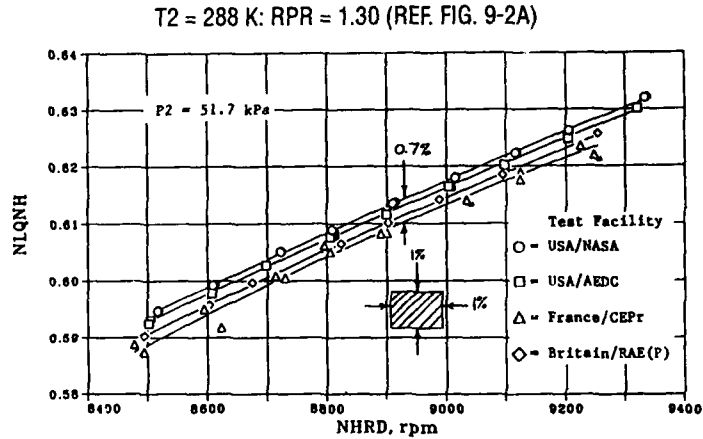


Figure 1. Typical rotor speed ratio results.

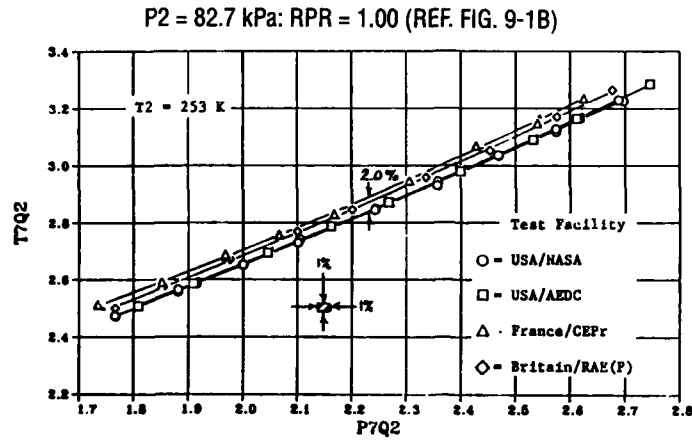
### $\Delta$ NLQNH VS. NHRD AT MID-THRUST VALUE

82.7/1.00/T2			P2/1.30/288			82.7/F 288		
TC	T2	$\Delta\%$	TC	P2	$\Delta\%$	TC	RPR	$\Delta\%$
1	253	0.5	6	82.7	0.4	3	1.00	0.5*
2	268	0.7	7	51.7	0.7	5	1.06	0.8
3	288	0.5*	8	34.5	0.8	6	1.30	0.4
4	308	0.7	9	20.7	0.8	10	1.70	0.7

\* DATA FROM ONLY 3 FACILITIES

- NO SYSTEMATIC EFFECT OF TEST ENVIRONMENTS
- $0.4\% \leq \text{OBSERVED DIFFERENCE} \leq 0.8\%$
- SMALLEST DIFFERENCES OF ANY PARAMETER SET
- THERMAL NONEQUILIBRIUM AT CEPr CONTRIBUTION 0 TO -0.3% (RANDOM)
- ENGINE CYCLE RE-MATCH CONTRIBUTION - 0.3% (SYSTEMATIC)
- $0.04\% \leq \text{DIFFERENCE W/O CEPr} \leq 0.6\%$

Figure 2. Differences in engine rotor speed ratio.



## NOTE:

- $T_7Q_2$  NEUTRAL OR INCREASING IN ORDER OF TESTS [NASA, AEDC, RAE (P)]
- PROBABLE  $P_7$  ERROR 2% LOW-INFLUENCE COEFFICIENT 0.6 (CEPr)
- REPEAT SCAN NOT VISIBLE (NASA, AEDC, CEPr)
- 98% OF DATA WITHIN 2% BAND

Figure 3. Typical engine temperature ratio results.

 $\Delta T_7Q_2$  VS.  $P_7Q_2$  AT MID-THRUST VALUE

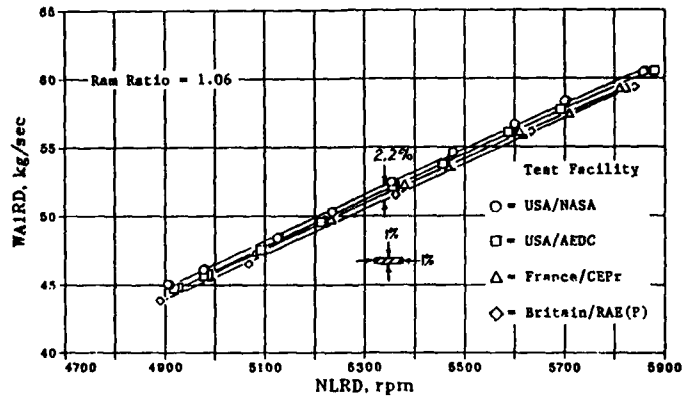
82.7/1.00/ $T_2$			$P_2/1.30/288$			82.7/RPR/288		
TC	$T_2$	$\Delta\%$	TC	$P_2$	$\Delta\%$	TC	RPR	$\Delta\%$
1	253	2.0	6	82.7	1.2	3	1.00	1.5*
2	268	2.0	7	51.7	1.3	5	1.06	1.2*
3	288	1.5*	8	34.5	0.7	6	1.30	1.2
4	308	1.5	9	20.7	0.6	10	1.70	1.5*

\* DATA FROM ONLY 3 FACILITIES

- POSSIBLE SYSTEMATIC EFFECT OF INCREASING  $T_2$  AND DECREASING  $P_2$
- $0.6\% \leq \text{OBSERVED DIFFERENCE} \leq 2.0\%$
- ENGINE CYCLE REMATCH CONTRIBUTION +0.3% (SYSTEMATIC)
- $P_7$  MEASUREMENT 2% LOW AT CEPr (INFLUENCE COEFF.  $\sim 0.6$ ) CONTRIBUTION +1.2%
- $0.3\% \leq \text{DIFFERENCE W/O CEPr} \leq 1.3\%$

Figure 4. Differences in engine temperature ratio.

P2 = 82.7 kPa; T2 = 288 K (REF. FIG. 9-3C)



NOTE:

- WA1RD NASA HIGHEST AND RAE(P) LOWEST
- REPEAT SCANS NOT VISIBLE OR ALONG CHARACTERISTIC (NASA, AEDC, CEPr)
- 88% OF DATA WITHIN 2% OF BAND

Figure 5. Typical engine airflow results.

Δ WAIRD VS. NLRD AT MID-THRUST VALUE

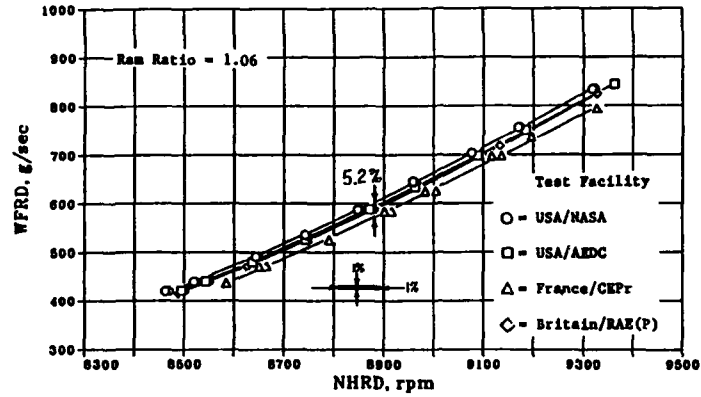
82.7/1.00/T2			P2/1.30/288			82.7/RPR/288		
TC	T2	Δ%	TC	P2	Δ%	TC	RPR	Δ%
1	253	2.6	6	82.7	1.6	3	1.00	1.3*
2	268	2.9	7	51.7	1.5	5	1.06	2.2
3	288	1.3*	8	34.5	3.6	6	1.30	1.6
4	308	2.0	9	20.7	2.2	10	1.70	1.6

\* DATA FROM ONLY 3 FACILITIES

- PROBABLE SYSTEMATIC EFFECT OF DECREASING P2
- 1.3% ≤ OBSERVED DIFFERENCE ≤ 3.6%
- UNEXPLAINED ANOMALY IN WA1RD AND NLRD DATA FROM CEPr AT TEST CONDITION 8
- INLET FLOW DISTORTION (TIP) CONTRIBUTION PROBABLY +0.5 TO +1%
- WA1RD AT RAE(P) LESS THAN WA2RD (REFEREE) BY - 1%
- 1.3% ≤ DIFFERENCE W/O CEPr TC8 ≤ 2.9%

Figure 6. Differences in engine airflow.

P2 = 82.7 kPa; T2 = 288 K (REF. FIG. 9-3D)



NOTE:

- WFRD DECREASING IN ORDER OF TESTS [NASA, AEDC, RAE(P)]
- REPEAT SCANS NOT VISIBLE OR ALONG CHARACTERISTIC (NASA, AEDC)
- REPEAT SCANS VISIBLE AND NOT ALONG CHARACTERISTIC (CEPr)
- SINGLE SCANS ONLY [RAE(P)]
- 63% OF DATA WITHIN 2% BAND (85% W/O CEPr)

Figure 7. Typical engine fuel flow results.

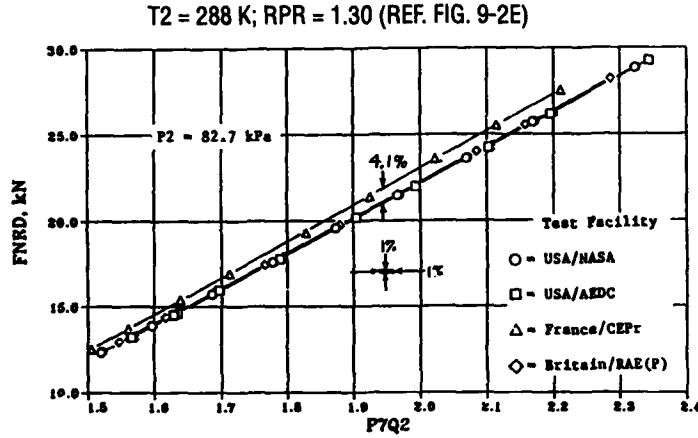
Δ WFRD VS. NHRD AT MID-THRUST VALUE

82.7/1.00/T2			P2/1.30/288			82.7/RPR/288		
TC	T2	Δ%	TC	P2	Δ%	TC	RPR	Δ%
1	253	4.6	6	82.7	3.8	3	1.00	4.3*
2	268	5.5	7	51.7	5.0	5	1.06	5.2
3	288	4.3*	8	34.5	4.0	6	1.30	3.8
4	308	5.3	9	20.7	4.1	10	1.70	5.1

\* DATA FROM ONLY 3 FACILITIES

- NO SYSTEMATIC EFFECT OF TEST ENVIRONMENTS
- 3.8% ≤ OBSERVED DIFFERENCE ≤ 5.5%
- THERMAL NONEQUILIBRIUM AT CEPr CONTRIBUTION 0 TO 2.5% (RANDOM)
- ENGINE CYCLE REMATCH CONTRIBUTION +0.5% (SYSTEMATIC)
- INLET FLOW DISTORTION (TIP) CONTRIBUTION PROBABLY +0.5 TO 1%
- WFRD (REFEREE) NOT OBTAINED AT RAE (P)
- FUEL PROPERTIES ANALYSIS (SPEC. GRAV., HEAT VALUE) CONTRIBUTION 0.04% TO 0.35%
- 1.0% ≤ DIFFERENCE W/O CEPr ≤ 3.0%

Figure 8. Differences in engine fuel flow.



- NOTE:
- FNRD TIGHTLY CLUSTERED [NASA, AEDC, RAE(P)]
  - PROBABLE P7 ERROR 2% LOW INFLUENCE COEFFICIENT 2.0 (CEPr)
  - REPEAT SCANS NOT VISIBLE (NASA, AEDC, CEPr)
  - 69% OF DATA WITHIN 2% BAND (92% W/O CEPr)

Figure 9. Typical engine net thrust results.

Δ FNRD VS. P7Q2 AT MID-THRUST VALUE

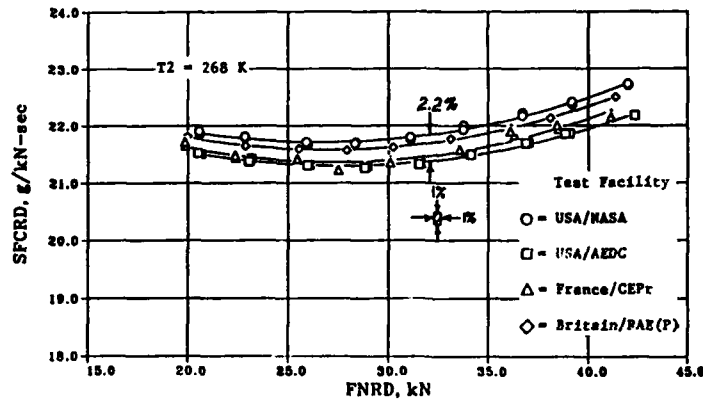
82.7/1.00/T2			P2/1.30/288			82.7/RPR/288		
TC	T2	Δ%	TC	P2	Δ%	TC	RPR	Δ%
1	253	3.4	6	82.7	4.1	3	1.00	3.9*
2	268	4.1	7	51.7	5.4	5	1.06	3.8*
3	288	3.9*	8	34.5	4.6	6	1.30	4.1
4	308	5.0	9	20.7	4.3	10	1.70	4.5*

\* DATA FROM ONLY 3 FACILITIES

- POSSIBLE SYSTEMATIC EFFECT OF INCREASING T2 AND INCREASING RPR
- 3.4% ≤ OBSERVED DIFFERENCE ≤ 5.4%
- P7 MEASUREMENT 2% LOW AT CEPr (INFLUENCE COEFF. -2) CONTRIBUTION 4%
- ENGINE REMATCH (DETERIORATION) CONTRIBUTION 0 TO -1% TO 0 (SYSTEMATIC)
- FLOW DISTORTION (TIP) AT ENGINE INLET CONTRIBUTION PROBABLY 0
- AEDC 3% LOWER THAN OTHER 3 FACILITIES AT TEST CONDITION 9 - CAUSE NOT DETERMINED
- 0.3% ≤ DIFFERENCE W/O CEPr ≤ 3.3%

Figure 10. Differences in engine net thrust.

P2 = 82.7 kPa; RPR = 1.00 (REF. FIG. 9-1F)



NOTE:

- SFCRD NASA HIGHEST AND AEDC LOWEST
- MANY REPEAT SCANS VISIBLE
- FNRD COMMON IN BOTH DEPENDENT AND INDEPENDENT VARIABLES
- 89% OF DATA WITHIN 2% BAND

Figure 11. Typical engine specific fuel consumption results.

Δ SFCRD VS. FNRD AT MID-THRUST VALUE

82.7/1.00/T2			P2/1.30/288			82.7/RPR/288		
TC	T2	Δ%	TC	P2	Δ%	TC	RPR	Δ%
1	253	2.4	6	82.7	1.9	3	1.00	1.7*
2	268	2.2	7	51.7	1.4	5	1.06	2.3
3	288	1.7*	8	34.5	0.9	6	1.30	1.9
4	308	2.0	9	20.7	2.1	10	1.70	1.5

\* DATA FROM ONLY 3 FACILITIES

- NO SYSTEMATIC EFFECTS OF TEST ENVIRONMENTS
- 0.9% ≤ OBSERVED DIFFERENCE ≤ 2.4%
- ENGINE REMATCH (DETERIORATION) CONTRIBUTION 0 TO ~+1%
- FLOW DISTORTION (TIP) AT ENGINE INLET CONTRIBUTION PROBABLY 0
- AEDC HIGHER THAN OTHER FACILITIES AT TEST CONDITION 9 - CAUSE NOT DETERMINED
- THERMAL NONEQUILIBRIUM AT CEPr CONTRIBUTION -0 (FORTUITOUS J-57 SPECIFIC)
- 0.9% ≤ DIFFERENCES ≤ 2.4%

Figure 12. Differences in engine specific fuel consumption.

ENGINE PARAMETER	FACTORS INCORPORATED IN FINAL ASSESSMENT (%)	FACTORS NOT INCORPORATED IN FINAL ASSESSMENT (%)
NLQNH VS. NHRD	(a) THERMAL NONEQUILIBRIUM CEP <sub>r</sub> ( $\leq -0.3$ )	(a) ENGINE CYCLE REMATCH (-0.3)
T7Q2 VS. P7Q2	(a) P7 MEASUREMENT CEP <sub>r</sub> ( $2 \times 0.61C = 1.2$ )	(a) ENGINE CYCLE REMATCH (+0.3)
WA1RD VS. NLRD		(a) INLET FLOW DISTORTION (TIP) ( $\rightarrow +0.5$ TO 1.0) (b) WA1RD < WA2RD (REFEREE) RAE (P) (-1.0) (c) UNDEFINED ANOMALY IN WA1RD, NLRD CEP <sub>r</sub> TC8
WFRD VS. NHRD	(a) THERMAL NONEQUILIBRIUM CEP <sub>r</sub> (0 TO -2.5)	(a) ENGINE CYCLE REMATCH (+0.5) (b) INLET FLOW DISTORTION (TIP) ( $\rightarrow +0.5$ TO 1.0) (c) FUEL PROPERTIES ANALYSIS ( $< 0.4$ ) (d) FUEL SYSTEM DIFFICULTIES (DATA NONRECOVER.)
FNRD VS. P7Q2	(a) P7 MEASUREMENT CEP <sub>r</sub> ( $2 \times 21C = 4$ )	(a) ENGINE CYCLE REMATCH (0 TO -1 TO 0) (b) INLET FLOW DISTORTION (TIP) ( $\rightarrow +0.5$ TO 1.0) (c) UNDEFINED ANOMALY IN FNRD AEDC TC9
SFCRD VS. FNRD	(a) NONE	(a) ENGINE CYCLE REMATCH (0 TO +1.0)

Figure 13. Assessments of interfacility differences.

REFERENCE TABLE 18-1

ENGINE PARAMETER (INDEPENDENT VARIABLE)	OVERALL PERCENTAGE SPREAD AT MID-THRUST (WITHOUT CEP <sub>r</sub> )	DATA WITHIN 2-PERCENT BAND, PERCENT (WITHOUT CEP <sub>r</sub> )
NLQNH (NHRD)	0.4 TO 0.8 (0.04 TO 0.8)	99
T7Q2 (P7Q2)	0.6 TO 2.0 (0.3 TO 1.3)	98
WA1RD (NLRD)	1.3 TO 3.6 (1.3 TO 2.9)	88
WFRD (NHRD)	3.8 TO 5.5 (1.0 TO 3.0)	63 (85)
FNRD (P7Q2)	3.4 TO 5.4 (0.3 TO 3.3)	69 (92)
SFCRD (FNRD)	0.9 TO 2.4 (0.9 TO 2.4)	89

Figure 14. Summary of differences between altitude facilities.

## COMPARISON OF GROUND-LEVEL TEST CELLS AND GROUND-LEVEL TO ALTITUDE TEST CELLS

by  
D.M. Rudnitski  
Section Head  
Engine Laboratory  
National Research Council Canada  
Ottawa, Ont. K1A 0P6  
CANADA

### SUMMARY

The Uniform Engine Test Program was set up to examine gas turbine test procedures, instrumentation techniques and data reduction methods employed by engine test facilities in several AGARD countries.

Two major classes of facilities participated, altitude and ground-level test beds. Two engines were to be operated in the test facilities, but as the program evolved, only one engine was tested in all the altitude facilities, and the other in the ground-level beds, with some overlap between. Thus the performance assessment had to be laid out with three specific comparison objectives:

- 1) altitude with altitude
- 2) ground-level with ground-level
- 3) ground-level with altitude

The previous lecture dealt with objective one, data comparisons of altitude with altitude. This lecture will deal with objectives two and three.

Steady-state performance of a J57-P-19 turbojet engine was evaluated in four ground-level test beds, three of them enclosed: NRCC, CEPr, and TUAF, and an open-air test bed at NAPC. Detailed inter-facility comparisons were made on the three basic engine parameters, airflow, net thrust, and specific fuel consumption, and reasons sought for any differences.

Objective three was to compare data taken in an altitude facility to those obtained in a ground-level test bed. As not all facilities tested both engines in the round-robin, engine SN 607594 was used for altitude to altitude and altitude to ground-level, and engine 615037 for ground-level bed comparison. AEDC was the only altitude facility capable of operation at sea-level-static conditions for both engines, which provided a direct comparison of the validity of the normalizing equations. CEPr tested one engine in both a ground-level bed and in their altitude facility. Significant data scatter and biases in the CEPr data made meaningful comparisons of dubious value, reducing the size of the database.

A summary of percentage differences for the three basic performance parameters evaluated at approximately the mid-thrust level is shown below.

Engine parameter	Independent variable	Inter-facility Spread % ground-level	Inter-facility spread - % ground-level/altitude
FNR <sup>3</sup>	P7Q2	0.7 (2.5) <sup>1</sup>	5.1 (3.0) <sup>2</sup>
SFCR <sup>3</sup>	FNR	1.8 (3.0) <sup>1</sup>	2.8
WA1R	NLR	1.9 (4.0) <sup>2</sup>	2.5

- NOTES: 1) Bracketed values include TUAF data  
2) Bracketed value excludes CEPr (Alt) data  
3) NRCC values for thrust approximately 1% low

In evaluating NAPC data, it was discovered that the thrust accounting procedures for enclosed test beds was not correctly defined by the GTP equations. NRCC corrected their data, which demonstrated that gross thrust was low by approximately 1.0%. Therefore any parameter for NRCC containing thrust will be low.

Once account is taken for the known anomalies, the inter-facility data agreement falls within the declared measurement uncertainty bands.

### LIST OF SYMBOLS

AEDC	Arnold Engineering Development Center
CEPr	Centre d'Essais des Propulseurs
FNR	Net Thrust Corrected to Sea-Level Conditions, kN
GTP	General Test Plan
NAPC	Naval Air Propulsion Centre
NASA	National Aeronautics and Space Administration Lewis Research Center
NHR	High Pressure Compressor Rotor Speed Corrected to Sea-Level Conditions, rpm

NLQNH	Ratio of Low Pressure Compressor to High Pressure Compressor Rotor Speeds
NLR	Low Pressure Compressor Rotor Speed Corrected to Sea-Level Conditions, rpm
NRCC	National Research Council of Canada
P2	Engine Inlet Total Pressure, kPa
P7	Exhaust Nozzle Inlet Total Pressure, kPa
P7Q2	Ratio of Exhaust Nozzle Inlet to Engine Inlet Total Pressure
PAMB	Static Pressure at Exhaust Nozzle Exit Plane, kPa
RAE(P)	Royal Aerospace Establishment Pyestock
RPR	Ram Pressure Ratio
SFCR	Specific Fuel Consumption Corrected to Sea-Level Conditions, g/kN-sec
SLS	Sea-Level Static Conditions (101 kPa, 1.0 RPR, 288 K)
T2	Engine Inlet Total Temperature, K
T7	Exhaust Nozzle Inlet Total Temperature, K
T7Q2	Ratio of Exhaust Nozzle Inlet to Engine Inlet Total Temperature
TC	Test Condition
TUAF	Turkish Air Force Supply and Maintenance Centre
UETP	AGARD-PEP Uniform Engine Test Program
WA1R	Facility Airflow Corrected to Sea-Level Conditions, kg/sec
WFER	Reference Fuel Mass Flow Corrected to Sea-Level Conditions, g/sec
WFR	Facility Fuel Mass Flow Corrected to Sea-Level Conditions, g/sec

## 1 INTRODUCTION

The previous lecture dealt with the observed differences of engine performance parameters obtained in four altitude facilities, NASA LeRC, AEDC, RAE(P), and CEPr. Ten test conditions were specified that varied inlet temperature, T2, inlet pressure, P2, and ram pressure ratio, RPR. An additional test condition, sea-level-static, was requested, but only one altitude facility, AEDC, was capable of operation at this point. The GTP (Ref. 1) specified that both J57 engines were to be tested at all facilities, be it altitude or ground-level. Due to operational and program constraints, not all agencies were able to fulfil this requirement: one engine, SN 607594, completed the rounds in the altitude facilities, and the other SN 615037, in the ground-level test facilities. Thus came the problem of addressing the altitude to ground-level test bed comparison. It was decided that comparisons of altitude cells would be based on data from engine 607594, ground-level beds based on data from engine 615037, and ground-level with altitude using engine 607594. This latter comparison was included as there has been evidence that the performance of an engine measured in an altitude cell at conditions close to ground-level can differ from that measured on a ground-level test bed. One agency, CEPr, tested engine 607594 in both an altitude tank and on a ground-level test bed.

Six sets of engine performance parameter relationships were selected to assess the differences in all the facilities. These were:

NLQNH vs. NHR	WA1R vs. NLR	FNR vs. P7Q2
T7Q2 vs. P7Q2	WFR vs. NHR	SFCR vs. FNR

The data presented for ground-level facilities are corrected to standard day conditions, whereas the altitude data are corrected to desired conditions. For data comparison between the facility types, the desired condition becomes sea-level-static, consistent with the equations in Ref. 2. None of the ground-level beds had environmental control, thus testing was conducted at the prevailing ambient conditions of temperature, pressure and humidity. With the exception of CEPr, which operated between  $277 < T2 < 283$  K, the required temperature corrections did not introduce any additional errors (Section 16.3 of Ref. 2).

The engine performance parameter relationships were developed by fitting second order, polynomial curve fits of the data points from each facility. To quantify inter-facility differences for the purpose of comparison, the maximum spread of each dependent parameter (expressed as a percentage of the median value) was calculated at approximately the mid-thrust point. The magnitude of the spreads shown were derived from tabulated data.

There are two sections for this data comparison. First, the ground-level facilities will be discussed, then second, the ground-level to altitude.

## 2 Ground-Level Facility Comparisons

Comparisons of the ground-level beds are based on data from engine 615037 acquired at NRCC, CEPr and TUAF, with comparable data obtained at the AEDC altitude facility at SLS conditions included for reference.

The data show the same general trends (curve slopes similar) and, with the exception of the TUAF data, are in moderately good agreement. The reasons why the TUAF data depart rather more from the mean than do the data from the other facilities are most probably due to the lack of empirical corrections for this particular engine type. The TUAF test stand is designed for pre- and post-overhaul testing of only those engines in the TUAF inventory; since the J57-19 is not one of these, cell correction factors were not available. In addition, manual recording of data increased the measurement uncertainty. The UETP results are not therefore considered representative of TUAF facility capability. Therefore, the TUAF data have not been included when calculating the percentage spreads between facilities, but they are included in the discussions which follow.

At the time of writing UETP AR 248 (Ref. 2), the data from the only outdoor stand, NACP, were not available for consideration in the detailed comparison. Subsequent analysis by NRCC and NACP, using these new data, revealed that the UETP calculation procedures in Appendix IV of Ref. 2 lead to results which differ slightly from those obtained using standard methods. Reference should be made to Appendix VIII of Ref. 2 for a discussion of the influence of environmental factors on the measurement of thrust in a ground-level test bed.

The graphical comparison in Section 3.5 and values quoted in Sections 18.3.5 and 18.3.6 of Ref. 2 do not contain the environmental corrections, and therefore should be viewed with caution. In this lecture, the figures from Appendix VIII of Ref. 2 will be used, as they include the NAPC data. For consistency with Section 9 of Ref. 2, the data are based on the equations in the GTP.

## 2.1 Rotor Speed Ratio

Rotor speed ratio as a function of corrected high rotor speed for the four ground-level facilities and one altitude facility is displayed as Figure 1. The curve shapes are all similar and show a maximum spread of 1.5%, bounded by TUAf at the top and CEPr at the bottom. Without TUAf data, the spread drops to 0.4-0.5%, which is similar to that observed in the altitude facilities.

A reason for this large shift in TUAf rotor speed ratio may be due to an expected pressure distortion at the compressor inlet, caused by the close proximity of the facility vertical inlet to the engine face. As the detailed pressure measurements were not recorded in TUAf, this hypothesis cannot be confirmed.

As in the altitude case, CEPr shows a significant separation between the points from the two data scans at each power setting. This separation indicates that the engine had not reached thermal equilibrium (see Section 18.2.1 of Ref. 2), and could account for these and other differences.

The NAPC data lie slightly above the CEPr values but below those of NRCC and AEDC which show very good agreement. It was shown that thermal stability was a problem at CEPr, however this was not the case at NAPC. The difference of 0.4% is just within the uncertainty limits of NHR. However, given that systematic cycle rematch could account for about a 0.3% change, the remaining difference is well within the measurement uncertainty (0.2 - 1.6%).

## 2.2 Temperature Ratio

The engine pumping characteristic, or temperature ratio versus pressure ratio is shown in Figure 2. The maximum spread of 1.1% (2.5% including TUAf) is less than that seen in the altitude facility comparisons (1.5 - 2.0% at unity ram ratio). TUAf data are not directly comparable due to the limited sampling at Station 7. (See Section 4.4 of Ref. 2).

Values of T7Q2 measured at CEPr and AEDC agree within 0.5%. The difference between NRCC and AEDC or CEPr is most likely caused by the method of computing T7 from point measurements. At NRCC, a large number of thermocouples progressively became unserviceable during the course of the test. As the procedure for accounting for unserviceable thermocouples in a highly non-homogeneous flow field was not the same at all facilities (see Appendix VI of Ref. 2), the derived T7 could be significantly different.

The addition of NAPC data created two distinct groups: CEPr with AEDC and NRCC with NAPC. The reason given for NRCC deviation was the treatment accorded to failed T7 instrumentation. The determination of P7 at NAPC was not in accordance with the test plan as only two of the four rakes were used. Given that the pressure profile was highly non-homogeneous, any comparison using NAPC data is not valid. However, the differences of 1.1% between the facilities were well within the uncertainty band (0.9 - 1.8%).

## 2.3 Airflow

Corrected engine airflow (WA1R) measured by the facility, as a function of corrected low-pressure-compressor rotor speed, is presented as Figure 3. The spread at the mid-thrust point was 1.8% (4.8% with TUAf). The highest value of WA1R was obtained from TUAf, the lowest from NRCC. AEDC values were in close agreement with CEPr and lie about mid-way between the two extremes. It should be noted that for purposes of this comparison, the reference value of airflow (WA2R) measured at TUAf was inserted as WA1R, as a facility measurement for airflow was not available.

The analysis presented in Section 14.4 of Ref. 2 through the use of flow functions, clearly demonstrated that AEDC had consistently good agreement (0.5%) between the two air metering locations, WA1R and WA2R. CEPr had a difference of approximately 1.3%, and NRCC 2.0%, which was attributed to a known measurement problem at Station 1.0 (WA1R). Based on the flow functions, and the data in Figure 3, it can be inferred that the airflow measured at AEDC must have been reasonably close to the true value. NRCC confirmed that their airflow was between 1.0 and 1.5% low because of difficulty in determining the discharge coefficient.

The NAPC WA1R data deviated in shape from the other facilities, especially at the extremes. A possible explanation for the unique shape of the NAPC data may lie in the short inlet section which results in sharp Station 1.0 pressure profiles as a function of engine power setting. Wind gusts also contributed to the problem as both the magnitude and direction changed throughout the test sequence, introducing additional errors.

Discounting TUAf and NRCC values due to defined problems, the agreement is better than 0.5%, well within the estimated measurement uncertainty (0.6 - 1.5%).

## 2.4 Fuel Flow

Corrected engine fuel flow (WFR), as a function of corrected high rotor speed is presented in Figure 4. The performance trends measured by all four facilities are consistent, but exhibit significant differences in level. At a given value of NHR the maximum spread is 3.5% (8% with TUAf). The CEPr data exhibited a considerable degree of scatter probably caused by engine thermal instability. The agreement between NRCC and AEDC was 1.0 - 1.3%, and between NRC and NAPC 0 - 0.5%, depending upon the power setting.

The comparison between the reference, engine mounted meters and the facility fuel measurements, is dealt with in Section 15 of Ref. 2. It was shown that the agreement between the two systems was very good, 0.3 - 0.6% for AEDC and NRCC, and 1.0% for CEPr. TUAf did not have a facility fuel flow measurement.

Evaluation of fuel properties, lower heating value and specific gravity added an additional difference of up to 0.35% (Appendix VII of Ref. 2). There were also some cycle rematch effects as seen in Figure 1. Considering these effects, and that the declared measurement uncertainty ranged from 0.9 - 2.5%, this agreement is quite good.

## 2.5 Net Thrust

Corrected net thrust as a function of engine pressure ratio (P7/Q2) is displayed as Figure 5. Discounting NACP data, the maximum spread is 0.7% (2.5% with TUAF) which is considerably less than the 3 to 4% seen in the altitude facilities at a ram ratio of unity. There are no discernable effects of inlet temperature mismatch from standard conditions ( $T_2 = 288 \text{ K}$ ). NACP data for P7 were not valid as measurements from only two of the four pressure rakes were recorded.

In spite of this good agreement, there were known problems in the sampling of P7, as swirl effects and failed or leaky probes considerably increased the uncertainty of the P7 measurement. Studies of gross thrust using nozzle coefficients and PS7 in Section 13 of Ref. 2, more clearly separated out the facility thrust measurements. Comparing nozzle coefficients, the spread increased from 0.7% to almost 2.0%, bounded by AEDC at the high end, and NRCC at the bottom. The main reason for this increase was in the definition of ambient pressure in an enclosed cell, and in the method of thrust accounting. Details of the accounting procedure are in Appendix VIII of Ref. 2. For the UETP, the effect of redefining the thrust accounting in the NRCC facility was to increase net thrust by almost 1.0%.

With the known inadequacies in the ground-level thrust data and P7 measurements, comparisons of FNR against P7/Q2 are not considered valid.

## 2.6 Specific Fuel Consumption

Corrected fuel consumption (SFCR) as a function of corrected net thrust (FNR) is shown in Figure 6. The performance trends from all facilities were consistent (curve slopes similar) except for data from TUAF which indicate a decreasing SFCR level with increasing FNR, crossing the other facility curves at the higher thrust levels. The spread in SFCR at FNR = 33 kN was 1.8% bounded by NRCC and AEDC (3.0% with TUAF).

The SFCR data for NACP exhibited a very large degree of scatter, in some cases up to 1.3% for back-to-back points. Again, it appears that the wind gusts affected the scale force thrust by altering the inlet momentum and the scrubbing drag on the test bed. With such scatter it is difficult to compare using curve fits, but the actual data points are still bounded by those obtained at AEDC and NRCC. The spread of data between AEDC and NRCC (1.8%) is just within the declared uncertainty band.

The problems with defining FNR in the previous section affects the SFCR calculation. Using the revised FNR, the difference in the SFCR spread between NRCC and AEDC has been reduced from 1.8 to 1.2% (Figure 7), and from 1.0 to 0.3% between NRCC and NACP. This agreement is considered very good.

## 2.7 Summary of Ground-Level Facility Differences

Engine SN 615037 was tested at four ground-level facilities, one of them an open-air test bed, and at an altitude facility operated at SLS conditions. The comparisons in the UETP were originally conducted without the benefit of the open-air bed data from NACP, but subsequent inclusion did not alter the differences. In fact, the data were crucial to rationalizing the discrepancies in the thrust accounting methodology in the enclosed ground-level facilities.

The figures in this lecture, extracted from Appendix VIII of Ref. 2, were used as they incorporated the NACP data. There are some differences in the percentage spread computed for Appendix VIII compared to those quoted in Section 9 and 18 of Ref. 2. Those listed in this paper and Appendix VIII are to be taken as correct, for they were systematically computed for all the ground-level facilities based on second-order curve fits of declared data. The tabulated results, with corrections incorporated, are displayed as Figure 8. As a reference, the estimated uncertainty band is listed for each parameter.

In general, the data agreement is quite good. Known anomalies have been identified, and when duly considered, virtually all data agree within the declared uncertainty limits.

## 3 Ground-Level/Altitude Facility Comparisons

The ground-level to altitude facility comparisons are based on data from Engine 607594 acquired at NASA, AEDC, RAE(P), CEPr and NRCC. With the exception of NASA, all the altitude facility data related to an inlet temperature of 288 K. Because Test Condition 3 (TC 3) for Engine 607594 was omitted by NASA due to a restricted test window, TC 4 (308 K) was substituted. In view of this difference and the uncertain magnitude of its effect on the levels of the parameters considered, the NASA data were disregarded when evaluating percentage spreads. However, to prevent misrepresentation of facility test capability, the NASA data were included in the facility comparisons.

The data from all altitude facilities, except AEDC, required use of the UETP equations to adjust the data from the as-tested inlet pressure of 82.7 kPa to the standard sea-level value of 101.3 kPa. While these adjustments could introduce discrepancies (see Sections 13 and 16 of Ref. 2) it was judged that the discrepancies would be negligibly small at the high pressure condition.

In Section 2.0 of this paper, data from engine SN 615037, obtained at the AEDC altitude facility operating at sea-level-static conditions, were included in the comparison of ground-level facilities. It was shown that if all identified anomalies were accounted for, the overall agreement was very good.

Having compared AEDC measurement capabilities for engine 615037, another comparison opportunity was created for engine 607594. As well as AEDC, data from two additional altitude facilities were available, CEPr and RAE(P), all operating at TC 3 (82.7 kPa, 1.00 RPR, 288 K). AEDC also obtained data at SLS conditions, TC 11, and in this comparison, both data sets were used to assess the suitability of the normalization equations provided in the GTP. CEPr tested the same engine in the altitude facility at TC 3, and in a ground-level test bed at TC 11. These data will be discussed, as they presented an opportunity for a direct 'in-house' comparison of measurement procedures.

In the figures that follow, data from AEDC TC 3 are not shown; they will however be used in the discussion where relevant. NASA TC 4 data are illustrated, but are not included in computing the percentage data spread.

Ref. 2 does not provide a direct comparison of AEDC TC 3 and TC 11. Since altitude to ground-level test bed data are normalized from TC 3 to TC 11, it must be demonstrated that the equations are valid. Figure 9 illustrates the percentage difference of each parameter pair using AEDC TC 11 measurements as the datum. Values for the parameter pairs were computed at approximately the mid-thrust point using second-order polynomial fitted data, as provided by NASA.

### 3.1 Rotor Speed Ratio

Rotor speed ratio, presented as Figure 10, shows a spread similar to that observed in the ground-level comparison in Section 2.1. Again, a very significant scatter in CEPr data was observed in both facilities, and is attributed to inadequate thermal stabilization of the engine. Agreement for AEDC between the two test conditions is within 0.25%, inside the declared measurement uncertainty band. With the exception of CEPr TC 3, both ground-level facilities were lower than the altitude ones. The overall spread, including CEPr data is 0.5%.

### 3.2 Temperature Ratio

Temperature ratio as a function of pressure ratio, Figure 11, is bounded at the high end by CEPr TC 3 and at the low end by NRCC. CEPr, again with significant data scatter, has a difference of 1.3% between their two facilities, whereas AEDC demonstrated a 0.4% bias between the two test conditions. In both CEPr and AEDC, the results obtained at TC 11 conditions were lower than those at TC 3.

There were difficulties with both T7 and P7 measurements, as discussed in Section 2.2, accounting for some of the differences. The overall spread of 2.3% is relatively large, but the quality of the measurements do not lead to credible conclusions.

### 3.3 Airflow

The airflow spread, 2.5%, is slightly larger than that observed in the previous comparisons (Figure 12). A bias in the TC 11 data relative to TC 3 at CEPr (2.0%) puts in question the measurement accuracy at TC 11 (see Figure 9). AEDC showed a difference of 0.4% between these two conditions. Discounting CEPr TC 11 airflow, the spread reduces to 1.4%. NRCC had problems establishing a flow coefficient, and consequently declared their airflow as low by about 1.0%. Notwithstanding this problem, the spread between facilities is within the measurement uncertainty.

### 3.4 Fuel Flow

Fuel flow as a function of corrected high rotor speed is shown as Figure 13. The indicated spread groups CEPr at the low end and the remaining facilities, tightly grouped, at the high end. In addition to this bias in excess of 2%, CEPr showed a large degree of data scatter, putting in doubt the validity of their data. AEDC TC 11, RAE(P) and NRCC agreed to within 0.5%, which is excellent agreement. AEDC TC 3 was 1% higher than TC 11, but as this difference is within the measurement uncertainty ( $\pm 1.25\%$ ), no further significance is accorded.

### 3.5 Net Thrust

Net thrust, Figure 14, exhibits quite a wide spread, up to 5%, bounded on the high side by CEPr, and the low side by NRCC. In Section 2.5, it was stated that NRCC values are known to be about 1.0% low by using the GTP equations. When proper account is made for this anomaly, NRCC would be about 0.7% lower than AEDC TC 11, which is well within the measurement uncertainty. CEPr consistently showed variance between TC 11 and TC 3, a difference of up to 2%, the altitude cell indicating high.

### 3.6 Specific Fuel Consumption

Specific fuel consumption plotted against net thrust is displayed as Figure 15. AEDC indicated the lowest SFC, and is in relatively good agreement for both TC 3 and 11, differing only by the fuel flow parameter. CEPr showed good agreement between TC 3 and TC 11, and with AEDC. The high thrust and low fuel flow values offset each other to achieve this result. NRCC is high as a result of the low thrust discussed in Section 3.5. The difference between AEDC and RAE(P) was attributed to the higher values of thrust at AEDC, as was discussed in Section 13 of Ref. 2.

### 3.7 Summary of Ground-Level and Altitude Facility Differences

In general, the data show that the highest values of dependent parameters are attributed to altitude facilities, and the lowest to a ground-level facility. A comparison of AEDC data at two test conditions did show some consistent differences, and with the exception of airflow, TC 11 always indicated a lower value, albeit within the declared measurement uncertainty.

The CEPr data were surprising in themselves, as there were not only large biases compared to the other test facilities, but also large biases between their own ground-level and altitude facility, in most cases overshadowing inter-facility differences.

Considering the known anomalies in NRCC airflow, and the thrust accounting procedures, NRCC data compare favourably with the other test agencies, all parameters being within the declared measurement uncertainties.

A table summarizing the ground-level to altitude differences is shown as Figure 16, and for reference Figure 17 generalizes the results from all the inter-facility comparisons.

## LIST OF REFERENCES

1. Subcommittee 01, AGARD Propulsion and Energetics Panel, Working Group 15, "Uniform Engine Testing Program General Test Plan," June 1983, (Revised edition).
2. Ashwood, P.F., principal author, and Mitchell, J.G., editor. "The Uniform Engine Test Programme-Report of PEP WG 15," AGARD Advisory Report No. 248, February 1990.

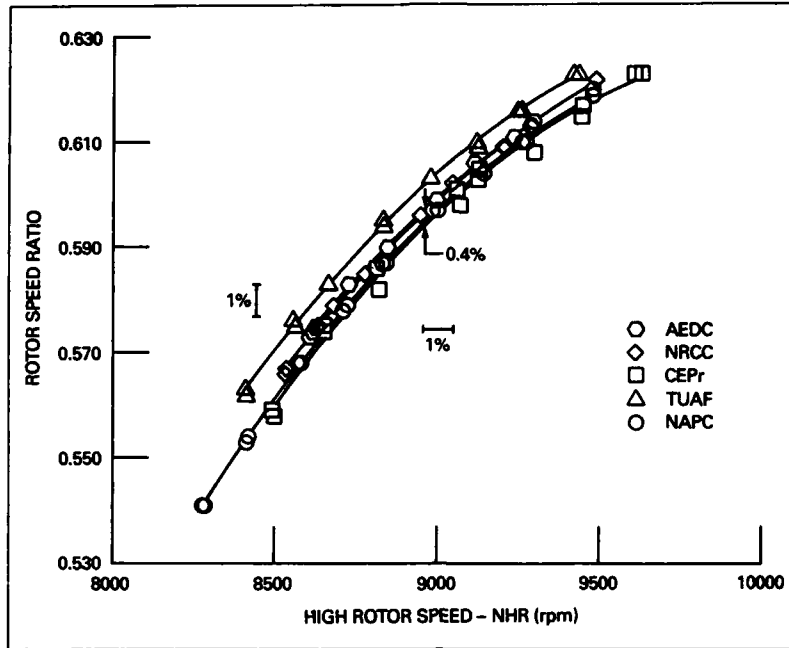


Figure 1 Rotor speed ratio - SN 615037

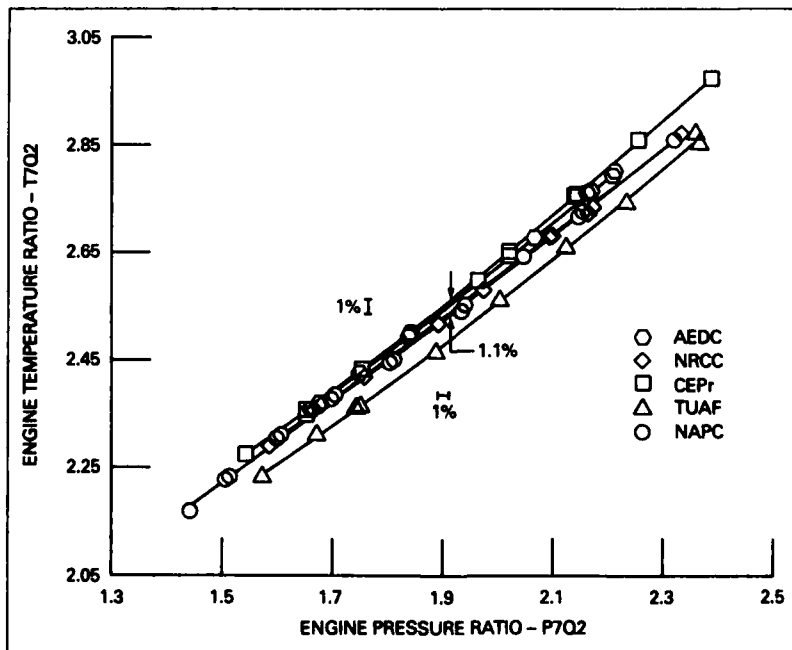


Figure 2 Engine temperature rise - SN 615037

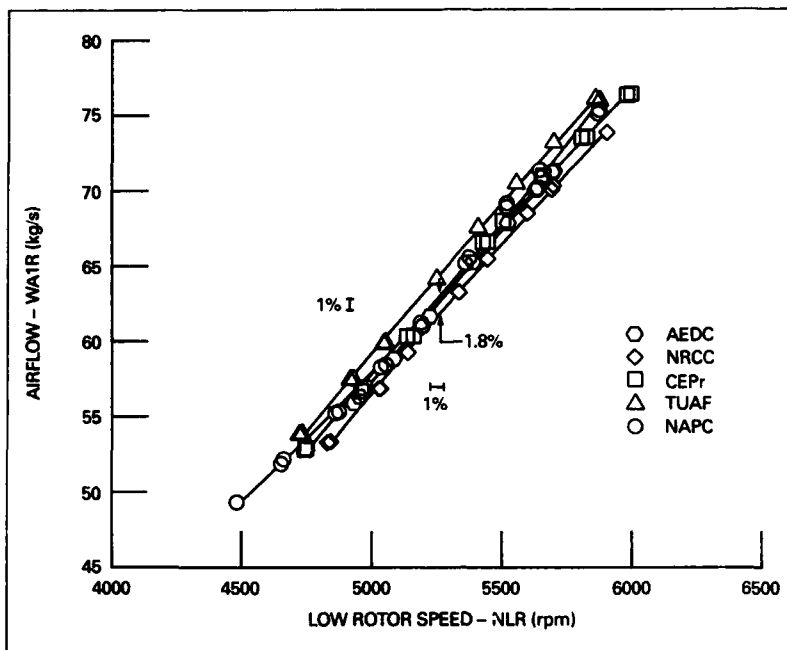


Figure 3 Facility measured airflow - SN 615037

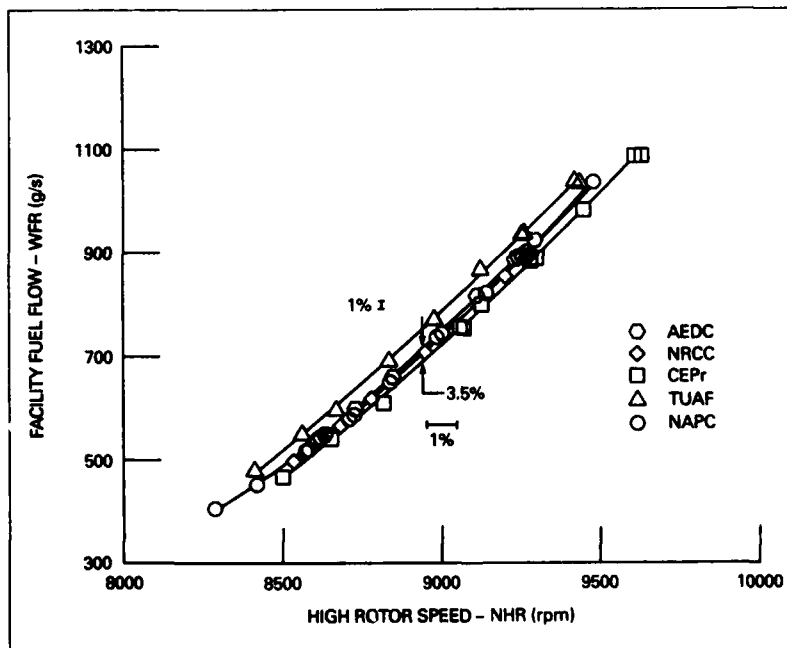


Figure 4 Facility measured fuel flow - SN 615037

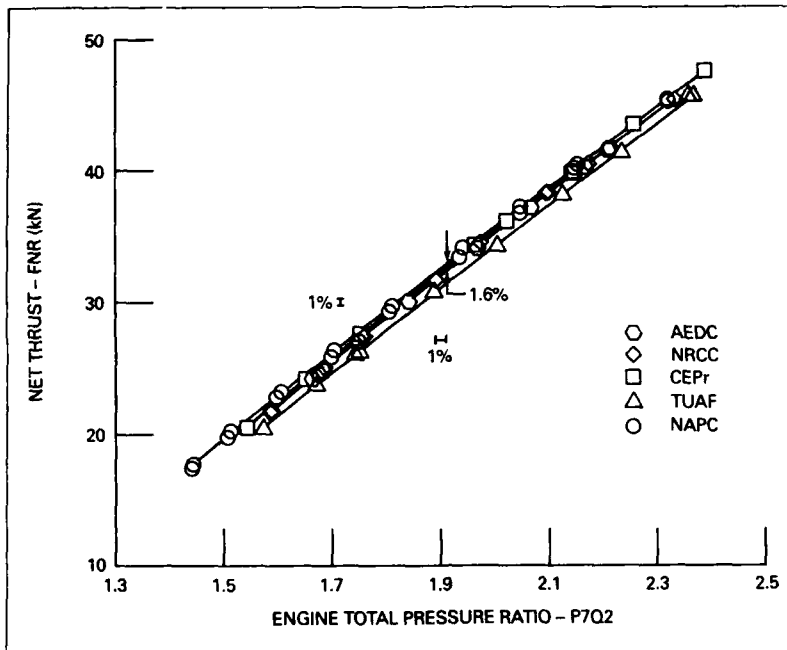


Figure 5 Net thrust vs. engine pressure ratio - SN 615037

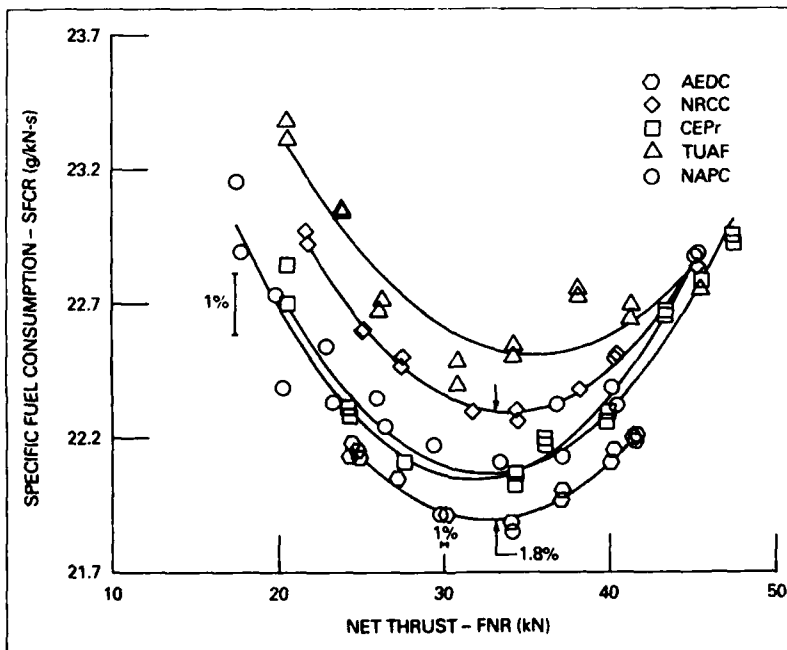


Figure 6 Specific fuel consumption - SN 615037

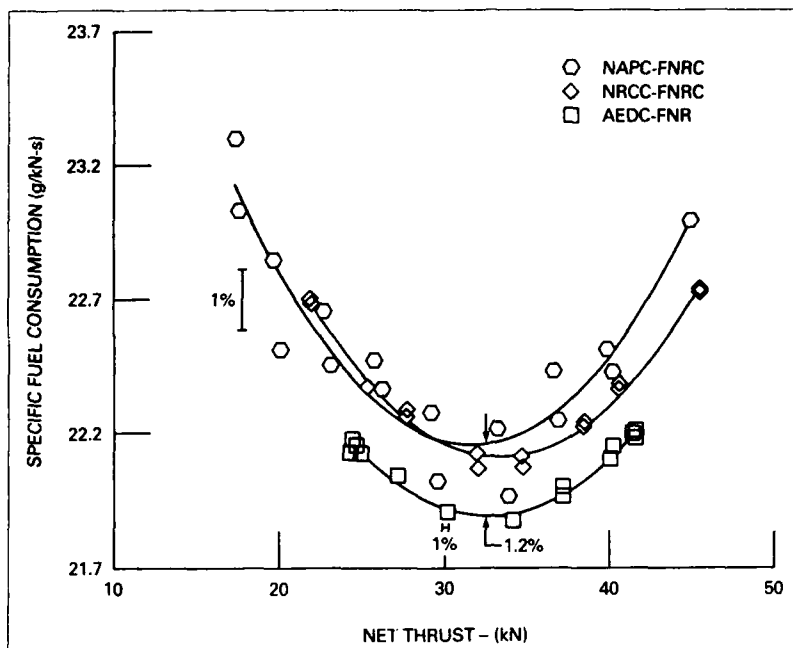
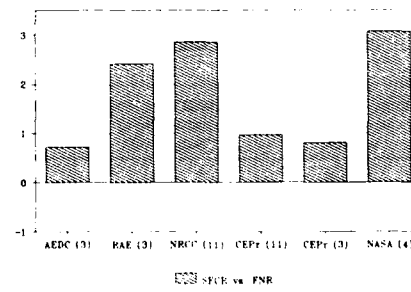
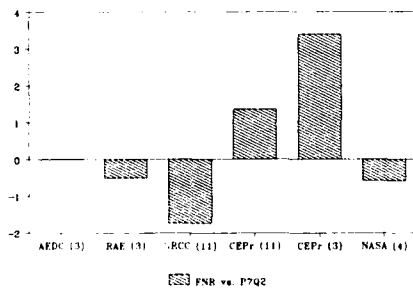
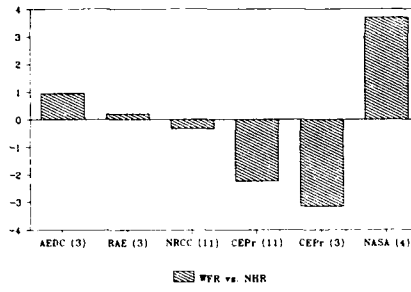
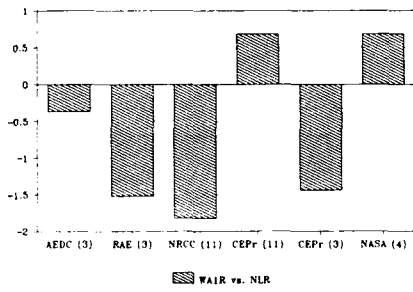
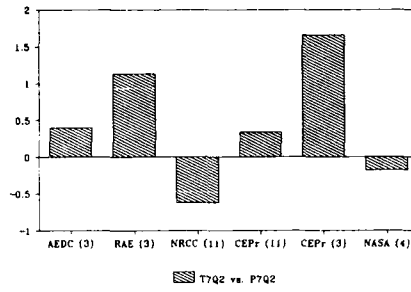
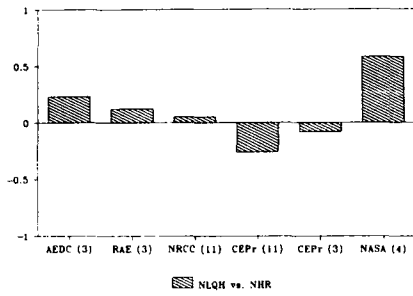


Figure 7 Specific fuel consumption - corrected - SN 615037

Ground-Level Bed Comparison (SLS Conditions) (NRCC, CEPr, TUAf, NAPC, AEDC)* SN 615037			
Engine Parameter (Independent variable)	Overall Percentage Spread at Mid-thrust (with TUAf)	Percentage Spread of Estimated Uncertainty	Comments
NLQNH (NHR)	0.5 (1.5)	0.2 to 1.6	Spread similar to that in altitude facilities.
T7Q2 (P7Q2)	1.1 (2.5)	0.9 to 1.8	Spread affected by failure of T7 thermocouples at NRCC
WA1R (NLR)	1.9 (4.0)	0.6 to 1.5	NRCC airflow low by 1 - 1.5%
WFR (NHR)	3.5 (6.0)	0.9 to 2.5	Spread reduced to 1.3% when CEPr values removed
FNR (P7Q2)	0.7 (2.5)	1.0 to 2.3	FNR incorrectly defined - see Appendix VIII. NAPC value not included
SFCR (FNR)	1.8 (3.0)	1.5 to 3.5	FNR incorrectly defined - see Appendix VIII. Agreement to within 1.2%

\* Tests in AEDC altitude cell at standard sea-level static conditions included for comparison.

Figure 8 Summary of Ground-Level Bed Differences



$$\% \text{ Difference} = \frac{\text{Facility} - \text{AEDC TC 11}}{\text{AEDC TC 11}} \times 100$$

Figure 9 Percentage Differences Referenced to AEDC TC 11 - SN 607594

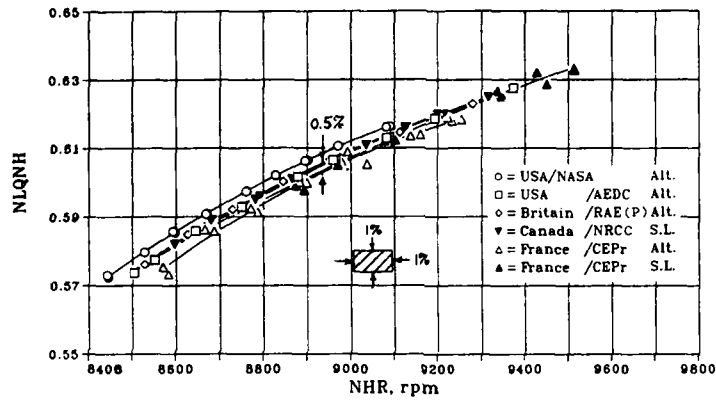


Figure 10 Rotor speed ratio - SN 607594

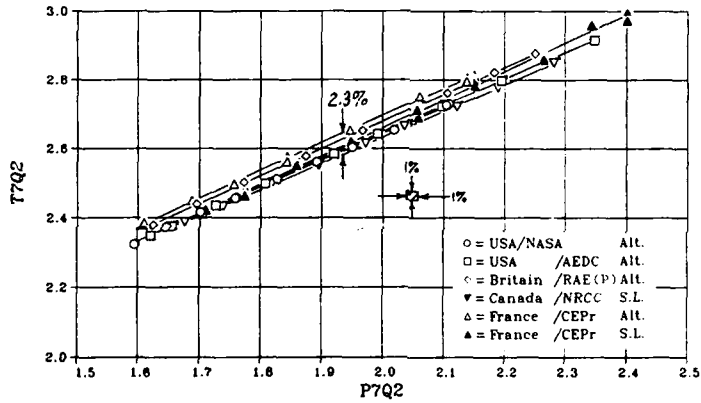


Figure 11 Engine temperature rise - SN 607594

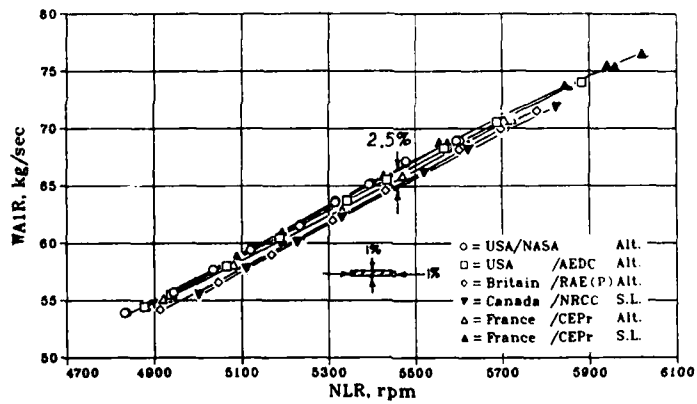


Figure 12 Facility measured airflow - SN 607594

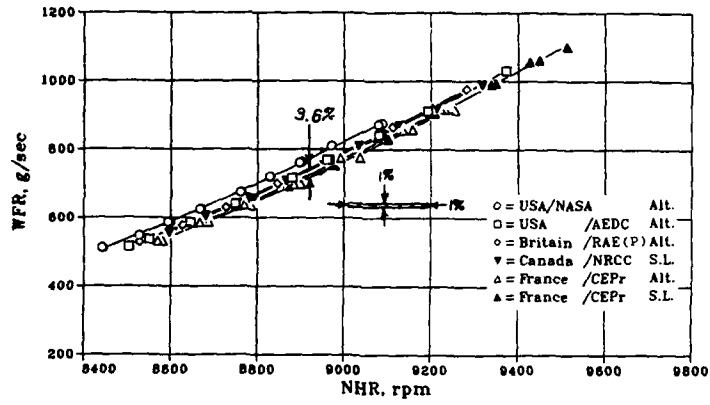


Figure 13 Facility measured fuel flow - SN 607594

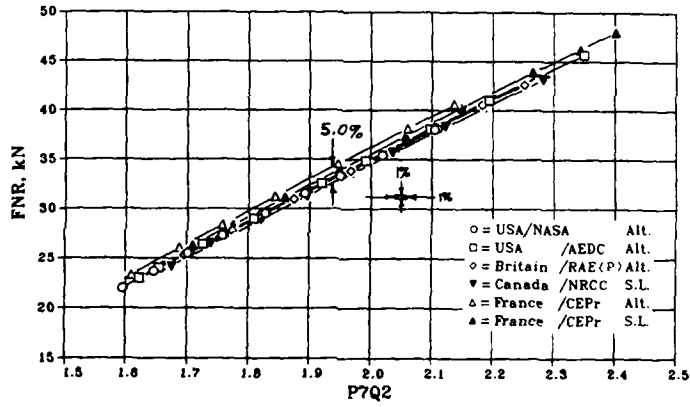


Figure 14 Net thrust vs. engine pressure ratio - SN 607594

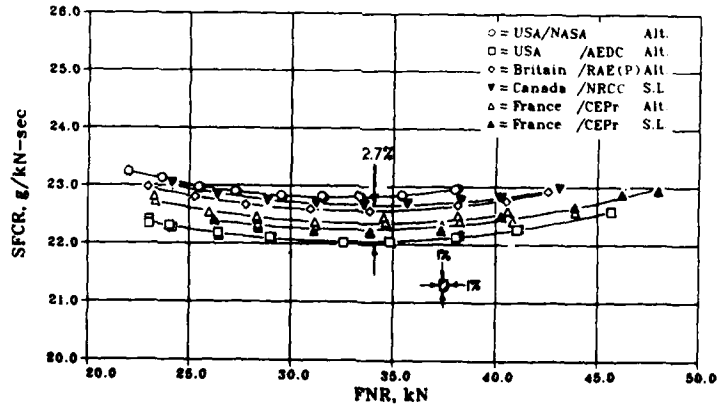


Figure 15 Specific fuel consumption - SN 607594

Engine Parameter (Independent Variable)	Overall Spread at mid-thrust (Percent)	Comments
NLQNH (NHRD)	0.5	
T7Q2 (P7Q2)	2.3	Spread affected by failure of T7 thermocouples at NRCC
WA1R (NLRD)	2.5	NRCC airflow low by 1.0 - 1.5% CEPr TC 11 in doubt
WFR (NHR)	3.4	CEPr has 2.0% bias, remaining facilities in excellent agreement
FNR (P7Q2)	5.1	Spread reduced to 3.0% if CEPr (Alt) non-equilibrium values removed. NRCC known to be 1% low
SFCR (FNR)	2.8	Max spread is between NRCC (GL) highest and AEDC (Alt) lowest

Figure 16 Ground-level to altitude facility comparisons - SN 607594

Percentage spread in performance parameters at mid-thrust point						
Engine parameter Independent variable	NLQNH NHRD	T7Q2 P7Q2	WA1RD NLRD	WFRD NHRD	FNRD P7Q2	SFCRD FNRD
Altitude facilities SN 607594	0.4 to 0.8	0.6 to 2.0	1.3 to 3.6	3.8 to 5.5	3.4 to 5.4	0.9 to 2.4
Engine parameter Independent Variable	NLQNH NHR	T7Q2 P7Q2	WA1R NLR	WFR NHR	FNR P7Q2	SFCR FNR
Ground-level facilities* Ground-level facilities† SN 615037	0.5 1.5	1.1 2.5	1.9 4.0	3.5 6.0	0.7 2.7	1.8 3.0
Engine parameter Independent variable	NLQNH NHRD	T7Q2 P7Q2	WA1RD NLRD	WFRD NHRD	FNRD P7Q2	SFCRD FNRD
Altitude and ground-level facilities SN 607594	0.5	2.3	2.5	3.4	5.1	2.8

\* Excluding TUAF

† Including TUAF

Figure 17 Summary of inter-facility comparisons

## MEASUREMENT UNCERTAINTY IN GAS TURBINE PERFORMANCE DETERMINATION

J.P.K. Vlegheert  
National Aerospace Lab (NLR) (rtd)  
POB 90502, 1006 BM Amsterdam, NL

## SUMMARY

A pre-test estimate of Data Uncertainty shows up weak links in the data chain and serves as a yardstick to judge whether observed differences in measured data are significant. On the other hand post-test analysis is essential to identify data validity problems.

The uncertainty estimates are based on the Abernethy concept, which splits total uncertainty in precision and bias.

With the help of an Error Audit four types of elemental errors are estimated for each of five Basic Physical Parameters. This error is then propagated to the Engine Performance Parameters, and from there to the Target Values on which the comparison is based.

Values for predicted errors are compared between the participating facilities and reasons for discrepancies are discussed.

Please see note about additional material on p.7-7.

## 1 INTRODUCTION

For accurate determination of the performance of a gas turbine it is desirable to do a number of measurements, preferably under different conditions. The results should be referred to standard conditions, making use of thermodynamic relations. Thus the results of different measurements can be compared. If any observed differences are larger than the previously estimated Data Uncertainty Limits, the measurement process should be checked for errors. But even if perfect agreement is obtained, the final result may still differ from the true value; there may be an offset or bias. This may show up if the test is repeated at a later date or in a different facility. However it is not possible to find out what is the true value; only whether observed differences are significant. That means the differences are true in so far that either the gas turbine, or the measurement technique, or both, have altered. A third possibility is that the error estimate was too optimistic: if a larger error is allowed the results could still be compatible.

It is not always possible to rely on previous experience for the estimated Data Uncertainty Limits; the make-up of data collection and processing can be different. Therefore existing data on uncertainty must be broken down to basic principles and then reassembled to fit the case under consideration. A pre-test assessment is important as it will show up weak points in the data collection chain, if there are any. On the other hand it is essential to conduct a post test analysis to identify possible data validity problems.

The process of estimating uncertainty limits consists of splitting the error in scatter and bias, determining both for a number of basic physical parameters and propagating the possible error to the final result. Test analysis entails calculating the end results in a number of different ways, using redundant information from the actual measurement data. By comparing these end results it can be checked whether the pre-test error estimate covers existing discrepancies, and if not, which parameter is at fault. A prerequisite is that obvious mistakes in the data processing must have been corrected or removed.

This report handles the error estimating technique used for the AGARD Uniform Engine Test Program (UETP), it gives values for the predicted Uncertainty Limits, and it compares Error Limit Estimates for the different participating facilities. It also gives some of the reasons for discrepancies in these estimates, and indicates a number of ways in which to check the end results for the post test analysis.

## 2 METHODOLOGY

Uncertainty estimates are based on the Abernethy concept, which splits total Uncertainty in two aspects: precision and bias. Precision, or random variation, scatter, is visible in a single series of experiments and can be determined statistically. This error reduces with an increasing number of data points. Bias, or systematic variation, offset, is constant for a single series of experiments and only shows up when several series are compared, and then not necessarily to its full extent.

Whether a certain error is called precision ( $s$ ) or bias ( $b$ ) depends on the extent of the experiment, the Defined Measurement Process (DMP). Calibration scatter reduces to an uncertainty in the calibration curve, which is a "fossilized" error, a bias, in the further experiment. However it is not the only bias, an unknown offset in the master instrument introduces a further bias element. Likewise scatter in any intermediate result may transform into a bias element further on in the calculation. There were marked differences between the facilities in their nomenclature of errors. This does not really matter as long as these differences are observed consistently throughout the estimation procedure. It does result however in detail error estimates not always being comparable.

For the UETP, different DMP's were employed by each of the test facilities to make pre-test error predictions, assessment and post test analysis. For instance, the RAE(P) DMP covers the uncertainty prediction and assessment of a single engine performance curve fitted (by least squares) to the test results for the nine engine power settings at a specified test condition. RAE(P)'s estimated Precision Index is based on

the predicted data scatter that will occur about a curve fit through the nine power settings. The predicted Precision Index is then verified by a post test determination using a third order curve fit through the test data and observing the residual standard deviation about the curve fit. Using the RAE(P) DMP, differences between a collection of curves, representing different test conditions and day-to-day variations, are classified as bias.

In contrast, the DMP used at AEDC for the UETP is based on the results of the overall measurement program for a given installation. Therefore estimates of the Precision Index at AEDC reflect the variations in the test results at the mid-thrust point, at a specified test condition for a given measurement system and test installation. They also include the variations that may result from tests on different days. Only the differences resulting from different measurement systems are classified as bias.

Precision and bias are kept separate throughout the error estimation procedure, only in the last step they are combined into a single number, the Error Limit Estimate. This must be a relevant combination of bias and precision. The latter value is a statistic, which lends itself to the calculation of confidence limits, within which the actual value can be reasonably expected to lie, in the absence of bias errors. It is however impossible to define a single rigorous statistic for the total error, because bias is an upper limit, which has unknown characteristics, and is to some extent dependent on engineering judgement. In fact the bias error can be thought of as the error remaining after corrections from the post test analysis have been exhausted. A working solution for the Error Limit Estimate (or Uncertainty Interval) is given in Section 3.7

### 3 UNCERTAINTY PREDICTION PROCEDURE

#### 3.1 DATA SEQUENCE

Basically a single measuring chain stretches from the flow field via probe and connecting line to the transducer, and from there usually via an electric line-sometimes pre-amplified- to multiplexer, amplifier, signal conditioner and A/D convertor, to be recorded. This measurement chain varies for each of the Basic Physical Parameters, which are force, pressure, temperature, pulse rate (giving RPM and Fuel Flow) and area (giving total force from pressure measurement)

Afterwards the signal is played back, an instrument calibration applied, and often a number of single measurements are combined to determine a value representative for the flow field, usually by averaging in space and/or time. These Basic Measurements are then used to calculate the Engine Performance Parameters (EPP), which are in referred form and constitute the end product of the measurement, e.g.  $WAIRD = WA \sqrt{1/2/288} / (P2/101325)$

Each dependent EPP can be given as a function of an independent parameter which can be chosen at will (usually RPM or EPR). For comparison either within or between facilities it is necessary to determine a Target Value of each dependent parameter. This requires an interpolation procedure, as it is not possible to set the exact test condition and engine power.

#### 3.2 ERROR PROPAGATION

Each step in the above-mentioned data sequence contributes to the overall data error in its own specific way. An overview is given below, each step is detailed in the following sections. The first step is to assess the elemental errors for a single measurement of each basic physical parameter. These errors are organized in four categories. Each item should be assessed separately for bias and precision; total bias and precision is then calculated by Root-Sum-Square (RSS) addition. Some aspects of the error in the effective flow field value or Basic Measurement are influenced by the number of single measurements incorporated. The next step is to propagate the error in each basic measurement to the Engine Performance Parameter. This is done by multiplying the b and s values by the appropriate Influence Coefficient (IC). The overall effect on the EPP is found by RSS addition. An important condition to justify RSS combination is that each item must be independent, this is sometimes not the case when there are common calibration errors. The error in the Target Value again partly depends on the number and disposition of the points used in the interpolation procedure. This aspect can be given by the Random Error Limit of Curve Fit (RELCF). Another error element is introduced because the Target Value is read from a curve at a chosen value of the independent variable, which itself is not error-free. This is the Curve Shift effect. Apart from that the Target Value has its own bias error. Finally the total Error Limit must be assessed by combining b and s.

#### 3.3 ELEMENTAL ERROR CATEGORIES

The Abernethy/Thompson method described in Ref. 2 details the evaluation of the elemental errors. These can be grouped in four categories for each measurement chain. However the groups defined in Ref. 2 were too general in scope for the purpose of a detailed assessment of the facility measurement uncertainties. Therefore a separate Error Audit was made up for each basic physical parameter, which lists the errors expected, but not necessarily in the order or in the subdivision as given in Ref. 2. An example (for force) is given in Table 3-1. For the purpose of explanation the categories of Ref. 2 are used in the underneath overview.

##### 3.3.1 CALIBRATION

Calibration errors are incurred because of hysteresis, drift and sensitivity of the instrument being calibrated. Also the calibration procedure, curve fit and resolution have an influence. Usually the instrument is calibrated against a Work Standard, the calibration of which should be traced back, ultimately to the National Standard, in steps via a Laboratory Standard and a Transfer Standard. This is called the Calibration Hierarchy. In each step the original bias of the less accurate instrument is replaced by the (smaller) error of the curve fit (see Section 3.6) combined with possible drift in time or due to calibration conditions (temperature effect). In order to trace these it is advisable to compare a number of calibrations done some time apart, say every 6 months.

### 3.3.2 DATA ACQUISITION

These errors can be caused by slight variations in exciter voltage, outside influences on data transmission and on the transducer, signal conditioning and recording. This results in non-repeatability. Sensor hysteresis could be allowed for if the measuring history is known, but this is usually not a practical proposition; anyway with most modern instruments hysteresis is small. Recording of the output of a single transducer is usually done in a matter of milliseconds or even less. To prevent aliasing errors, high-frequency components of the signal have to be eliminated by a low-pass filter. As this introduces some lag, a settling time has to be allowed in the case that a number of probes is multiplexed on to a single transducer. Usually the tube transient - in the case of multiplexed pressure channels - can be made negligible by using a low-volume transducer, which is close-coupled to the scanning valve. Of course overall faster sampling is possible if each channel is allocated to a separate transducer. The scatter of any single measured point can be reduced by taking a number of readings during a dwell and averaging the result.

### 3.3.3 DATA REDUCTION

Resolution errors and calibration curve fit errors can usually be made negligible, compared with the other categories. As an error of half the biggest error elsewhere only contributes 10% to the overall error when added RSS, it is not effective to use extreme resolution in the computational hardware and software. Calibration curve fit errors can be minimized by choosing the appropriate functional relationship, qualified by visual and numerical inspection. When a higher than second order curve fit is used, it is important that the calibration points are spaced evenly, otherwise the densely populated part may introduce a calibration bias in the sparsely populated part.

### 3.3.4 OTHER EFFECTS

These do not quite fit in with the above-named categories and are referred to by different names, such as Non-Instrument effects, Sensor System errors, Errors of Method, etc. In general they are concerned with the interaction between the medium and the measuring chain. They are usually difficult to separate, and unfortunately often rather large. Examples are the sensitivity of pressure probes and hole patterns to flow angle, and the variability of pressure- and temperature patterns over the cross section of the flow. A possible error of method is constituted by the assumption that static pressure is constant over the parallel section of the flow area in the engine inlet. The mechanics of the thrust stand can introduce bias and/or precision errors in the thrust stand zero. The transducer zero can be checked mid-run by taking up the load separately, but the thrust stand zero can only be checked in quiescent conditions, and then may be different from the value during the run. Pre-test and post-test zero are different, and it is usually assumed - but without true justification - that the test zero lies in between. Fuel flow measuring errors can occur because of the longitudinal vortices induced by the flow turning a corner (Beltrami flow); these vortices can be difficult to suppress.

## 3.4 BASIC MEASUREMENT ERROR

The precision component of the basic measurement error will be reduced with a larger number of sampling locations; generally with a factor equal to  $\sqrt{n}$ , where  $n$  is the number of locations. The bias error is not influenced by  $n$ , however, and the pattern variation can introduce extra bias. This variation can be reduced with an aperiodic sample, where the number of sampling locations is chosen deliberately different from the natural pattern in the flow, as for instance exists behind the burners in the combustion chamber. Often reproducibility of the pattern is more important than a true thermodynamic average. This however may result in unrealistic values for efficiencies or nozzle factors. Failure of any probe in a multi-probe sensor system can alter the effective average value. A procedure was used to interpolate between neighbouring probes, but this does not eliminate the error.

## 3.5 ENGINE PERFORMANCE PARAMETERS

The General Test Plan (Ref.1) gives the standard equations used to calculate engine performance parameters from the basic measurements. The influence of an error in any basic measurement on the outcome can be determined either by Taylor series expansion or numerically by perturbing the equation for a difference in that parameter, keeping all other parameters constant at their nominal value. The latter method is preferred because it accounts for implicit as well as explicit functional relationships. The resulting Influence Coefficient is expressed as the percentage variation of the calculated EPP for a one percent deviation of a single input parameter  $I$

$$\text{Influence Coefficient IC} = (\Delta \text{EPP} / \text{EPP}) / (\Delta I / I)$$

For small perturbations non-linearity effects will be insignificant, but the value of IC will vary over the operating range. Bias and precision of the EPP can be determined by adding the product  $\text{IC} * (\Delta I / I)$  for all relevant input parameters by RSS addition, separately for  $b$  and  $s$ . An example is given in table 3-2. Since the IC depends on hardware installation and measurement configuration, direct comparison between facilities is not possible.

### 3.6 TARGET VALUE

The Target Value of an EPP must be read from a correlation against the chosen independent variable (usually RPM or EPR) at a chosen value of that variable. Usually this is done for each test condition, which - for the case of UETP - consists of nine power settings. One aspect of the error in the EPP Target Value is given by the Random Error Limit of Curve Fit (RELCF), which is calculated from the Residual Standard Deviation (RSD) - also called Standard Error of Estimate (SEE) - of the points relative to a curve, fitted by the method of least squares. In calculating RELCF account is taken of the number of points and their longitudinal distribution; in so far that mid-curve the error is smaller than towards the ends. RELCF reduces with approximately  $\sqrt{\text{RSD}(n)}$ . The principle of the method is detailed in Ref.17. RELCF only takes account of the scatter during the one test condition; also precision errors may exist which cause the other test conditions to deviate, and apart from that there may be bias errors. These were evaluated separately in the previous section; in a different way by some facilities.

Any uncertainty in the chosen dependent variable translates into a discrepancy  $\Delta\text{EPP}$  of the Target Value, even though it has no effect on the individual EPP values. This Curve Shift effect depends on the curve slope, as is illustrated in Fig 3-1. In the case that a single error source influences both the dependent- and the independent parameter (like temperature influence on airflow and referred RPM) the Curve Shift error must not be calculated separately and added RSS as the errors are dependent. Instead a resultant error must be calculated in which the direct and the indirect (via curve shift) effects of the error source are added algebraically. This error contribution must be substituted for the original simple temperature error in the RSS error estimate for airflow.

An example for airflow is given underneath, with the functional relationship:

$$\begin{aligned} \text{with the shorthand notation} \quad & \text{WA}^* = f(\text{N}^*) \\ & \text{WA}^* = \text{WA} \sqrt{\text{T}} / \text{A} * \text{P} \\ & \text{N}^* = \text{N} / \sqrt{\text{T}} \end{aligned}$$

$$\begin{aligned} \text{in which} \quad & d\text{WA}/\text{WA} = d\text{WA}^*/\text{WA}^* + d\text{A}/\text{A} + d\text{P}/\text{P} - 1/2 d\text{T}/\text{T} \\ \text{and} \quad & d\text{WA}^*/\text{WA}^* = df(\text{N}^*)/d\text{N}^* * d\text{N}^*/\text{N}^* \\ & \text{and} \quad d\text{N}^*/\text{N}^* = d\text{N}/\text{N} - 1/2 d\text{T}/\text{T} \end{aligned}$$

$$\text{with the curve slope factor} \quad (\text{WAN}^*) = df(\text{N}^*)/d\text{N}^* = d\text{WA}^*/\text{WA}^* / d\text{N}^*/\text{N}^*$$

$$\text{it follows that } d\text{WA}/\text{WA} = d\text{A}/\text{A} + d\text{P}/\text{P} + d\text{N}/\text{N} * (\text{WAN}^*) - 1/2 d\text{T}/\text{T} (1 + (\text{WAN}^*))$$

The latter factor must be substituted for the simple contribution of temperature error if no curve shift is considered. The influence of the curve shift effect for the above case is additive for a temperature error; for fuel flow it is subtractive because the relation for that case is given by:

$$\text{WF}^* = \text{WF} / \text{P} * \sqrt{\text{T}} = f(\text{N}^*)$$

The curve shift effect can quite easily be dominant because the curve slope effect is large; it is about 3 for the case of airflow and 7 to 8 for fuel flow.

### 3.7 UNCERTAINTY INTERVAL

It was mentioned before, that a single rigorous statistic for the total error limit or Uncertainty Interval cannot be given. Usually the more or less arbitrary standard of bias plus a multiple of the precision index is used:

$$U = \pm(B + t_{95} * S)$$

in which  $t_{95}$  is the 95th percentile point for the two-tailed Student's "t" distribution, defining the limits within which 95% of the points are expected to lie in the absence of bias errors. If the predicted  $S$  is determined from a large number of points ( $n \gg 30$ ) the value  $t_{95} = 2.0$  can be taken; Monte Carlo simulations have shown that the coverage of  $U$  is about 99% (Ref. 16). The average Target Value of 10 test conditions numbers 9 degrees of freedom, for which case the  $t_{95} = 2.26$ . The Target Values for a certain EPP must be within a band of  $\pm U$  for all test conditions. If this is not the case either a data error exists or an important aspect of the uncertainty estimate has been overlooked.

An alternative for the value of the Uncertainty Interval is:

$$U = \pm \text{SQRT}((B^2 + (t_{95} * S)^2))$$

The coverage of this value is 95%, therefore it is indicated by  $U_{95}$ . In the case of RAE(P),  $S$  was estimated to be the scatter from which RELCF for the EPP is calculated. This is a small value; both values of  $U$  are similar and nearly equal to their  $B$ . This is not the case for the other facilities, because their definition of  $B$  and  $S$  is different, as are the numerical values. The resulting Uncertainty Interval should be compatible with the RAE(P) value.

## 4 TESTING PROCEDURE

### 4.1 INSTRUMENTATION

Referee instrumentation, consisting of inlet rakes and a modified tailpipe with rakes, developed by the first participant (NASA LeRC), is detailed in Ref. 1. This instrumentation system travelled with the engines, but each participant used its own transducers (except for engine fuel flow) and recording system. Apart from the referee instrumentation, each participant used its standard test cell instrumentation to determine engine performance, including separate fuel flow meters and an instrumented thrust stand. Items

like inlet conditions and air mass flow were thus measured double, allowing cross checks to be made, c.q. flow coefficients to be evaluated. AEDC used a choked venturi in its facility determination of air mass flow, which was deemed to be more accurate because of the higher pressure differentials involved.

Most participants used electronic absolute pressure gauges, except RAE(P) which employed differential gauges relative to a high-accuracy barometer. This system is more accurate at near-atmospheric pressure, but less so at the high-altitude condition, as then the differential pressure is large. The depression in the airmeter throat is measured differentially, with an absolute transducer as back-up.

For elevated temperatures thermocouples were used; for lower temperatures also resistance probes. Details are given in the facility reports; Ref. 5 to 11. Fuel flow was generally measured with turbine-type volume-flow transducers with separate fuel temperature measurement to calculate density. Only RAE(P) used displacement meters for the facility measurements, which were reported to be more accurate.

#### 4.2 SCANNING SYSTEMS

Most facilities used a combination of sequential scanning and multiplexing; the latter usually for the individual probes in a rake. Mostly mechanical scanning was used for pressure, where a number of pressure lines are connected in sequence to a single transducer. This resulted in cycle times of 20 seconds for NASA, who used low volume transducers, 1 minute for AEDC with more accurate larger volume transducers, which required longer stabilisation, and 6 minutes for NRCC, who used only a few transducers, one for each pressure range.

RAE(P) used electronic scanning for the UETP, with separate transducers for each tapping (sometimes two per tap). This allows a scanning cycle to be completed in 5 seconds. A measuring point then consists of a number of scanning cycles, with a check for consistency. Also NASA used electronic scanning in its repeat test. Different scanning systems are illustrated in Fig 4-1.

TuAF employed manual registration, with pressure taps manifolded to water manometers. Their cycle time was around 6 minutes; the readings were digitized manually for further processing on a computer. Testing procedure consisted of setting the engine power, allowing 4 minutes for the engine to stabilize, record a performance point, and a repeat point two minutes later. With the longer recording times these two points were taken back-to-back.

#### 4.3 CALIBRATION, DATA CHECK

Calibration was done at least once a day. In some cases the scanning cycle included a number of calibration points, that were also measured by a Work Standard; in this way an on-line calibration check can be effected. This is not possible with electronic scanning, but the system can be calibrated between tests; at NASA on command or automatically every 20 minutes, by switching all transducers over to a calibration manifold (see Fig 4-1).

Calibration point anomalies or data consistency checks can be used to trigger an alarm if set tolerances are exceeded. This allows the test operator to break off the test for closer scrutiny, which saves getting doubtful data. This can be carried as far as calculating the RELCF value on-line for some Engine Performance Parameters, and repeating points which appear to be outliers. Analysis must be carried out off-line; outliers must only be deleted if a good technical reason can be found; they could indicate a shortcoming in the instrumentation or even in the set-up of the experiment, or a anomalies in the test article.

#### 4.4 TRANSDUCER ERROR VARIATION

Instrument manufacturers brochures usually give a guaranteed error limit at Full Scale Output (FSO), which is assumed constant in absolute value over the whole range. This constant absolute error model results in a pessimistic estimate of uncertainty at the low end of the measuring range. NASA used this model, but with their own experimentally found value for the FSO error for each transducer type.

AEDC used the constant percent error model, with the error specified at 10 percent FSO. From zero to 10% FSO a constant absolute value was assumed for the error. This model results in a pessimistic estimate at the top end of the range, see Fig 4-2.

RAE(P) used the linear error model, in which the error is determined at both zero input and at FSO. It is then assumed to vary linearly between these values. This gives the closest representation of the measurement error over the total range, but it somewhat overestimates the error at the low end. Typically the absolute value of their zero error is in the order of 20% of that at FSO.

### 5 UNCERTAINTY ESTIMATES

#### 5.1 INTRODUCTION, ERROR AUDIT

At the start of the UETP, bias and precision error estimates in airflow, net thrust and SFC were calculated by the different facilities. An interim review showed large variations. To try and solve these an Error Audit was put together, which detailed the errors in the measuring system for the basic physical parameters (Ref. 3). All facilities have used this Error Audit in their final Uncertainty Assessment, but not necessarily in all its detail. Depending on local practice, errors were grouped differently, with the result that it is not possible to give average results for the separate categories mentioned in Section 3.3. This is for instance the case with an end-to-end calibration.

Also the allocation of bias and precision errors differed between facilities. Hysteresis errors were typically classed by NRCC and RAE(P) as bias and by AEDC and NASA as precision. Another example is the error from repeated application of the calibration pressure standard to the pressure measurement system. RAE(P) classed this type of error as bias, NASA as precision, and AEDC as part bias and part precision. This reflects the differences in calibration procedure and error assessment, specifically those in the

Defined Measurement Process, indicated in Section 2. The Uncertainty Interval  $U = \pm(B + 2*S)$  generally agreed within one percentage point for all facilities.

## 5.2 BASIC MEASUREMENTS

The errors in the basic measurements are given for three typical test conditions, taken as TC 3 and TC 9 for the Altitude Test Facilities (ATF) and TC 11 for the Ground Level Test Beds. These represent design inlet pressures of 82.7, 20.7 and 101.3 kPa respectively, or 12.0, 3.0 and 14.7 psi. The variation in temperature and in ram pressure ratio did not result in significant variation of error, therefore only different pressure levels have been considered. Fig 5-1 summarizes the RSS of the elemental errors for each of the basic measurements, split up in bias and twice the precision for each of the facilities. Due to the difference in DMP, NASA and AEDC generally attribute a larger portion of the total error to precision than did CEPR and RAE(P). The value of the percentage range of the estimated Uncertainty Interval is summarized in the table underneath:

	RPM	P2	T2	WF	FS
TC3	.02-.5	.1-.5	.3-.6	.2-1.1	.3-.7
TC9	.02-.5	.3-1.2	.3-.4	.5-1.6	.6-3.0

TC11 .02-.5 .2-.3 .3-.8 .4-.6 .4-.5

There is one item in which the difference in estimated error is significantly more than the one percent quoted in 5.1 and that is the Scale Force (FS). Fig 5-1 shows that this is mainly due to AEDC quoting a low value for their error at altitude.

## 5.3 ENGINE PERFORMANCE PARAMETERS

The errors for the EPP's NRD (referred RPM, either NH or NL), the speed ratio NLQNH, the Engine Pressure Ratio  $EPR = P7Q2$ , the temperature ratio  $T7Q2$ , referred airflow WAIRD, referred fuel flow WFRD, referred net thrust FNRD and referred Specific Fuel Consumption SFCRD, are given in Fig 5-2 for the Target Value (i.e. about mid-range of the power settings) and for the same conditions as indicated in the previous section. The Uncertainty Limits are summarized in the table below:

	NRD	NLQNH	P7Q2	T7Q2	WAIRD	WFRD	FNRD	SFCRD
TC3	.16-.55	.02-.7	.1-.7	.3-.6	.6-.8	.4-1.3	.5-1.2	.6-1.7
TC9	.2-.5	.02-.7	.5-1.1	.3-.6	.8-2.6	.4-1.7	1.6-3.2	2.1-3.5
TC11	.4-.7	.1-.8	.2-.3	.5-.9	.3-.7	.4-1.1	.5-.6	.9-1.2

These errors are quoted exclusive of curve shift errors, as these vary with the independent parameter, and therefore can only be given in combination. In Fig 5-3 the differences in the end results for the ATF's are compared with two different Uncertainty Intervals determined from the above table. One is the Estimated Maximum Logical Uncertainty Interval, determined from the sum of the largest value and the largest but one; this seemed more logical than twice the largest value. The other is the Median; that is the middle value, which is not influenced by a possible extreme estimate, as would be the average.

Fig 5-3 shows that for Airflow the estimated uncertainties agree very well with the differences actually found. For SFC the uncertainty estimate seems a bit pessimistic. For three out of four ATF's the Net Thrust error estimate is very pessimistic; the result for the fourth ATF evidently contains an error, which has not yet been found. The expected increase with altitude in net thrust error is borne out in practice. This is not the case with SFC.

## 6 TEST DATA ANALYSIS

### 6.1 PREPARATIONS

Test data analysis is not necessarily carried out post-test. To begin with, all computer processing must be checked out thoroughly before the test, including the application of calibrations and the equations for calculation of the average flow field values and the performance parameters. It must be checked that the correct calibrations are applied and possible calibration check points must be monitored. These remarks seem self-evident, but it is surprising how many errors were found in the end results due to simple oversights in these basic matters, especially for a non-standard program, as UETP was to some extent.

### 6.2 VALIDATION OF SINGLE RESULTS

Usually anomalies in calibration check points and in data compatibility- if more than one scan is used to average a point- are flagged, and analysed later, unless a drastic error occurs. At RAE(P) the measured performance parameters were correlated with referred RPM and the RELCF determined on-line to be able to repeat a point if an outlier occurs, while engine, facility and instrumentation are still running. Fig 6-1 gives these RELCF values for all ten test conditions; it shows the expected increase with altitude for the net thrust values and also that for TC 5 the variation is more than the expected value. This TC 5 was run on different days; plotting the separate points shows that these line up on two curves, which show an offset at low thrust, probably due to day-to-day variation in the calibration (Fig. 6-2) To show up differences not the absolute value is plotted, but the difference with the straight line connecting the end points of the first curve. It does not matter what reference is taken, as long as it is the same one for all points to be compared.

The large RELCF for TC 1 could not be traced.

Post-test calculation of RELCF for the other facilities showed overall large values for CEPr. It transpired that in this case shorter stabilisation times were used for the engine. Fig 6-3 shows that not only the scatter between points is larger, but that marked differences occur between the first and second data scan, with an overall offset. This was not expected, as the engine power setting was deliberately chosen to alternate between approach from below and from above. The differences were not correlated with this approach direction.

### 6.3 VALIDATION USING FUNDAMENTAL INFORMATION

It has been mentioned before that comparison of results from the different test conditions is often possible in referred form. This can be done within the facility. For thrust it must be taken into account that referred values for different intake pressure (simulated altitude) may decrease with intake pressure due to Reynold's effect. A similar result would obtain, however, if there is a constant absolute error in the thrust indication. For the case of UETP, where intake pressure differed by a factor four, a 1% error at high intake pressure then results in a 4% error at altitude, with a systematic variation in-between. To determine whether this is Reynold's effect or measuring error, the thrust coefficient can be calculated.

$CG = \text{measured thrust} / \text{calculated thrust}$   
 in which the gross thrust is measured with the test stand, corrected for inlet momentum, and calculated from the total pressure in the jet pipe. This value is practically independent of Reynold's effect; any systematic variation therefore indicates a measuring error. Most performance parameters can be correlated against different independent variables; measuring accuracy and curve shift effect will determine the preferable correlation with the least scatter. Fig 6-4 shows a number of possibilities in a schematic of data flow. Some values could be calculated which should be constant for the relevant engine, (at least part-range) like the turbine flow function, or show only small variation (like CG), thereby eliminating the curve shift effect.

### 6.4 VALIDATION BETWEEN FACILITIES

A useful exercise to compare data from different facilities is to collect them in a data envelope. The shape of this envelope does not reflect the data accuracy. It must not be confused with the confidence limit, which is narrow where a lot of data is available and wide if there is little data, while the shape of the data envelope is the opposite. However if the envelope shrinks with the use of another independent parameter, this is definitely an indication of better accuracy. Fig 6-5 shows that for each test condition the points correlate well (RELCF = .15 to .35%) but that between test conditions a random spread exists. For a single facility the bandwidth of 1.4% of thrust coefficient vs NPR based on total pressure shrinks to 1.0% if static pressure is used. Also the overall picture for all facilities improves and test conditions with deviating accuracy can be indicated. This is for instance the case with TC 9 at CEPr where an instrument failure occurred and the less accurate back-up instrument had to be used (Fig. 6-6 and 6-7) Reading the results at one value of the independent parameter, the confidence limit of the average value can be calculated. For the above case with bandwidth 1.4% the standard deviation of CG values is  $RMS = .48\%$ . The degrees of freedom number 9, resulting in  $t_{95} = 2.26$  and

$$SE = t_{95} * RMS / \sqrt{N} = .37$$

If the average values from different facilities differ more than this Standard Error, both groups do not belong to the same population, i.e. there are bias elements at work. In this way data can be judged without pre-test estimates for the accuracy, although of course analysis requires detailed estimates to be able to find a likely culprit.

The Conclusions, References, tables and figures will all be found in AG-307 or AR-248, as listed below.

<u>LS- 169</u>	<u>AG- 307</u>
Conclusions	= p-18
References	= p-19
Table 3-1	= Table 3-1A ; p-20
Table 3-2	= Table 5-1A and 5-1B ; p-27
Fig 3-1	= Fig 3.1 ; p-34
Fig 4-1	= Fig 4.1 ; p-34
Fig 4-2	= Fig 6.2 ; p-37
Fig 5-1	= Fig 5.4 ; p-36
Fig 5-2	= Fig 5.5 ; p-36
Fig 5-3	= Fig 6.7 ; p-39
Fig 6-1	= Fig 6.3 ; p-37
Fig 6-2	= Fig 6.4 ; p-37
Fig 6-3	= Fig 6.6 ; p-38
Fig 6-4	= Fig 6.1 ; p-37
	<u>AR- 248</u>
Fig 6-5	= Fig.13-1 ; p-54
Fig 6-6	= Fig.13-2 ; p-54
Fig 6-7	= Fig.13-3 ; p-55

## EXPERIENCE IN DEVELOPING AN IMPROVED DESIGN OF EXPERIMENT (LESSONS LEARNED)

By  
Robert E. Smith, Jr.  
Vice President and Chief Scientist  
Sverdrup Technology, Inc./AEDC Group  
Arnold Engineering Development Center  
Arnold Air Force Base, TN USA

### SUMMARY

The design of the experiment for the AGARD PEP Uniform Engine Test Program was a highly successful effort. The plan and organization for this program included contemporary recording of lessons learned regarding improvements to the design of the UETP experiment.

Nine major lessons learned were identified which provide the opportunity for improvements in the design of experiments for future programs having a scope and complexity similar to the UETP. These lessons learned were spread across the seven key technical elements of the experiment as follows:

ELEMENT	LESSON LEARNED
Test Article	Validated Engine Math Model
Matrix of Variables	Engine Performance Tracking
Experimental Measurements	Referee Tailpipe Measurements Engine Inlet Turbulence
Test Method	Compressor Inlet Flow Distortion Engine Thermal Stabilization
Test Data Processing	Lapse Characteristics for Engine Performance
Measurement Uncertainty	Defined Measurement Process
Reporting	Data Comparison Strategies

In addition, one lesson learned related to the management of major, round-robin programs.

### LIST OF SYMBOLS

NASA	National Aeronautics and Space Administration
NRCC	National Research Council of Canada
RAE(P)	Royal Aerospace Establishment Pyestock
UETP	AGARD-PEP Uniform Engine Test Program

### 1.0 INTRODUCTION

The UETP was a pioneering effort in the design of the experiment for this major, multi-national test program. The experiment was designed to provide information which could be used to quantify the similarities and differences in performance measurement capabilities of various turbine engine test facilities located within the NATO countries. As with any engineering undertaking of this magnitude, there is much to be learned from a critical examination of the strengths and weaknesses of the engineering processes used in the conduct of this program. This lecture focuses on the design of the UETP experiment. Subsequent lectures in this series will focus on other aspects of this program.

The learning opportunities in the UETP were especially large in area of design of experiments because no existing publications which defined experiments of the scope and complexity of the UETP could be located. Therefore, this design effort did not have a documented information base to serve as a starting point for the evolution of the design.

To take full advantage of this unique opportunity to advance the state of the art of design of experiments, the chairman of AGARD-PEP Working Group 15 established a plan for contemporary recording of the "lessons learned," i.e., what worked well and what needed improvement, during this effort. This plan was in effect from very near the beginning of the UETP to its completion.

All aspects of this design are documented in Ref. 1. Those areas of the design needing improvement were noted as they were discovered in the course of the planning, testing, analysis, and reporting phases of the UETP. This lecture focuses only on these improvement areas, and as such, it provides a compilation of those "lessons learned." This compilation, when used in conjunction with Ref. 1, provides a basis for improved design of future experiments having the scope and complexity of the UETP.

The seven major elements or building blocks of the UETP experiment are (Ref. Section 1.0 - Lecture 2):

1. Selection of Test Articles
2. Specification of Matrix Variables
3. Identification of Experimental Measurements
4. Definition of Test Methodology
5. Specification of Test Data Processing
6. Definition of Measurement Uncertainty
7. Content of Reports

This UETP lessons learned discussion will include an eighth element, as follows:

8. Management of Round-Robin Experiments

The details of the UETP experiment are documented in Ref. 1. Summaries of many of the strengths of the design of this experiment and of the improvements needed are included in Section 19 of Ref. 2.

## 2.0 IMPROVEMENTS IN DESIGN OF UETP EXPERIMENT

The lessons learned relative to needed improvements in the UETP experiments are discussed for all seven major technical elements and for one program management element in the following sections. Items which are not discussed in the following sections generally met the needs and objectives of the UETP in a satisfactory manner.

At the conclusion of each section, a subjective assessment is provided of the importance of each improvement to the success of a future application similar to the UETP. The importance levels used are (1) desirable, (2) necessary, and (3) mandatory where "desirable" connotes only small gains in the quality of the experimental results and "mandatory" indicates that the program results will be severely compromised unless the improvement is incorporated. Some of these assessments are strongly influenced by the basic characteristics of the test engine and power control system as noted in each section.

### 2.1 Selection of Test Article

Availability of a validated mathematical model of the steady-state performance of the engine was not identified as a requirement of the UETP engine selection process (Section 3-Ref. 2). In fact, no such model existed for the selected J57-PW-19W. The key requirement is for a "validated" code. Several models for similar J57 engines did exist, but none had been validated to establish the quantitative relationship between the model performance and the actual engine performance at the means and extremes of the populations of production and overhauled engines within the ranges of the UETP test conditions.

As was learned during the analysis phase of the program, the diagnostics of some of the observed differences in engine performance between facilities (e.g., effect of unplanned variations in ram pressure ratio and engine inlet temperature) were not possible because no validated engine math model was available. Further, in some cases where the diagnosis could be made, the lack of an engine model reduced the confidence in the results. In one very important area, i.e., comparison of altitude test facility performance and ground-level test facility performance, the lack of a model increased the uncertainty of the comparative results.

The availability of a validated math model of the engine should be a primary requirement in future engine selections. This new requirement ranges from "desirable" for an engine and control system having configuration and logic similar to the J57 up to "mandatory" for engines and control systems using multiple variable geometries and control logics.

The lesson learned relative to "Validated Engine Math Model" is summarized in Fig. 1.

### 2.2 Matrix of Variables

The General Test Plan (Ref. 1) required that engine performance changes during the lifetime of the UETP be established by conducting the first tests and the last tests in the same test facility and measuring the overall change in performance. This plan was later revised to include bookkeeping engine performance changes that occurred at each facility. This bookkeeping was accomplished by having each facility conduct a repeat test at the completion of testing at the same test conditions as were used at the start of its test program. Neither of these approaches was successful because the engine performance changes were smaller than the errors of the facility measurement systems. Finally, during the analysis phase of the program a third method was developed. This method was based on the referee diagnostic measurements (Section 2.3 - Lecture 2) at operating conditions which minimized the precision errors (Section 11. -Ref 2).

As was learned during this analysis effort, the selected methods of tracking changes in engine performance with time were very labor intensive and yielded results with poor precision.

In future test programs, a portion of the test matrix at each facility should be dedicated to tracking engine performance. Referee measurement systems, not just referee sensors, should be used for such tracking. Finally, the test conditions should be selected to provide minimum precision of measurements. This improved approach ranges from "necessary" for an engine and control system similar to the J-57 up to "mandatory" for self-adaptive engine control systems.

The lesson learned relative to "Engine Performance Tracking" is summarized in Fig. 1.

### 2.3 Experimental Measurements

Difficulties in obtaining accurate values of tailpipe referee conditions (especially total pressure) were anticipated during the UETP planning. The test engines were modified and special instrumentation arrays were installed in an attempt to obtain reliable tailpipe measurements (Section 4 - Ref. 2). The degree of difficulty in

making these measurements was, however, underestimated, and unreliable measurements of tailpipe total pressure resulted. (Section 14.3 and 18.2.2-Ref.2).

In future programs, additional analysis and/or experiments should be conducted before the official testing begins to confirm that the tailpipe sensors exhibit little or no sensitivity to small changes in engine operating conditions. Installation of flow-mixing devices or flow-straightening systems upstream of the measurement planes might be required to achieve the desired insensitivity to changes in engine operation. An improved design is "necessary" for all configurations.

The lesson learned relative to "Referee Tailpipe Measurements" is summarized in Fig. 2.

Characterization of the turbulence in the engine inlet airflow at each test installation was a requirement for the UETP (Section 4-Ref. 2). However, the referee instrumentation requirements and the data processing requirements were inadequate, and a usable characterization of turbulence at each facility was not obtained (Section 12.2-Ref. 2).

An improved approach to characterize engine inlet turbulence should be developed for future programs. These improvements are rated as "desirable" for all configurations.

The lesson learned relative to "Engine Inlet Turbulence" is summarized in Fig. 2.

#### 2.4 Test Methodology

Different approaches were used by the various agencies to design the aerodynamics of the air supply systems upstream of the facility/engine inlet interface. As a result a wide range of inlet distortion (total pressure profiles) was produced at the compressor inlet (Section 12 and 17 - Ref. 2).

For future programs improved definition of the aerodynamic conditions at the facility/engine inlet interface is warranted. Improved definition of compressor inlet flow distortion limits is evaluated as "necessary" for all configurations.

The lesson learned relative to "Compressor Inlet Flow Distortion" is summarized in Fig. 3.

Rather simple elapsed time criteria were specified in the General Test Plan (Section 8.4-Ref. 1) to provide for thermal stabilization of the engine and test facility before steady-state data were acquired. The prescribed approach was validated during the first test entry at NASA and was reverified at RAE(P) and NRCC (Section 12-Ref. 2). However, thermal nonequilibrium effects were present in some data (Section 18.2.1 and 18.2.2 - Ref. 2).

An improved specification of test stabilization criteria is needed for future test programs. This improvement ranges from "necessary" for an engine and control system similar to the J-57 up to "mandatory" for engine controls employing closed-loop engine temperature control.

The lesson learned relative to "Engine Thermal Stabilization" is summarized in Fig. 3.

#### 2.5 Test Data Processing

The General Test Plan (Ref.1) required that the measured engine performance be corrected (referred) to the desired test conditions using the traditional performance generalization parameters. These techniques did not provide the desired level of precision because of the basic limitations of the method (Section 16-Ref. 2).

For future test programs, validated values of the influence coefficients for the effects of inlet temperature (temperature lapse) and ram pressure ratio should be specified for the adjustment of test data to desired conditions. These validated values can be obtained from measured data or from validated engine math models. This improved specification ranges from "necessary" for an engine and control system similar to the J57 up to "mandatory" for a multi-variable engine and control system.

The lesson learned relative to "Lapse Characteristics for Engine Performance" is summarized in Fig. 4.

#### 2.6 MEASUREMENT UNCERTAINTY

Initial efforts to determine the measurement uncertainty at each test agency revealed that the definition of the methodology specified in the General Test Plan (Ref. 1) was incomplete. A special sub-group was formed to complete the definition of the methodology (Lecture 7 and Ref. 3). The sub-group completed this work on a timely basis; the most important contributions were in the areas of the elemental error audit and the Defined Measurement Processes (DMP). The DMP encompasses the overall procedure, including calibration, etc., to arrive at a desired test result using a specified installation (Ref 3).

An improved specification of the methodology to be used to estimate pretest measurement uncertainties and to determine posttest measurement uncertainties is needed for future programs. The improvements should be focused in the areas of elemental error audits and Defined Measurement Processes. The improved specification is rated as "necessary" for all configurations.

The lesson learned relative to "Defined Measurement Process" is summarized in Fig. 4.

#### 2.7 REPORTING

The data comparison strategies to be used for UETP were not identified in the General Test Plan (Ref. 1). Rather, these strategies were evolved during the analysis phase of the program. This evolution was very labor intensive and substantially prolonged the analysis effort.

For future programs, a predetermined plan for data comparison should be incorporated into the design of the experiment. This improvement in the design of the experiment is rated as "desirable" for all configurations.

The lesson learned relative to "Data Comparison Strategies" is summarized in Fig. 5.

## 2.8 Management of Round-Robin Experiments

Throughout the lifetime of AGARD-PEP Working Group 15, all decisions were made and all directions were established during plenary sessions of the Working Group. This conservative management style was completely appropriate for the UETP because of the uniqueness of this program.

Building on the foundation provided by the UETP, future programs could be managed more efficiently if the Working Group chartered and empowered an executive steering group to make decisions and provide directions in defined areas. This smaller group could be more responsive in addressing many technical details. The executive steering group would provide a double benefit to the program by first providing more timely decisions/directions in designated areas, and second, by reducing the detailed technical workload at the plenary sessions, thus permitting the full Working Group to address more effectively major programmatic matters. This management change is "desirable" for all programs having the scope and complexity and, now, the maturity of the UETP.

The lesson learned relative to "Executive Steering Group" is summarized in Fig.5.

## LIST OF REFERENCES

1. Subcommittee 01, AGARD Propulsion and Energetics Panel, Working Group 15, "Uniform Engine Testing Program General Test Plan," June 1983, (Revised Edition).
2. Ashwood, P. F., principal author, and Mitchell, J. G., editor, "The Uniform Engine Test Programme - Report of PEP WG15," AGARD Advisory Report No. 248, February 1990.
3. Vleghert, J. P. K., editor, "Measurement Uncertainty Within the Uniform Engine Test Program," AGARDograph 307, May 1989.

- TEST ARTICLE: VALIDATED ENGINE MATH MODEL
  - UETP EXPERIENCE
    - (a) INCREASED DIFFICULTY/REDUCED CONFIDENCE - DIAGNOSTICS OF INTERFACILITY  $\Delta$ 'S
    - (b) INCREASED UNCERTAINTY - COMPARISON OF ATF'S AND GLTF'S
  - LESSON LEARNED
    - INCLUDE ENGINE MATH MODEL AS PRIMARY REQUIREMENT IN ENGINE SELECTION
  - APPLICATION:
    - DESIRABLE - SIMPLE ENGINE /CONTROL
    - MANDATORY - MULTI-VARIABLE ENGINE/CONTROL
- MATRIX OF VARIABLES: ENGINE PERFORMANCE TRACKING
  - UETP EXPERIENCE
    - LABOR INTENSIVE, POOR PRECISION - ENGINE PERFORMANCE TRACKING
  - LESSONS LEARNED
    - REQUIRE TEST MATRIX AT EACH FACILITY - USE REFEREE MEAS. SYS.
  - APPLICATION:
    - NECESSARY - SIMPLE ENGINE/CONTROL
    - MANDATORY - SELF-ADAPTIVE ENGINE CONTROL

Figure 1. Lessons learned, test article and matrix of variables.

- EXPERIMENTAL MEASUREMENTS: REFEREE TAILPIPE MEASUREMENTS
  - UETP EXPERIENCE
    - UNRELIABLE MEASUREMENT OF TAILPIPE REFEREE CONDITIONS
  - LESSON LEARNED
    - SELECT REFEREE TAILPIPE SENSORS WITH REDUCED SENSITIVITY
  - APPLICATION:
    - NECESSARY - ALL CONFIGURATIONS
- EXPERIMENTAL MEASUREMENTS: ENGINE INLET TURBULENCE
  - UETP EXPERIENCE
    - INADEQUATE CHARACTERIZATION - ENGINE INLET DYNAMIC PRESSURE
  - LESSON LEARNED
    - IMPROVE SPECIFICATION OF DYNAMIC MEASUREMENT REQUIREMENTS
  - APPLICATION:
    - DESIRABLE - ALL CONFIGURATIONS

Figure 2. Lessons learned, experimental measurements.

- TEST METHOD (INSTALLATION): COMPRESSOR INLET FLOW DISTORTION
  - UETP EXPERIENCE  
WIDE RANGE OF INLET FLOW DISTORTION
  - LESSON LEARNED  
IMPROVE DEFINITION OF AERODYNAMIC CONDITIONS AT ENGINE INLET/INTERFACE
  - APPLICATION:  
NECESSARY - ALL CONFIGURATIONS
  
- TEST METHOD (OPERATION): ENGINE THERMAL STABILIZATION
  - UETP EXPERIENCE  
THERMAL NONEQUILIBRIUM EFFECTS PRESENT IN SOME DATA
  - LESSON LEARNED  
IMPROVE SPECIFICATION OF TEST STABILITY CRITERIA
  - APPLICATION:  
NECESSARY - SIMPLE ENGINE/CONTROL  
MANDATORY: CLOSED-LOOP ENGINE TEMPERATURE CONTROL

Figure 3. Lessons learned, test method.

- TEST DATA PROCESSING: LAPSE CHARACTERISTIC FOR ENGINE PERFORMANCE
  - UETP EXPERIENCE  
POOR PRECISION - REFERRED ENGINE PERFORMANCE GENERALIZATION
  - LESSON LEARNED  
REQUIRE USE OF MEASURED LAPSE CHARACTERISTICS TO ADJUST PERFORMANCE
  - APPLICATION:  
NECESSARY - SIMPLE ENGINE/CONTROL  
MANDATORY - MULTI-VARIABLE ENGINE CONTROL
  
- MEASUREMENT UNCERTAINTY: DEFINED MEASUREMENT PROCESS (DMP)
  - UETP EXPERIENCE  
INADEQUATE SPECIFICATION OF DMP, E.G., ELEMENTAL ERROR AUDIT
  - LESSON LEARNED  
IMPROVE SPECIFICATION OF UNCERTAINTY METHODOLOGY
  - APPLICATION:  
NECESSARY - ALL CONFIGURATIONS

Figure 4. Lessons learned, test data processing and measurement uncertainty.

- REPORTING: DATA COMPARISON STRATEGIES
  - UETP EXPERIENCE  
DATA COMPARISON STRATEGIES EVOLVED DURING ANALYSIS
  - LESSON LEARNED  
INCORPORATE PRE-DETERMINED PLAN FOR DATA COMPARISON
  - APPLICATION:  
DESIRABLE - ALL CONFIGURATIONS
  
- PROGRAM MANAGEMENT: EXECUTIVE STEERING GROUP
  - UETP EXPERIENCE  
DIRECTIONS/DECISIONS BY COMMITTEE OF THE WHOLE
  - LESSON LEARNED  
CHARTER AND EMPOWER AN EXECUTIVE STEERING GROUP
  - APPLICATION:  
DESIRABLE - ALL CONFIGURATIONS

Figure 5. Lessons learned, reporting and program management.

AGARD LECTURE SERIES 169  
UNIFORM ENGINE TEST PROGRAMME

EXPERIENCE IN DEVELOPING AN IMPROVED ALTITUDE TEST CAPABILITY

A. R. Osborn  
Propulsion Department  
Royal Aerospace Establishment  
Pyestock, Farnborough, Hants GU14 0LS, England

Copyright (C) Controller HMSO London 1990

SUMMARY

Each test site benefitted in different ways from participating in the UETP, not least from observing how other test sites approached the testing, through participating in the Working Group discussions on procedures and methods of analysis.

A review of the lessons learnt by the participants during the altitude testing of the UETP has been carried out and a strategy proposed for an improved altitude test capability. Many of the good practices proposed for a better test capability are based on experience found to be successful at RAE, Pyestock, in the UK.

1 INTRODUCTION

The objectives, typical results and the technical difficulties experienced in the UETP have been extensively explained in preceding lectures. By this stage, the reader should have a good grasp of the principles employed in altitude engine testing and should need no further detailed explanation of the fundamentals. This Paper will, therefore, explore the major areas of difficulty experienced in the UETP and propose possible solutions and good practice which should enable future altitude engine tests to have a greater chance of success.

Organisations with different approaches to testing took part in the UETP and therefore the range of lessons learnt varied from one test facility to the other, everyone learning something to their advantage. Every test site was able to measure their facility bias for the first time and compare this with their predictions; a unique opportunity in the international field of turbine engine testing. This section of the Lecture Series will attempt to summarise the lessons learnt by all participants and will be complementary to the lessons learnt during sea-level testing, although some test sites will obviously only be associated with certain of the items listed. The subjects covered will especially be appropriate to altitude turbine engine testing, which has a different set of problems to contend with compared with ground-level test stands. For example, altitude testing often entails instrumentation that must accommodate a much wider range of measurement, in particular pressure, thrust and fuel flow. There again, environmental conditions within the altitude test cell can be unfriendly to delicate instrumentation systems. These are the well known problems, but the items listed below should introduce fresh insight into the preparation needed in staging turbine engine altitude tests with the objective of obtaining the best possible results.

2 INLET DUCTING

Almost all Gas Turbine Engine Altitude Test Facilities install the engine such that the inlet air flows through ducting directly into the engine, while the whole assembly is mounted in a test chamber to maintain the appropriate altitude pressure. This type of arrangement is generally called 'connected' testing and enables the engine flight conditions to be closely controlled by a relatively simple plant layout. An example of a typical altitude test cell is shown in Fig 1 where the layout of RAE(P) Cell 3, the UK test facility used in the UETP, is depicted. The design of the inlet ducting needs special attention so that it provides the engine under test with a total pressure profile which is closely related to the flow field the engine would experience in the actual aircraft installation in flight. At the same time, the inlet ducting usually incorporates some method of determining engine airflow which is a primary measurement requirement. In addition, some form of control of the total inlet pressure is provisioned so that the correct flight test condition can be set. An elaborate instrumentation array is also usually required to accurately determine the value of mean inlet total pressure. Some of this equipment can disturb the flow and produce a distorted pressure profile if care in the design of the equipment is ignored.

The following advice is given based on experience gained from the UETP. The inlet ducting design should, where divergence is necessary, keep the divergence angle to a minimum, an included angle greater than 7° should be avoided. If possible, instrumentation intrusion in the inlet ducting should be kept to the minimum commensurate with the requirements to obtain accurate mean measurements. This may initially entail exploratory tests to investigate the complexity of the flow field using extensive sampling, but this can then probably be reduced for subsequent engine performance tests by careful positioning of a minimum instrumentation array. Any flow distortion unavoidably created by upstream control devices or duct geometries may be attenuated by a combination of gauzes and flow straighteners. The exact location and quantity of these devices can only be determined experimentally.

3 NOZZLE/EXHAUST DIFFUSER COUPLING

The need to use exhaust diffusers in altitude test cells to optimise the pressure recovery in the exhaust duct so that the exhausters machines are employed efficiently, also needs careful consideration. Since the test facility must be configured to produce the minimum secondary airflow so that minimum exhauster energy is used to achieve a given altitude, this can lead to mis-match between engine and exhaust diffuser airflow for good pressure recovery. It is normal practice to optimise the diffuser geometry for the maximum engine airflow condition. Fig 2 shows that there is no single installation configuration which all test facilities adopted. Therefore, at other flight conditions there is the possibility of recirculating exhaust flows which may have an

impact on the local nozzle environmental flow field. With some engine installations, secondary chokes or orifice plates may need to be fitted to the exhaust diffuser entry to minimise these effects.

It is recommended that the flow field in the vicinity of the afterbody/nozzle of the engine is explored by using a ring of statics to determine the local static pressure. In addition, the provision of surface static pressure tappings along the engine outer carcass with some statics surrounded by perforated enclosures, 'tea bag statics', at the nozzle exit plane will help to determine if pressure gradients are present. Steps can then be taken to correct for boattail forces and pressure area terms in the derivation of engine thrust.

The degree of pressure gradients that can be generated is a function of the geometry of the nozzle/exhaust diffuser interface. It might therefore be prudent to design the engine installation so that not only can the axial distance of the engine be varied with respect to the diffuser entry, but also the size of the diffuser entry can be varied by the application of chokes and orifice plates. No specific recommendations can be made because solutions to minimise these effects depend on the layout and capability of the test cell and air pumping plant, which varies between facilities.

#### 4 ENGINE STABILISATION

The UETP General Test plan specified a five minute stabilisation period before steady-state performance data were collected. This time was arrived at after NASA had carried out exploratory tests in their facility to determine when aero thermodynamic stabilisation was reached. In addition, both RAE(P) and MRCC carried out investigations of engine settling time during tests in their facilities. Fig 3 shows the result obtained at test Condition 6 during the RAE(P) tests. During the UETP the CEPR facility tested the engine at altitude and due to priority requirements did not always adhere to the recommended five minute waiting time. This policy gave a larger scatter in their data when compared with data obtained at NASA, AEDC and RAE(P).

Based on these experiences it is recommended that any tests on a new type engine in an altitude facility should be planned to contain a test to determine engine/test plant stabilisation times at the earliest opportunity. Specific recommendations cannot be made since times depend on engine size, cycle temperatures, cell environmental conditions, instrumentation response and plant control response. All these factors vary for different installations and cannot be predicted. However, the test plan should be constructed so that conditions are explored both in an increasing and decreasing engine power lever movement and with different flight conditions. It is appreciated that this may not be possible in early tests, but even if only one test is carried out with data scans at one minute intervals to determine stabilisation time, then a generous factor can be applied to the stabilisation period to account for potentially more difficult conditions.

#### 5 PERFORMANCE RETENTION TESTS

In all engine performance tests it is very important to keep track of engine deterioration and therefore test programmes should be planned to enable this element to be measured. The UETP plan was specifically organised to enable performance retention to be determined by:-

(a) Requesting each participating altitude test facility repeat at the end of their test series the same performance test condition that was set up for their first test. This enabled deterioration during each altitude test to be determined provided it was larger than the combination of day-to-day bias plus precision uncertainty for that particular test facility. The results obtained at RAE(P) for their tests are shown in Fig 4.

(b) NASA carried out tests on two occasions, at the start and finish of all the altitude tests. This again enabled engine deterioration to be tracked providing it was larger than the longer term bias and precision uncertainty for the NASA test facility.

As concluded earlier in the Lecture Series the UETP performance retention was determined to be very good with negligible deterioration. This was probably due to the combination of an engine 'running in' period at NASA prior to the start of the UETP and the rugged design of the J57 engine.

Even though the carefully laid out plan of the UETP did not reveal engine deterioration for the reasons outlined above, it is recommended that similar practices are applied in all engine altitude tests of this nature so that engine health can be monitored at all stages. A further recommendation would consist of repeating a single test condition on a day-to-day basis at a specific engine power setting so that not only is engine health checked, but also the data gathering system is checked for integrity and consistency.

#### 6 UNCERTAINTY ANALYSIS AS A GUIDE TO MEASUREMENT SYSTEM DESIGN

This Lecture Series has already outlined an extensive insight into uncertainty analysis in engine turbine testing, setting out methods and results. There is, however, a spin-off from such methodology which can guide the test engineers in either selecting or tailoring measurement systems to achieve certain objectives or indicating areas where measurement improvement is required. It must not be forgotten, however, that financial considerations and pressures of time can also play a major role in the measurement criteria, which may overwhelm the technical considerations based on uncertainty analysis recommendations.

The first step, well before testing commences, is to specify the degree of accuracy required to identify the engine performance. It must be remembered that comparative tests on development engines of the same type in the same test facility using the same measurement process will attract a lower uncertainty spread. In this case, some bias errors will be common and can therefore be discounted. Not all bias errors, however, may be ignored since some changes in the complete test set-up are inevitable, and in any case, instrumentation drift must be accounted.

The measurement process can now be specified, based on the test criteria, and the uncertainty prediction analysis carried out. The complete analysis will reveal whether the specified performance accuracy will be achieved. If this accuracy has just been satisfied then no further action will be required. However, if the specified accuracy has not been achieved the analysis will show where measurement process improvements should be

attempted. These modifications can then be incorporated in the measurement process and the uncertainty prediction repeated. This process can be repeated until the test objectives are satisfied. If the accuracy needs are extensively exceeded it may be possible to relax the complexity of the measurement process, to use simpler, lower cost instruments, and still achieve the objective. All these criteria need to be examined before testing commences, but the application of this quality control should continue during and after testing, particularly with a post test analysis which will confirm that the original objectives and estimates are valid. The UETP experience should give confidence in applying those methods used and explained in AG 307, which were proved to be successful.

#### 7 ON-LINE ANALYSIS

Altitude engine testing is an expensive operation due to the combined need for complex test plant and the high energy to achieve the flight conditions. It is therefore important to provide every means of ensuring the measured data are satisfactory and it has already been stated that good pre-test planning plays an important role in this process. However, the need for on-line data analysis and checking is equally important, since this is the period when the high energy costs are expended. RAE(P) have long ago instituted a three-stage on-line data checking system and other test sites have similar arrangements to ensure good data are obtained.

The RAE(P) system is explained here briefly as an example of good practice:-

The first-stage on-line check following a data scan involves a combination of automatic computer software checks and manual checking of individual measured parameters. The computer checking is configured so that measurement stability is interrogated by multi-sampling methods. In addition, outlier detection is applied to multi-measured parameters or pressure and temperature arrays and those measurements detected to be in error are deleted. Methods are then applied to re-calculate mean pressures or temperatures, etc or re-constitute a measurement based on interpolation or extrapolation techniques. Similarly, manual checking procedures are carried out in parallel, deletions or manipulations implemented and the data reprocessed.

The second stage on-line checks involve an engineer using a suite of computer programmes to check that pressure and temperature arrays are giving acceptable pressure and temperature profiles, based on past experience or past test results. Also aerothermodynamic data derived from test plant measurements should be correlated with pre-determined established functions, again based on previous experience. These techniques are heavily dependent on good graphical displays on a series of VDU terminals which can be rapidly multiplexed so that the data can be checked before the next test scan is required. A typical graphical output examined during this stage at RAE(P) is shown in Fig 5.

The third stage on-line check is carried out by an engine performance engineer, who uses calculated engine performance parameters to compare against past test results or sea-level test results. Fig 6 shows a sample of a typical graphical output used during this stage, one of twenty four such plots used at RAE(P). Again assistance with these checks is provided by a rapid multiplexed graphical computer software suite with additional statistical software aids.

Using these checking procedures at each test scan, and also looking for trends as test conditions progress, has enabled RAE(P) to provide a test capability which gives high quality data at an economic cost.

#### 8 USING NOZZLE COEFFICIENTS FOR PERFORMANCE COMPARISONS

Nozzle coefficients, both airflow and thrust, were shown to be good parameters to use for performance comparisons during the UETP. It must be emphasised that these characteristics are only useful for a fixed geometry convergent or convergent-divergent nozzle. The uncertainties involved with variable area nozzles, which can include substantial leakage, make these geometries unsuitable for this type of analysis.

Nozzle coefficients plotted against nozzle pressure ratio are a suitable on-line analysis parameter to check on thrust and airflow measurement consistency during tests, being very sensitive to small measurement changes or errors. Figs 7 and 8 show the on-line results of such an analysis for all ten test conditions for the RAE(P) UETP results. The good collapse of the data indicates consistent thrust and airflow measurement in this case.

Nozzle coefficients can also be used to check thrust and airflow measurements between different test facilities, or to determine thrust in flight. Both these procedures are heavily dependent on good nozzle inlet total pressure and temperature measurements. If it is possible to position pressure and temperature measurement arrays in the nozzle tailpipe, then a suitable position should be selected where the effects of swirl and turbine strut wakes are a minimum. It must be realised that this area within the engine is a harsh environment for measurement probe integrity and therefore failures must be expected. The UETP showed that nozzle tailpipe static pressure measurement was more rugged than the total pressure probes and was also insensitive to secondary flows within this region. It is probably advisable to use such a static pressure measurement to determine total pressure in combination with a tailpipe area and a value for gamma, than to rely on a total pressure measurement array. Even if this technique leads to a bias in nozzle total pressure measurement, because errors can be introduced both from estimates of area and the flow assumptions introduced into the calculation, at least it will be consistent across all tests if the same procedure is adopted.

If total pressure and temperature arrays are used then these instrument arrays must be maintained in good working condition at all test sites if consistency is to be retained.

Although the UETP included tests on an open air stand at MAPC, Trenton, these tests unfortunately came too late to be of any real benefit to be included in the overall analysis. However, if nozzle coefficients are to be used as thrust and airflow measurement comparitors, it is recommended that these be determined during an open air stand test on a day with negligible wind velocity. Only in this type of test can installation effects be declared a minimum and true datum nozzle coefficients determined. Of course, this datum still depends on good placement of nozzle entry instrumentation as indicated earlier.

## 9 FUEL FLOW MEASUREMENT

The UETP showed that consistent fuel flow measurement across all altitude test sites was difficult to achieve. The fuel flow measurement comparisons gave differences of the order of 4 to 5 percent at a high rotor speed, the largest differences for any primary performance parameter. The difficulties in fuel flow measurement arise from many considerations. Firstly, there is the wide variation in flows with altitude, typically from 0.1 litre/s to 4.0 litre/s, a ratio of 40:1. Leakage flows in the measurement instruments, whether they be turbine or positive displacement meters, are a major problem. In addition, where turbine meters are used the fuel viscosity and installation has a significant effect on volume flow measurement. The fuel viscosity, in turn, is dependent on temperature and fuel properties and needs to be determined accurately. Some of these difficulties can be resolved by calibrating the meters in a high quality test rig over their expected operating range using gravimetric measurements.

At RAE(P) positive displacement meters are used for steady-state performance measurements of fuel flow. Two meters are used in series in the test cell to calculate fuel flow and both meters are calibrated in their respective positions in the calibration facility. These meters are of the sliding vane or reciprocating piston type, the former giving 2.25 litre/rev and the later 0.5 litre/rev respectively. These are regularly calibrated in the RAE(P) calibration laboratory, which uses gravimetric measurements. The meters are not sensitive to installation pipework. Figures 9 and 10 show examples of the RAE(P) calibration methodology and a typical fuel meter calibration history chart. These meters have been found to give consistent performance over many years and the UETP confirmed their choice to be based on sound principles.

Other problems arise in fuel flow measurement, namely the conversion from volume flow to mass flow and also the determination of calorific value. The mass flow determination is dependent on a measurement of density, which in itself can prove difficult. If hand measurements are taken during a test there is the problem of variability between different manual readings both of the hydrometer and the temperature measurement. The same problems may be present in an automatic reading by remote sensing because these devices generally rely on a resonating cylinder which is sensitive to fuel temperature.

Fuel calorific value is also a difficult measurement and is not covered by an international standard. Confusion can arise because some agencies use heat per unit mass and others heat per unit weight in air. In these cases it is important to use the correct fuel density (ie mass or weight) for the results to be consistent. The calorific value used to be determined by bomb calorimeter and some agencies still use this technique, but others have adopted the use of Nuclear Magnetic Resonance (NMR) techniques, which employ hydrogen and sulphur content combined with a multiple regression equation.

All the above remarks have been made to highlight the great care needed in the measurement of fuel flow. It must therefore be recommended that an engine testing agency should give a proportionate effort to providing a high quality fuel measurement process if specific fuel consumption performance is a prime test objective.

## 10 THRUST MEASUREMENT CALIBRATION CHECKS

The ultimate check on any load measurement system in an altitude test facility is a centre-line pull applied at the engine centre-line position. There is no doubt that this test provides a great deal of confidence in load measurement capabilities if performed for a given test facility. However, to plan such a test is very time-consuming and requires the provision of special frameworks to enable the load to be applied at the appropriate position. Alternatively, a procedure should be set up to check the load measurement system on a regular basis by designing a system to apply loads to the thrust frame at an appropriate position.

Most test sites have some means of applying loads to the measuring load cell and a master load cell simultaneously, with the engine installed, to provide load cell calibrations. By adopting such a procedure, thrust calibration history charts or records can be kept to maintain consistency over long periods. Then, if any anomaly shows up in the charts the load measurement system can be investigated for extraneous fixed or variable loads caused by unscheduled installation factors. These may be the result of additional mass addition to the thrust frame or additional bridging between the earth and metric parts of the load measurement system. Fig 11 shows a typical thrust calibration history chart kept at RAE(P). The difference from a nominal load is plotted at three different load levels of 25, 50 and 70 kW and the generally low scatter on these plots indicates the slope of the load cell has remained relatively constant. The changes in the 0 kW level indicate the change in zero load during either an engine installation, as instrumentation, etc is added or the change from one engine installation to the next. The detail is to some extent unimportant in this figure, but it does demonstrate the good practice of maintaining calibration histories, which increase confidence in the measurement process capability.

## 11 CONCLUDING REMARKS

The Uniform Engine Test Programme provided a unique opportunity for aero engine test facilities in Europe and North America to evaluate their test procedures and methods of analysis by testing the same engines over an agreed range of operating conditions. Each test site benefited in different ways from participating in the UETP, not least from observing how other test sites approached the testing, through participating in working group discussions on procedures and methods of analysis. The encouraging results of the UETP, giving bias errors within prediction and precision errors of not greater than 0.3 percent are highly creditable and a good reflection on the test procedures used in the test facilities.

The UETP involved the Pratt & Whitney, J57 two-spool turbojet which is not representative of more advanced military turbofan engines now under development. Turbofan engines are likely to be more sensitive to installation effects such as exhaust nozzle to diffuser spacing, inlet pressure profile and Reynolds Number. Test facilities may need to pay greater attention to these factors in any future joint test programme. It is expected that those items highlighted in this lecture together with the good practice guidance will help to improve the procedures of all test facilities.

**REFERENCES**

1. Ashwood, P.F., 'The Uniform Engine Test Programme'. Report of the Propulsion and Energetics Panel Working Group 15. AGARD AR 248, February 1990.
2. Mitchell, J.G., 'Uniform Test Engine Testing Programme'. General Test Plan, January 1983. Revised June 1983.

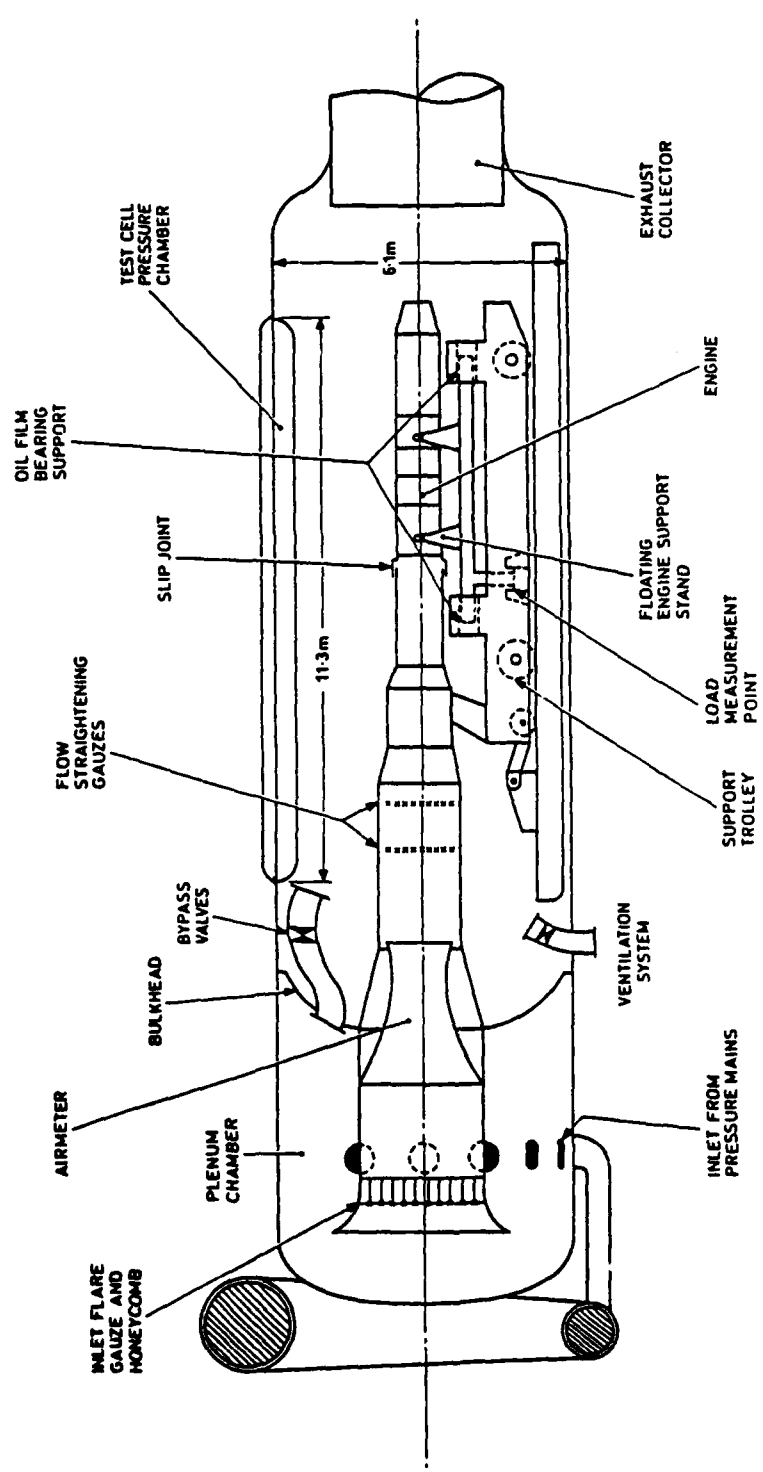
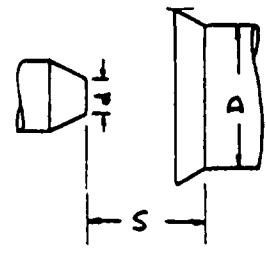


FIG.1 TYPICAL ENGINE INSTALLATION IN RAE (P) ALTITUDE CELL 3

d = 550 mm (nominal)



	D mm	S mm	$\frac{D}{d}$	$\frac{S}{d}$
NASA PSL3	1016	660	1.85	1.20
AEDC T2	1700	250	3.09	0.45
CEPr R6	1800	580	3.27	1.05
RAE(P) Cell 3	2134	1412	3.88	2.57
NRCC Cell 5	838	457	1.52	0.83
CEPr TO	1930	650	3.51	1.18
TUAF	1830	1500	3.33	2.73

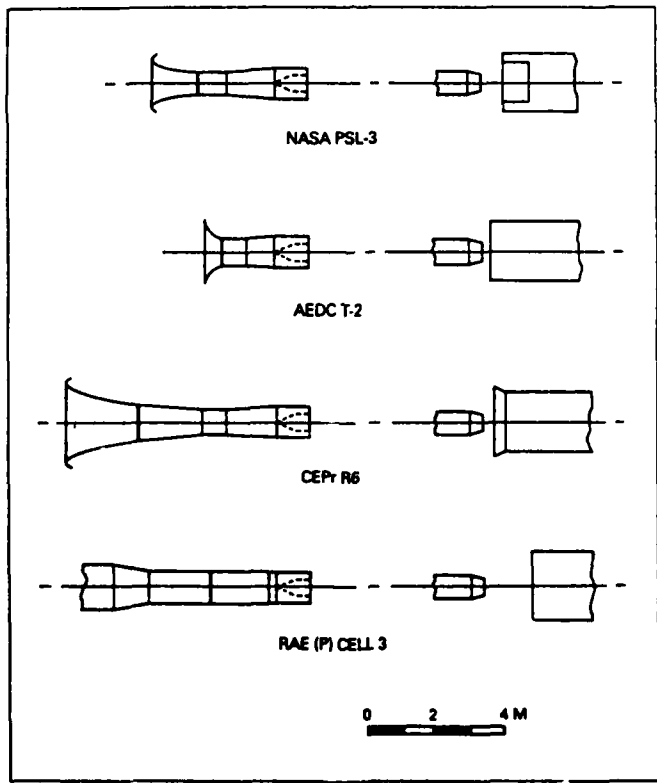


Fig. 2 Comparison of inlet and exhaust geometries —

Fig 3A Fuel flow and thrust during stabilisation time

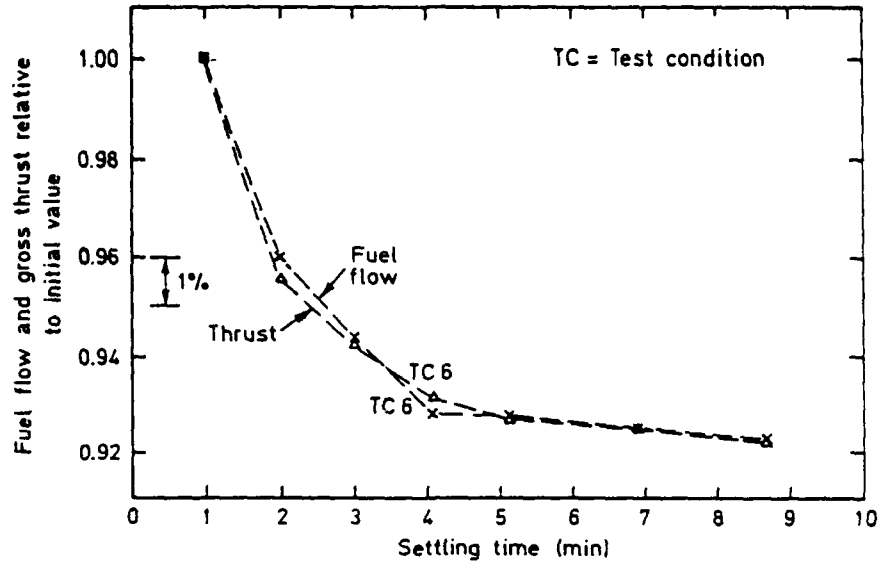


Fig 3B Inlet and cell pressures during stabilisation time

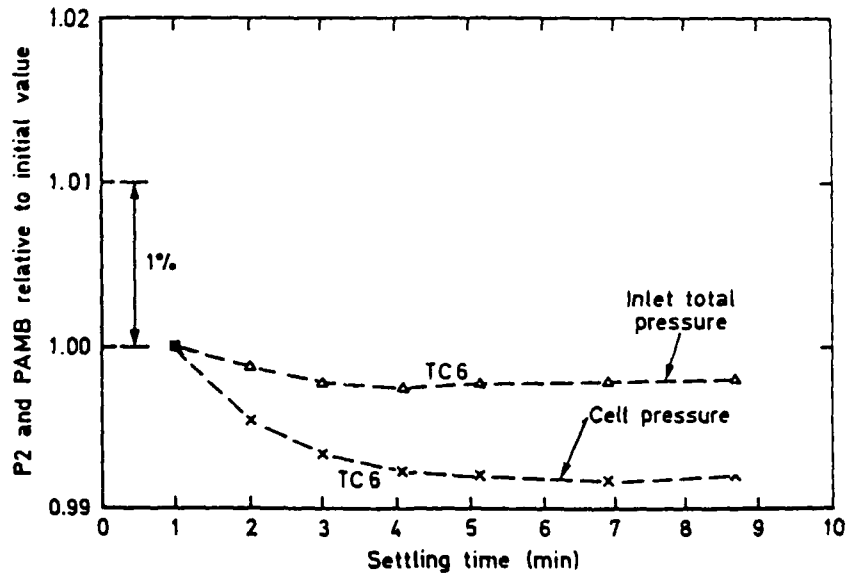


FIG.3 ENGINE STABILISATION

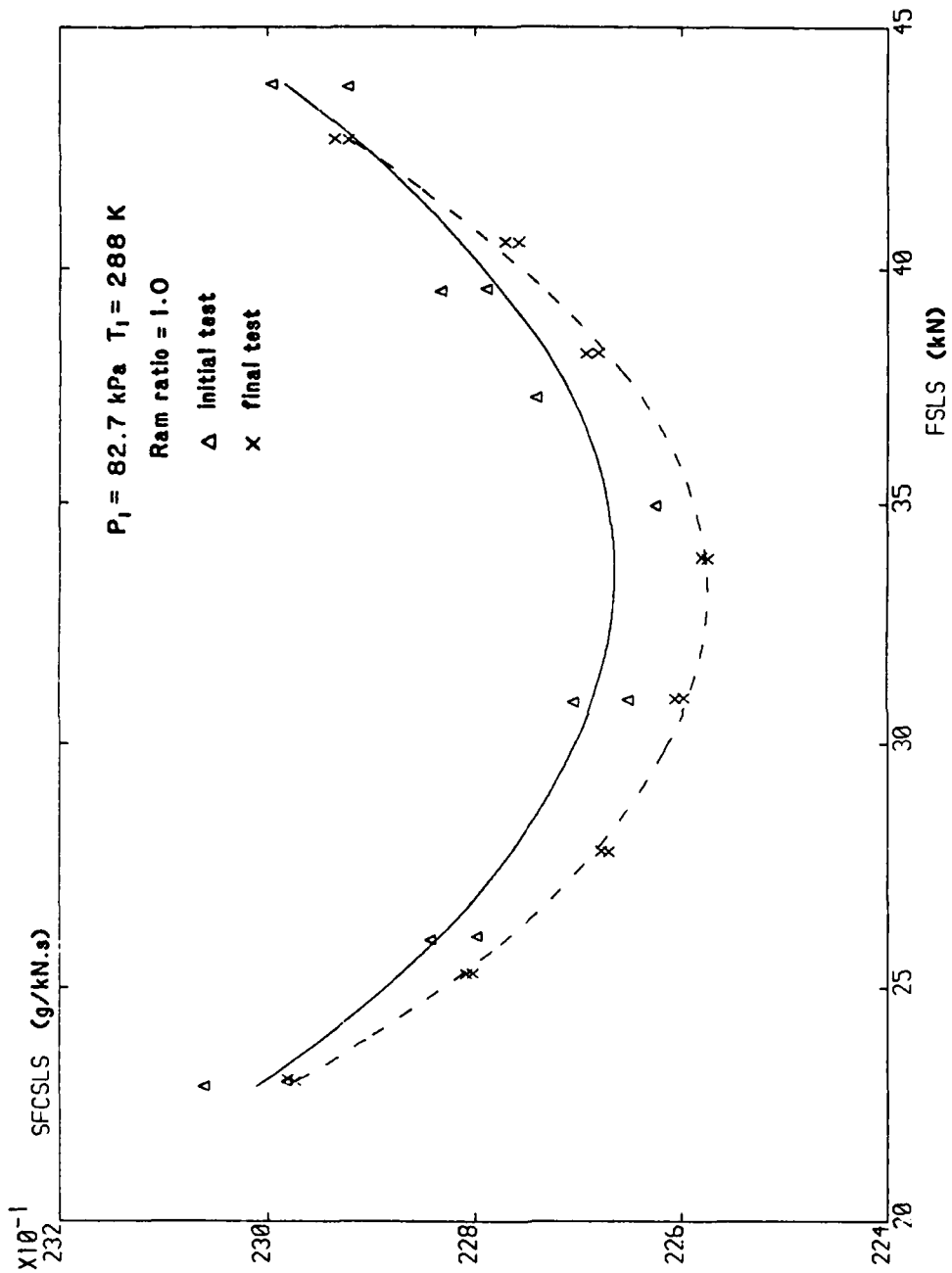


FIG. 4

THE SPECIFIC FUEL CONSUMPTION  
COMPARISON FOR THE FIRST AND  
FINAL TESTS AT RAE PYESTOCK

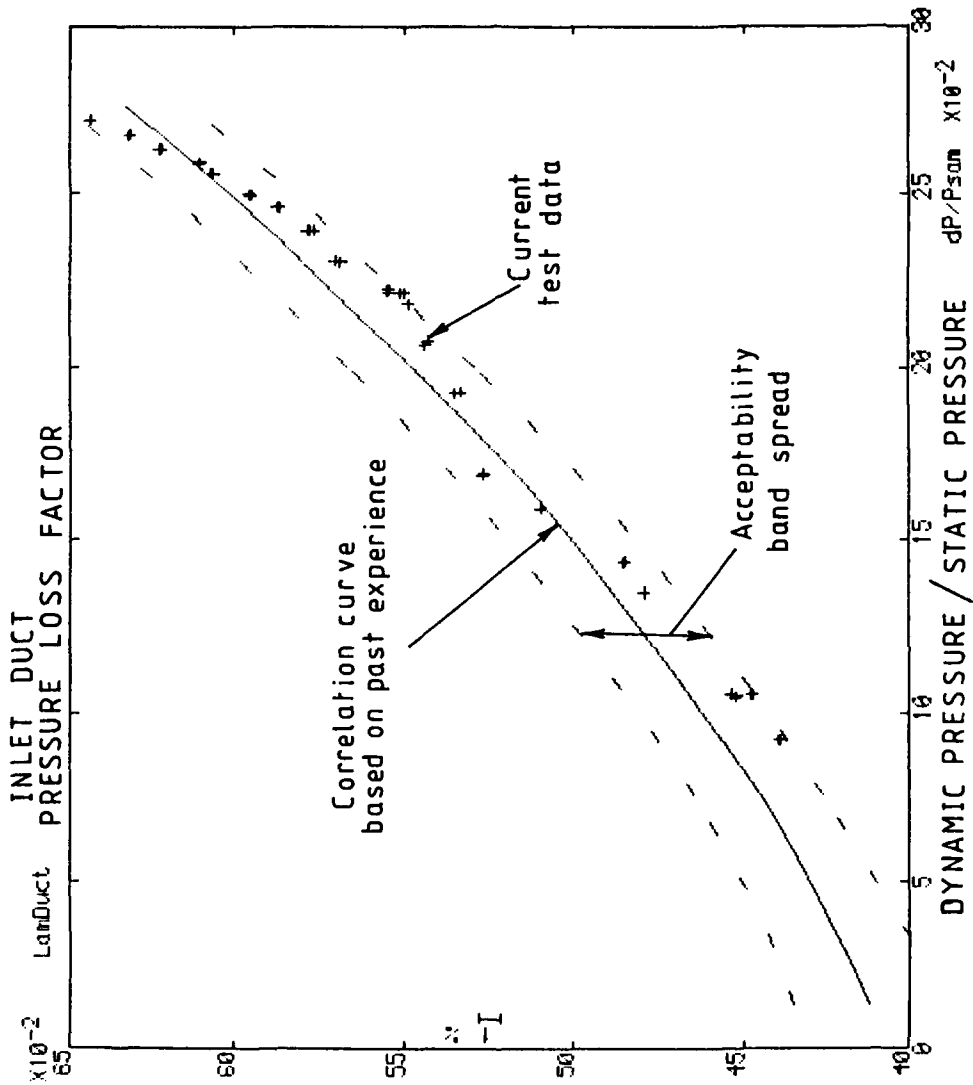


FIG. 5 EXAMPLE OF RAE(P) SECOND STAGE ON-LINE ANALYSIS GRAPH

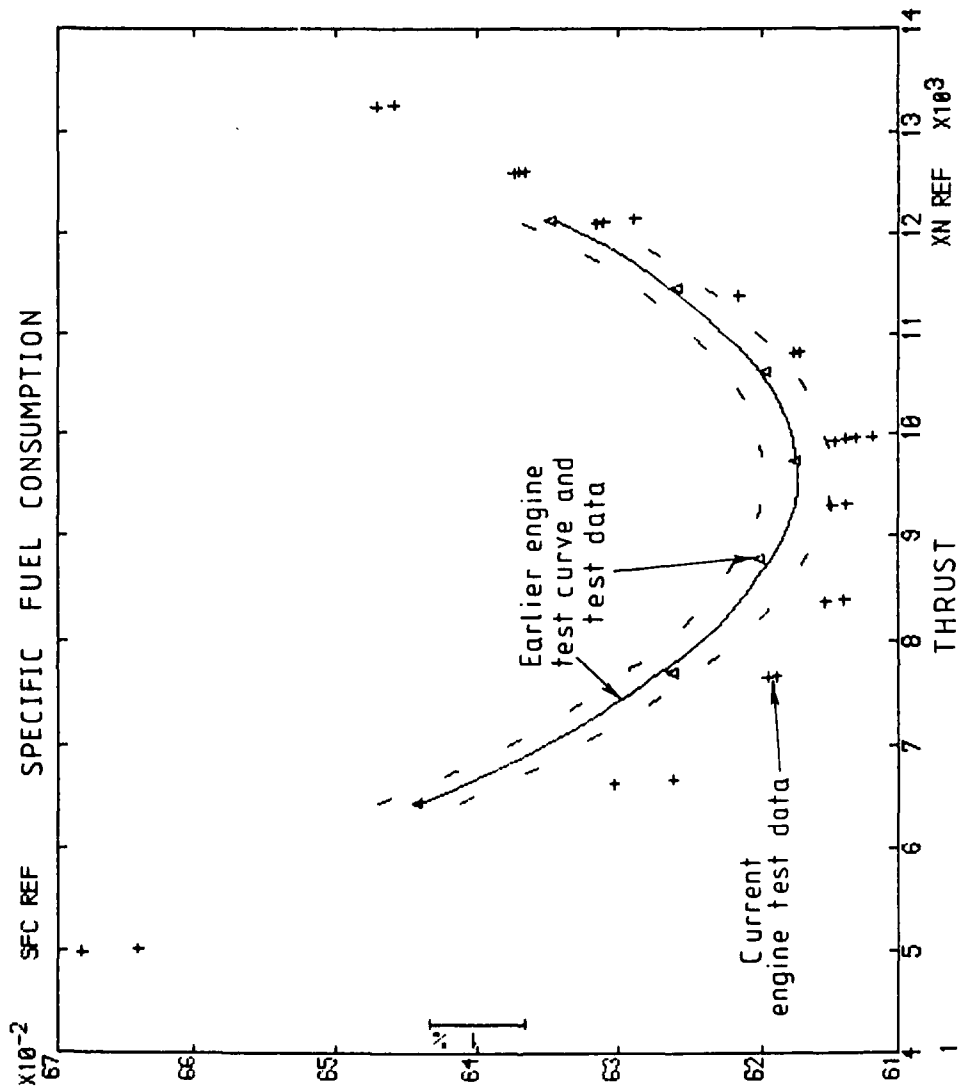


FIG.6 EXAMPLE OF RAE P THIRD STAGE ON-LINE ANALYSIS GRAPH

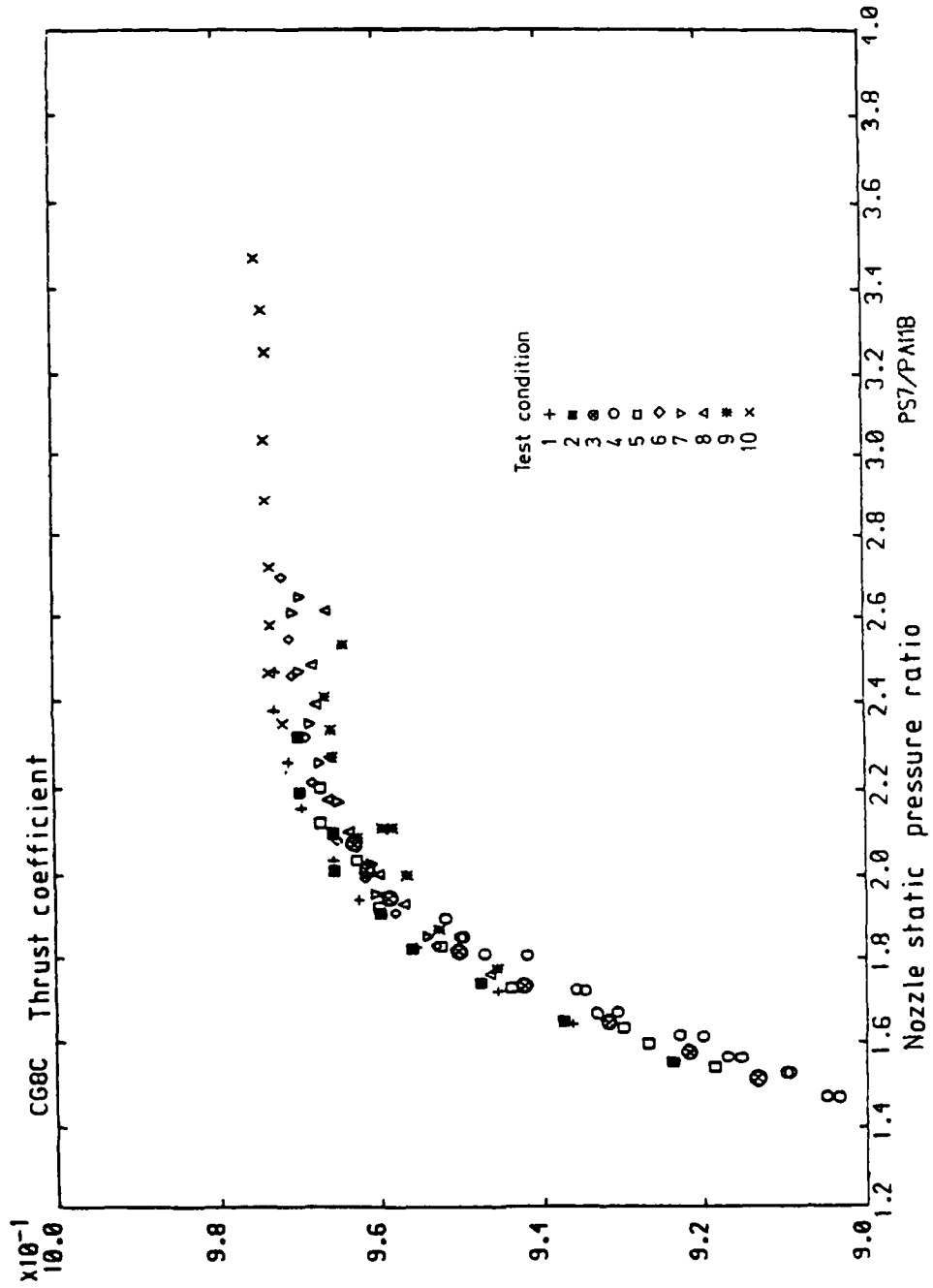


FIG.7 GROSS THRUST COEFFICIENT FOR ALL FLIGHT CONDITIONS IN THE R.A.E. TEST FACILITY

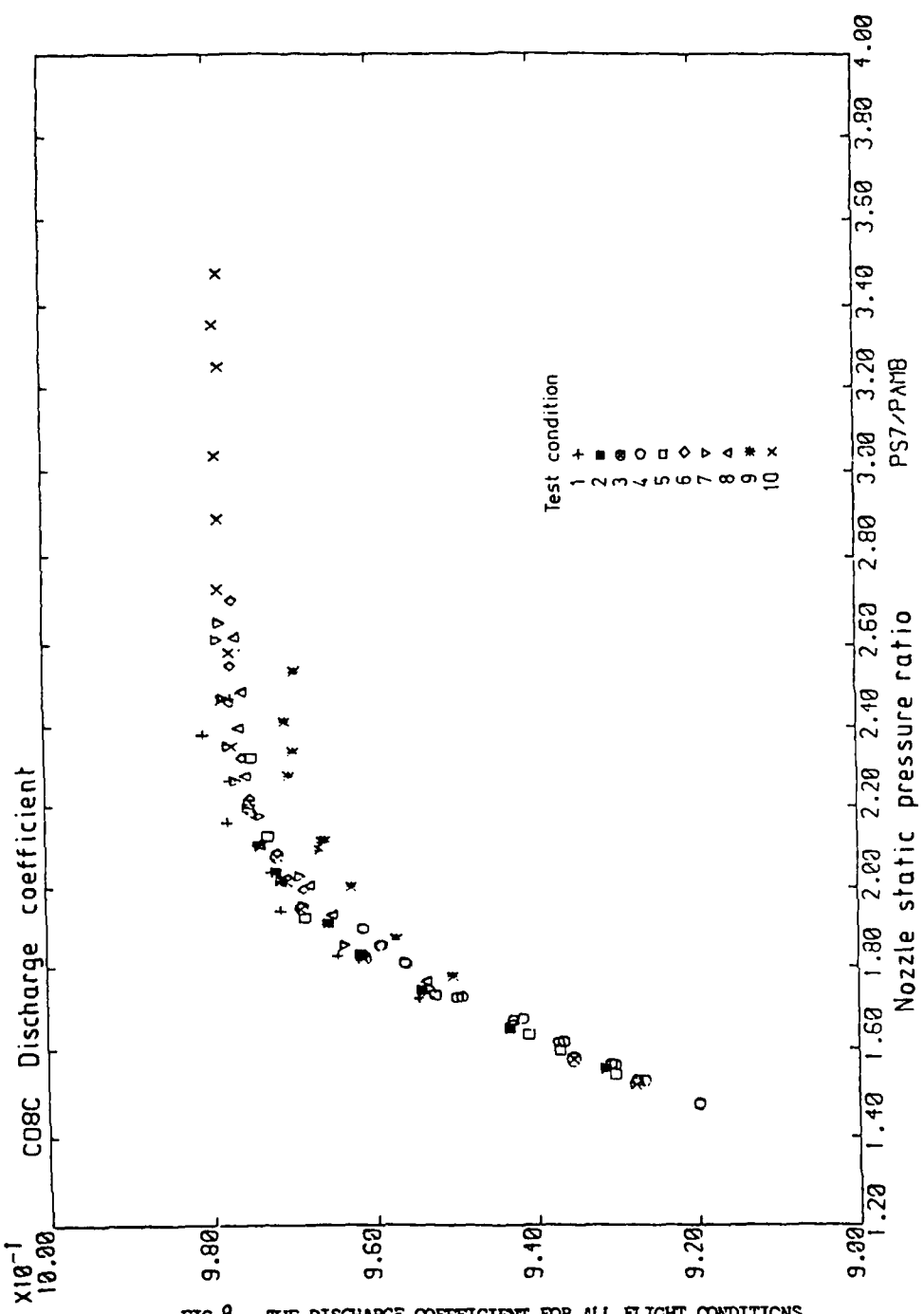
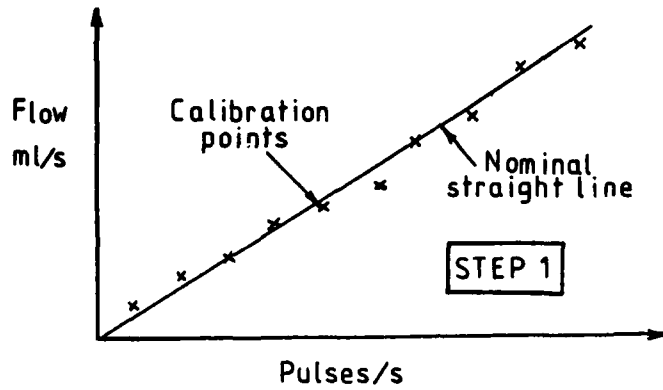


FIG 8 - THE DISCHARGE COEFFICIENT FOR ALL FLIGHT CONDITIONS IN THE RAE TEST FACILITY



- DURING TEST
- 1) Measure pulses
  - 2) Calculate nominal flow
  - 3) Add correction
    - a) from straight line
    - or b) from hyperbola

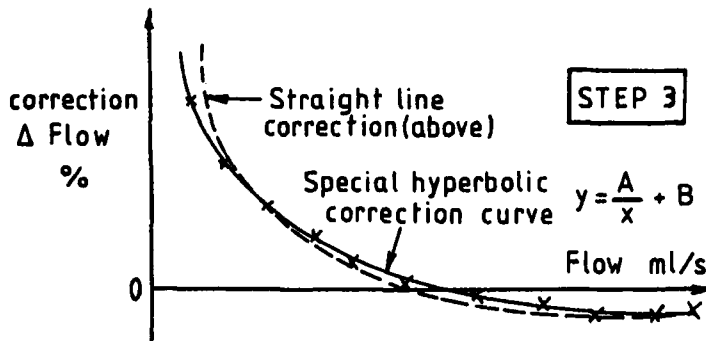
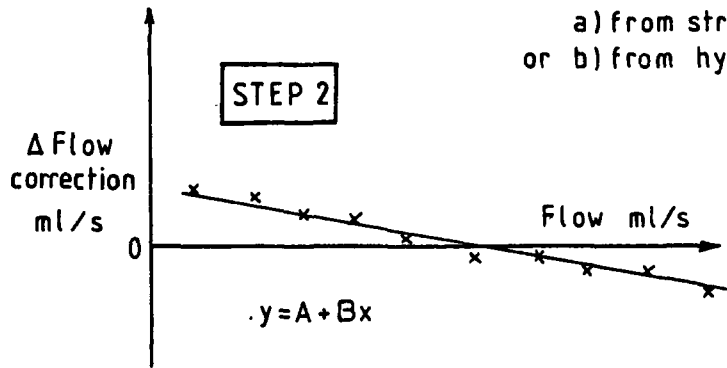


FIG. 9 RAE(P) FUEL METER CALIBRATION METHODOLOGY

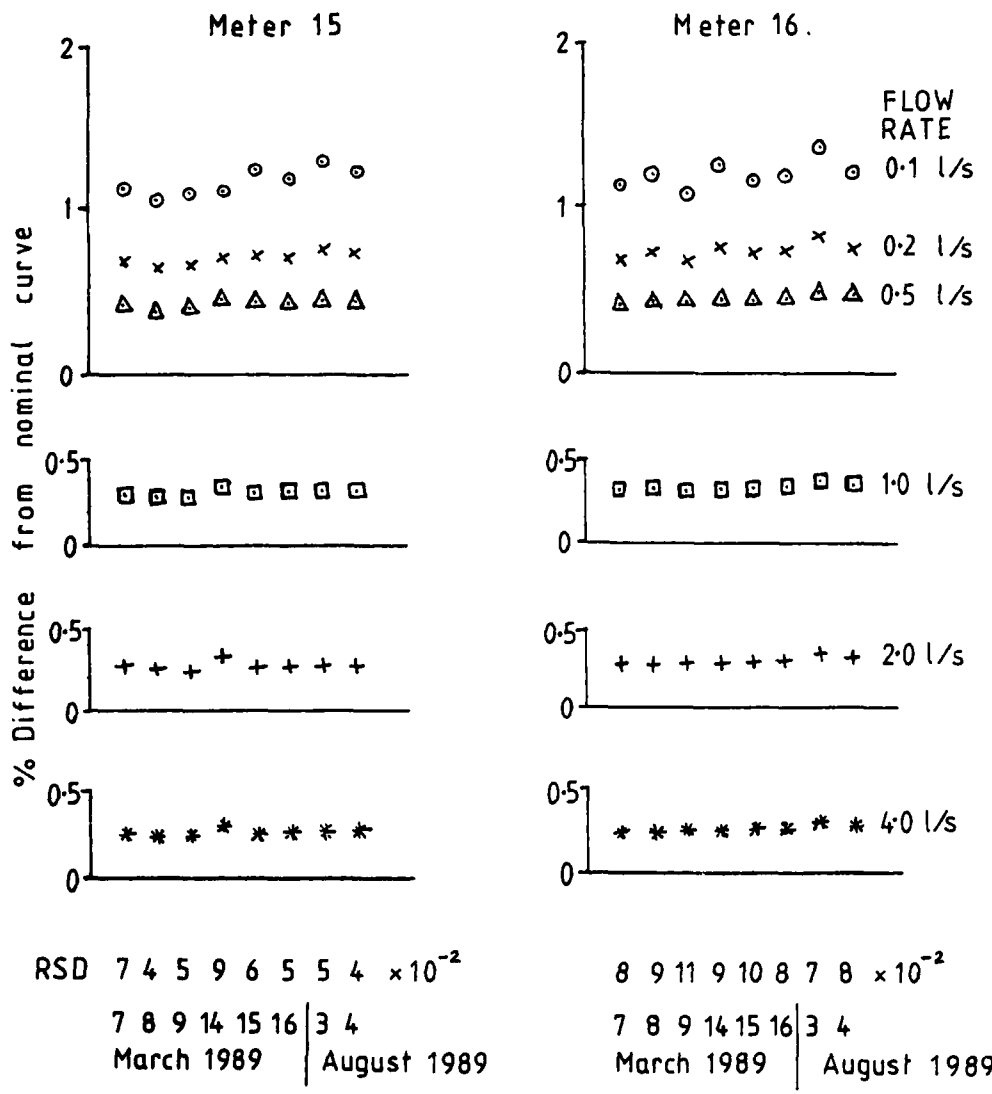


FIG.10 TYPICAL R.A.E.(P) FUEL METER CALIBRATION HISTORY CHART

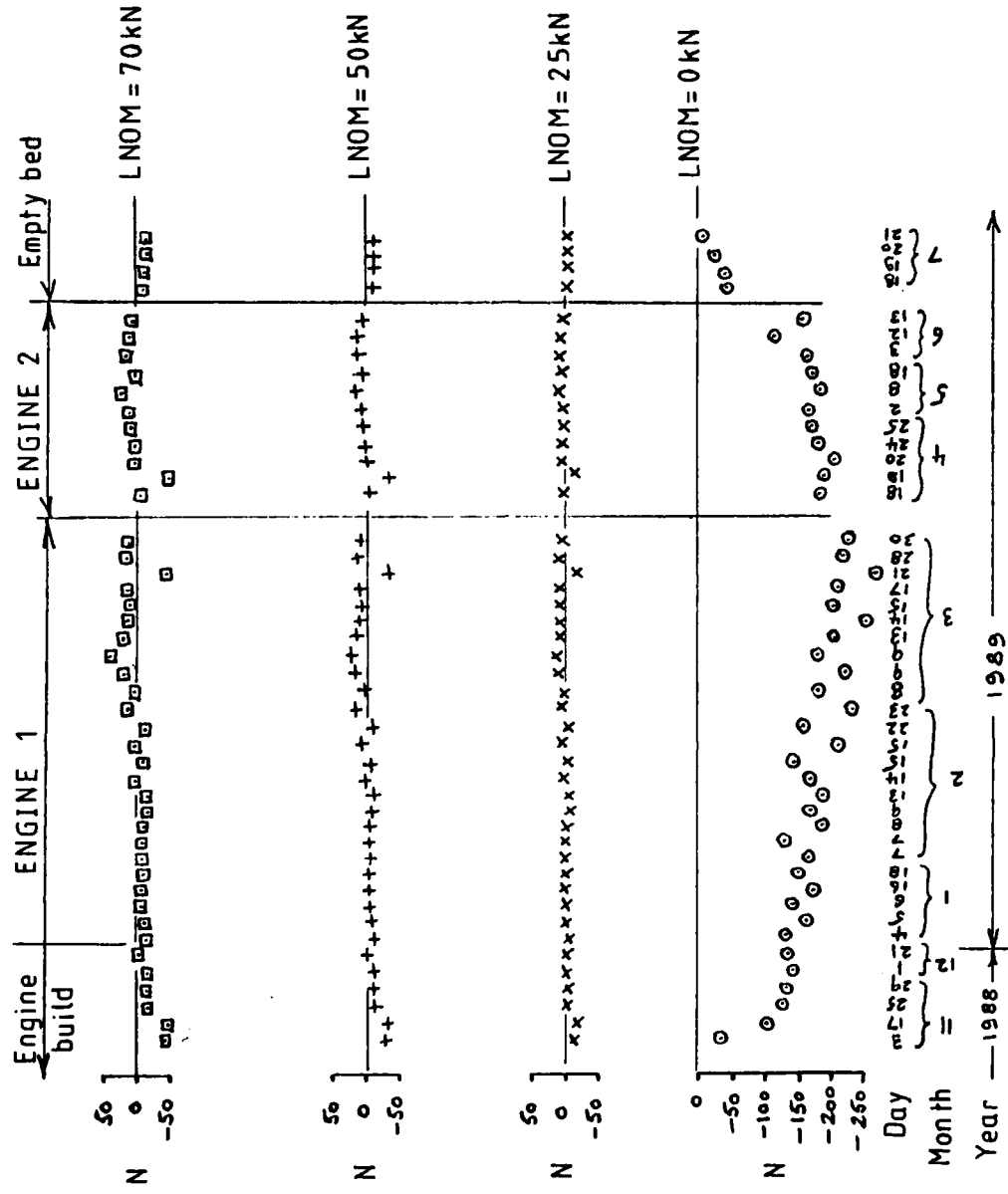


FIG.11 TYPICAL RAE(P) THRUST CALIBRATION HISTORY CHART

## EXPERIENCE IN DEVELOPING AN IMPROVED GROUND-LEVEL TEST CAPABILITY

by  
D.M. Rudnikski  
Section Head  
Engine Laboratory  
National Research Council Canada  
Ottawa, Ont. K1A 0R6  
CANADA

### SUMMARY

Enclosed ground-level cell engine testing requires a thorough understanding of engine and test cell aerodynamic interaction to ensure accurate and repeatable engine performance evaluation. The key elements of cell design have been identified and design considerations outlined. Some examples of practices employed at NRCC have been listed, a number of them directly reflecting experience gained from the UETP.

### 1 INTRODUCTION

Two major classes of engine test facilities were used in the UETP, altitude or direct connect, and the ground-level test cell. Of the two, only the altitude facility can simulate the complete altitude - Mach number envelope that an engine could experience in service. Ground-level cells are relegated to operate under prevailing environmental conditions of pressure, temperature and humidity. Despite this limitation, the ground-level bed still serves as a cost effective tool at the production, post-overhaul, and research and development level.

One of the objectives in the UETP was to compare engine performance obtained in each class of facility, and rationalize any observed differences. A difficulty encountered in the comparison was the inability of the altitude facilities, except one, to operate at the same environmental test conditions as the ground-level cells. Corrections to these data using relatively simple normalization equations were shown to be quite limited in application, and hence introduced additional bias errors.

There were other instances of uncertainties that only became evident during the process of data comparison and rationalization. This section of the Lecture Series will address some of the essential points to consider for determining engine performance in ground-level test cells. A number of common issues have already been identified in the previous lecture on altitude test capability, and will therefore not be repeated. In the sections that follow, three topic areas will be discussed, test cell design considerations, performance measurements and performance calculations.

### 2 GROUND-LEVEL CELL DESIGN CONSIDERATIONS

Ground-level cells can be sub-divided into two groups, the outdoor stand, and the indoor or enclosed test cell. Of the two, the outdoor stand is less common, although it provides the best possible datum to which the 'artificial' situation of enclosed test cells, both sea-level and altitude, can be compared. In a 'no-wind' condition, the scale force measurement is a direct reading of gross thrust at the given temperature and pressure. Its major limitation is that it is subject to the ambient environment, data quality being strongly affected by wind strength and direction, humidity, and precipitation. Another drawback is the lack of acoustic attenuation at both the inlet and exhaust, which is the major reason for bringing an engine indoors.

While acoustically beneficial, the 'raison d'être' for being outdoors, a uniform static pressure field with no approach momentum, is lost. Cell aerodynamic effects, created by the interaction of the engine with the inlet, test chamber, and exhaust collector, to some degree alter the pressure field and introduce an inlet momentum term that must be accounted for.

Several documents on design considerations for enclosed test facilities have been produced, and excerpts from two of these (Ref. 3, 4) are reprinted with permission.

Common aerodynamic test cell problems such as inlet pressure and temperature distortion and airflow recirculation can contribute to uncertainty about engine performance measurements. In an extreme case, the engine inlet airflow distortion can result in compressor stall and cause severe engine damage.

The principal components of the test cell system are the inlet plenum, the engine test chamber and the exhaust section. Each must be designed for its individual function and for its compatibility with the others, with respect to aerothermodynamic and acoustic performance. The design concept for large turbofan and afterburning turbojet engines is shown in Figure 1. The major elements of the cell and its features are discussed in the following sections.

#### 2.1 Inlet Plenum

The primary function of the inlet plenum is to deliver clean and adequate (both in quality and quantity) airflow to the test chamber. The inlet plenum should be designed to provide stable inlet flow upstream the engine inlet and to eliminate problems caused by physical and environmental conditions. The intake may be either horizontal or vertical with turning vanes, but must allow for cell operation independent of outside wind direction and magnitude so that testing can be conducted without unnecessary restrictions due to weather. The inlet flow must be treated to isolate the variations in the outside wind to reduce test cell distortion. Losses in the inlet system will be reflected in cell depression. Common inlet plenum accessories include screens, honeycomb, turning vanes (for vertical inlets), silencer baffles and possibly filters.

In the UETP, only one facility had a vertical inlet lined with acoustic baffles. There were neither turning vanes nor flow straighteners, and the proximity of the engine bellmouth to the vertical inlet is thought to have introduced flow distortions to the engine face altering engine performance. As individual pressure measurements were not recorded, there is no definitive proof of this speculation.

## 2.2 Test Chamber

A test chamber includes the engine thrust frame, and cell supporting equipment, such as lift platforms, ladders, engine monorails, and so on. Careful attention must be paid to the design of the test chamber to minimize or eliminate projections in the flow field which affect portions of the flow which enters the engine. Such projections can cause wakes and distortions in the bellmouth and produce unacceptable variations in engine performance. In addition, consideration should be given to those aspects of the test chamber design which affect the airflow in the vicinity of the engine to ensure that air is not recirculating and reingested by the engine. Reingestion of cell flow can produce temperature distortions in the compressor and adversely affect performance. Also, test chamber recirculation can reduce the accuracy of thrust correction measurements.

An important factor in test section design is the geometric ratio of engine diameter to the cross-sectional area of the cell. Another significant design consideration is the bypass ratio, which is defined as the ratio of the secondary air flowing past the engine to the airflow entering the engine inlet. Both the bypass ratio and the area ratio have a direct influence on the velocity of the air bypassing the engine, which should preferably be less than 10 m/s (Ref. 5). To meet this requirement, the maximum engine size for a given test section may be approximated by:

$$W_e = \frac{12 * A_{cell}}{(\alpha + 1)}$$

where  $W_e$  - maximum engine airflow (kg/s)

$A_{cell}$  - test section flow area ( $m^2$ )

$\alpha$  - bypass ratio

High bypass air velocities cause a reduction in static pressure along the engine length, resulting in forces that would not occur in open-air testing. These pressures acting on the engine will alter the measured thrust by producing axial buoyancy forces. The major effect of these buoyancy forces is generally near the exhaust end of the engine where the secondary flow velocities are high. If the flow velocity in the test section is significant, tailpipe ambient pressure will be reduced relative to the engine inlet pressure. The result is equivalent to the engine operating with an apparent forward velocity, and at a slightly higher altitude. The use of a high loss protective screen in front of the engine may lower the inlet pressure to the engine even further.

Flow along the test section wall experiences a rapid acceleration as it approaches the engine bellmouth, since the flow captured by the engine has a cross-sectional area larger than the engine itself. Boundary layer analysis (Ref. 6) indicates that flow along the wall separates for all cell bypass ratios. The separation location moves downstream as the bypass ratio increases. For high bypass ratios, the separation point moves downstream of the bellmouth entry plane, which will prevent vortex ingestion. For low bypass ratios, the flow separation point moves upstream of the bellmouth inlet, which may lead to vortex formation. Keeping the separation point at or behind the bellmouth inlet should reduce vortex formation.

Temperature distortion, generally caused by test cell flow recirculation, will adversely affect compressor performance similar to velocity distortion. Engine performance is strongly dependent on inlet temperature, hence location errors in temperature measurement caused by exhaust gas recirculation is a possibility. Such could be the case if screen mounted thermocouples are used. In addition to temperature distortion, cell recirculation can cause the engine external body forces to fluctuate which will reduce engine thrust measurement accuracy.

## 2.3 Exhaust System

Probably the greatest impact on engine performance is the design of the exhaust system. The exhaust system not only controls the amount of secondary airflow in the cell, but it also controls the back pressure on the engine, the sound absorption, and the production of exhaust pollution. Most modern engine testing facilities use an augmentor tube to capture the engine exhaust gas and induce secondary airflow through the cell. The exhaust is directed into the augmentor tube, through a diffuser, and then expelled into the atmosphere. The augmentor tube acts in combination with the engine exhaust momentum to form an ejector, which entrains cool, secondary air from the test cell. In the past, augmentor design was basically an art and test facility people had only quantified some of the parameters concerning ejector performance (Ref. 7).

The secondary or bypass flow is important for cooling the exterior of the turbine casing and the exhaust duct of the engine, as well as the exhaust silencer and the augmentor tube itself. It is preferable to use an augmentor tube that has a collector which can be moved relative to the engine exhaust plane, and a variety of insert sizes to modify the flow area. This type of design allows easier control over the airflow pumping requirements, noise, and local static pressure at the jet nozzle exit plane. More importantly, the quantity of secondary air entrained is crucial for proper engine testing. Too little secondary air allows recirculation of exhaust gases within the cell, resulting in overheating of the engine components and the augmentor tube. Too much secondary air causes excessive static pressure gradients between the engine inlet and exhaust planes, which require large corrections to the measured thrust. However, sufficient secondary air must be entrained to lower the kinetic energy of the exhaust, to allow the silencing equipment to perform properly. Turbofan engines, for example, tend to overpump the system and the augmentor tube must be modified to restrict the amount of entrained air.

The major design elements of an augmentor tube include the nozzle/augmentor diameter ratio, the inlet configuration, the engine airflow, the spacing between the engine nozzle and augmentor tube, and the engine exhaust temperature. Each of the parameters will have an effect on the cell bypass ratio, the total cell airflow, and the pressure, temperature, and velocity profiles in the augmentor tube.

The collector to engine nozzle diameter ratio is a very important parameter in the augmentor design. The bypass ratio decreases with decreasing diameter ratio because of the reduced secondary flow area (Ref. 6). As the diameter ratio increases, the entrance losses become less important because the secondary air enters the augmentor tube in a more axial direction. A converging-diverging engine nozzle will reduce the bypass ratio because of the increased secondary flow blockage from the diverging nozzle flow, and because of the decreased diameter ratio from a modulating nozzle.

An example of the effect of nozzle to collector size is shown as Figure 2 (Ref. 6) based on 1/12 scale model experiments of the NRCC No. 5 test cell. Nozzle pressure ratio and nozzle to collector spacing were held constant while varying collector diameter for a given nozzle size. For a given nozzle size (relative to the test cell cross-section), the entrainment ratio varies almost linearly to a maximum value and then drops off.

The spacing between the engine nozzle and augmentor tube has less influence on the secondary airflow. The bypass ratio increases slightly with spacing because of reduced blockage of the nozzle and then decreases because of increased flow blockage of the spreading exhaust plume (Ref. 7). More importantly, the spacing affects the static pressure field at the nozzle exit, which ideally should be the same as the static pressure field around the engine. Increasing the spacing causes an increase in the noise produced within the cell, because of the larger shear layer between the jet exhaust stream and the low-velocity secondary air.

The ground-level facilities in the UETP had a diameter ratio ranging from 1.5 to 3.5 and nozzle spacings from 0.8 to 2.7 (Figure 3). It can be reasonably expected that the pressure field around the nozzle varied for each installation and had a direct influence on the thrust accounting equations. This effect for the NRCC facility will be discussed in a later section.

The secondary cell bypass flow is also a function of the engine exhaust temperature. The cell bypass ratio varies approximately as the square root of the ratio of the exhaust total temperature to the engine inlet total temperature (Ref. 8). Military engines, because of their inherently higher exhaust plume temperatures, induce higher bypass ratios.

## 2.4 Summary of Design Considerations

The effects of enclosed test cells on engine performance are primarily aerodynamic. Before embarking on new cell designs or modifications to existing facilities it is best to construct a scale model of approximately 1/12 size and evaluate individual cell components for their effects on the total system. The key areas for evaluation are shown as Figure 4 (Ref. 9).

## 3 Performance Measurements

Engine performance in a ground-level cell is generally defined as thrust, fuel flow, and to a lesser degree airflow. In an altitude facility, airflow is required for the definition of thrust, whereas in a ground-level cell this is normally not the case. The exception is if the installation incorporates a decoupled bellmouth, and the bellmouth forces are not transmitted to the thrust stand. For this situation, the thrust accounting procedures become similar to those employed for altitude facilities, and engine airflow must be determined.

In this section, airflow and fuel measurements will be briefly discussed, but thrust will be dealt with more rigorously.

### 3.1 Airflow

Airflow is in most cases obtained through the use of smooth-approach orifices conforming to ASME standards. Measurements of pressure, temperature and area at the throat of the air meter are required for the calculation. The air meter itself has to be calibrated against another standard, or by carefully traversing the throat with pitot probes and establishing a flow coefficient. The accuracy and repeatability of this device may be affected by flow distortion or turbulence approaching the engine.

These are two cautions that must be observed when using an airmeter of this type. One is the assumption of uniform static pressure across the measurement plane, and the other is the high measurement precision required in what is a relatively low Mach no. flow field. Uniformity of static pressure must be confirmed by traversing the measurement plane, and also ensuring that no flow distortions from upstream disturbances are present. The low Mach no. inherent in the measurement plane can be increased by locally reducing the area, followed by a diffuser to the engine face. Diffusers do thicken up the boundary layer and may alter engine performance.

In the UETP, NRCC and TUAF had low Mach no. directly coupled airmeters, while CEPr had a necked-down airmeter, followed by a diffuser which was decoupled from the thrust stand (Figure 5 from Ref. 2). Inherently, the CEPr airmeter should have provided the most consistent and accurate results, which proved to be the case (Section 18.3.3 of Ref. 2). NRCC had difficulties in establishing a flow coefficient because of a double accounting of the boundary layer growth. TUAF airflow measurements are believed to have suffered from inflow distortion effects, but as the pitot probes data were not individually recorded, it is only speculative.

### 3.2 Fuel Flow

The most commonly used system to measure fuel flow is a volumetric turbine type device coupled to a variable time base digital readout instrument. The sensors, at least two in series, when installed with flow straighteners upstream and downstream, are accurate and reliable. Fuel density and viscosity are calculated from temperatures measured at the meters. If a wide range of flow is required, as in the case of afterburning engines, a multi-manifold fuel system should be installed near the fuel inlet to the engine. With time, bearing wear will degrade the accuracy of the meters and introduce non-linearities in the low flow range. For this reason, periodic calibrations are necessary. A typical calibration is shown in Figure 6. The required inputs are frequency and viscosity (temperature dependent); with the output the so called "K" factor. Actual fuel specific gravity at the fuel temperature and the frequency are combined to produce actual gravimetric fuel flow.

Note from Figure 6 that when operated in the linear range, the value of viscosity is not very important. Only if the meter were 'incorrectly' operated in the non-linear low-flow range, would viscosity be significant.

Positive displacement meters were used by one altitude facility in the UETP. Whether positive displacement or turbine type, corrections must be made for specific gravity and lower heating value. Volumetric meters should both be calibrated using a fluid of similar viscosity and specific gravity to jet fuel, but the effect of non-compliance would be much less for positive displacement meters.

The method of calibration, whether volumetric or gravimetric can also introduce errors as was discussed in an earlier lecture. In a controlled 'round-robin' test of calibration facilities, it was shown that the spread in results was up to 0.5%, with a demonstrated bias of at least 0.2% between volume and gravimetric calibrators (Figure 7).

In the UETP, there was quite a large scatter in the results, and although the reference meters were the primary basis of comparison, operational difficulties in some facilities rendered these data unusable.

### 3.3 Scale Force Measurement

The system most commonly used to measure the thrust of a turbojet or turbofan utilizes strain gauge type load cells. They may be mounted near the front or at the rear of the thrust stand in compression or tension. The forward location is preferred to reduce the possibility of errors due to thermal radiation from the engine exhaust. The thrust measuring system should be designed to minimize false loading of the load cell due to temperature gradients in the structure and/or calibration in a different horizontal plane than the thrust loading.

Stand stiffness, spring rate, and hysteresis have to be accounted for as there may be measurable deflections of the thrust cell relative to the ground reference. Squeezing the thrust cell with a reference load cell in the plane of the measurement cell could conceivably calibrate the overall system on a routine basis. However, because the engine thrust vector is some distance above the load cell, a centre-pull calibration with the engine in place is mandatory, as the overturning moment induced in the stand can cause the flexures to change loading from tension to compression. Should this happen, the calibration will likely be non-linear, unrepeatable, and sensitive to changes in mass.

### 3.4 Thrust Accounting

In an outdoor facility, the engine operates in a uniform static pressure field; thus the pressure in the plane of the nozzle exit is the same as that surrounding the engine. For this situation, with still air conditions, the measured thrust on the load cell is equal to the engine gross thrust. In an indoor facility, an exhaust collector is generally placed in close proximity to the nozzle exit, creating an ejector effect, thereby inducing secondary airflow through the test cell. This placement, combined with the secondary airflow entering the collector, locally modifies the static pressure field at the nozzle exit.

For this situation, the engine static pressure environment is different from that measured by the trailing edge statics, the value of which was defined as PAMB in the UETP General Test Plan (Ref. 1). To overcome this difficulty, all pressure forces were referred to a plane upstream of the engine inlet, which when added to the scale force and momentum terms, yielded a value for gross thrust (Figure 8 from Ref. 3).

In this installation, the bellmouth is mechanically coupled to the engine stand. The locations of the planes of accounting are somewhat arbitrary, except for the exhaust exit plane. The requirements for planes 0 and b are uniform static pressure and velocity. Definition of planes 0 and b might prove difficult in test cells that have distorted flow fields, which may occur with a vertical inlet.

The sum of the forces acting on the control volume, under steady-state conditions, is equal to the change in axial momentum across the control volume. A summary of the pertinent equations is as follows:

$$F_m + A_d P_0 - A_{pb} P_M - A_d P_0 + F_d + F_f - F_w - W_0 V_0 + W_b V_b - W_0 V_0$$

where  $F_d$  - drag force on the thrust frame  
 $F_f$  - friction drag on the engine  
 $F_w$  - friction drag on the walls

The most significant aerodynamic component of the thrust measurement is the intrinsic inlet momentum, which produces a force on the engine as a result of drawing air into the test cell (Ref. 10). For static engine testing, the magnitude of this force may be substantial. Since this force is, in effect, a drag term, it must be added to the measured thrust of the engine. A complete breakdown of all the terms is given in Ref. 3, but for illustrative purposes, the size of the individual components for NRCC is shown in Figure 9.

CEPr had a detached bellmouth in their facility, thus the thrust accounting more closely approximates that for altitude cells.

## 4 Performance Calculations

### 4.1 Ambient Corrections

Corrections for ambient temperature and pressure are absolutely necessary for engine performance evaluation. It was shown in Section 16 of Ref. 2 that the standard corrections are valid only over a very limited range of excursion from standard day conditions. More complex engines employing variable geometry would deviate even further using simplistic corrections, thus the need for an empirical engine model or 'cycle deck' for data reduction and comparison.

Another factor of concern to ground-level cells is the presence of humidity in the inlet air. Engine performance is significantly affected by high humidity in the intake air. While air properties ( $C_p$ ,  $\gamma$ , MW,  $R$  - specific heats, molecular weight, and gas constant) can be corrected for reasonably low levels of absolute humidity, high relative humidity may result in condensation in the engine inlet. The phase change from vapour to liquid in the accelerating air inflow stream results in a temperature rise in the air stream, which is difficult to handle precisely for airflow calculations. Subsequent evaporation in the fan stream reverses the process. Furthermore, wetness of fan blade surfaces may affect fan efficiency. Visible moisture in the air could also enter the pressure probes introducing biases in the pressure measurements. Thus, in order to avoid condensation in the air inlet stream, the following atmospheric limitations should be observed:

maximum relative humidity: 75%  
 maximum absolute humidity: 14 g water/kg air (98 grains)

The thermodynamic properties of moist air may be determined by a weighted average of the properties of the two components - dry air (subscript a) and water vapour (subscript w). Based on absolute humidity,  $q$ , in grams of water vapour per kilogram of dry air, the following equivalent dry air properties can be defined:

$$C_p = \frac{1000 C_{p,a} + q C_{p,w}}{1000 + q} \quad (\text{specific heat at constant pressure})$$

$$C_v = \frac{1000 C_{v,a} + q C_{v,w}}{1000 + q} \quad (\text{specific heat at constant volume})$$

$$\gamma = \frac{1000 C_{p,a} + q C_{p,w}}{1000 C_{v,a} + q C_{v,w}} \quad (\text{ratio of specific heats})$$

$$R = \frac{1000 R_a + q R_w}{1000 + q} \quad (\text{gas constant})$$

This approximate method and its experimental verification is described in Ref. 11. It yields corrections to obtain dry thrust and airflow at constant rotor speed, ram pressure ratio, and inlet temperature.

Recent studies of available literature show that while the above corrections apply in a number of cases, they are by no means all-inclusive. As a result, an AGARD PEP study group has been formed to critically review the literature and produce a document with application guidelines.

Corrections of ground-level gross thrust were shown not to agree with the equations listed in Ref. 1. It was shown that corrections using the tailpipe mounted ambient pressure sensor (PAMB) were invalid. The PAMB measurement was directly influenced by the nozzle to collector spacing and size ratio, and thus was not indicative of the pressure field surrounding the engine. To account for this interference for the J57 engine, corrections of thrust in ground-level cells is simply:

$$FGR = FQ\delta$$

rather than:

$$FGR = (FQ\delta) + (AQ\delta)(PAMB - P2AV)$$

as defined for ground-level cells in the UETP (Ref. 2).

#### 4.2 Flow Coefficient

The use of nozzle flow coefficients for validation of facility measured thrust and airflow also has application to ground-level test cells. The technique was well documented in Section 13 of Ref. 2, and in the previous lecture, thus will not be repeated here. Turbine flow functions also have some use, but to be valid the final nozzle must operate in a choked condition, which may limit their use to high pressure ratio engines. Variable area final nozzles, as are typified by afterburning engines, make this technique less useful, for the geometric area must be a repeatable known value.

#### 4.3 Data Handling and Presentation

Experimental programs such as the UETP can produce voluminous quantities of data, especially if an automated data gathering and handling system is used. There is a great tendency to measure everything that is possible often without regard as to how the data will later be presented. Complete reduction, cataloguing, analysis and storage of the data should be done within several days (preferably the same day) of the test. Memories of those present during the test are sometimes very short. A good example is this Lecture Series. It is difficult

to recall all the thought processes that were used at the time of the data comparison, with the consequence that some important items may have been overlooked.

Some specific items that were encountered at NRCC were:

- i) The use of software to selectively eliminate faulty sensor values can be risky. Typical software programs calculate a rake average and then attempt to eliminate outliers. Certain stations within the engine have severe pressure or temperature gradients, thus good data would be removed for the wrong reason. Another difficulty with outliers is trying to decide when to throw out an entire test point because of one bad sensor, or removing one sensor as faulty if it is only intermittent.
- ii) Curvefitting of certain parameters using a quadratic equation may lead to erroneous results, e.g., SFC, turbine efficiency, etc., because of their very non-linear shape. Polynomial curve fitting should be employed instead.
- iii) Test planning and execution should include repeat data points within a run and across runs within a test series. An engine thermodynamic model should be available to estimate the ranges of measurements, to derive temperature lapse rates and to assess changes in performance or to detect bad sensors.
- iv) Measurement uncertainty analysis should include a complete error audit of all error sources for key parameters. A complete description of the calculation algorithms for all performance parameters is necessary. Error models for transducers will have a major effect on the system accuracy. The comparison of curvefitted data must include the errors introduced by the curve slope effect and the effects of common measurements in both the dependent and independent parameters.

## 5 Concluding Remarks

Ground-level test cells, despite their limitations on environmental control fulfill an important role in assessing engine performance. Enclosed test cells require a number of corrections to the measured value of thrust to obtain an uninstalled gross thrust. These corrections may be analytically derived from detailed measurements in a test facility, or may be established by comparing enclosed test facility results to some standard datum. A universally accepted datum is an outdoor test stand, which when utilized in conditions of zero wind, measures gross thrust directly as scale force. With future engines growing in terms of thrust and airflow, the importance of the test cell design and the thrust corrections needed to account for the "test cell effect" will increase dramatically. A better understanding of the interaction between the engine and its immediate surroundings will enhance the quality and efficiency of engine testing in the future.

## REFERENCES

1. Subcommittee 01, AGARD Propulsion and Energetics Panel, Working Group 15, "Uniform Engine Test Program - General Test Plan", June 1983 (Revised Edition).
2. Ashwood, P.F., principal author, and Mitchell, J.G., editor, "The Uniform Engine Test Programme - Report of PEP - WG15", AGARD Advisory Report No. 248, February 1990.
3. MacLeod, J.D. "A Derivation of Gross Thrust for a Sea-Level Jet Engine Test Cell". Division of Mechanical Engineering, National Research Council Canada. DM-009. September 1988.
4. SAE EG-1E. "Design Considerations for Enclosed Turbofan/Turbojet Engine Test Cells". Draft submitted to SAE EG-1E Subcommittee. February 1988.
5. SAE. "Gas Turbine Engine Test Cell Correlation". Society of Automotive Engineers, Inc., Warrendale, PA. SAE APR 741. 1976.
6. Kromer, S.L., and Dietrich, D.A. "Flowfield Analysis of Low Bypass Ratio Test Cells". Journal of Aircraft, 22(2): 99-100. 1985.
7. Sapp, C.N., Jr., and Netzer, D.W. "Experimental Investigation of Turbojet Test Cell Augmentors". Naval Postgraduate School, Monterey, CA. SPS67-78-009. 1978.
8. Hastings, R.R. "A Simulation of a Jet Engine Test Cell". Division of Mechanical Engineering, National Research Council Canada, Ottawa, Ont. LTR-ENG-110. 1983.
9. Hoelmer, W., and Smith, T.E. "GE Aircraft Engine Test Cell Aerodynamic Design Specification". March 1989.
10. Oates, G.C. "The Aerothermodynamics of Aircraft Gas Turbine Engine and Rocket Propulsion". American Institute of Aeronautics and Astronautics, New York, NY. 1984.
11. Grabe, W., and Bird, J. "Humidity Effects on Gas Turbine Performance". Division of Mechanical Engineering, National Research Council Canada. TR-ENG-003. December 1988.

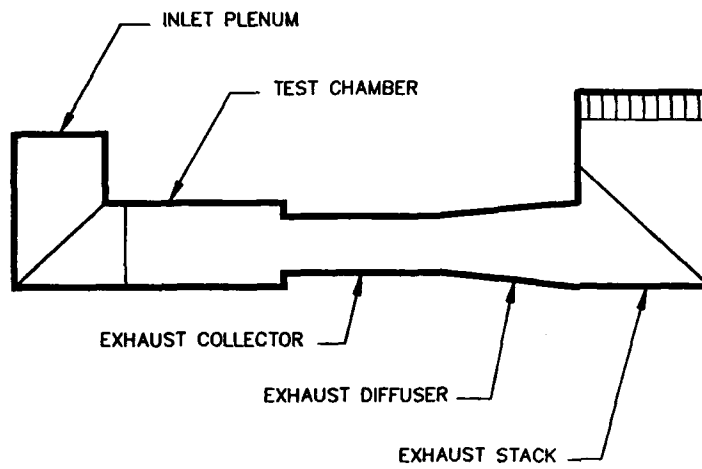


Figure 1 Major test cell areas of consideration

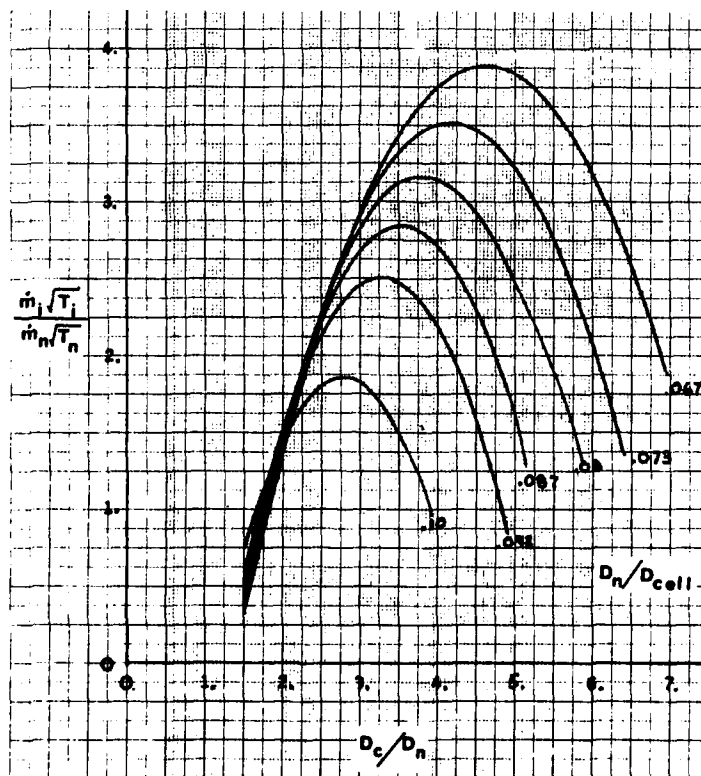
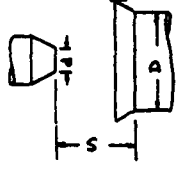


Figure 2 Nozzle and collector effects on entrainment ratio

$d = 550 \text{ mm (nominal)}$



	D mm	S mm	$\frac{D}{d}$	$\frac{S}{d}$
NASA PSL3	1016	660	1.85	1.20
AEDC T2	1700	250	3.09	0.45
CEPr R6	1800	580	3.27	1.05
RAE(F) Cell 3	2134	1412	3.88	2.57
NRCC Cell 5	838	457	1.52	0.83
CEPr TO	1930	650	3.51	1.18
TUAF	1830	1500	3.33	2.73

Figure 3 Comparison of exhaust geometries

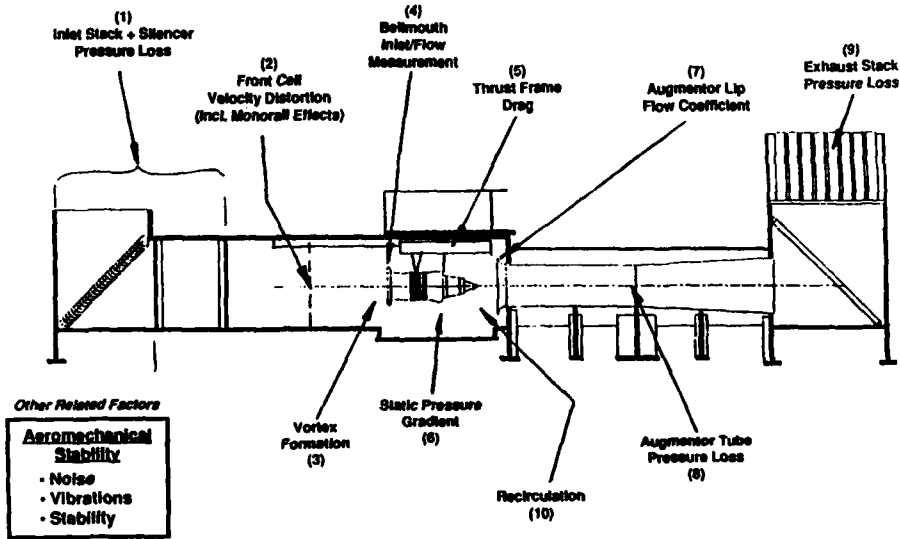


Figure 4 Test cell aerodynamic design factors

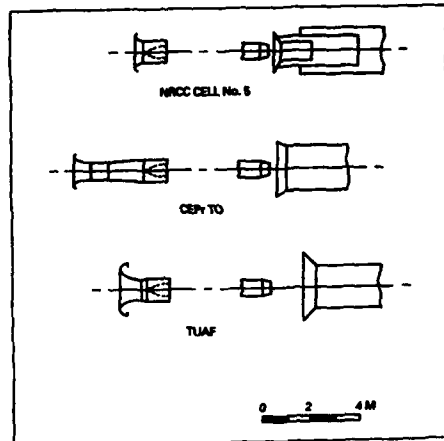


Figure 5 Comparison of inlet and exhaust geometries - ground-level cells

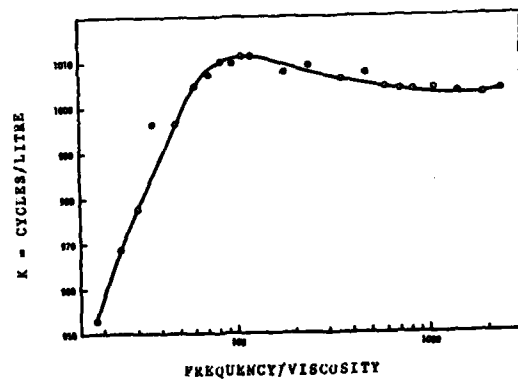


Figure 6 Typical turbine meter calibration

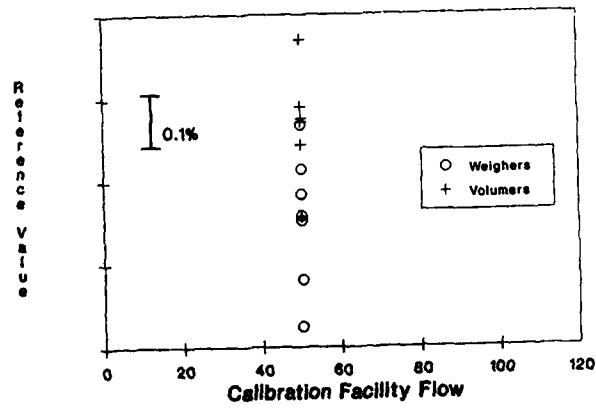


Figure 7 NIST round-robin calibration results

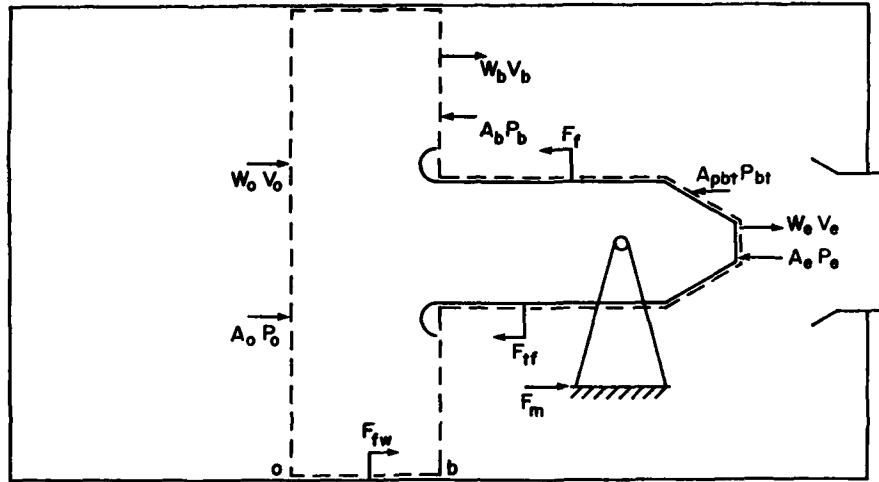


Figure 8 Engine and test cell control volume

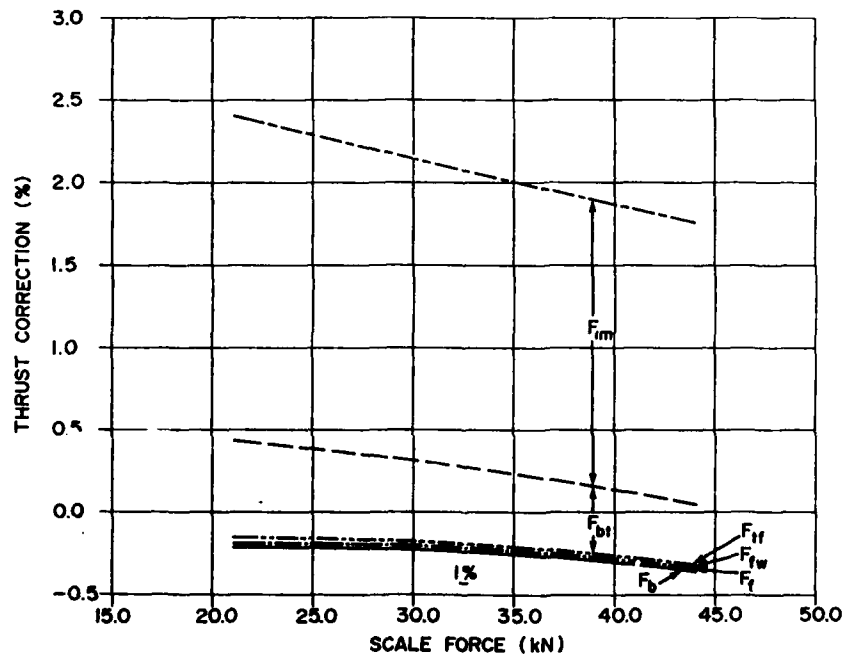


Figure 9 Correction factor comparison

AGARD

ADVISORY GROUP FOR AEROSPACE RESEARCH AND DEVELOPMENT  
NORTH ATLANTIC TREATY ORGANIZATION

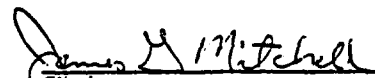
UNIFORM ENGINE TESTING PROGRAM  
GENERAL TEST PLAN

Propulsion and Energetics Panel  
Sub-Committee 01  
Airbreathing Engine Testing and Test Facilities

Working Group Number 15

REVISED December 1982

Approved By:

  
Chairman  
AGARD Working Group 15

UNIFORM ENGINE TESTING PROGRAM  
GENERAL TEST PLAN

REVISIONS FROM JANUARY 1982 GTP

<u>PAGE</u>	<u>DESCRIPTION</u>
26	Added specific gravity to fuel analysis requirements
37-53	NASA revised standard equations
42	Added note pertaining to fuel viscosity adjustment
54-58	NASA revised nomenclature
69	Corrected exhaust nozzle terms to correspond with nomenclature
72	NASA revised format for facility test report
77	Revised MIL power speed settings for engine S/N F615037
80	Revised format for test summary sheet
89	NASA revised instrumentation sheets
106-109	Revised parameter identification for standard AGARD engine performance plots
110-111	NASA revised format for test summary result sheets
126	Plot identification changed to indicate overall compressor pressure ratio

In addition to above changes several other minor changes have been made (i.e. changing Hz to RPM and adding parenthesis & brackets to equations).

REVISIONS FROM SEPTEMBER 1982 GTP

<u>PAGE</u>	<u>DESCRIPTION</u>
34	Revised Engine Power Settings for Sea-Level Testing
55	Correction to Nomenclature
56	Correction to Nomenclature

<u>PAGE</u>	<u>DESCRIPTION</u>
59	Correction to Nomenclature
117-118	Revised Engine Starting and Shutdown Procedures
126	Revised Limit for Exhaust Gas Temperature
135-138	Appendix V added with attachment
37-54	Various revisions and clarifications added to Standard Equations for UETP
81-82	Addition to TABLE III of Section C and D for Bleed Closed and Open Settings
61	Addition to Calculation, Engine Data and Facility Data groups

NOTE: \* in right margin denotes revision from September 1982 General Test Plan

REVISIONS FROM DECEMBER 1982 GTP

<u>PAGE</u>	<u>DESCRIPTION</u>
10	Deleted "1" from Dr. Mitchell's Telephone Number
12	Added/corrected telephone numbers/telex numbers, changed non-panel member from France and changed title for Mr. M. Holmes of United Kingdom as well as name of establishment
16	Changed C.E.Pr. Representative to M. F. Fagegaltier and name of participant No. 4 from National Gas Turbine Establishment to Royal Aircraft Establishment (Pyestock)
17	Changed AEDC Representative (Air Force) from J. F. Soileau to A. E. Burwell
19	Changed from Nat. Gas Turbine Estab. to Royal Aircraft Estab. (Pyestock)
111	Changed Parameter Name
112	Changed Parameter Name

**PREFACE**

Presented herein is a general test plan which specifies common test hardware, instrumentation, data acquisition, and data processing procedures for the AGARD Uniform Engine Test Program (AGARD-UETP). This plan should serve as a guideline for the preparation of each participant's test plan and as a control document for the definition of the test engine and related test hardware. The general test plan is being compiled and maintained by the Arnold Engineering Development Center and material pertaining to the plan should be forwarded to the Working Group Chairman (Dr. J. G. Mitchell).

## TABLE OF CONTENTS

	<u>Page</u>
1.0 INTRODUCTION . . . . .	9
2.0 AGARD-UETP MEMBERSHIP. . . . .	10
3.0 AGARD-UETP OBJECTIVES AND MEMBERSHIP RESPONSIBILITIES	
3.1 Program Objectives. . . . .	14
3.2 AGARD Working Group 15 Authority/ Responsibilities. . . . .	14
4.0 AGARD-UETP TEST PARTICIPANTS . . . . .	16
5.0 PARTICIPANT TEST OBJECTIVES AND RESPONSIBILITIES	
5.1 Facility Test Objectives. . . . .	18
5.2 Participant Responsibilities. . . . .	18
5.3 Participant Test Schedule . . . . .	19
6.0 ENGINE DESCRIPTION	
6.1 General Description . . . . .	20
6.2 Compressor Bleeds . . . . .	20
6.3 Oil Cooler. . . . .	21
6.4 Engine Exhaust Nozzle . . . . .	21
6.5 Engine Instrumentation. . . . .	22
6.5.1 General. . . . .	22
6.5.2 Station Designation and Nomenclature . . . . .	22
6.5.3 Instrumentation Connections and Identification . . . . .	22
6.5.4 Referee Instrumentation Requirements . . . . .	23
6.5.5 Dynamic Pressure Transducers . . . . .	23
6.6 Spare Parts . . . . .	23

<b>7.0</b>	<b>TEST INSTALLATION REQUIREMENTS</b>	
7.1	General . . . . .	24
7.2	Engine Inlet Hardware . . . . .	24
7.3	Test Cell Cooling and Flow Gradients. . . . .	24
7.4	Engine Mount System . . . . .	25
7.5	Engine Installation Interface Definitions . . . . .	25
7.6	Engine Fuel System. . . . .	27
7.7	Power Lever Shaft Schedule and Rigging. . . . .	27
7.8	Electrical System Requirements. . . . .	28
7.9	Lubricating Oil System. . . . .	28
7.10	Hardware Items Available to UETP Participants . . . . .	28
7.11	Available Drawings for UETP . . . . .	30
<b>8.0</b>	<b>TEST PROCEDURES</b>	
8.1	Operating Procedures	
8.1.1	Engine . . . . .	31
8.1.2	Trim . . . . .	31
8.2	Pretest Checks	
8.2.1	Ignition Checks. . . . .	31
8.2.2	Fuel System Leak Checks. . . . .	32
8.2.3	Windmilling Check. . . . .	32
8.2.4	Engine Oil Service . . . . .	32
8.2.5	Engine Inspection. . . . .	32
8.3	Engine Posttest Inspection. . . . .	32
8.4	Test Conditions . . . . .	32
8.4.1	Altitude Testing . . . . .	32
8.4.2	Sea-level Testing. . . . .	34
8.5	Log Requirements. . . . .	34

9.0	TEST DATA REQUIREMENTS	
9.1	Acquisition . . . . .	36
9.2	Editing and Validation. . . . .	36
9.3	Standard Equations for UETP . . . . .	36
9.4	Nomenclature. . . . .	55
9.5	Data Presentation Format. . . . .	59
9.6	Format for Data Transmittal . . . . .	60
9.7	Suggested Performance Parameters. . . . .	69
9.8	Performance Plot . . . . .	70
9.9	Data and Report Transmittal . . . . .	70
10.0	ERROR ASSESSMENT . . . . .	71
11.0	REPORTING	
11.1	Facility Test Plan Format . . . . .	72
11.2	Facility Test Report. . . . .	73
12.0	ENGINE PRESERVATION AND SHIPPING	
12.1	Engine Preservation (Altitude Facilities) . . . . .	74
12.2	Engine Preservation (Sea-Level Test Facilities). . . . .	75
12.3	Engine Waterwash. . . . .	76
12.4	Shipping. . . . .	76
	<b>TABLES</b>	
I.	Referee Instrumentation Recommendations . . . . .	77
II.	Mil Power Settings for Trim Check . . . . .	78
III.	Test Conditions . . . . .	79
A.	Engine No. 1, S/N 607594. . . . .	79
B.	Engine No. 2, S/N F615037 . . . . .	80
C.	Sea-Level Facilities-Bleed Closed Settings. . . . .	81
D.	Sea-Level Facilities-Bleed Open Settings. . . . .	82

IV. Test Summary Sheet. . . . .	83
V. Description of Data Measurement Systems . . . . .	84
A. Pressures . . . . .	84
B. Temperatures. . . . .	85
VI. Identification of Elemental Error Sources . . . . .	86
VII. Estimated Measurement Uncertainties . . . . .	87
VIII. Estimated Performance Parameter Uncertainties . . . . .	88

#### FIGURES

1. Pratt & Whitney Aircraft J57-P-19W Turbojet Engine. . . . .	89
2. Modified Tailpipe and Reference Nozzle Assy.. . . . .	90
3. UETP Engine Instrumentation Station Locations . . . . .	91
4. Engine Internal Aerodynamic Pressure & Temperature Instrumentation . . . . .	92-101
5. Engine Installation in NASA Supplied Test Stand . . . . .	102-104
6. Engine Inlet Bulletnose . . . . .	105
7. NASA Bulletnose and Engine Inlet Instrumentation Spool Piece Design. . . . .	106
8. Engine Lubricating Oil System Schematic . . . . .	107
9. J57 Installation at NASA LeRc . . . . .	108
10. Standard AGARD Engine Performance Plots . . . . .	109-114

#### APPENDICES

I. Recommended Spare Parts for J57 Unified Engine Test Program . . . . .	116
II. Spectrometric Oil Analysis Program Sample (SOAP) Limits for J57-P-19W Engine. . . . .	118
III. Engine Operating Procedures . . . . .	119
IV. Engine Operational Limits . . . . .	130
V. Calculation of Kinematic Viscosity Constants. . . . .	135

## 1.0 INTRODUCTION

The overall purpose of the AGARD-Uniform Engine Test Program (UETP) is to bring an understanding of turbine engine ground test data for participating AGARD countries to a common denominator, and to improve test techniques, instrumentation and test equipment for turbine engine testing. The improved understanding and methods are to be achieved through a comparative engine test program. In this program, two J57P-19W nonafterburning turbojet engines are to be made available from the U.S. Air Force. The plug type nozzle of the J57 will be replaced with a cylindrical tailpipe and a reference convergent nozzle. The intent of replacing the exhaust nozzle is to simplify the installation of nozzle instrumentation and the calculation of nozzle performance. Certain fixed instrumentation will be provided to travel with the engine. This reference instrumentation will be used to set test conditions, monitor engine health and engine performance degradation. The basic objectives of the UETP is that each participant use those facility test procedures, instrumentation arrangements and analysis methods that are consistent with their normal practices to define three basic engine performance parameters: airflow rate, net thrust, and specific fuel consumption.

NASA Lewis Research Center will initiate the test program and be responsible for the initial program management. Two newly overhauled engines will be delivered from the U.S. Air Force Logistics Command to NASA Lewis Research Center for modification and checkout prior to the initiation of the UETP. The initial and final participant facility tests of the UETP will be conducted at NASA Lewis Research Center. Test data from the final retest at NASA Lewis Research Center will be used to assess engine performance degradation.

The purpose of this document, the General Test Plan (GTP), is to specify participant common test hardware, instrumentation, data acquisition, data processing procedures and will serve both as a guideline for the preparation of the participants test plan and as a control document for the definition of the test engine and related test hardware.

## 2.0 AGARD-UETP MEMBERSHIP

## AGARD Propulsion and Energetics Panel (PEP) Working Group 15:

Panel Membership

Chairman: Dr. J. G. Mitchell  
 Technical Director for Operations  
 Headquarters Arnold Engineering  
 Development Center (AFSC)  
 Arnold AF Station, Tennessee 37389  
 TELE: 1(615)455-2611 x 7621

BELGIUM

M. le Prof. R. Jacques  
 Ecole Royale Militaire  
 30 Avenue de la Renaissance  
 1040 Bruxelles  
 TELE: 02-7339794 x 378 or 246

CANADA

Dr. W. L. MacMillian  
 National Defense Headquarters  
 CRAD/DST (OV)  
 101 Colonel By Drive  
 Ottawa, Ontario D1A 0K2  
 TELE:

FRANCE

Ing en Chef de l'Armement J.  
 Cocheteux  
 Service Technique des Programmes  
 Aeronautiques  
 4 Avenue de la Porte d'Issy  
 75996 Paris Armees  
 France  
 TELE:

GERMANY

Dr. D. K. Hennecke  
 Motoren und Turbinen Union  
 GmbH (MTU)  
 Abt. EW  
 Dachauerstrasse 665  
 8000 Munchen 50  
 TELE:

ITALY

Dr. Ing. G. Maoli  
 FIAT S.p.A.  
 Via L. Bissolati 57  
 00187 Roma  
 TELE:

NETHERLANDS

Ir. J. P. K. Vlegghert  
 National Aerospace Laboratory  
 P. O. Box 90502  
 Anthony Fokkerweg 2  
 1059 CM Amsterdam  
 TELE:

TURKEY

Professor Dr. A. Ucer  
 Middle East Technical University  
 O D T U  
 Makina Muh. Bolumu  
 Ankara, Turkey  
 TELE:

UNITED KINGDOM

Mr. A. J. B. Jackson  
 Rolls-Royce Limited  
 Aero Division  
 P. O. Box 31  
 Derby DE2 8BJ  
 TELE: (0332) 42424 x 1009

Mr N.A. Mitchell  
 Rolls-Royce Limited  
 P.O.Box 3  
 Filton, Bristol  
 BS12 7QE

UNITED STATES

Mr. A. A. Martino  
Director, Measurement &  
Information Systems Department  
Naval Air Propulsion Center, Code  
PE4

P. O. Box 7176  
Trenton, New Jersey 08628  
TELE: (609) 836-5713

NON-PANEL MEMBERSCANADA

Mr. D. M. Rudnitski  
 Division of Mechanical Engineering  
 National Research Council  
 Engine Laboratory  
 Montreal Road Lab., Bldg. M-7  
 Ottawa, Ontario K1A 0R6, Canada  
 TELE: (613) 993-2214  
 TELEX: 053 3386

FRANCE

M. F. Fagegaltier  
 Centre d'Essais des Propulseurs  
 91406 Orsay  
 TELE: (6) 941-8150  
 TELEX: 692148

GERMANY

Prof. Dr-Ing. W. Braig  
 Institut fur Luftfahrt-Antriebe  
 Stuttgart University  
 Pfaffenwaldring 6  
 7000 Stuttgart 80  
 TELE: (0711) 685-3597

TURKEY

Captain Fehmi Algun  
 Turkish Air Force Command Logistics  
 Technical Department  
 Hv. K. K. ligi Lojistik Bsk. ligi  
 Bakanliklar/Ankara  
 Turkey  
 TELE: 41 199099, ext. 696 or 139  
 TELEX: 42688 TRHKK

UNITED KINGDOM

Mr. P. F. Ashwood  
 36 Lynch Road  
 Farnham  
 Surrey GU98BY  
 TELE: (0252) 714295

Mr. M. Holmes  
 Head of Engine Test Operations  
 Dept.  
 Royal Aircraft Establishment  
 (Pyestock)  
 Farnborough, Hants GU14 OLS  
 TELE: (0252) 544411 x 6132

UNITED STATES

Mr. Richard Connell  
 PE-62  
 Naval Air Propulsion Center  
 P. O. Box 7176  
 Trenton, New Jersey 08628  
 TELE:

Mr. J. T. Tate  
 Program Manager, Aeropropulsion  
 Programs Dept.  
 Sverdrup Technology, Inc., AEDC  
 Group  
 Arnold Air Force Station,  
 Tennessee 37389  
 TELE: (615) 455-2611, ext. 7203

Mr. W. M. Braithwaite  
 (MS 500-207)  
 Aeronautics Directorate  
 NASA Lewis Research Center  
 21000 Brookpart Road  
 Cleveland, Ohio 44135  
 TELE: (216) 433-4000, ext. 5502

OVERVIEW COMMITTEE

Dr. J. G. Mitchell, Chairman

M. J. Cocheteux

Dr. D. K. Hennecke

Mr. A. J. B. Jackson

Prof. R. Jacques

Dr. M. L. MacMillan

Ir. J. P. Vleghert

### 3.0 AGARD UETP OBJECTIVES AND MEMBERSHIP RESPONSIBILITIES

#### 3.1 PROGRAM OBJECTIVES

##### General

To provide a basis for upgrading the standards of turbine engine testing within AGARD countries by comparing test procedures, instrumentation techniques, and data reduction methods, thereby increasing confidence in performance data obtained from engine test facilities.

To compare the performance of an engine measured in ground-level test facilities and in altitude facilities at the same non-dimensional conditions and establish the reasons for any observed differences.

##### Specific

Define, initiate, and monitor a facility-to-facility comparative engine test program.

Compare the engine performance measured in the various facilities and resolve any observed differences.

Prepare an AGARDograph summarizing the results.

#### 3.2 AGARD WORKING GROUP 15 AUTHORITY/RESPONSIBILITIES

1. Prepare and maintain the General Test Plan.
2. Formulate program objectives.
3. Define and implement program pretest and posttest study requirements.
4. Arrange logistic support activities and provide procedures for logistic support.
5. Arrange for interfacility written material to be translated and transmitted in a timely manner.
6. Review participant's Engine-Test-Plans for format and content and oversee changes.
7. Establish procedures for the exchange of information among test participants.
8. Establish procedures to resolve test participant inquiries.
9. Resolve differences in participant engine performance data.

10. Prepare program AGARDographs.
11. Assure test continuity via an Overview Committee.
  - a. Define interim participant test reporting requirements.
  - b. Provide early review/assessment of selected data from each participant's test program.
  - c. Provide technical advisory services to the AGARD-PEP-Working Group 15 Chairman, as required, to assure participant compliance with UETP procedures.
  - d. Provide technical advisory services to the AGARD-PEP-Working Group 15 chairman, as required, to assure consistency in engine performance data reported by participants.

## 4.0 AGARD-UETP TEST PARTICIPANTS

1. Facility: NASA Lewis Research Center
  - Representative: Mr J. Biesiadry
  - 21000 Brookpark Road
  - Mailing Address Cleveland, Ohio 44135
  - Type Test: Altitude
2. Facility: Naval Air Propulsion Center
  - Representative: Mr. R. Connell
  - Mailing Address: P. O. Box 7176
  - Trenton, New Jersey 08628.
  - USA
  - Type Test: Sea-Level
3. Facility: National Research Council
  - ✓ Representative: Mr. D. M. Rudnitski
  - Mailing Address: Engine Laboratory
  - Ottawa Ontario IIA OR6
  - Canada
  - Type Test: Sea-Level
4. Facility: Royal Aircraft Establishment (Pyestock)
  - Representative: Mr. M. Holmes
  - Mailing Address: Farnborough
  - Hants GU15 OLS
  - England
  - Type Test: Altitude
5. Facility: Centre d'Essais des Propulseurs
  - ✓ Representative: M. F. Fagegaltier
  - Mailing Address: Saclay
  - 91406 Orsay
  - France
  - Type Test: Altitude and Sea-Level

6. Facility: Engine Overhaul Division  
Representative: Captain Fehmi Algun  
Mailing Address: Turkish Air Force Command Logistics  
Technical Department  
Hv. K. K. Igi Lojistik Bsk. Igi  
Bakanliklar/Ankara  
Turkey  
Type Test: Sea-Level
7. Facility: Arnold Engineering Development Center (AEDC)  
Representative: Mr. J. T. Tate (Sverdrup Technology, Inc.)  
Mailing Address: Arnold Air Force Station  
Tennessee 37389  
USA  
Type Test: Altitude and Sea-Level

5.0 PARTICIPANT TEST  
OBJECTIVES AND RESPONSIBILITIES

5.1 FACILITY-TEST OBJECTIVES

1. Assess turbine engine performance at specified test conditions and engine power levels using facility test procedures, instrumentation arrangements and analysis methods consistent with participants' normal practices.
2. Report test results in a specified form/format which will enhance direct comparison and correlation with test results reported by other test participants.

5.2 PARTICIPANT RESPONSIBILITIES

1. Provide a pretest Facility Test Plan which defines the following:
  - Test installation.
  - Instrumentation schematics.
  - Data acquisition system.
  - Test hardware.
  - Data reduction procedures and equations.
  - Estimated measurement uncertainty.
  - Engine operational procedures.
  - Engine service systems (fuel, oil, electrical).
  - Basic engine performance systems (thrust, airflow, and fuel flow).
2. Conduct testing to provide an assessment of specified engine performance at specified test environmental conditions and engine power levels.
3. Prepare and transmit a final data package in accordance with the requirements of the General Test Plan.
4. Prepare and transmit a final test report in accordance with the requirements of the General Test Plan.
5. Support the Working Group in making the interfacility data evaluations and in the preparation of the final report, as required.

**5.3 PARTICIPANT TENTATIVE TEST SCHEDULE**

Engine delivery to NASA Lewis Research Center	30 November 1980
Engine instrumentation and checkout completed	1 May 1981
Testing completed and engine shipped	15 December 1981
Arrival at Arnold Engineering Development Center, U.S.A.	1 January 1982
Testing completed and engines shipped	24 May 1982
Arrival at National Research Laboratory, Canada	1 June 1982
Testing completed and engines shipped	1 September 1982
Arrival at Centre d'Essais des Propulseurs, France	1 October 1982
Testing completed and engines shipped	1 March 1983
Arrival at Royal Aircraft Establishment (Pyestock), England	1 April 1983
Testing completed and engines shipped	1 July 1983
Arrival at Engine Overhaul Division, Turkey	1 August 1983
Testing completed and engines shipped	1 November 1983
Arrival at Naval Air Propulsion Center, U.S.A.	1 December 1983
Testing completed and engines shipped	1 March 1984
Arrival at NASA Lewis Research Center	15 March 1984
Testing completed and engines shipped	15 June 1984
Arrival at Oklahoma City Air Logistics Center, U.S.A.	

## 6.0 ENGINE DESCRIPTION

### 6.1 GENERAL DESCRIPTION

The test engines will be U. S. Air Force supplied J57-P-19W turbojet engines. The J57-P-19W engine (Fig. 1) is an axial-flow, two spool non-augmented turbojet with a fixed-area exhaust nozzle. Rated sea-level-static thrust is 46.71 kN (10,500 lb) at military power. The engine inlet diameter is .932 m (36.7 in), and the maximum engine dry weight is approximately 1882 Kg (4150 lb).

The engine compression system is a sixteen-stage two-spool compressor with an overall pressure ratio of 11.3:1 and a rated airflow of 74.843 kg/sec (165 lb/sec) at sea-level-static, military power conditions. The nine-stage, low-pressure compressor (LPC) is connected by a through-shaft to a two-stage, low-pressure turbine. The seven-stage, high-pressure compressor (HPC) is connected by a hollow shaft to the single-stage, high-pressure turbine. An intercompressor bleed discharges air overboard through a bleed port during starting and low power operation.

The combustor section consists of an annular diffuser and a cannular combustor unit with eight flame tubes. Each flame tube contains six dual-orifice fuel spray nozzles. Ignition is accomplished by spark igniters located in flame tubes 4 and 5. Combustion spreads to the other flame tubes by means of cross-over tubes welded to the forward section of each chamber. Power to the spark ignition is provided by a 7-amp, 24-vdc external source.

Engine fuel is metered by a hydromechanical fuel control as a function of power lever position, high-pressure compressor rotor speed, compressor inlet temperature, and compressor discharge pressure. High pressure rotor speed, at a fixed power lever position, is biased by compressor inlet temperature; burner pressure is limited to a maximum of approximately 1,378 kPa (200 psia).

The test engines are production-configuration USAF J57-P-19W turbojet engines (S/N P607594 and S/N F615037) modified to provide (1) a cylindrical tailpipe and converging exhaust nozzle assembly, (2) a "referee" Uniform Engine Testing Program Instrumentation Package, and (3) a water/oil cooler to replace the aircraft oil cooler. The test program does not require horsepower extraction, water-injection, customer bleed, or anti-ice.

### 6.2 COMPRESSOR BLEEDS

The production engine configuration (J57-P-19W) utilizes two compressor bleed valves (left and right). Operation of the engine with the bleed valves in this configuration limits the high-power rotor speed range (with both bleeds closed) to approximately 26.18 Hz (250 rpm) (High-Pressure Rotor Speed). This limited speed range prevents use of the test procedure recommended by the PEP Working Group 15 (nine steady-state power levels between the bleed-closed power level and the

military engine power level). Operation of the engine with the right-hand compressor bleed blocked off will allow a high-power rotor speed range of approximately 800 rpm (High-Pressure Rotor Speed) between the bleed-closed power level and the military engine power level. The increased rotor speed range should allow use of the PEP Working Group No. 15 recommended test procedure.

The bill-of-material configuration of the J-57 engine models designed for "fighter" applications (J57-21B and J57-23B models for example) have blanked-off right-hand compressor bleed ports (right and left hand ports are defined as looking upstream). However, the single-bleed engine configurations have a "larger" left-hand bleed port opening than the left-hand bleed port opening of the two-bleed engine configurations as noted below:

	<u>"FIGHTER ENGINES"</u>	<u>"BOMBER ENGINES"</u>
Left Bleed	4.3 Diam. Orifice	3.25 Diam. Orifice
Right Bleed	CAPPED	2.20 Diam. Orifice

For this test program, the engine bleeds have been modified to a "fighter" configuration in order to increase the bleed close operating range.

### 6.3 OIL COOLER

Engine operation requires the use of an external oil cooler. A test stand mounted oil cooler will be used and shipped with the engine. This oil cooler, which will use water as the coolant, is to maintain the oil temperature at 366.48°K (200°F) at the outlet of the oil cooler. There is no operational requirement to perform heat transfer calculations.

### 6.4 ENGINE EXHAUST NOZZLE

Because the tailcone on the standard J57-P-19W extends through the nozzle exit plane (see Fig. 1), the Bill-of-Material nozzle will be replaced by a cylindrical tailpipe and a reference convergent nozzle both fabricated by rolling sheet metal (Fig. 2). The cylindrical tailpipe will provide a more suitable platform for the extensive pressure and temperature instrumentation needed to establish nozzle inlet conditions. This approach, however, does require a calibration test run with the new tailpipe-nozzle assembly to size the nozzle so that engine performance can be restored to approximately the nominal value. NASA LeRC has accepted the responsibility of fabricating the nozzles and conducting the calibration. Even though two engines will be available for the program, it is planned to use only one tailpipe-nozzle assembly.

## 6.5 ENGINE INSTRUMENTATION

### 6.5.1 General

The test instrumentation package will consist of facility-peculiar or primary instrumentation and engine-peculiar or referee instrumentation. The primary instrumentation will consist of that required by each facility to determine engine fuel flow, airflow, thrust, and test cell environmental conditions. The referee instrumentation will be mounted on the engine or support stand by NASA and travel with the engine.

### 6.5.2 Station Designation and Nomenclature

The station designations for the referee instrumentation conform to SAE-755A (Aerospace Recommended Practice for Gas Turbine Engine Steady-State Performance Presentation for Digital Computer Programs) and are shown in Fig. 3. Diagrams showing the number and types of aerodynamic instrumentation to be installed in the test engines are shown in Fig. 4.

All instrumentation measurements (except rotor speeds) will be made with facility supplied sensors. Engine fuel flow rates will be measured with both facility supplied fuel flowmeters and engine-supplied fuel flowmeters.

Each engine will be provided with its own flowmeter system (2 flowmeters, piping and thermocouple). This system has been calibrated and therefore should not be disassembled without the authorization of the Working Group Chairman. The fuel flow system calibration data will be provided by NASA LeRC.

All engine inlet and internal aerodynamic instrumentation must be inspected prior to and following each phase of the UETP program. NASA LeRC has the responsibility of fabricating the referee instrument probes. NASA LeRC will also certify the probes for engine use, but assumes no responsibility for their continued safe use once shipped from their facility.

### 6.5.3 Instrumentation Connectors and Identification

The engines will be delivered with most instrumentation terminating on "patch-panels" which are attached to the engine inlet duct (Station 2.0 Instrumentation Ring), to the engine intermediate case, and to the Engine Tailpipe Section.

NASA will provide 1/8 inch Swagelock fittings for pressure lines and standard 2-pin quick-disconnect connector for thermocouples. Conversion fittings to make the transition between fractional and metric tubing do exist. NASA will provide assistance relative to connector problems to those facilities which anticipate problems (upon request to NASA Working Group Representatives). The possibility exists that mating connectors can be provided for pressure and temperature instrumentation. Mating connectors will be provided for the fuel flowmeter (AN fitting) and speed sensor (BNC connectors).

All instrumentation connections and electrical connector interfaces will be identified by name.

#### 6.5.4 Referee Instrumentation Requirements

The required referee instrumentation parameters quantity and measurement ranges are listed in Table I. Also noted in the Table are parameters to be measured in facility control rooms for engine health monitoring.

#### 6.5.5 Dynamic Pressure Transducers

Each test participant must supply two Kulite Model STL5-140-5D or equivalent pressure transducers for their portion of the test program. These transducers are to be used at engine station 2 (refer to Fig. 4 for specific location) to monitor the turbulence characteristics (i.e.  $P$  RMS from 0 to 1000 Hzs) of the engine inlet airflow. The RMS values should be included as part of the steady-state data system.

#### 6.6 SPARE PARTS

A list of spare parts to accompany the engines are presented in Appendix I. The items listed as expendables in Appendix I will be shipped with the engine. The items listed as major parts are not currently available. Any additional parts required will have to be requisitioned through the U.S. Air Force Logistics Command. On-site representation to provide logistic support will not be provided. Requests for spare parts should be made through the Working Group Chairman, Dr. J. G. Mitchell.

## 7.0 TEST INSTALLATION REQUIREMENTS

### 7.1 GENERAL

The J57-P-19W engines will be shipped to each test facility on standard wheel dollies. The engines will be mounted on a NASA supplied test stand which in turn may be mounted on each participant's facility thrust bed by facility personnel. The engine installation in the NASA Test Stand is shown in Fig. 5.

### 7.2 ENGINE INLET HARDWARE

The engine inlet bulletnose is an aircraft part and will not be used for the UETP. NASA LeRC will fabricate an engine bulletnose from U. S. Air Force drawings and modify the part to aid in support of the engine inlet instrumentation probe array. A schematic of the bulletnose and instrumentation spool piece design is presented in Fig. 6. NASA will only fabricate one bulletnose, instrumentation spool piece, and complete set of inlet temperature and pressure rakes. NASA will provide some spare probes for the inlet rakes.

NRCC will install a 60cm long airflow measuring section in front of the station 2 spool piece that necessitates removing the NASA supplied nose cone and replacing it with one of their own design. Test data will be gathered with both nose cones to quantify the effects of this change. The bellmouth and airflow measuring section could be made available to other participants if necessary after the NRCC tests. NRCC will, however, quote the test results based on the NASA bulletnose configuration.

Each participant will use a bellmouth and airflow measuring section of their own design. The method of attaching facility hardware to the NASA instrumentation spool section and the thrust unloading (i.e., slip seal) or thrust accounting methods for such hardware will be of the participants' choosing. The bellmouth and inlet ducting used by NASA may be available for participant use, if required. The NASA engine inlet hardware is shown in Fig. 7.

### 7.3 TEST CELL COOLING AND FLOW GRADIENTS

The amount and type (i.e., conditioned or atmospheric) of test cell cooling air should be monitored. If it is not practical to measure the mass flow rate of the cooling air, test cell air velocities should be estimated using pitot-static pressure measurements. In addition, wall static pressure taps should be used to identify test cell pressure gradients. A minimum of four axial pressure measurement stations are required with one of the stations being in the exit plane of the engine nozzle. At each test cell wall measurement station a minimum of two pressures, 180 degrees apart, should be installed.

#### 7.4 ENGINE MOUNT SYSTEM

The engine mount framework is NASA supplied and connects directly to the engine test stand shown schematically in Fig. 5. The engine mount frame consists of two overhead intermediate case mounts and one rear mounting framework which connects to the engine turbine case at two locations. The test stand, in addition to supporting the engine, includes instrumentation patch panels, supports the NASA supplied water/oil cooler. The fuel flow meter package will be attached to the engine.

#### 7.5 ENGINE INSTALLATION INTERFACE DEFINITIONS

Engine installation interfaces are defined as follows:

- A. P&WA installation drawing 225601 should be used as reference for mounting and hookup of engines.
- B. The engine should be supported at the intermediate and the turbine exhaust case. Typical test mounts would be a "dog house" stand. A stand of this type will be supplied by NASA-Lewis.
- C. The following stand interfaces are required for engine test.
  1. Fuel inlet - Requires a flanged connector to match fuel pump inlet. Flange is shown at 4A of Sheet 1 of installation drawing. The stand fuel system should be capable of delivering up to 45,359 kg/hr (10,000 lb/hr) of Jet-A.
  2. Ignition system - The test facility must supply 24 volts DC @ 7 amps. Use a 3106-14S-9S or equivalent connector. Ignition is on only during start cycle.
  3. Oil system (Refer to Fig. 8)
    - a. The engine has its own oil tank but an external oil cooler must be provided. A jumper tube between pads "J" and "AS" on the inlet case front accessory drive support will be supplied with the engine. Pads are shown at 18F and 19F, Sheet 1 of installation drawing. Remove the P/N 240060 oil cooler to oil tank inlet tube. The stand oil cooler should be plumbed between the attachment points for this tube.
    - b. There is a remote oil fill adapter available at the oil tank. See Sheet 1 of installation drawing, "L" at 16B.

- c. NASA-Lewis will provide a visual oil sight gage. It can be connected to the oil tank drain valve located at the left rear of oil tank. The drain valve handle must be wired to the open position.
  - d. Breather pressurizing valve is located at the front top of oil tank. The pad for connecting to stand breather line is shown at 18E, Sheet 2, of installation drawing.
4. Turbine exhaust gas temperature connector (TT5)\* - There are four chromel alumel probes mounted in the turbine exhaust case. Probes are normally connected by an averaging harness. To read individual TT5 temperatures, disconnect the averaging harness from the probes and run individual leads to a stand mounted switch box. The switch box should have TT5 averaging capability. These engines have dual junction probes, which allow use of the B/M averaging harness along with individual leads.
  5. Turbine exhaust gas pressure (PT5) - There is one B/M PT5 probe in the turbine exhaust case.
  6. Overboard drains - There are three overboard drains required.
    - a) P&D valve plus burner - 1.0625-12-3 fitting
    - b) Fuel pump and control seal drain - .4375 - 20NF-3 fitting
    - c) Static oil drain - .500 - 20NF-3 fitting
  7. PLA connection - May be installed on the engine cross shaft on either side of engine. Required interface is shown on sheet 2 of installation drawing at 11D.
  8. Tachometers - The engine has provisions for an NL tachometer on the low rotor gearbox and an NH tachometer on the main gearbox. Tachometer ratios are 0.717:1 and 0.433:1, respectively. NASA-Lewis will provide the engine tachometers.

\*NOTE: Engine Station designations in this report conform to SAE-755A which are not consistent with engine station designations specified in the J57 tech order manual.

## 7.6 ENGINE FUEL SYSTEM

The engines will be supplied with a fuel system consisting of a fuel pump, hydro-mechanical fuel control, fuel pressurization and dump valve, and engine fuel manifold and spray nozzles. In addition, each engine will be modified to include a NASA supplied fuel flowmeter package located between the fuel control and P&D valve.

The engines will use Jet-A or Jet-A-1 fuel and shall require a facility supplied fuel delivery system to the fuel pump inlet. The facility shall include in this fuel system an emergency shutoff valve and a 10-40 micron filter upstream of the fuel pump inlet.

Fuel samples shall be taken from near the engine fuel pump inlet prior to each engine performance test period. The fuel sample will be analyzed for viscosity, specific gravity and lower heating value. The results of the analyses shall be reported in the final data packages. In addition, two fuel samples from each facility will be provided for comparative analysis by the Canadian Fuel Laboratories.

The following fuel properties will be determined: distillation range, sulphur content, net heat of combustion (by calculation and bomb calorimeter), aromatics content, hydrogen content, smoke point, naphthalene content, thermal stability, and specific gravity. Engine test agencies are to arrange shipment of two gallons (approximately 8-10 liters) of fuel in clean, well-sealed containers to:

Dr R. B. Whyte  
Fuels and Lubricants Laboratory  
National Research Council  
Montreal Road  
Ottawa, Ontario  
Canada  
K1A 0R6

Mark containers: "Fuel Samples, AGARD Uniform Engine Test Program"

(For further information, Dr Whyte may be contacted by telephone: (613) 993-2415.)

## 7.7 POWER LEVER SHAFT SCHEDULE AND RIGGING

The power lever positioning system shall be facility supplied to position the single fuel control power lever shaft (accessible from either side of engine). The power lever has 100 degs of rotation from cutoff to military stop. Pin holes are provided along the shaft face for position calibration at idle and military. Increasing power lever angle is in the counterclockwise direction when viewed from the engine left side. The power lever angular position is to be recorded using a facility supplied potentiometer mounted to the PLA shaft.

### 7.8 ELECTRICAL SYSTEM REQUIREMENTS

The engine uses a high-energy capacitor type ignition system that provides a source of very high energy. The ignition system consists of two identical, independent units, one for each ignition plug, with a common power source. Power to the system requires a 7 amp, 24 vdc external source. (See T.O. 2J-J57-13 for additional information.)

### 7.9 LUBRICATING OIL SYSTEM

The engine lubrication system is of a self-contained high pressure design (Fig. 8). It consists of a pressure system which supplies lubrication to the main engine bearings and to the accessory drives. Oil is drained through a scavenge system, from the bearing compartments and from the accessories, and is pumped through an external mounted water/oil cooler and returned to the engine oil tank for storage. The engine main oil tank which is mounted on the front compressor rear case is connected to the inlet side of the oil pressure pump, thereby completing the oil flow cycle. A breather system connecting the individual bearing compartments and the oil tank with the breather pressurizing valve completes the engine lubricating system.

The lubricating oil to be used is MIL-L-7808. The water/oil cooler shall require a facility water supply rate of 0 to 1,261.8 ml/sec (20 gpm) and a regulating valve to maintain oil temperature out of the cooler at  $366.48 \pm 5.6^{\circ}\text{K}$  ( $200 \pm 10^{\circ}\text{F}$ ).

An engine oil sample must be obtained immediately (within 15 minutes) following each test period for spectrometric oil analysis (SOAP). The SOAP limits for the J57-P-19W are listed in the engine operational limits (Appendix II). (See T.O. 2J-J57-13 for additional information.)

### 7.10 HARDWARE ITEMS AVAILABLE TO UETP PARTICIPANTS

A preliminary list of hardware and instrumentation to be used for the NASA-LeRC phase of the UETP and to be shipped with the engines is presented below. Also included is a list of recommended spare parts, only some of which have been received at NASA LeRC. Such information as instrument qualification procedures, qualification data (if desired, must be requested from NASA-Lewis), instrument and hardware drawings, etc. will be provided with the items listed, but NASA-LeRC will not assume responsibility for any hardware or instrumentation once it leaves NASA-LeRC. It is the responsibility of each UETP participant to insure that any hardware or instrumentation used in its engine test facility meets the operational and safety requirements for that facility.

Preliminarily, the instrumentation and hardware available, are as follows:

1. Items 6, 9 and 20 shown in Fig. 9.

2. Instrumentation shown in Fig. 4. Instrumentation-facility interface will be through bulkheads located at the engine inlet, compressor exit and tailpipe-nozzle assembly using 1/8 inch Swagelock fittings for pressure lines and Marlin, Type K, connectors (i.e., standard 2-pin quick-disconnect connectors) for thermocouples. Only chromel-alumel thermocouples will be used.
3. Two fuel flow meters per engine with appropriate instrumentation for temperature and accompanying tubing and AN fittings.
4. One oil cooler and accompanying tubing and AN fittings.
5. Accelerometer mounting pads located on the inlet case, diffuser case, turbine exhaust case and accessory drive case plus two mounting pads located inside the center body spool piece to monitor the vibrations transmitted from the center body nose cone (Item 9, Fig. 9) to the engine.
6. Tachometer - generators to measure the low rotor and high rotor speeds along with BNC connectors.
7. Mating electrical connector for the ignition system.
8. One mating spline for the PLA shaft.
9. No pressure transducers or accelerometers will be shipped with the engine.
10. An air starter will be provided with each engine. The starter should not be removed from the engine for testing in altitude facilities.

## 7.11 AVAILABLE DRAWINGS FOR UETP

The following drawings are available from NASA LeRC.

<u>DESCRIPTION</u>	<u>DRAWING NO.</u>
Fixed Duct	CF 505693, Item 1
Split Duct	CF 505694, Item 2
Outer Body Spool Piece	CF 505695, Sht. 1
Center Body Nose Cone	CF 505695, Sht. 2
Nose Cone Adapter	CF 505695, Sht. 2
Center Body Spool Piece	CF 505695, Sht. 1
Engine Nozzle Support	CF 505696, Item 4
Engine Stand	CF 505696, Items 1-2
Wide Flange Beam	No Drawing
8 x 8 x 31 lb/ft x 12 ft long	
J57 Nozzle (Calibration)	CF 505709
J57 Reference Nozzle	CF 505710
Seal Duct	CF 505694, Items 3-4
Mount-Front Engine (i.e., Dog House Engine Support)	CF 505713, Shts. 1-2
PWA Engine Installation	PWA 225601, Shts. 1-4
PWA Lifting Sling, Part #PWA XD515745	No Drawing
NASA Installation Assembly	CR 505712

## 8.0 TEST PROCEDURES

### 8.1 OPERATING PROCEDURES

#### 8.1.1 Engine

Engine procedures required for all test facilities are:

- a. Engine starting and shutdown.
- b. Engine and fuel control system functional check.
- c. Engine depreservation and fuel/oil leak check.
- d. Engine performance testing.

Specifics for these procedures are provided in Appendix III\*. The engines will be operated within the limits in Technical Order 2J-J57-13. Engine operational limits are listed in Appendix IV\*.

#### 8.1.2 Trim

The engines will be retrimmed at NASA with Jet A fuel to approximately those values obtained by the USAF when it trimmed the engines using JP4 fuel. The engine trim should be checked for each engine at the military power setting (PLA = 90°). The mechanical speeds at military conditions for each test condition are contained in Table II. If the measured mechanical speed deviates more than 50 rpm from these values, the Working Group Chairman should be notified.

Note that engine trim checks and trim adjustments should not be required for the conduct of the AGARD UETP. The engines were trimmed prior to the initiation of the UETP by NASA. In the event that the desired engine power settings cannot be obtained (due to engine "trim slip" or "engine deterioration"), the chairman of Working Group 15 should be contacted for direction and or authorization of any corrective engine maintenance action.

### 8.2 PRETEST CHECKS

#### 8.2.1 Ignition Check

The functioning of the ignition system shall be checked prior to windmilling the engine and with both rotors at rest. Audible sparking shall be confirmed prior to continuing the program.

\*Procedures and operational limits provided in Appendices III and IV are for informational purposes only, the official procedures and limits are those specified by Technical Order 2J-J57-13.

#### 8.2.2 Fuel System Leak Check

With facility fuel supply connected to engine and pressurized from 206.84 (30) to 344.74 kPa (50 psia), the engine shall be closely examined for fuel leaks. All leaks shall be repaired prior to continuing the program.

#### 8.2.3 Windmilling Check

The engine shall be windmilled to an NH 1500 rpm or via the air starter to NH 2500 rpm (max. one minute) prior to each test period to check vibration levels, rotor speed indications, and oil system priming. The engine and lubricating system plumbing shall be examined for oil leaks. All leaks shall be repaired prior to continuing the program.

#### 8.2.4 Engine Oil Servicing

The prerun check list shall include a check of the oil sight gage (if available), or tank dip stick before each engine run.

#### 8.2.5 Engine Inspection

The engine inlet area shall be visually inspected for foreign object damage, foreign objects in the engine inlet area, oil leaks, and inlet duct instrumentation condition. The exhaust area shall be checked for damage or oil leaks.

#### 8.3 Engine Posttest Inspection

The engine inlet area shall be visually inspected for foreign object damage, oil leakage and freedom of rotation. The inlet shall be inspected for signs of tip rub, blade cracking, etc. The exhaust area shall be inspected visually for signs of damage or oil leakage.

#### 8.4 TEST CONDITIONS

The UETP has two sets of test conditions; one applicable to altitude test facilities and one to sea-level test facilities.

At each test facility, dew point or specific humidity should be recorded for every data point. Due to possibilities of condensation affecting Tt2, running should not be attempted at high levels of relative humidity at the engine inlet.

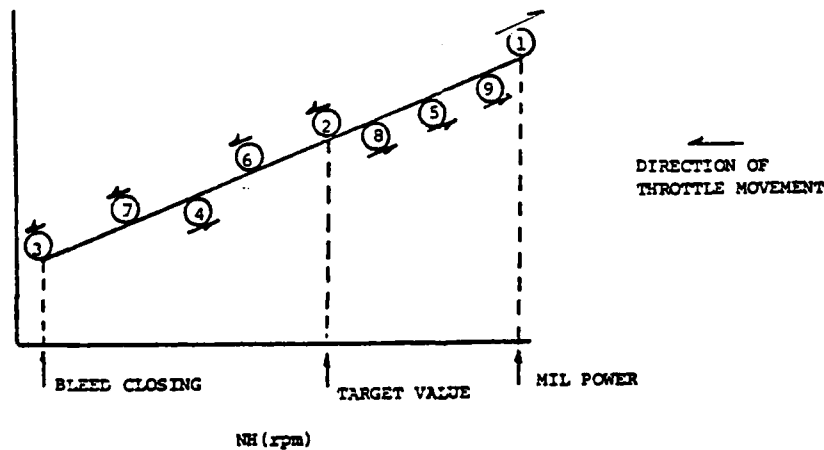
##### 8.4.1 Altitude Testing

Conditioned air will be supplied to the engine inlet at the total pressure and temperature corresponding to the desired test conditions. Engine inlet total pressure will be defined as the numerical average of the 20 total pressure probe measurements at Station 2.0. Station 2.0 boundary layer rakes will not be used in the determination of P2. Engine inlet total temperature will be defined as the numerical average of the

10 total temperature probe measurements at Station 2.0. A recovery factor of 1.0 is to be used for all Station 2.0 temperature probes. The test conditions for the altitude test facilities are presented in Table III. For each test condition, data scans will be taken at nine engine power settings approximately equally spaced between mil power and the speed at which the bleed valves start to open (the specific NH speed power settings are defined in Table III). The test sequence for the nine NH speed settings are: \*

1. Mil power
2. Target value
3. Bleed valve opening limit
4. Between 3 and 2
5. Between 2 and 1
6. Between 2 and 4
7. Between 4 and 3
8. Between 2 and 5
9. Between 5 and 1

Graphically, the test sequence appears as follows:



When approaching each setting, the throttle lever will be moved slowly towards the throttle position where the required speed is expected to be achieved and the engine allowed to stabilize. The set speed should be within  $\pm 25$  rpm of the desired. In going between two set speeds, the throttle direction must not change. In the event of a speed overshoot outside of the tolerance band, the throttle setting should be backed up approximately 100 rpm and the speed reset.

At each power setting two data scans will be obtained. The intent is to obtain stabilized engine aerodynamic performance (i.e. stabilized gas path). It is estimated that stabilized performance can be assessed within five minutes at set conditions for the initial data scan; and within two minutes for the repeat data scan.

#### 8.4.2 Sea-Level Testing

For sea-level testing, the engine inlet total pressure and temperature will be defined as specified for altitude testing (Section 8.4.1). The proposed test conditions for the sea-level tests are ambient conditions with a RAM ratio of 1.0. Two regions of engine operation are specified:

1. From engine power settings from bleeds just close speed to mil power (i.e. same as the altitude facilities), and
2. From engine power settings from bleeds just open speed to idle power.

As most sea-level test beds do not have environmental control, the engine power settings will have to be established at each test temperature. For the high power region, values of NH have to be established for bleed valve closed (BVC) and MIL power. By dividing up the test range into 8 equal increments, 9 values of NH are obtained. The sequence of power settings is the same as in Sec. 8.4.1. and detailed in Table III. Two data scans after engine stabilization will be taken at each test condition. For the low power region, the speed range between idle and bleed valve closure will also be divided up into 9 equally spaced values of NH and power settings sequenced in the same manner as per the high speed range. Table III outlines the test points and sequence.

#### 8.5 LOG REQUIREMENTS

The AGARD logging requirements for each J57 engine are as follows:

1. Windmill time.
2. Engine hot time.
3. Military (i.e. PLA = 90°) and max EGT (i.e. T5 = 1130°F) time.

4. Maintenance and repair records.
5. Spectrometric oil analysis results.
6. Test summary sheets.

These logs are to be shipped with each engine.

## 9.0 TEST DATA REQUIREMENTS

### 9.1 ACQUISITION

Each participant's test report should include a flow diagram of the data acquisition system used to record and process outputs from steady-state, transient and high-response transducers. The type hardware and software used for data acquisition and data sampling rates per second per channel should be identified.

### 9.2 EDITING AND VALIDATION

The test participant procedures for editing data should be identified in the test report. Redundant data and data rejection processes should be described. Procedures for handling missing data such as the loss of a sample and outliers should also be presented.

### 9.3 STANDARD EQUATIONS FOR UETP

The following calculations will be made by each test participant. NASA LeRc will provide a sample set of inputs and outputs for the purpose of checking the equations.

**SUBJECT:** Clarification of Shorthand Notation Used to Describe the Uniform Engine Testing Program (UETP) Standard Equations.

The following example is presented to assist those unfamiliar with the shorthand notation used to describe the equations in the reference document. The example chosen refers to the calculation of average temperature at the engine inlet, station 2 (see AVERAGES, Station 2, T2AV).

SHORTHAND NOTATION

T2AV = Avg (T2AVOA, T2AVOB, T2AVOC, T2AVOD, T2AVOE)  
 where: T2AVO\$ = Avg (T2\$14, T2\$32)  
 where: \$ = A, B, C, D, E

NOTE: The symbol "\$" is used to describe a sequence of measurements made at the location denoted by A, B, C, etc. "A" indicates measurements in ring A; B in ring B, etc. This can further be seen by comparison with the algebraic equation.

ALGEBRAIC EQUIVALENT

$$T2AV = \frac{T2AVOA + T2AVOB + T2AVOC + T2AVOD + T2AVOE}{5}$$

$$\text{where: } T2AVOA = \frac{T2A14 + T2A32}{2}$$

$$\text{where: } T2AVOB = \frac{T2B14 + T2B32}{2}$$

$$T2AVOE = \frac{T2E14 + T2E32}{2}$$

where: T2A14, T2A32, T2B14, ..., T2E32 represent instrumentation as shown in figure 4A of the GTP

NASA would be pleased to explain the equations further for those UETP participants who may still have questions. However, it is requested that these questions be addressed to specific areas of concern.

STANDARD EQUATIONS FOR UETP

AGARD-UETP test participants may use facility-developed standard procedures for the determination of gas properties, such as the specific heat ratio ( $\gamma$ ). The following relationship for the specific heat ratio ( $\gamma$ ) in the Standard Equations has been provided by NASA for use, as desired, by test participants who do not desire to use their facility-developed standard procedures: \*

The relationship used for the specific heat ratio ( $\gamma$ ) in the Standard Equations is as follows:

Equation For  $\gamma$  - No Dissociation

$$\gamma_{\text{gas}} = \left\{ 1 - \frac{(1 + f) (0.28705 + 2.0620 \left( \frac{m}{m+1} \right) f)}{\sum_{i=0}^2 \left[ f \left( \frac{a_i m + b_i}{m+1} \right) + c_i \right] T^i} \right\}$$

Where:  $f$  = FAR = Fuel Air Ratio  
 $i$  = Summation index, 0, 1, 2  
 $m$  = H/C = Hydrogen Carbon Ratio of fuel  
 $T$  = Gas Temperature, K

Constants (Joule/(gr-K))

$i$	$a_i$			$b_i$			$c_i$		
0	8.983	761	<sup>b</sup> 899-00	(-)	1.127	218 529-01	9.497	901	502-01
1	5.006	943	032-04		3.018	887 416-03	1.607	549	922-04
2	2.260	316	157-06	(-)	1.258	866 682-06	2.616	006	174-08

a  $R_{\text{gas}} = R_{\text{air}} + (8.314/2M_{\text{H}_2}) (m/m+1) f$ , Joules/gr - K)  
 $= 0.28705 + 2.0620 (m/m+1) f$

b Exponent of 10, e.g.,  $a_1 = 5.006 \ 943 \ 032 \times 10^{-4}$  \*

AVERAGES

The "avg( )" function indicates that the arithmetic average of the parameters is to be calculated. For example:

$$\text{avg}(X,Y,Z) \Rightarrow (X+Y+Z)/3$$

The "wtavg( )" function indicates that an area weighted average is to be taken. The parameters are given in pairs; the first value is a parameter to be averaged and the second value is its associated weighting factor. For example:

$$\text{wtavg}(X,A1,Y,A2,Z,A3) \Rightarrow [(X \cdot A1) + (Y \cdot A2) + (Z \cdot A3)] / (A1 + A2 + A3)$$

The averages to be calculated are as follows:

Station 2

$$T2AV = \text{avg}(T2AV0A, T2AV0B, T2AV0C, T2AV0D, T2AV0E)$$

$$\text{where: } T2AV0\$ = \text{avg}(T2\$14, T2\$32)$$

$$\text{where: } \$ = A, B, C, D, E$$

$$P2AV = \text{avg}(P2AV0A, P2AV0B, P2AV0C, P2AV0D, P2AV0E)$$

$$\text{where: } P2AV0\$ = \text{avg}(P2\$00, P2\$09, P2\$18, P2\$27)$$

$$\text{where: } \$ = A, B, C, D, E$$

$$PBI2AV0\$ = \text{avg}(PBI2\$07, PBI2\$25)$$

$$\text{where: } \$ = A, B, C, D, E$$

PBO2AV0\$ = avg(PBL2\$05,PBL2\$23)

where: \$ = A,B,C,D,E,F,G,H

PS2AV = utavg(PS2AV0A,R2A,PS2AV0B,R2B)

where: PS2AV0\$ = avg(PS2\$01,PS2\$10,PS2\$19,PS2\$28)

where: \$ = A,B

R2A = .24384

R2B = .48006

Station 3

T3AV = avg(T3AV0A,T3AV0B,T3AV0C)

where: T3AV0\$ = avg(T3\$11,T3\$25)

where: \$ = A,B,C

P3AV = avg(P3AV0A,P3AV0B,P3AV0C)

where: P3AV0\$ = avg(P3\$08,P3\$28)

where: \$ = A,B,C

Station 3.1

PS31AV = avg(PS31A03,PS31A33)

Station 5

T5AV = avg(T5A02,T5A11,T5A20,T5A29)

P5AV = P5AV30

Station 7

T7AV = wtavg(T7AV0A,A7A,T7AV0B,A7B,T7AV0C,A7C,T7AV0D,A7D,  
T7AV0E,A7E,T7AV0F,A7F,T7AV0G,A7G,T7AV0H,A7H,  
T7AV0I,A7I,T7AV0J,A7J,T7AV0K,A7K,T7AV0L,A7L,  
T7AV0M,A7M,T7AV0N,A7N,T7AV0O,A7O,T7AV0P,A7P,  
T7AV0Q,A7Q,T7AV0R,A7R)

where: T7AV0\$ = avg(T7\$01,T7\$19)

where: \$ = B,D,F,H,J,L,N,P,R

T7AV0\$ = avg(T7\$10,T7\$28)

where: \$ = A,C,E,G,I,K,M,O,Q

A7A = 3.5363	A7G = 24.3211	A7M = 45.7303
A7B = 6.4882	A7H = 27.8893	A7N = 49.2983
A7C = 10.0484	A7I = 31.4575	A7O = 52.8666
A7D = 13.6186	A7J = 35.0257	A7P = 56.4348
A7E = 17.1847	A7K = 38.5939	A7Q = 60.0031
A7F = 20.7529	A7L = 42.1621	A7R = 107.1122

P7AV = wtavg(P7AV0A,A7A,P7AV0B,A7B,P7AV0C,A7C,P7AV0D,A7D,  
P7AV0E,A7E,P7AV0F,A7F,P7AV0G,A7G,P7AV0H,A7H,  
P7AV0I,A7I,P7AV0J,A7J,P7AV0K,A7K,P7AV0L,A7L,  
P7AV0M,A7M,P7AV0N,A7N,P7AV0O,A7O,P7AV0P,A7P,  
P7AV0Q,A7Q,P7AV0R,A7R)

where: P7AV0\$ = avg(P7\$01,P7\$19)

where: \$ = A,C,E,G,I,K,M,O,Q

P7AV0\$ = avg(P7\$10,P7\$28)

where: \$ = B,D,F,H,J,L,N,P,R

PS7AV = avg(PS7A00,PS7A09,PS7A16,PS7A27)

TM7AV = avg(TM7A02, TM7A11, TM7A20, TM7A29)

Station 0.4

P04AV = avg(P04A08, P04A17, P04A26, P04A35)

Station 0.5

P05AV = avg(P05A08, P05A17, P05A26, P05A35)

Station 0.8

P08AV = avg(P08A03, P08A12, P08A21, P08A30)

Fuel Flow

WFE = avg(WFE1, WFE2)

ENGINE FUEL FLOW CALCULATION

WFES = WFEsV \* 0.99902 \* SG60 \* (1 + CEX \* (288.7 - TWF))

where: S = 1.2

SG60 = from fuel sample

CEX =  $9.126 \cdot 10^{-4}$

$$WFESV = (WFESAC/KS)$$

$$\text{where: } KS = f(WFESAC/v)$$

$$\text{where: } v = Z \cdot \exp[-0.7487 - (3.295 \cdot Z) + (0.6119 \cdot Z^2) - (0.3193 \cdot Z^3)]$$

$$\text{where: } Z = Z' - 0.7$$

$$\text{where: } \log_{10}(\log_{10}(Z')) = A - B \cdot \log_{10}(1.8 \cdot TWF)$$

$$\text{where: } A = 10.9047^*$$

$$B = 4.1325^*$$

Functions for KS: let  $X = \ln(WFESAC/v)$

#### Engine 1

$$K1 = (0.0006034297 \cdot X^5) - (0.017081179 \cdot X^4) + (0.1919556 \cdot X^3) - (1.070272 \cdot X^2) + (2.95902 \cdot X) - 2.69471$$

$$K2 = (0.001614871 \cdot X^5) - (0.0471595 \cdot X^4) + (0.548617 \cdot X^3) - (3.17926 \cdot X^2) + (9.18249 \cdot X) - 10.04551$$

#### Engine 2

$$K1 = (0.001164908 \cdot X^5) - (0.033784435 \cdot X^4) + (0.388961646 \cdot X^3) - (2.2213515 \cdot X^2) + (6.2889063 \cdot X) - 6.5115769$$

$$K2 = (0.000797802 \cdot X^5) - (0.023476177 \cdot X^4) + (0.27411549 \cdot X^3) - (1.5865434 \cdot X^2) + (4.5458990 \cdot X) - 4.6202107$$

### AIRFLOW

#### Station 2 - Ideal

$$WAI2 = 1000 \cdot P2AV \cdot M12 \cdot A2 \left( \frac{\gamma}{R} \right) \left( \frac{1}{T2AV} \right) \left( \frac{P52AV}{P2AV} \right)^{\frac{\gamma}{\gamma-1}} \left( \frac{1}{2} \right)$$

\* Constants A and B are to be evaluated for each fuel batch.  
See Appendix V for calculation procedure as per ASTM D341.

$$\text{where: } M12 = \{[2/(\gamma-1)]\{(P2AV/PS2AV)\}^{\gamma} - 1\}\}^{1/2}$$

$$R = 287.05$$

$$\gamma = f(T2AV)$$

$$A2 = A2S(1 + \Lambda(TM1AV - 296))^{1/2}$$

$$\text{where: } \Lambda = 16.2 \cdot 10^{-6}$$

$$A2S = 0.53992$$

$$CD2 = WA1/WA12$$

Station 2 - Integrated

$$WA2 = (1/2) \sum_{n=2}^{18} WA2QA_n(AP2_j, -AP2_k)$$

$$M2AV = (1/2) [1/(AP2_j - AP2_k)] \sum_{n=2}^{18} M2_n(AP2_j, -AP2_k)$$

$$\text{where: } j = n-1$$

$$k = n+1$$

$$WA2QA_n = 1000 \cdot P2_n \cdot M2_n [(\gamma/R)(1/T2_n)(PS2_n/P2_n)\}^{\gamma} - 1\}\}^{1/2}$$

$$M2_n = \{[2/(\gamma-1)]\{(P2_n/PS2_n)\}^{\gamma} - 1\}\}^{1/2}$$

$$PS2_n = C_n \cdot PS2AV0A + (1 - C_n) \cdot PS2AV0B$$

$$R = 287.05$$

$$\gamma = f(T2AV)$$

$$AP2_n = AP2S_n [1 + A(TM1AV - 294)]^2$$

$$\text{where: } A = 16.2 \cdot 10^{-6}$$

Table Of Pressure And Temperature Relations And Areas

n	P2	C	T2	AP2S
1	-	-	-	0.72712
2	PBO2AV0H	0.0134	T2AV0D	0.71756
3	PBO2AV0G	0.0334	T2AV0D	0.70336
4	PBO2AV0F	0.0534	T2AV0D	0.68924
5	PBO2AV0E	0.0736	T2AV0D	0.67533
6	PBO2AV0D	0.0937	T2AV0D	0.66149
7	PBO2AV0C	0.1137	T2AV0D	0.64787
8	PBO2AV0B	0.1473	T2AV0D	0.62538
9	PBO2AV0A	0.1874	T2AV0D	0.59897
10	P2AV0D	0.2403	T2AV0D	0.56510
11	P2AV0C	0.4203	T2AV0C	0.45705
12	P2AV0B	0.6232	T2AV0B	0.34903
13	P2AV0A	0.8608	T2AV0A	0.24097
14	PBI2AV0E	0.8229	T2AV0A	0.21102
15	PBI2AV0D	0.9097	T2AV0A	0.20588
16	PBI2AV0C	0.9365	T2AV0A	0.20080
17	PBI2AV0B	0.9772	T2AV0A	0.19579
18	PBI2AV0A	0.9900	T2AV0A	0.19084
19	-	-	-	0.18720

Station 8 - Ideal

$$\text{Calculate: } M8 = \left( \frac{T2}{\gamma - 1} \right) \left[ \left( \frac{P7AV}{PAMB} \right)^{\frac{\gamma}{\gamma - 1}} - 1 \right]^{\frac{1}{2}}$$

$$\text{where: } \gamma = f(P5, T5, FAR)$$

$$\text{where: For } PAMB > 0.53685 \cdot P7AV$$

$$P5 = PAMB$$

$$T5 = T7AV \left( \frac{PAMB}{P7AV} \right)^{0.25926}$$

For  $PAMB \leq 0.53685 \cdot P7AV$   
 $PS = 0.53685 \cdot P7AV$   
 $TS = 0.85106 \cdot T7AV$

For  $M8 \geq 1$

$$WIS = 1000 \cdot P7AV \cdot A8 \left[ \left( \frac{\gamma}{R'} \right) \left( \frac{1}{T7AV} \right) \left( \frac{2}{\gamma+1} \right)^{\frac{1}{2}} \left( \frac{\gamma+1}{\gamma-1} \right)^{\frac{1}{2}} \right]^{\frac{1}{2}}$$

For  $M8 < 1$

$$WIS = 1000 \cdot P7AV \cdot M8 \cdot A8 \left[ \left( \frac{\gamma}{R'} \right) \left( \frac{1}{T7AV} \right) \left( \frac{PAMB}{P7AV} \right)^{\frac{1}{2}} \left( \frac{\gamma+1}{\gamma} \right)^{\frac{1}{2}} \right]^{\frac{1}{2}}$$

where:  $A8 = A8S(1 + \Lambda(TM7AV - 294))^{\frac{1}{2}}$

where:  $\Lambda = 11.52 \cdot 10^{-6}$

$A8S = 0.2376$

$R' = 8314.32/MW$

where:  $MW = f(PS7AV, TS7, FAR)$  or as specified by each facility.

$WAI8 = WIS - (WF/1000)$

$CDS = WAI/WAI8$

IDEAL NOZZLE GROSS THRUST

For  $M8 > 1$

$$FGIS = \left\{ \left[ 2 \left( \frac{2}{\gamma+1} \right)^{\frac{1}{2}} \left( \frac{1}{\gamma-1} \right)^{\frac{1}{2}} \right] \left( \frac{P7AV}{PAMB} - 1 \right) PAMB \cdot A8 \right\}$$

For  $M8 \leq 1$

$$\left\{ \left[ 2 \left( \frac{2}{\gamma+1} \right)^{\frac{1}{2}} \left( \frac{1}{\gamma-1} \right)^{\frac{1}{2}} \right] \left( \frac{P7AV}{PAMB} - 1 \right) PAMB \cdot A8 \right\}$$

$FGIS = \gamma \cdot PAMB \cdot M8^{\frac{1}{2}} \cdot A8$

The one is subtracted after the product of terms.

WRONG EQ

WRIGHT EQ

where:  $A_8$  is defined in Station 8 airflow calculation

$\gamma = f(PS, TS, FAR)$  or as specified by each facility \*

where: For  $PAMB > 0.53685 \cdot P7AV$

$PS = PAMB$

$TS = T7AV(PAMB/P7AV)^{0.25926}$

For  $PAMB \leq 0.53685 \cdot P7AV$

$PS = 0.53685 \cdot P7AV$

$TS = 0.85106 \cdot T7AV$

\*  $CG_8 = FG/FGI_8$

$CV_8 = CG_8/CD_8$

#### NET THRUST

$FN = FG - FRAM$

where:

$FRAM = (WAI/1000) \{ 2 \cdot R \cdot T2AV(\gamma/(\gamma-1)) [ 1 - (PAMB/P2AV)^{((\gamma-1)/\gamma)} ] \}^{1/2}$

where:  $\gamma = f(T2AV)$

$R = 287.05$

#### CALCULATIONS USING FUEL FLOW

$$SFC = WF/FN$$

$$FAR = (WF/1000)/WA1$$

CALCULATIONS USING ROTOR SPEEDS

$$NLPER = NL/58.58$$

$$NHPER = NH/97.0$$

$$NLQNH = NL/NH$$

PRESSURE AND TEMPERATURE RATIOS AND EFFICIENCIES

Engine Pressure And Temperature Ratios

$$P5Q2 = P5AV/P2AV$$

$$P7Q2 = P7AV/P2AV$$

$$T5Q2 = T5AV/T2AV$$

$$T7Q2 = T7AV/T2AV$$

RAM Ratio

$$P2QAMB = P2AV/PAMB$$

Compressor Performance

$$P3Q2 = P3AV/P2AV$$

$$T3Q2 = T3AV/T2AV$$

$$EC = [P3Q2 \uparrow ((\gamma_{23}-1)/\gamma_{23}) - 1] / (T3Q2 - 1)$$

$$\text{where: } \gamma_{23} = (2/3)\gamma_2 + (1/3)\gamma_3'$$

$$\text{where: } \gamma_2 = f(T2AV)$$

$$\gamma_3' = f[T2AV \cdot P3Q2 \uparrow ((\gamma_2 - 1)/\gamma_2)]$$

Nozzle Pressure Ratio

$$P7QAMB = P7AV/PAMB$$

ALTITUDE , MACH NO. AND REYNOLDS NUMBER INDEXAltitude

For PAMB > 22.63273

$$ALT = 158.1[1 - (PAMB/101.325) \uparrow 0.1902543] / 0.00356616$$

For 5.47485 ≤ PAMB ≤ 22.63273

$$ALT = 11000 - [6341.545 \cdot \ln(PAMB/22.63273)]$$

For PAMB < 5.47485

A-50

$$\text{ALT} = 20000 + \{216650 [(5.47485/\text{PAMB}) + 0.029271 - 1]\}$$

FLIGHT MACH NUMBER

$$M = \{[2/(\gamma - 1)] \{ (P2AV/\text{PAMB}) \}^{\{(\gamma - 1)/\gamma\}} - 1\} \}^{1/2}$$

where:  $\gamma = f(T2AV)$

Reynolds Number Index

$$\text{RNI} = \{ (P2AV/101.325) \{ (T2AV/288.15) + 0.38311 \} \} / \{ 1.38311 (T2AV/288.15) \}^{1/2}$$

CORRECTIONS TO SEA LEVEL SPECIFIED PAM AND LHV

Correction Parameters

$$\delta = P2AV/101.325$$
$$\theta = T2AV/288.15$$
$$\theta' = \theta^{1/2}$$

Airflow

$$\text{WAIR} = \text{WA1} \cdot \theta' / \delta$$

Fuel Flow

$$WFR = [WF/(8 \cdot \theta')] (LHV/42960)$$

Thrust

$$FGR = (FG/S) + (A8/S) (PAMB - (P2AV/RAMSPC))$$

where: RAMSPC = 1.0	for	P2QAMB ≤ 1.03
1.06	for	1.03 < P2QAMB ≤ 1.15
1.3	for	1.15 < P2QAMB ≤ 1.5
1.7	for	1.5 < P2QAMB

or  
1.0 for Sea Level and Out Door Stands

A8 is defined in Station 8 airflow calculation

$$FNR = FGR - FRAMSP$$

where: FRAMSP = 0.0	for	P2QAMB ≤ 1.03
0.09777 * WAIR	for	1.03 < P2QAMB ≤ 1.15
0.20449 * WAIR	for	1.15 < P2QAMB ≤ 1.5
0.28539 * WAIR	for	1.5 < P2QAMB

$$FSLS = (FG/\theta') + (A8/S) (PAMB - P2AV)$$

Specific Fuel Consumption

$$SFCR = WFR/FNR$$

$$SFCSLs = WFR/FSLS$$

Fuel-Air Ratio

$$FARR = (FAR/\theta)(LHV/42960)$$

Rotor Speeds

$$MLR = NL/\theta'$$

$$MLPERR = NLPER/\theta'$$

$$NHR = NH/\theta'$$

$$NHPERR = NHPER/\theta'$$

CORRECTIONS TO SPECIFIED CONDITIONS

Correction Parameters

$$\delta D = P2AV/P2SPEC$$

where: P2SPEC =	20.684 for	P2AV ≤ 28	2.999 for	P2AV ≤ 40.6
	34.474 for	28 < P2AV ≤ 41	4.799 for	40.6 < P2AV ≤ 54.5
	51.711 for	41 < P2AV ≤ 69	7.490 for	54.5 < P2AV ≤ 110.0
	82.737 for	69 < P2AV ≤ 90	11.990 for	110.0 < P2AV ≤ 120.0
	101.325 for	90 < P2AV	14.692 for	120.0 < P2AV

$$\theta D = T2AV/T2SPEC$$

where: T2SPEC =	253 for	T2AV ≤ 261	426 for	T2AV ≤ 410.6
	268 for	261 < T2AV ≤ 278	431 for	410.6 < T2AV ≤ 501
	288 for	278 < T2AV ≤ 297	519 for	501 < T2AV ≤ 525.8
	308 for	297 < T2AV	555 for	525.8 < T2AV

$$\theta D' = \theta D \uparrow (1/2)$$

Airflow

$$WAIRD = WA1 \cdot \theta D' / \delta D$$

Fuel Flow

$$WFRD = (WF / (\delta D \cdot \theta D')) (LHV / 42960)$$

Thrust

$$FGRD = (FG / \delta D) + (A8 / \delta D) [PAMB - (P2AV / RAMSPC)]$$

where: RAMSPC = 1.0	for	P2QAMB ≤ 1.03
1.06	for	1.03 < P2QAMB ≤ 1.15
1.3	for	1.15 < P2QAMB ≤ 1.5
1.7	for	1.5 < P2QAMB

A8 is defined in Station 8 airflow calculation

$$FNRD = FGRD - FRMSPD$$

where:

FRMSPD =	0.0	for	P2QAMB ≤ 1.03
	0.0057598 * WAIRD * T2SPEC <sup>1/2</sup>	for	1.03 < P2QAMB ≤ 1.15
	0.0120451 * WAIRD * T2SPEC <sup>1/2</sup>	for	1.15 < P2QAMB ≤ 1.5
	0.0162108 * WAIRD * T2SPEC <sup>1/2</sup>	for	1.5 < P2QAMB

\*

\*

Specific Fuel Consumption

$$SFCRD = WFRD / FNRD$$

Fuel-Air Ratio

$$FARRD = (FAR/\theta D)(LHV/42960)$$

Rotor Speeds

$$MLRD = NL/\theta D'$$

$$MLPRRD = NLPER/\theta D'$$

$$NHRD = NH/\theta D'$$

$$NHPRRD = NHPER/\theta D'$$

## 9.4 NOMENCLATURE

The nomenclature to be used for the UETP is presented in the following table.

TABLE OF SYMBOLS

<u>Parameter</u>	<u>Parameter Identification</u>	<u>Units</u>
ALT	Altitude	m
A2	Flow area at Station 2	m <sup>2</sup>
A2S	Station 2 flow area measurement at 294 K	m <sup>2</sup>
A7A - A7R	Station 7 area weights	m <sup>2</sup>
A8	Flow area at Station 8	m <sup>2</sup>
A8S	Station 8 flow area measurement at 294 K	m <sup>2</sup>
CD2	Station 2 flow coefficient based on Station 1 (Facility) airflow measurement	*
CD8	Station 8 flow coefficient based on Station 1 (Facility) airflow measurement	*
CEX	Coefficient of thermal expansion of fuel	1/K
CG8	Exhaust nozzle thrust coefficient	
CV8	Exhaust nozzle velocity coefficient	
EC	Compressor efficiency	
FAR	Fuel air ratio	
FG	Gross thrust measured by facility	kN
FGI8	Ideal one-dimensional gross thrust	kN
FN	Net thrust measured by facility	kN
FRAM	Calculated flight ram drag	kN
K1, K2	Fuel flow turbine meter K factors	cycle/ml

M	Calculated flight Mach number	
MI2	One-dimensional, ideal Mach number at Station 2	
M2AV	Average Mach number at Station 2	*
M8	One-dimensional, ideal Mach number at Station 8	
MW	Molecular weight of exhaust gas	Kg/Kg - mole *
NH	High pressure compressor rotational speed	RPM
NHPER	High pressure compressor percent of rated rotational speed	%
NL	Low pressure compressor rotational speed	RPM
NLPER	Low pressure compressor percent of rated rotational speed	%
NLQNH	Ratio of low pressure compressor speed to high pressure compressor speed	
PAMB	Ambient pressure	kPa
P04AV	Average pressure at Station 04	kPa
P05AV	Average pressure at Station 05	kPa
P08AV	Average pressure at Station 08	kPa
P2AV	Average total pressure at Station 2	kPa
P2AV0A - P2AV0E	Average ring total pressures at Station 2	kPa
PS2AV	Average static pressure at Station 2	kPa
P2QAMB	P2AV/PAMB, RAM Ratio	
P3AV	Average total pressure at Station 3	kPa
P3AV0A - P3AV0C	Average ring total pressures at Station 3	kPa

P3Q2	P3AV/P2AV	
PS31AV	Average static pressure at Station 31	kPa
P5AV	Average total pressure at Station 5	kPa
P5Q2	P5AV/P2AV	
P7AV	Average total pressure at Station 7	kPa
P7AV0A - P7AV0R	Average ring total pressures at Station 7	kPa
P7QAMB	P7AV/PAMB	
P7Q2	Engine Pressure Ratio, P7AV/P2AV	
PS7AV	Average static pressure at Station 7	kPa
R	Gas constant of air	J/(kg·K)
R'	Gas constant of exhaust gas	J/(kg·K)
RNI	Reynolds number index	
SG60	Specific gravity of fuel at 289 K	
SFC	Specific fuel consumption	g/(kN·s)
TM1AV	Average duct metal temperature at Station 1 and Station 2	K
TWF	Fuel temperature	K
T2AV	Average total temperature at Station 2	K
T2AV0A - T2AV0E	Average ring total temperatures Station 2	K
T3AV	Average total temperature at Station 3	K
T3AV0A - T3AV0C	Average ring total temperatures at Station 3	K
T3Q2	T3AV/T2AV	

T5AV	Average total temperature at Station 5	K
T5Q2	T5AV/T2AV	
T7AV	Average total temperature at Station 7	K
T7Q2	Engine Temperature Ratio, T7AV/T2AV	
T7AV0A - T7AV0R	Average ring total temperature at Station 7	K
TM7AV	Average exhaust nozzle metal temperature at Station 7	K
WA1	Facility airflow rate measurement	kg/s
WA2	Airflow calculated at Station 2.0	kg/s
WAI2	One-dimensional, ideal airflow at Station 2	kg/s
WAI8	One-dimensional, ideal airflow at Station 8	kg/s
WF	Facility fuel flow measurement	g/s
WFE1, WFE2	Fuel mass flow rate measured at engine flow meters (On Summary Output Sheet - frequency output of engine flow meters)	g/s
WFE1AC, WFE2AC	Frequency output of engine flow meters	Hz
WFE1V, WFE2V	Fuel volumetric flow rate measured at engine flow meters	ml/s
WI8	One dimensional, ideal exhaust gas flow at Station 8	kg/s
$\delta$	Pressure correction to Sea Level	
$\gamma$	Ratio of specific heats	
$\gamma_2$	Ratio of specific heats at engine inlet	

$\gamma_{21}$	Effective ratio of specific heats across the compressor	
$\gamma_3$	Ideal process ratio of specific heats at compressor exit	
$\lambda$	Coefficient of thermal expansion of metal	1/k
$\theta$	Temperature correction to Sea Level	
$\nu$	Fuel viscosity	cSt

#### Suffixes

D	Parameter corrected to desired conditions
R	Parameter is corrected to Sea Level conditions, desired RAM ratio and for fuel lower heating value

#### 9.5 DATA PRESENTATION FORMAT

A standard data presentation format sheet will be included in each participant's final data package. The standard units to be used for the Test Summary Sheets, the Test Conditions Summary Package, and the Engineering Units Tape will be the International System of Units (SI). The units are as follows:

<u>PARAMETER</u>	<u>SI</u>
Pressure	kilopascals (kPa)
Temperature	kelvin (K)
Airflow	kilograms/ second (kg/s)
Fuel Flow (Mass)	grams/second (g/s)
Fuel Flow (Volume)	milliliters/ second (ml/s)
Frequency	hertz (Hz)

Rotor Speed	revolutions/ min (RPM)
Rotor Speed (Percent)	percent (%)
Thrust	kilonewtons (kN)
Specific Fuel Consumption	grams/kilo- newton*second (g/kN*s)
Altitude	meters (m)
Power Lever Angle	degrees (deg)
Lower Heating Value	joules/gram (J/g)

The Test Summary Sheet is presented in Table IV.

#### 9.6 FORMAT FOR DATA TRANSMITTAL

Steady-state data readings selected from the data will be sent to the UETP participants on digital magnetic tapes supplied by the requesting agency along with a summary of each data reading after the Chairman of Working Group 15 has approved their release. The general format for the data tapes and the summary are described below. The number of steady-state data points per tape will be variable depending upon the frequency of testing and the number of data points per test period. A brief written log will be included with each tape.

#### Tape Format

The tapes will be non-labeled, fixed record length (physical and logical record length equal 132 bytes), 9-track, 1600 BPI, ASCII code with odd parity. Each logical group of information on tape will be of the form:

RECORD #	
1	Keyword MSUB MREC
2	Description of Data
3	N
4	X(1) X(2) ..... X(i)
.	.
.	.
.	.
m	X(j) ... X(n-1) X(n)

Keyword MSUB MREC: A six-character alphanumeric word which identifies the type of information contained in the group followed by two integers. MSUB Indicates the number of subgroups contained within the group. MREC indicates the number of records contained in the group, not including the keyword record. Format: (1X, A6, 20I6, 5X)

Description of Data: Signal record of free form alphanumeric information which describes and defines subgroups of information. Format: (1X 21A6, 5X)

N: An integer which indicates the number of units (words or word pairs) of information. Format: (1X, 21I6, 5X)

X: N units of data of type specified by keyword. Format: Dependent on group type. ID and UNITS groups will be (1X, 21A6, 5X). CALCULATION, ENGINE DATA and FACILITY DATA groups will be (1X, E15.8, A1, 3X). \*

With this structure for each logical group of information, the tape can be read in the following manner:

```

JJ Read KEYWRD,MSUB,MREC      Keyword MSUB MREC
   If (KEYWRD = AAAAAA) Go to KK
       .
       .
   If (KEYWRD = BBBBBB) Go to LL

KK Do MSUB times, then return to JJ
   Read DESCRIPTOR           Description of Data
   Read N
   Read (X(I), I = 1, N)
       .
       .
LL Skip MREC Records
   Go to JJ

```

Note: "Read" means read under format control

the logical end of tape will be denoted by a physical end of file mark.

All alphanumeric information will be left justified within its denoted field.

#### TAPE CONTENT

There will be five types of logical groups of information with subgroup structure handled by descriptor of type of data. Following is a description of each group (subgroup) that will be on tape.

ID GROUP

Keyword : ID 1 3  
 Descriptor : UNIFORM ENGINE TESTING PROGRAM  
 N : 21

The ID group will contain alphanumeric information to uniquely identify the accompanying steady state data point.

Word	Alphanumeric	Purpose
1-12	USA NASA LEWIS RESEARCH CENTER	Location
13-17	PSL-3	Facility
18-19	YYMMDDHHmmSS	Date Recorded*
20	YYMMDD	Date Processed*
21	NNNN	Data Point Number

\* YY - Year (81)  
 MM - Month (01-12)  
 DD - Day (01-31)  
 HH - Hour (00-24)  
 mm - Minute (00-60)  
 SS - Second (00-60)

UNITS GROUP

Keyword : UNITS 1 3  
 Descriptor : CUSTOMARY SI  
 N : 18

The descriptor and the units given will be those actually used on the

tape, that is, either Customary or SI, not both.

Word	Units	Parameter
1-2	LBF/IN <sup>2</sup>   KPA	Pressure
3	R   K	Temperature
4-5	LBM/SEC   KG/S	Airflow
6	LBM/HR   G/S	Fuel Flow (WF, WFE)
7	GFM   ML/S	Fuel Flow (WFE1AC, WFE2AC)
8	HZ   HZ	Fuel Flow (WFE1, WFE2)
9	RPM   RPM	Rotor Speed
10	%   %	Rotor Speed (Percent)
11	LBF   KN	Thrust
12-13	LBM/HR/LBF   G/KN.S	Specific Fuel Consumption
14	FT   M	Altitude
15	DEG   DEG	Power Lever Angle
16-17	BTU/LBM   J/G	Lower Heating Value
18	MIL/MM	Engine Vibration

The information units in the following groups will occur in word pairs. The first word of each pair will be the value in engineering units, the second word will be an alphanumeric flag character; it will be either blank ( ) or contain an asterisk (\*). If it is blank its accompanying data value is good data. If it contains an asterisk, its accompanying data value is erroneous or at least questionable.

The following groups are based on the data taken and calculations made at Lewis Research Center. The tape format is defined so that each facility can easily customize the information reported on tape to fit their own data and calculations. The Calculation Group and Engine Data Group should be essentially the same for all facilities, however the Facility Data Group would be expected to vary with each facility. Each facility should provide an index for their tapes which identifies the information in their Facility Data Group and any other deviations from the following list.

#### CALCULATION GROUP:

Keyword : CALC 8 31  
 Descriptor : Dependent on subgroup  
 M : Dependent on subgroup

The subgroups are as follows:

Descriptor : SUMMARY OF TEST CONDITIONS  
 M : 12  
 Word Value  
 Pair

1 ALT	9 FM
2 RNI	10 NUPER
3 P2AV	11 NUPER
4 T2AV	12 SFC

5 PAMB  
6 M  
7 WA1  
8 WF

Descriptor : STATION AVERAGES  
M : 17

Word Value  
Pair  
1 T00AV            9 PS31AV            17 P08AV  
2 PS00AV           10 T5AV  
3 T2AV             11 P5AV  
4 P2AV             12 T7AV  
5 PS2A             13 P7AV  
6 PS13A05          14 PS7AV  
7 T1AV             15 P04AV  
8 P1AV             16 P05AV

Descriptor : AIRFLOW  
M : 12

Word Value  
Pair  
1 WA1  
2 WA1R  
3 WA2  
4 M2AV  
5 WA1Z  
6 CD2  
7 WA1B  
8 WA1C  
9 WA1S  
10 CD8  
11 CVA  
12 WA1RD

Descriptor : THRUST  
M : 12

Word Value  
Pair  
1 FG  
2 FGR  
3 FN  
4 FNR  
5 FGLS  
6 CGS  
7 FRAM  
8 FGRD  
9 FNRD  
10 FRAMSP  
11 FRMSPD  
12 FSLs

Descriptor : SPEEDS  
M : 13

Word Value  
Pair  
1 NL  
2 NLR  
3 NLPER  
4 NLGNH  
5 NLRD  
6 NLPRD

4 MLPERR            12 NHRD  
 5 NH                13 NHPRRD  
 6 NHR  
 7 NHPER  
 8 NHPERR

Descriptor : FUEL FLOW

N : 11

Word Value

Pair

1 WF  
 2 WFR                9 WFRD  
 3 WFE                10 SFCHR  
 4 WFE1               11 SFCSLS  
 5 WFE2  
 6 SFC  
 7 SFCH  
 8 LHV

Descriptor : ENGINE PRES. & TEMP. RATIOS

N : 6

Word Value

Pair

1 PSQ2                5 P7Q2  
 2 TSQ2                6 T7Q2  
 3 P2QAMB  
 4 P7QAMB

Descriptor : COMPRESSOR PERFORMANCE

N : 3

Word Value

Pair

1 P3Q2  
 2 T3Q2  
 3 EC

#### ENGINE DATA GROUP

Keyword : ENGDAT 3 33

Descriptor : Dependent on subgroup

N : Dependent on subgroup

The subgroups are as follows:

Descriptor : PRESSURES

N : 124

Word Value

Pair

1 PS2A01	9 P2A00	17 P2D09	25 P2B27
2 PS2B01	10 P2B00	18 P2E09	26 P2C27
3 PS2A10	11 P2C00	19 P2A18	27 P2D27

4 PS2B10	12 P2D00	20 P2B18	28 P2E27
5 PS2A19	13 P2E00	21 P2C18	29 PBL2A05
6 PS2B19	14 P2A09	22 P2D18	30 PBL2B05
7 PS2A28	15 P2B09	23 P2E18	31 PBL2C05
8 PS2B28	16 P2C09	24 P2A27	32 PBL2D05
33 PBL2E05	41 PBL2E07	49 PBL2H23	57 P3B08
34 PBL2F05	42 PBL2A23	50 PBL2A25	58 P3C08
35 PBL2G05	43 PBL2B23	51 PBL2B25	59 P3A28
36 PBL2H05	44 PBL2C23	52 PBL2C25	60 P3B28
37 PBL2A07	45 PBL2D23	53 PBL2D25	61 P3C28
38 PBL2B07	46 PBL2E23	54 PBL2E25	62 PS31A03
39 PBL2C07	47 PBL2F23	55 PS13A05	63 PS31A13
40 PBL2D07	48 PBL2G23	56 P3A08	64 P5AV30
65 PS7A00	73 P7I01	81 P7H10	89 P7E19
66 PS7A09	74 P7K01	82 P7J10	90 P7G19
67 PS7A18	75 P7M01	83 P7L10	91 P7I19
68 PS7A27	76 P7O01	84 P7N10	92 P7K19
69 P7A01	77 P7Q01	85 P7P10	93 P7M19
70 P7C01	78 P7B10	86 P7R10	94 P7O19
71 P7E01	79 P7D10	87 P7A19	95 P7Q19
72 P7G01	80 P7F10	88 P7C19	96 P7B28
97 P7D28	105 P04A35	113 P08A03	121 PB
98 P7F28	106 P04A08	114 P08A12	122 PCP
99 P7H28	107 P04A17	115 P08A21	123 PB14A12
100 P7J28	108 P04A26	116 P08A30	124 PB14A21
101 P7L28	109 P05A35	117 MCF	
102 P7N28	110 P05A08	118 PMS	
103 P7P28	111 P05A17	119 PF0	
104 P7R28	112 P05A26	120 PF2	

Descriptor : TEMPERATURES  
 N : 69

Word Value  
 Pair

1 T2A14	9 T2D32	17 T5H	25 TM7A29
2 T2B14	10 T2E32	18 T5A02	26 T7B01
3 T2C14	11 T3A11	19 T5A11	27 T7D01
4 T2D14	12 T3B11	20 T5A20	28 T7F01
5 T2E14	13 T3C11	21 T5A29	29 T7H01
6 T2A32	14 T3A25	22 TM7AC2	30 T7J01
7 T2B32	15 T3B25	23 TM7A11	31 T7L01
8 T2C32	16 T3C25	24 TM7A20	32 T7M01
33 T7P01	41 T7M10	49 T7L19	57 T7I28
34 T7R01	42 T7O10	50 T7N19	58 T7K28
35 T7A10	43 T7Q10	51 T7P19	59 T7M28
36 T7C10	44 T7B19	52 T7R19	60 T7O28
37 T7E10	45 T7D19	53 T7A28	61 T7Q28

38 T7G10	46 T7F19	54 T7C28	62 TB14A12
39 T7I10	47 T7H19	55 T7E28	63 TB14B12
40 T7K10	48 T7J19	56 T7G28	64 TB14A21
65 TB14B21			
66 TOILCOOL			
67 MOT			
68 TFO			
69 TMF			

Descriptor : MISCELLANEOUS  
 N : 12  
 Word Value  
 Pair

1 WFE1AC	9 VCBH
2 WFE2AC	10 VCBV
3 WFE1	11 NLAC
4 WFE2	12 NHAC
5 VIC	
6 VDC	
7 VTC	
8 VAD	

FACILITY DATA GROUP

Keyword : FACDAT 3 25  
 Descriptor : Dependent on subgroup  
 N : Dependent on subgroup

The subgroups are as follows:

Descriptor : PRESSURES  
 N : 91  
 Word Value  
 Pair

1 PS00A00	9 PS01B24	17 PS03A24	25 PBL1C08
2 PS00A09	10 PS02A00	18 PS03B24	26 PBL1E08
3 PS00A27	11 PS02A12	19 PS1A00	27 PBL1G08
4 PS01A00	12 PS02A24	20 PS1A09	28 PBL1I08
5 PS01B00	13 PS03A00	21 PS1A18	29 PBL1K08
6 PS01A12	14 PS03B00	22 PS1A27	30 PBL1M08
7 PS01B12	15 PS03A12	23 P1A08	31 P1A17
8 PS01A24	16 PS03B12	24 PBL1A08	32 PBL1S17
33 PBL1D17	41 PBL1C26	49 PBL1D35	57 PS1A14
34 PBL1F17	42 PBL1E26	50 PBL1F35	58 PS1B14
35 PBL1H17	43 PBL1G26	51 PBL1H35	59 PS1C14
36 PBL1J17	44 PBL1I26	52 PBL1J35	60 PS1D14
37 PBL1L17	45 PBL1K26	53 PBL1L35	61 P1A14
38 PBL1M17	46 PBL1M26	54 PBL1M35	62 P1B14
39 P1A26	47 P1A35	55 PS1A13	63 P1C14

40 PBL1A26	48 PBL1B35	56 PS1A31	64 PID14
65 PS1A32	73 PS2B01T	81 PSFLO	89 PINK8
66 PS1B32	74 PS2A17M	82 PINK1	90 PINK9
67 PS1C32	75 PS2A35M	83 PINK2	91 PINK7P
68 PS1D32	76 P2C00T	84 PINK3	
69 P1A32	77 P3B08T	85 PINK4	
70 P1B32	78 PS31A03T	86 PINK5	
71 P1C32	79 P05A09T	87 PINK6	
72 P1D32	80 DPFLO	88 PINK7	

Descriptor : TEMPERATURES

N : 43

Word Value

Pair

1 T09A	9 T00C18	17 TM1A34	25 TTANK2
2 T00B00	10 T00D18	18 T1A14	26 TTANK3
3 T00C30	11 T00B27	19 T1B14	27 TTANK4
4 T00D00	12 T00C27	20 T1C14	28 TTANK5
5 T00B09	13 T00D27	21 T1A32	29 TTANK6
6 T00C09	14 TM1A07	22 T1B32	30 TTANK7
7 T00D09	15 TM1A16	23 T1C23	31 TTANK8
8 T00B18	16 TM1A25	24 TTANK1	32 TTANK9
33 TTANK10	41 TULROD		
34 TFFL1	42 TLRROD		
35 TFFL2	43 TURROD		
36 TFPL1			
37 TFPL2			
38 TFFAC			
39 TSFLO			
40 TLLROD			

Descriptor : MISCELLANEOUS

N : 10

Word Value

Pair

1 FML1	9 WFLND
2 FML2	10 PLA
3 FPL1	
4 FPL2	
5 WFL1AC	
6 WFL2AC	
7 WFL1AC	
8 WFL2AC	

### 9.7 SUGGESTED PERFORMANCE PARAMETERS

The objective of the Uniform Engine Testing Program is the comparison of performance parameters as processed by the various test centers. There must be sufficient commonality of instrumentation and procedures to permit data interpretation and analysis. Although the instrumentation will not be extensive enough to permit accurate evaluation of absolute levels of performance, comparative results can be obtained by using the same instrumentation and calibrations, e.g., mv to k, at the various test sites. A common set of parameters is required. The proposed instrumentation layout has been designed to allow calculation of representative performance parameters. These should permit comparison of calculation techniques as well as engine deterioration. It is proposed that the following engine parameters be computed by all participants and submitted in addition to the basic pressure, temperature and flow data:

#### SUGGESTED PERFORMANCE PARAMETERS\*

##### INLET

1. Actual and corrected airflow
2. Reynolds number index
3. Inlet Mach number
4. Inlet Flow coefficient
5.  $(\frac{\Delta P}{P})$  RMS,  $0 < f < 1000$  Hz

##### OVERALL

1. Rotor speeds - actual and corrected
  2. Ratio of rotor speeds
  3. Fuel flow - actual and corrected
  4. Engine pressure and temperature ratios
  5. Nozzle pressure ratio
  6. Thrust and specific fuel consumption - actual and corrected
- \* A preliminary list of equations is included in Section 9.6.

COMPRESSION SYSTEM

1. Pressure ratios
2. Temperature ratios
3. Adiabatic efficiency

Pressure and temperature instrumentation at the exit of the high compressor has been requested to permit the calculation of representative compressor efficiency. While not "true", in an absolute sense, the calculated efficiency would serve to illustrate differences in computational methods and techniques for evaluating thermodynamic properties. Comparison of the efficiency throughout the program will permit evaluation of engine deterioration.

EXHAUST NOZZLE

1. Flow coefficient =  $f(WA1, WFE)/f(P7AV, T7AV, PAMB, A8)$ .
2. Thrust coefficient =  $f(FG Meas)/f(P7AV, T7AV, PAMB, A8)$ .
3. Velocity coefficient =  $f(FG Meas)/f(P7AV, T7AV, PAMB, WA1, WFE)$ .

The purpose of these calculations is to provide a basis for comparative evaluation of normal facility airflow and thrust measurements. The levels or trends of the flow coefficient relative to the effective velocity coefficient (ratio of "Measured" effective velocity to ideal effective velocity) are different if the error is in jet thrust rather than airflow. Such comparisons can be used to increase confidence and detect gross anomalies in facility measurements.

## 9.8 PERFORMANCE PLOTS

A standard set of performance plots for each test condition will be included in each participant's final data package. The Standard Aqard Engine Performance Plots are shown in Figures 10a., b., c., d., e., and f.

## 9.9 DATA AND REPORT TRANSMITTAL

Ten copies of the facility final data package should be transmitted to the Chairman of Working Group 15 within 60 calendar days after test completion (2nd engine preservation). The final data package should include documentation (i.e. test summary report) that briefly explains the data, test procedures, test article, and test facility. Twenty copies of the facility final report should be transmitted to the chairman within 140 calendar days after transmittal of the final data package. Distribution of the data package and test report will be made only to those facilities that have completed the test program and transmitted the final test report to the chairman.

### 10.0 ERROR ASSESSMENT

Each participant's test plan will include a pretest estimate of the measurement uncertainty anticipated for engine airflow, net thrust and specific fuel consumption at the target speed (see Section 8). The measurement uncertainty analysis to be used is the method proposed by Dr. R. B. Abernethy and J. W. Thompson, Jr. which is presented in "Handbook - Uncertainty and Gas Turbine Measurement", AEDC-Tr-73-5. Pretest measurement uncertainties will be made for the following test conditions at the target engine power NH as specified in Section 8.4:

<u>Facility</u>	<u>Inlet Pressure</u>	<u>Ram Ratio</u>	<u>Inlet Temperature</u>
Altitude	82.7 (KPa)	1.00	288°K
Altitude	20.7 (KPa)	1.30	288°K
Sea-Level	100.0 (KPa)	1.00	288°K
Sea-Level*	100.0 (KPa)	1.00	288°K

\* At a low NH engine power setting to be specified by the Overview Committee.

A posttest measurement uncertainty estimate of engine airflow, net thrust, and specific fuel consumption will be made at the target speed of each test condition and will be included in the participant's final test report along with an estimate of the elemental source errors for each individual measurement used to derive these parameters. The final test report will contain four tables relating to measurement uncertainty. Examples of the recommended format for the measurement uncertainty tables are presented in Tables V-VIII.

**11.0 REPORTING**

**11.1 FACILITY TEST PLAN FORMAT**

**Revision Sheet**

**Table of Contents**

<b>Section 1.0</b>	<b>Introduction (Background)</b>
<b>Section 2.0</b>	<b>Test Objectives and Responsibilities</b>
<b>Section 3.0</b>	<b>Description (Installation)</b>
	<b>3.1 Test Facility</b>
	<b>3.2 Engine</b>
<b>Section 4.0</b>	<b>Testing</b>
	<b>4.1 Test Conditions</b>
	<b>4.2 Procedures</b>
<b>Section 5.0</b>	<b>Instrumentation</b>
	<b>5.1 Test Cell</b>
	<b>5.2 Engine</b>
	<b>5.3 Calibration Procedures</b>
<b>Section 6.0</b>	<b>Data Handling</b>
	<b>6.1 Calculation Procedures</b>
	<b>6.2 Data Adjustment Procedures</b>
	<b>6.3 Error Evaluation</b>
<b>Section 7.0</b>	<b>Schedule</b>
	<b>References</b>
	<b>Tables</b>
	<b>Figures</b>

**11.2 FACILITY TEST REPORT (to be specified by Overview Committee)**

Tentative outline is:

Cover

Preface

Table of Contents

Nomenclature

Section 1.0 Introduction

Section 2.0 Apparatus

2.1 Test Facility

2.2 Test Article

2.3 Test Instrumentation

Section 3.0 Test Description

3.1 Test Conditions and Procedures

3.2 Corrections

3.3 Data Reduction

3.4 Uncertainty/Precision of Measurement

Section 4.0 Testing Results

4.1 Techniques used for Data Analysis

4.2 Results

Section 5.0 Concluding Remarks

Section 6.0 References

Tables

Figures (Standard Format Plots to be provided by NASA from each test participants AGARD data tape)

Appendices

12.0 ENGINE PRESERVATION AND SHIPPING  
(Refer to T.O. 2J-J57-13 for Official Procedures)

12.1. ENGINE PRESERVATION (Altitude Facilities)

1. The engine fuel system will be preserved after completion of testing using oil conforming to Military Specification MIL-L-6081, Grade 1010.
2. Prior to cell air-on, disconnect pressurizing and dump valve control tube at dump valve and discard oil seal. Plug end of tube with suitable fitting and leave dump valve connection open to cell ambient pressure.
3. Disconnect fuel in-line to fuel pump and connect it to 1010 oil supply at 172.37 kPa g (25 psig) pressure. Oil temperature should be greater than 283.15°K (50°F).
4. Set conditions  $P_2 = P_{AMB} = 55.16 \pm 1.38$  kPa ( $8 \pm .2$  psia),  $T_2 =$  ambient temperature.
5. Ensure engine ignition remains de-energized for this program procedure.
6. Slowly increase  $P_2$  to achieve  $N_2 = 1500 \pm 100$  rpm. Record Transient Data.

---

CAUTION

- A. Ensure  $N_1$  indication.
  - B. Ensure MOP  $\leq 330.95$  kPa (48 psia) within 15 sec after start windmill.
- 
7. Advance PLA to military setting (90 deg). When preservation oil is observed flowing from drain, slowly retard PLA to cutoff (0 deg). Return to military setting, and return to cutoff. RTD.
  8. Return test cell to ambient conditions.
  9. Using a new seal, install and secure dump valve control tube and lockwire nut.
  10. After completion of fuel system preservation, engine oil shall be drained by opening main oil drain valve, oil inlet drain valve, filter drain valve (located on oil pumps and accessory drive housing), two tank drain valves, and drain plug on accessory drive adapter.

11. Allow engine to stand until excess oil has drained; close drain valves and replace drain plug. Coat drain plug with preservative oil prior to reinstallation.

#### 12.2 ENGINE PRESERVATION (Sea-Level Test Facilities)

1. Engine fuel system shall be preserved after completion of testing using oil conforming to Military Specification, MIL-L-6081, Grade 1010.

---

#### CAUTION

Extreme care shall be taken to prevent foreign material from entering engine fuel system. Equipment shall be provided with filters and/or strainers of no coarser mesh (200 mesh) than those used in engine.

- 
2. Disconnect pressurizing and dump valve control tube at dump valve, and discard oil seal. Plug end of tube with suitable fitting and leave dump valve connection open to atmosphere.
  3. Disconnect fuel in-line to fuel pump and connect it to supply of slushing oil at pressure of 2 -- 25 psig, at temperature of 50° -- 90°F (10° -- 32°C).
  4. With ignition OFF and with test stand fuel shutoff valve CLOSED, move power lever to FULL OPEN position. Motor engine with starter until preservation oil is observed to flow from dump valve overboard drain. During motoring period power lever shall be moved from MILITARY, to OFF, to MILITARY.

---

#### CAUTION

Ensure drain valve control tube elbow is correctly installed and has not been inadvertently located in MILITARY pressure tap opening.

---

NOTE: Check main oil fuel pump, and fuel control strainers, for evidence of leakage.

5. Using new seal, install and secure dump valve control tube and lockwire nut.

6. After completion of the fuel system preservation engine oil shall be drained, by opening main oil drain valve, oil inlet drain valve, filter drain valve (located on oil pumps and accessory drive housing), two tank drain valves, and drain plug on accessory drive adapter.
7. Allow engine to stand until all excess oil has drained; close drain valves and replace drain plug. Coat drain plug with preservative oil prior to reinstallation.

#### 12.3 ENGINE WATERWASH

Only in the unlikely event that a 10.47 Hz (100 rpm) drop in rated speed occurs, should an engine waterwash be considered. NASA has no plans to do a waterwash and, following a Pratt and Whitney's suggestion, recommends that it not be done unless absolutely necessary and then only with approval of the steering committee.

#### 12.4 SHIPPING

To be specified by AGARD Working Group.

TABIE 1  
REFRESH INSTRUMENTATION RECOMMENDATIONS

Station No.	Description	Parameter Name	Number	SI (English) Minimum	Instrument-Range Maximum	Engine Health Parameters (1)
2.0	Static Pressure	PS2	8	10.34 (1.5)	103.42 KPa (15 psia)	
2.0	High Response Static Pressure	PS2K	2	10.34 (1.5)	"	X
2.0	Total Pressure	P2	46	10.34 (1.5)	"	X
2.0	Total Temperature	T2	10	244.3 (-20)	310.90K (100°F)	X
2.0	Skin Temperature	TH2A	2	"	"	
1.3	Static Pressure	PS13	1	34.47 (5.)	344.7 KPa (50 psia)	X
1.4	Bleed Discharge Total Pressure	PS13	1	34.47 (5.)	344.7 KPa (50 psia)	X
1.4	Bleed Discharge Total Temperature	TS13	4	255.4 (0.)	609.8°K (800°F)	X
1.4	Total Pressure	P3	6	206.8 (30.)	206.8 KPa (300 psia)	X
3.0	Total Temperature	T3	6	255.4 (0.)	609.8°K (800°F)	X
3.0	Static Pressure	PS11	2	206.8 (30.)	206.8 KPa (300 psia)	X
3.1	Total Pressure	PS11	1	34.47 (5.)	344.7 KPa (50 psia)	X
5.0	Total Temperature	TS5	5	255.4 (0.)	1088.7°K (1500°F)	X
7.0	Static Pressure	PS7	4	34.47 (5.)	344.7 KPa (50 psia)	X
7.0	Total Pressure	P7	36	34.47 (5.)	344.7 KPa (50 psia)	X
7.0	Total Temperature	T7	36	255.4 (0.)	1088.7°K (1500°F)	X
7.0	Skin Temperature	TH7	4	255.4 (0.)	1088.7°K (1500°F)	X
7.0	Skin Temperature	TH8	2	255.4 (0.)	1088.7°K (1500°F)	X
0.4, 0.5 and 0.8	Static Pressure	PS	12	10.34 (1.5)	103.42 KPa (15 psia)	X
Oil System	Oil Broather Pressure	POB	1	-69.95 (-10)	60.95 KPa (10 psia)	X
	Main Oil Pressure	MOU	1	60.95 (10.)	60.95 KPa (10 psia)	X
	Oil Temperature Into Oil Cooler	TOCI	1	255.4 (0.)	422°K (300°F)	X
	Oil Temperature Out of Cooler	TOCO	1	255.4 (0.)	477.6°K (400°F)	X
	Fuel Pump Inlet Pressure	FP1	1	255.4 (0.)	477.6°K (400°F)	X
	Fuel Pump Discharge Pressure	FP2	1	68.95 (10.)	369.5 KPa (100 psia)	X
	Fuel Pump Inlet Temperature	TF1	1	344.7 (50.)	344.7 KPa (50 psia)	X
	Engine Flowmeter Discharge Temperature	TEFO	1	377.6 (40.)	310.90K (100°F)	X
	Power Lever Angle	PLA	2	0. (0.)	477.6°K (400°F)	X
	Inlet Case Vibration	VIC	1	0. (0.)	1047.2 Hz (1000 rpm)	X
	Diffuser Case Vibration	VDC	1	0. (0.)	100 deg	X
	Turbine Exhaust Case Vibration	VTEC	1	0. (0.)	10 mile	X
	Accessory Drive Case Vibration	VADC	1	0. (0.)	10 mile	X
	Turbine Cooling Air Supply Pressure	PTCA	1	0. (0.)	10 mile	X
	Engine Fuel Flow	WFE	2	0. (0.)	206.8 KPa (300 psia)	X
					12599.8 g/sec (1000 lbm/hr)	X

NOTE: (1) Recommended for display in facility control room for engine health monitoring.

## Compressor Speeds Revised /31/82

TABLE II

## MIL POWER SETTINGS FOR TRIM CHECK

A. Engine No. 1, S/N 607594

<u>Inlet Total Pressure, P2</u>	<u>Ram Ratio</u>	<u>Inlet Total Temperature, T2</u>	<u>High Compressor Speed at Mil or Max EGT, NH</u>
Kpa (psia)		$^{\circ}$ K ( $^{\circ}$ F)	
82.7 (12.0)	1.00	288 (59)	9330
82.7 (12.0)	1.00	253 (-4)	9215
82.7 (12.0)	1.00	268 (23)	9272
82.7 (12.0)	1.00	308 (95)	9385
82.7 (12.0)	1.06	288 (59)	9337
82.7 (12.0)	1.30	288 (59)	9348
82.7 (12.0)	1.70	288 (59)	9319
51.7 (7.5)	1.30	288 (59)	9316
34.5 (5.0)	1.30	288 (59)	9209
20.7 (3.0)	1.30	288 (59)	9135

B. Engine No. 2, S/N F615037

<u>Inlet Total Pressure, P2</u>	<u>Ram Ratio</u>	<u>Inlet Total Temperature, T2</u>	<u>High Compressor Speed at Mil or Max EGT, NH</u>
Kpa (psia)		$^{\circ}$ K ( $^{\circ}$ F)	
82.7 (12.0)	1.00	288 (59)	9520
82.7 (12.0)	1.00	253 (-4)	9409
82.7 (12.0)	1.00	268 (23)	9459
82.7 (12.0)	1.00	308 (95)	9570
82.7 (12.0)	1.06	288 (59)	9536
82.7 (12.0)	1.30	288 (59)	9515
82.7 (12.0)	1.70	288 (59)	9514
51.7 (7.5)	1.30	288 (59)	9497
34.5 (5.0)	1.30	288 (59)	9426
20.7 (3.0)	1.30	288 (59)	9320

TABLE III

## UFTP TEST CONDITIONS

## A. Engine No. 1, S/N 607594

Inlet Total Pressure, P <sub>2</sub>		Ram Ratio	Altitude Facilities		(1) High Compressor Speed, NH
KPa	(psia)		Inlet Total Temperature, T <sub>2</sub>	OK	
* 101.3 (2)	(14.7)	1.00	288	288	MIL, 8875, 8475, 8650, 9100, 8750, 0550, (3) 8975, 9200
82.7	(12.0)	1.00	288	288	MIL, 8875, 8475, 8650, 9100, 8750, 8550, 8975, 9200
82.7	(12.0)	1.00	253	(-4)	MIL, 8675, 8200, 8450, 8950, 8575, 8325, 8825, 9075
82.7	(12.0)	1.00	268	(23)	MIL, 8775, 8300, 8550, 9025, 8650, 8425, 8900, 9125
82.7	(12.0)	1.00	308	(95)	MIL, 9075, 8750, 8900, 9225, 9000, 8825, 9150, 9300
82.7	(12.0)	1.06	288	(59)	MIL, 8875, 8475, 8650, 9100, 8750, 8550, 8975, 9200
82.7	(12.0)	1.30	288	(59)	MIL, 8875, 8475, 8650, 9100, 8750, 8550, 8975, 9200
82.7	(12.0)	1.70	288	(59)	MIL, 8875, 8475, 8650, 9100, 8750, 8550, 8975, 9200
51.7	( 7.5)	1.30	288	(59)	MIL, 8900, 8500, 8700, 9100, 8600, 8600, 9000, 9200
34.5	( 5.0)	1.30	288	(59)	MIL, 8825, 8400, 8625, 9000, 8725, 8550, 8925, 9100
20.7	( 3.0)	1.30	288	(59)	MIL, 8750, 8425, 8625, 8950, 8700, 8525, 8875, 9025

(1) 9 throttle speed settings specified by NASA LeRC.

(2) The first condition run in the test series will be repeated at the end of the test program to evaluate engine deterioration or variation.

(3) MIL is Military Power (i.e., PLA = 90°). However, set PLA ≤ 90° to maintain T<sub>5</sub> ≤ 1130°F.

\*Optional test condition for altitude facilities.

Compressor Speeds revised 3/31/82

TABLE III (Continued)  
B. Engine No. 2, S/N F615037

Inlet Total Pressure, P2	Ram Ratio	Altitude Facilities		(1) High Compressor Speed, MIL
		Inlet Total Temperature, T2	OK	
* 101.3 (2)	1.00	288	(159)	MIL, 9000, 8600, 8750, 9250, 8875, 8625, 9125, 9375
82.7	1.00	288	(59)	MIL, 9000, 8600, 8750, 9250, 8875, 8625, 9125, 9375
82.7	1.00	253	(-4)	MIL, 8800, 8200, 8500, 9100, 8650, 8350, 8950, 9250
82.7	1.00	268	(23)	MIL, 8925, 8400, 8650, 9175, 8800, 8525, 9025, 9325
82.7	1.00	308	(95)	MIL, 9200, 8875, 9025, 9375, 9125, 8950, 9300, 9475
82.7	1.06	288	(59)	MIL, 9000, 8600, 8750, 9250, 8875, 8625, 9125, 9375
82.7	1.30	288	(59)	MIL, 9000, 8600, 8750, 9250, 8875, 8625, 9125, 9375
82.7	1.70	288	(59)	MIL, 9000, 8600, 8750, 9250, 8875, 8625, 9125, 9375
51.7	1.30	288	(59)	MIL, 8925, 8450, 8650, 9200, 8800, 8525, 9050, 9325
34.5	1.30	288	(59)	MIL, 8925, 8450, 8700, 9175, 8800, 8575, 9050, 9275
20.7	1.30	288	(59)	MIL, 8875, 8450, 8675, 9100, 8775, 8550, 8975, 9200

(1) 9 throttle speed settings specified by NASA LERC.

(2) The first condition run in the test series will be repeated at the end of the test program to evaluate engine deterioration or variation.

(3) MIL is Military Power (i.e., PLA = 90°). However, set PLA ≤ 90° to maintain T5 ≤ 1130°F.

\*Optional test condition for altitude facilities.

TABLE III (Continued)

\*

## C. Sea-Level Facilities-Bleed Closed Settings

SPEED SETTING	HIGH COMPRESSOR SPEED CALCULATION	HIGH COMPRESSOR SPEED, NH
N1	$N_{MIL}$	RPM
N2	$\frac{(N1+N3)}{2}$	RPM
N3	$N_{BVC} + 30$	RPM
N4	$\frac{(N2+N3)}{2}$	RPM
N5	$\frac{(N1+N2)}{2}$	RPM
N6	$\frac{(N2+N4)}{2}$	RPM
N7	$\frac{(N3+N4)}{2}$	RPM
N8	$\frac{(N2+N5)}{2}$	RPM
N9	$\frac{(N1+N5)}{2}$	RPM
$N_{BVC}^t$		RPM

TABLE III (Concluded)

\*

## D. Sea-Level Facilities-Bleed Open Settings

TEST POINTS - LOW RANGE

TEST POINT	SPEED CALCULATIONS	HP SPEED (N <sub>2</sub> )
N10	$N_{BVC}^{-30}$	RPM
N11	$\frac{(N10+N12)}{2}$	RPM
N12	$N_{IDLE}$	RPM
N13	$\frac{(N11+N12)}{2}$	RPM
N14	$\frac{(N10+N11)}{2}$	RPM
N15	$\frac{(N11+N13)}{2}$	RPM
N16	$\frac{(N12+N13)}{2}$	RPM
N17	$\frac{(N11+N14)}{2}$	
N18	$\frac{(N10+N14)}{2}$	
$N_{BVC}^?$		RPM

TABLE IV  
 TEST SUMMARY SHEET (EXAMPLE)  
 UNIFORM ENGINE TESTING PROGRAM  
 LOCATION: USA NASA LEHRS RESEARCH CENTER FACILITY: PSL-3 RECORDED: YY-MM-DD-HH-mm-SS PROCESSED: YY-MM-DD POINT: NNNN

SUMMARY OF TEST CONDITIONS

ALT NNNNNN M WAI NNNNNN KG/S  
 BNI NNNNNN WF NNNNNN G/S  
 P23V NNNNNN KPA FN NNNNNN KN  
 T23V NNNNNN K ALPER NNNNNN X  
 PAMB NNNNNN KPA MUPER NNNNNN X  
 N NNNNNN SFC NNNNNN G/KN.S

STA	STATION AVERAGES		AIRFLOW (KG/S)				THRUST (KN)				SPEEDS (RPM)			
	T (K)	P (KPA)	WAI	WAI2	WAI3	WAI4	WAI5	WAI6	WAI7	WAI8	WAI9	WAI10	WAI11	WAI12
00	NNNNN	NNNNN	NNNNN	NNNNN	NNNNN	NNNNN	NNNNN	NNNNN	NNNNN	NNNNN	NNNNN	NNNNN	NNNNN	NNNNN
2	NNNNN	NNNNN	NNNNN	NNNNN	NNNNN	NNNNN	NNNNN	NNNNN	NNNNN	NNNNN	NNNNN	NNNNN	NNNNN	NNNNN
13	NNNNN	NNNNN	NNNNN	NNNNN	NNNNN	NNNNN	NNNNN	NNNNN	NNNNN	NNNNN	NNNNN	NNNNN	NNNNN	NNNNN
3	NNNNN	NNNNN	NNNNN	NNNNN	NNNNN	NNNNN	NNNNN	NNNNN	NNNNN	NNNNN	NNNNN	NNNNN	NNNNN	NNNNN
5	NNNNN	NNNNN	NNNNN	NNNNN	NNNNN	NNNNN	NNNNN	NNNNN	NNNNN	NNNNN	NNNNN	NNNNN	NNNNN	NNNNN
7	NNNNN	NNNNN	NNNNN	NNNNN	NNNNN	NNNNN	NNNNN	NNNNN	NNNNN	NNNNN	NNNNN	NNNNN	NNNNN	NNNNN
04	NNNNN	NNNNN	NNNNN	NNNNN	NNNNN	NNNNN	NNNNN	NNNNN	NNNNN	NNNNN	NNNNN	NNNNN	NNNNN	NNNNN
05	NNNNN	NNNNN	NNNNN	NNNNN	NNNNN	NNNNN	NNNNN	NNNNN	NNNNN	NNNNN	NNNNN	NNNNN	NNNNN	NNNNN
08	NNNNN	NNNNN	NNNNN	NNNNN	NNNNN	NNNNN	NNNNN	NNNNN	NNNNN	NNNNN	NNNNN	NNNNN	NNNNN	NNNNN

ENGINE PRES.  
 & TEMP. RATIOS  
 P5Q2 NNNNNN  
 T5Q2 NNNNNN  
 P2QAMB NNNNNN  
 P7QAMB NNNNNN  
 P7Q2 NNNNNN  
 T7Q2 NNNNNN

COMPRESSOR PERFORMANCE  
 P3Q2 NNNNNN  
 T3Q2 NNNNNN  
 EC NNNNNN

TABLE V  
DESCRIPTION OF DATA MEASUREMENT SYSTEMS (Example)

## A. Pressures

Parameter Designation	Type Measured Device	Type Recording Device	Method of System Calibration
Venturi Inlet Total Pressure Station 00	Bonded Strain Gage-Type Transducers (TABERS)	Automatic Multiple Pressure Scanning onto Sequential Sampling Millivolt-to-Digital Converter, and Magnetic Storage Data Acquisition	Inplace Application of Multiple Pressure Levels Measured with a Working Standard Pressure Calibrator Calibrated in Standards Laboratory
Engine Inlet Total Pressures Station 2.0			
Combustor Inlet Total Pressures Station 3.0			
IPT Turbine Exit Total Pressures Station 5.0			
Exhaust Nozzle Inlet Total Pressure Station 7.0			
Exhaust Nozzle Exit Ambient Pressure Station 0.8			

TABLE 7 (Concluded)

## B. Temperatures

Parameter Designation	Type Measuring Device	Type Recording Device	Method of System Calibration
Venturi Inlet Total Temp. Station 00	Chromel-Alumel Temperature Transducer	Sequential Sampling Millivolt-to-Digital Operator and Magnetic Tape Storage Data Acquisition System	Millivolt Substitution on MB 8 Temperature vs Millivolt Table
Engine Inlet Total Temp. Station 2.0			
Exhaust Nozzle Inlet Total Temperature Station 7.0			
Fuel Temp.			

## C. Others

Parameter Designation	Type Measuring Device	Type Recording Device	Method of System Calibration
Scale Force	Bonded Strain-Gage-Type Force Transducer	Sequential Samplings (Same as Above)	Inplace Application of Working Standard Load Cell Calibrated on Standards Laboratory
Fuel Flow	Turbine-Type Flowmeters		Laboratory Calibration
Air Flow	Choked Venturis		Procedures and Methods Verified with a Primary Standard (i.e. Weigh Tank)

TABLE VI  
IDENTIFICATION OF ELEMENTAL ERROR SOURCES (Example)

Parameter - Scale Force  
Measurement Range - 44.5 kN to 66.7 kN (10K to 15K lbf)

Error Source	Precision Indexes			Bias Limits**	
	Percent of Reading	Unit of Measurement, $\mu$ (lbf)	Degrees of Freedom	Percent of Reading	Unit of Measurement, $\mu$ (lbf)
I. Calibration (Transfer Error): National Std. to Laboratory Std. Laboratory Std. to Working Std. Working Std. to Meas. Instr.	+8.9 (+1)		5		+13.34 (+3)
	+13.34 (+3)		4		+17.8 (+4)
	+22.2 (+5)		16		+26.7 (+6)
		$S_{cal} = +27.6$ (+6.2)	$df_{cal} = 23$		$B_{cal} = +34.7$ (+7.8)
II. Data Acquisition: Excitation Voltage Electrical Simulation Signal Conditioning Recording Device Force Transducer Thrust Stand Mechanics Environmental Effects	+8.9 (+2)		>30		+13.34 (+3)
	+8.9 (+2)		>30		+13.34 (+3)
	+0.9 (+2)		>30		+13.34 (+3)
			>20		+13.34 (+3)
	+31.1 (+7)		>30		+4.4 (+0.1)
	+13.34 (+3)		>30		+22.2 (+5)
		+8.9 (+2)	>30		+22.2 (+5)
		$S_{D.A.} = +39.14$ (+8.8)	$df_{D.A.} > 30$		$B_{D.A.} = +41.4$ (+9.3)
III. Data Reduction: Calibration Curve Fit Computer Resolution	0				
	0				
		$S_{total} = +48.04$ (+10.8)	$df_{total} = 52$		$B_{total} = +55.6$ (+12.5)

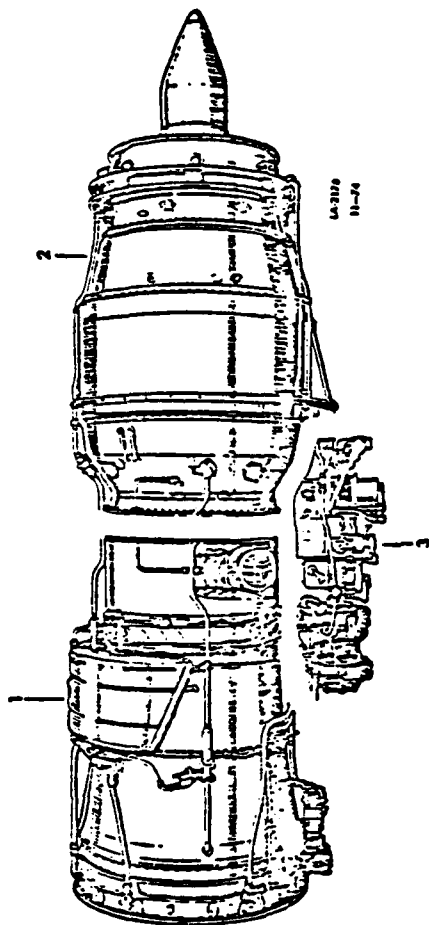
\*A similar table can be generated for each measured value.  
\*\*The method of numerical determination should be described (refer to AEDC-TR-73-5 for requirements)  
for each elemental error source identified in this table.

TABLE VII  
ESTIMATED MEASUREMENT UNCERTAINTIES (Example)

Parameter Designation	Measurement of Range	Precision Index (S)			Bias (B)			Uncertainty (Net)	
		Percent of Reading	Unit of Measurement	Degree of Freedom	Percent of Reading	Unit of Measurement	Percent of Reading	Unit of Measurement	
Venturi Inlet Total Pressure Station 00	96.53 to 172.4 kPa (14 to 25 psia)	0.03	--	30	0.06	--	0.12		
	34.47 to 68.95 kPa (5 to 10 psia)	0.08	--	30	0.15	--	0.31		
Venturi Inlet Total Temp. Station 00	272.2 to 533.3°K 490 to 960°R	--	.28°K 0.44°R	30	--	1.03°K 1.86°R		1.52°K 2.74°R	
	22.2K to 44.5K, N (5K to 10K, lbf)	--	35.6N (8 lbf)	30	--	62.3N (14 lbf)		131.4N (30 lbf)	
Scale Force	44.5K to 66.7K, N (10K to 15K, lbf)	--	35.6N (8 lbf)	30	--	66.7N (15 lbf)		137.9N (31 lbf)	
	2.52K to 100.8K, g/sec (2K to 80K, lbm/hr)	0.08	--	30	0.25	--	0.41	--	

TABLE VIII  
ESTIMATED PERFORMANCE PARAMETER UNCERTAINTIES (Example)

P2 (kPa)		T2 (°K)		Test Conditions		Airflow				Net Thrust				Specific Fuel Consumption			
				Ram Ratio	Hub Speed (Target Value) Hz (rpm)	Precision (S) %	Degree of Freedom	Bias (B) %	Uncertainty (U) %	Precision (S) %	Degree of Freedom	Bias (B) %	Uncertainty (U) %	Precision (S) %	Degree of Freedom	Bias (B) %	Uncertainty (U) %
02	200			1.0	(853.5)	.13	23	.2	0.5	0.08	30	.21	.37	.10	30	.30	0.50
20.7	200			1.3	(853.5)	.14	19	.26	0.6	.22	30	.50	.94	.20	30	.01	1.4



1. Compressor section
2. Combustion chamber, turbine, and exhaust sections
3. Accessory section

FIG. 1 PRATT & WHITNEY AIRCRAFT J57-P-19W TURBOJET ENGINE.

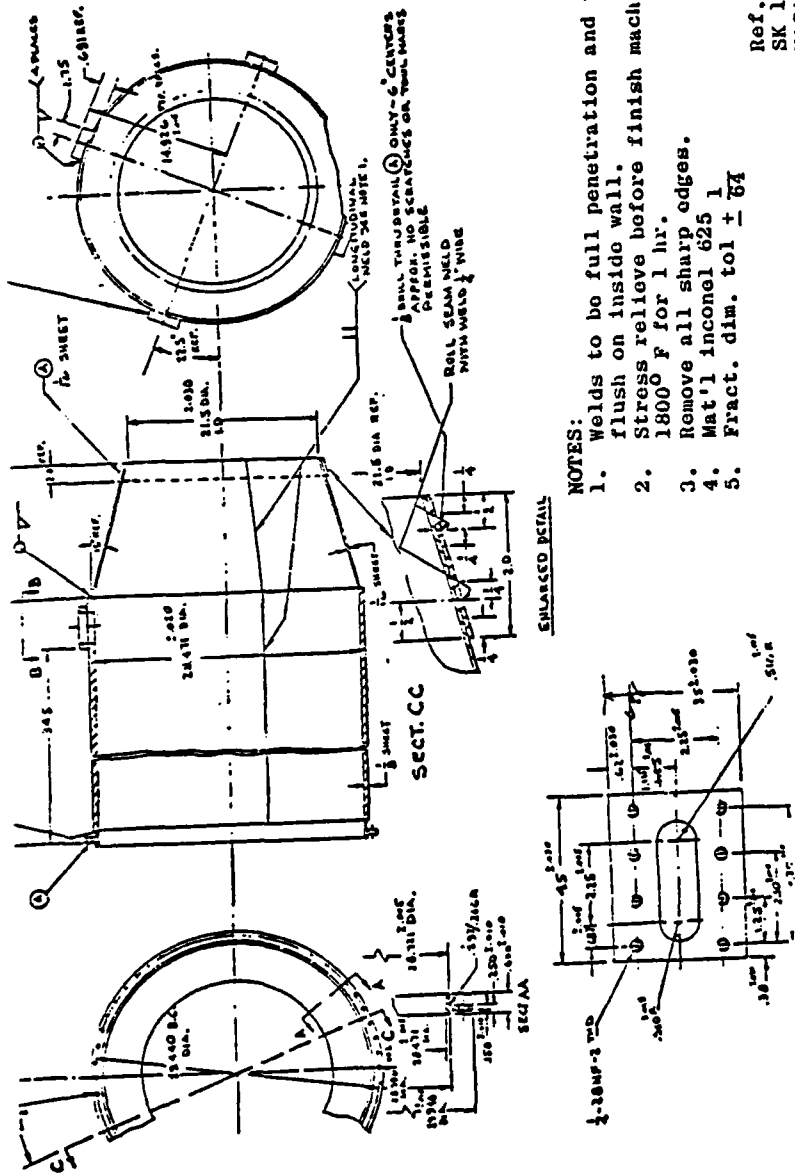
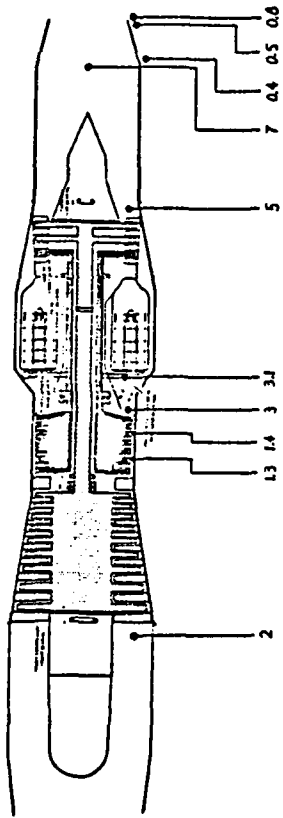


FIG. 2 MODIFIED TAILPIPE AND REFERENCE NOZZLE ASSEMBLY

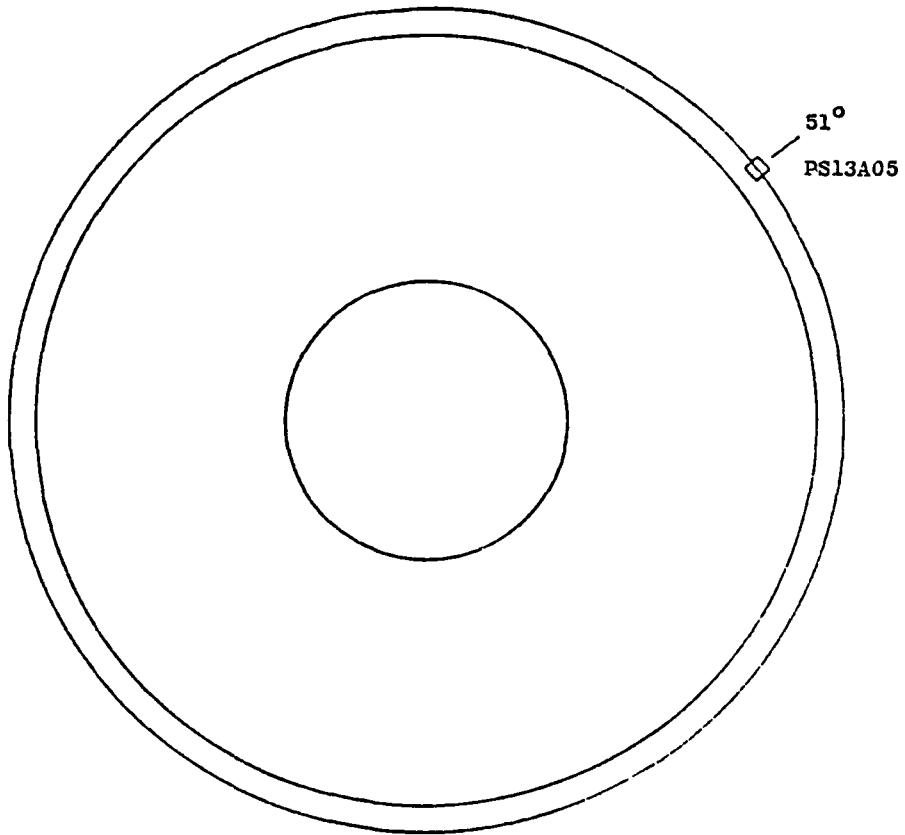


ENGINE INSTRUMENTATION STATION LOCATIONS

STATION NO.	DESCRIPTION
2.0	ENGINE OR LPC INLET
1.3	LPC BLEED ANNULUS
1.4	LPC BLEED PORT
3.0	COMBUSTOR INLET
3.1	COMBUSTOR DIFFUSER EXIT
5.0	LPT EXIT
7.0	EXHAUST NOZZLE INLET
0.4	EXHAUST NOZZLE EXIT (EXTERNAL)
0.5	EXHAUST NOZZLE (EXTERNAL)
0.8	EXHAUST NOZZLE (EXTERNAL) (TEA BAG STATIC)

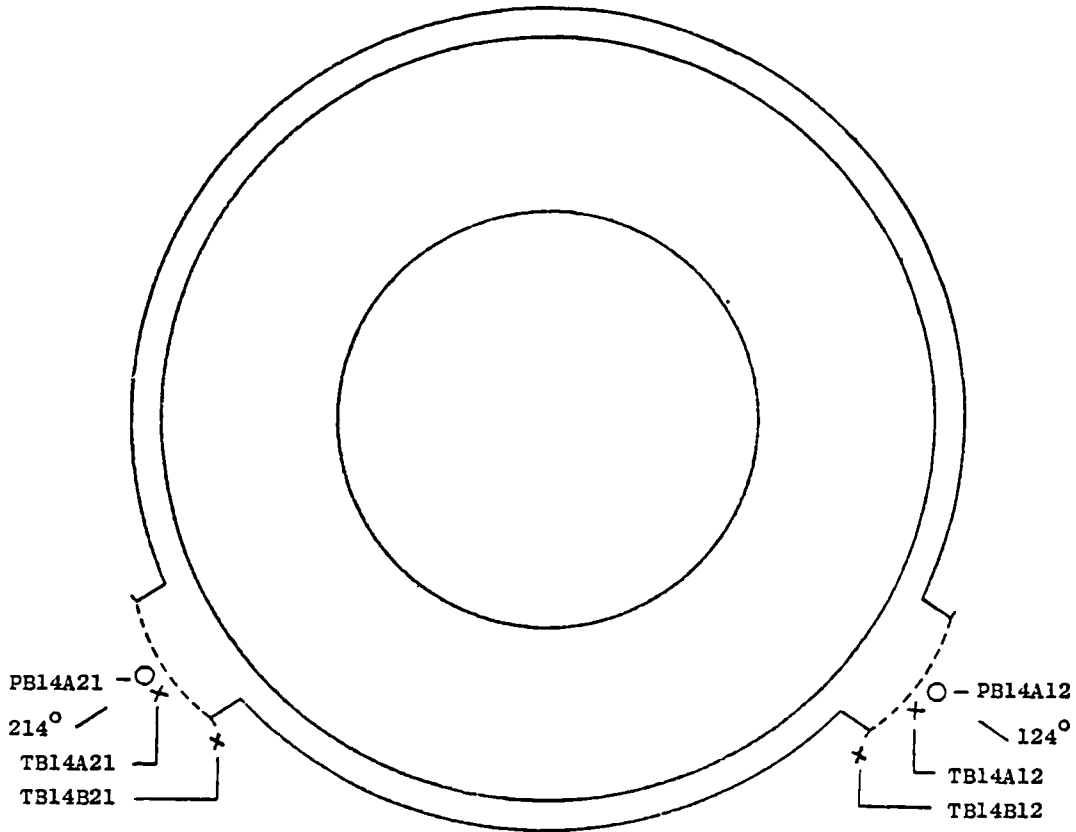
FIG. 3. UETP ENGINE INSTRUMENTATION STATION LOCATIONS





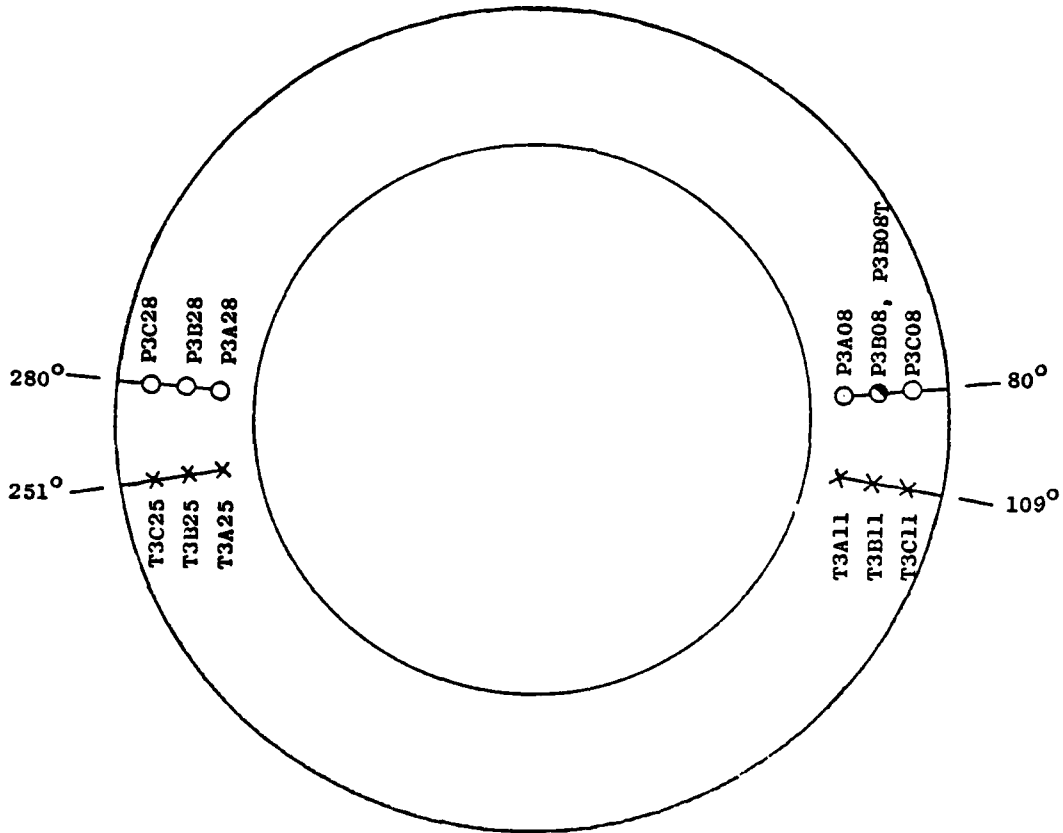
B. STATION 1.3  
LOW COMP. BLEED ANNULUS

FIG. 4 (CONTINUED)



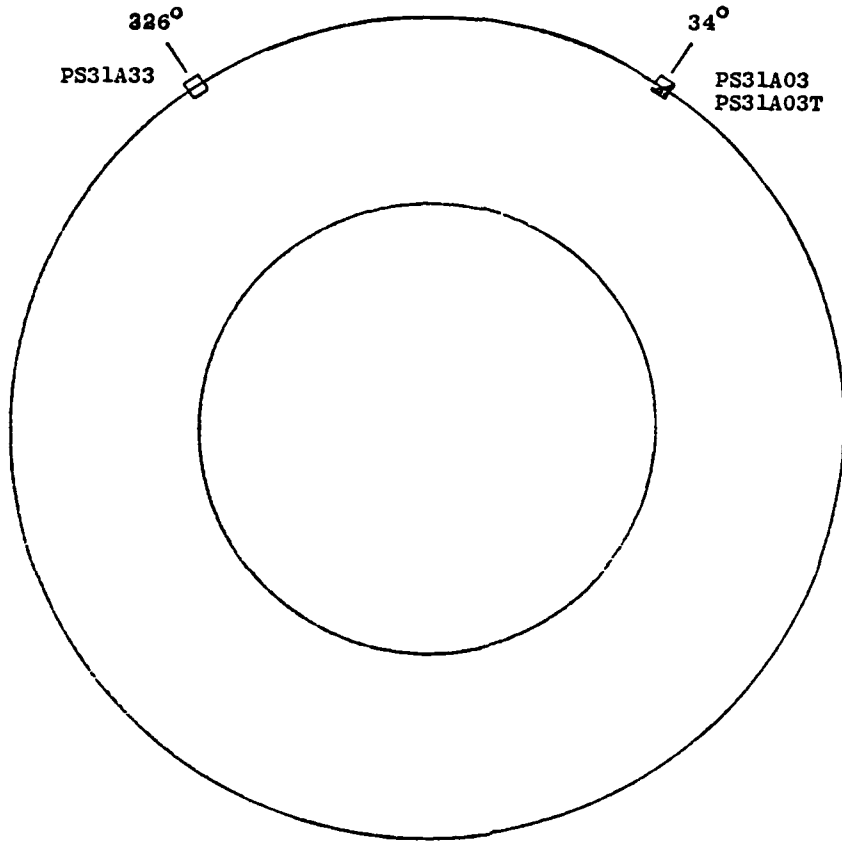
C. STATION 1.4  
LOW COMP. BLEED

FIG. 4 (CONTINUED)



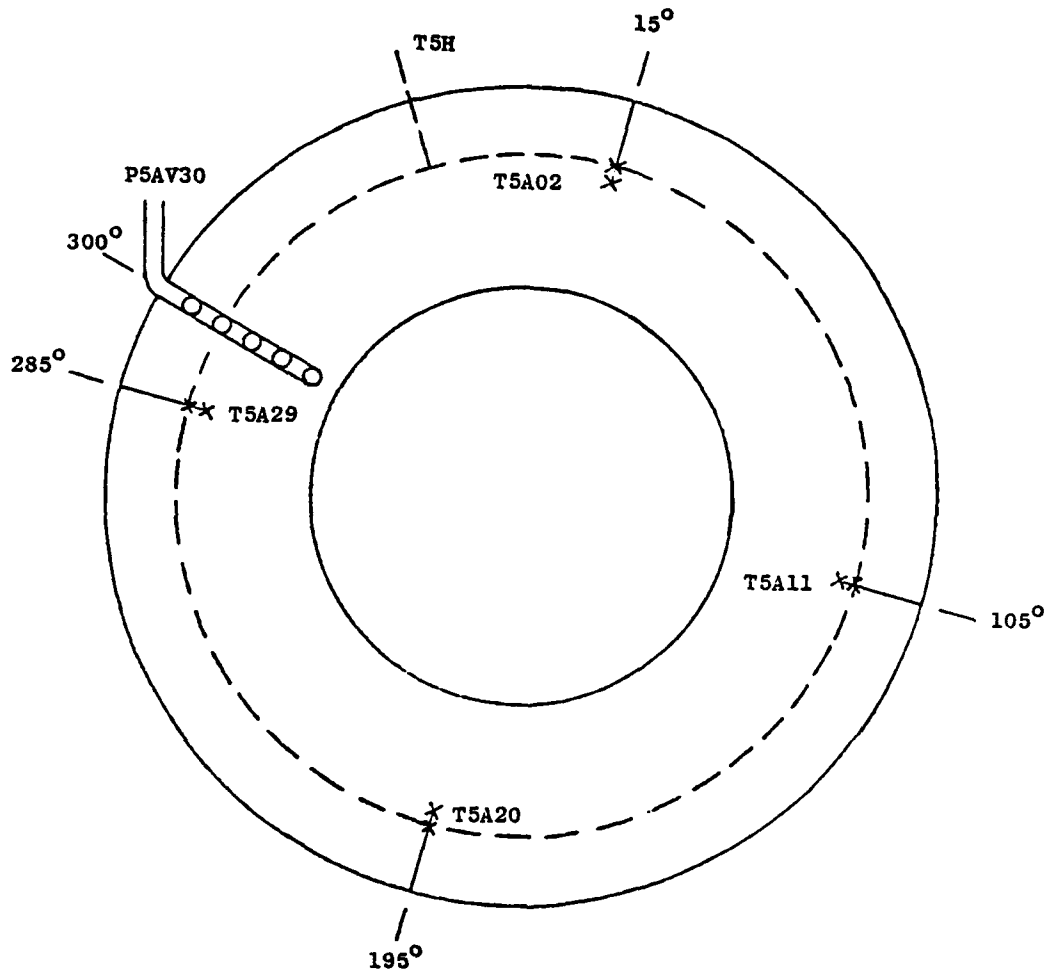
D. STATION 3  
COMBUSTOR INLET

FIG. 4 (CONTINUED)



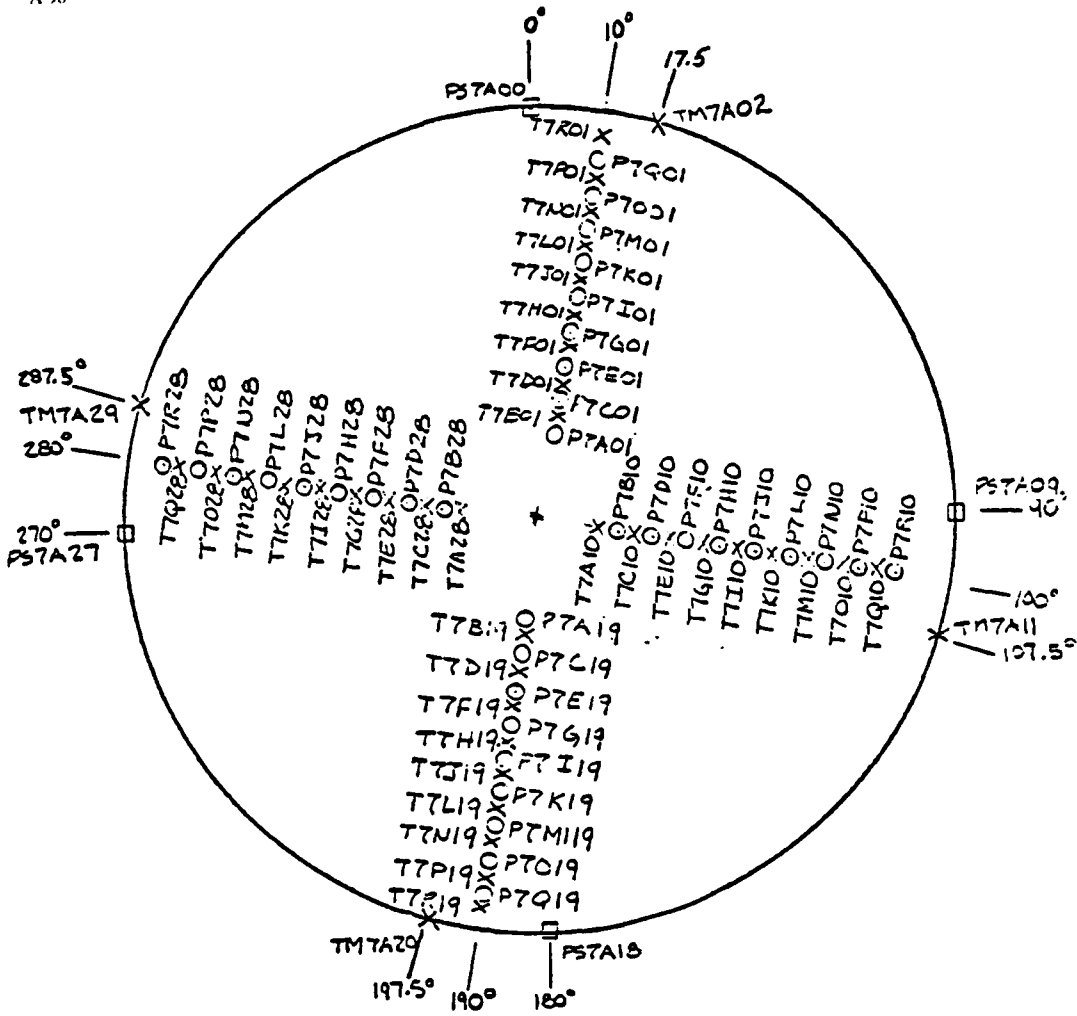
E. STATION 3.1  
COMBUSTOR DIFFUSER EXIT

FIG. 4 (CONTINUED)



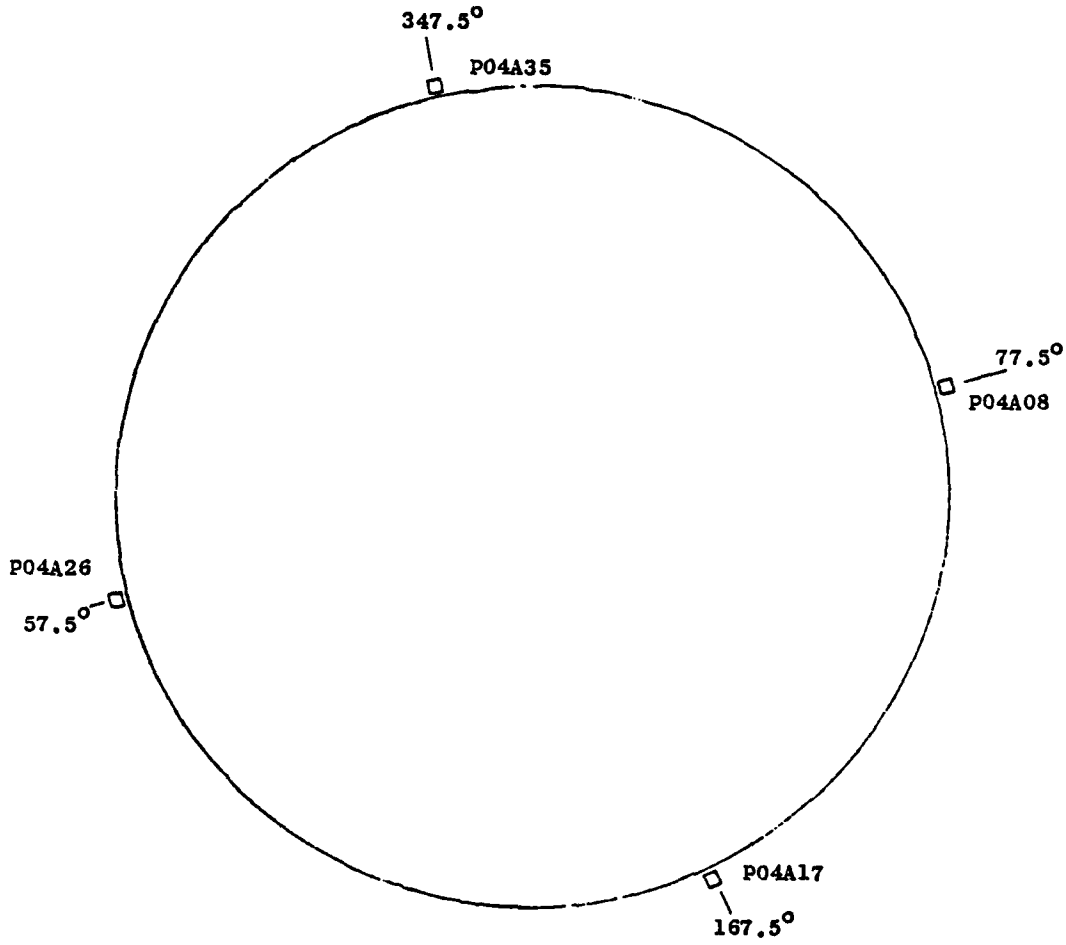
F. STATION 5  
LPT EXIT

FIG. 4. (CONTINUED)



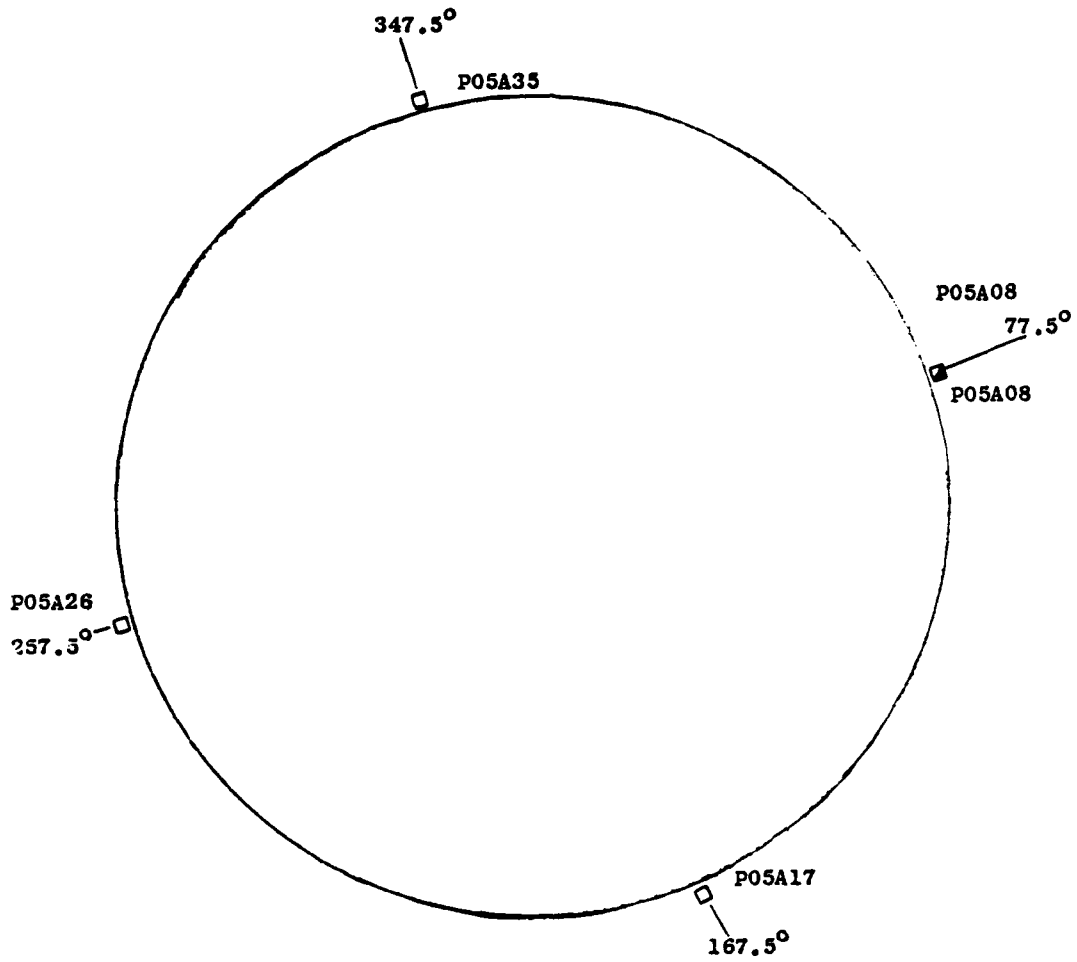
G. STATION 7  
EXHAUST NOZZLE INLET

FIG. 4 (CONTINUED)



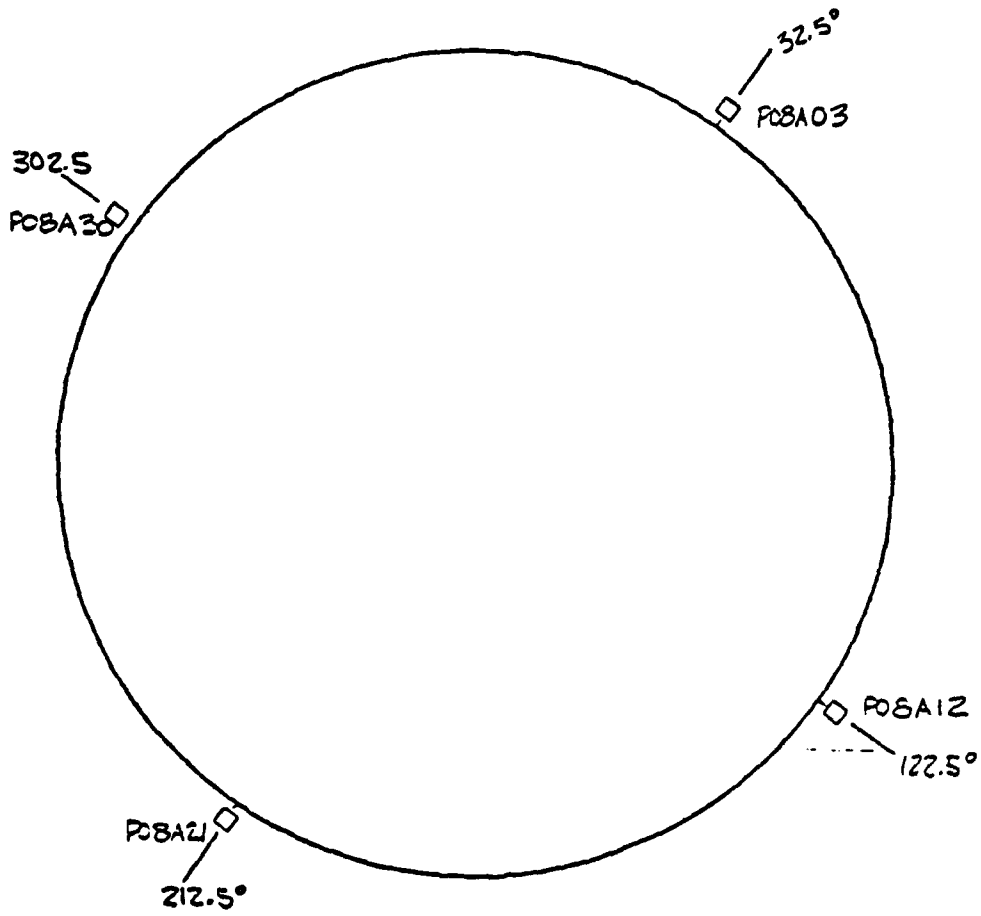
H. STATION 0.4  
EXHAUST NOZZLE EXIT (EXTERNAL)

FIG. 4. (CONTINUED)



I. STATION 0.5  
EXHAUST NOZZLE (EXTERNAL)

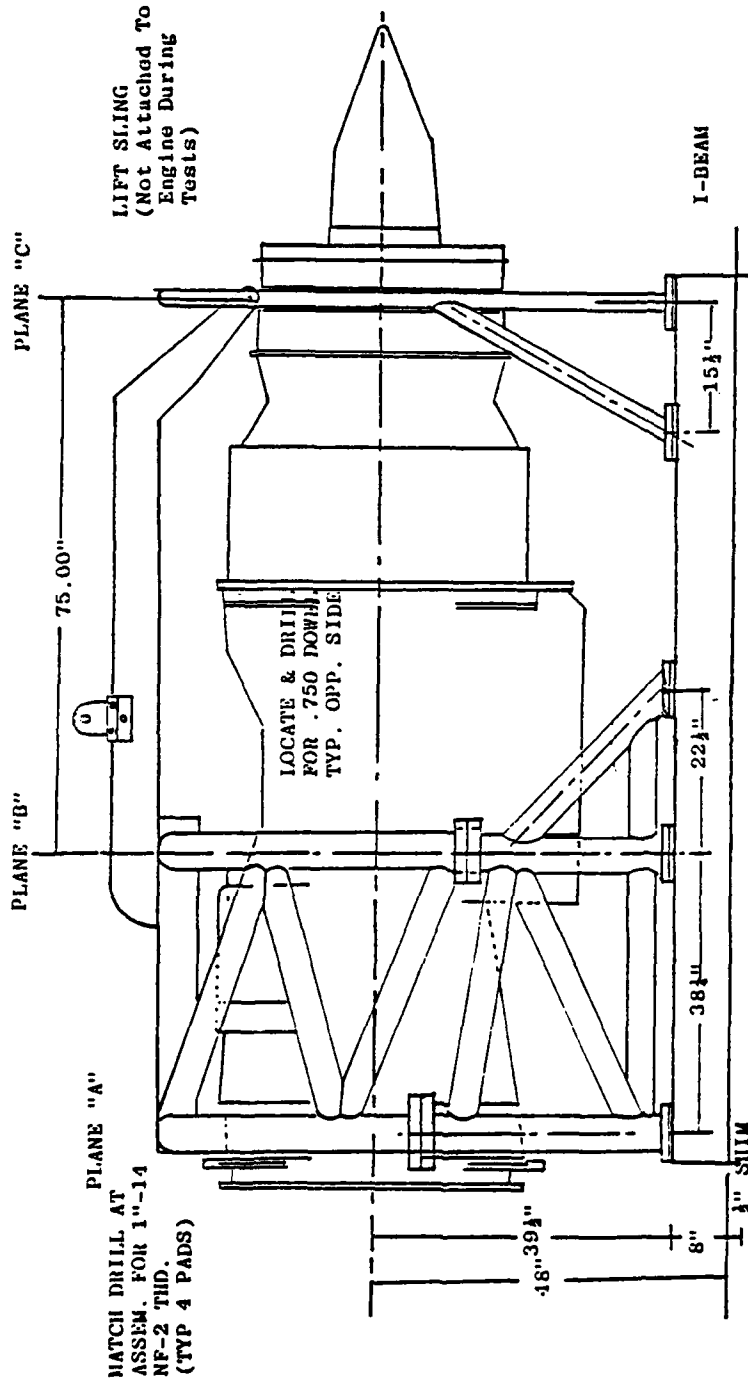
FIG. 4. (CONTINUED)



J. STATION 0.8  
EXHAUST NOZZLE (EXTERNAL)

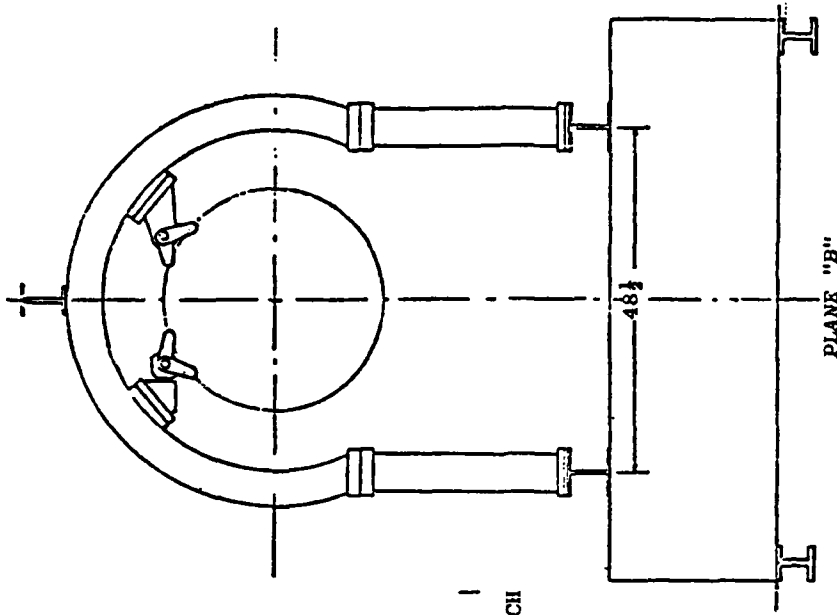
FIG. 4 (CONCLUDED)

NASA SKETCH

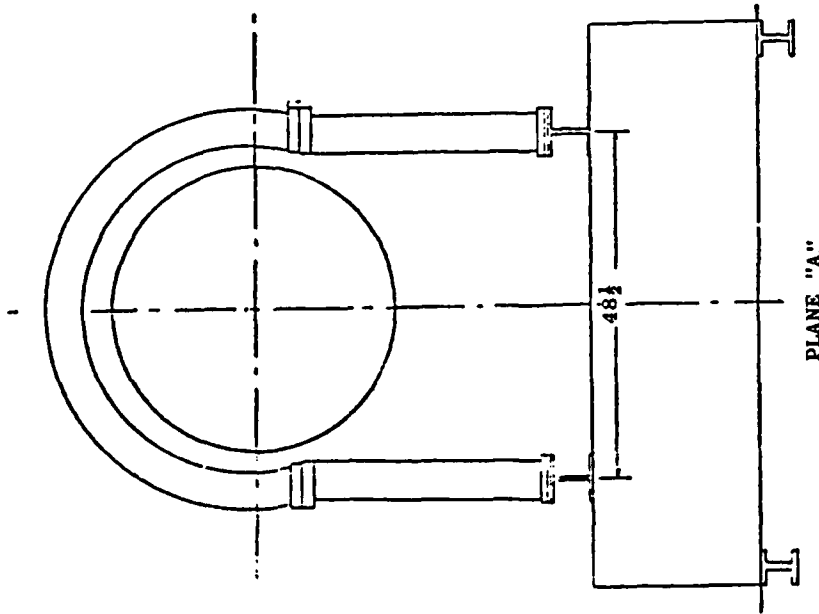


(a) Side View

FIG. 5 ENGINE INSTALLATION IN NASA SUPPLIED TEST STAND

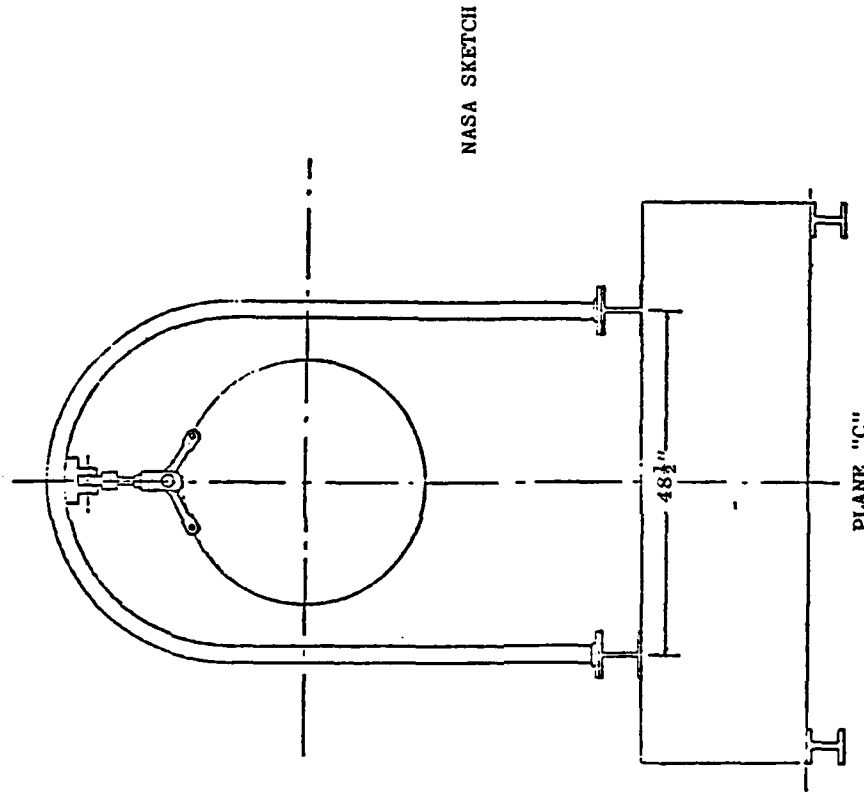


(c) Front View at Plane B



(b) Front View at Plane A

FIG. 5 CONTINUED



(d) Front View at Plane C

FIG. 5 CONCLUDED

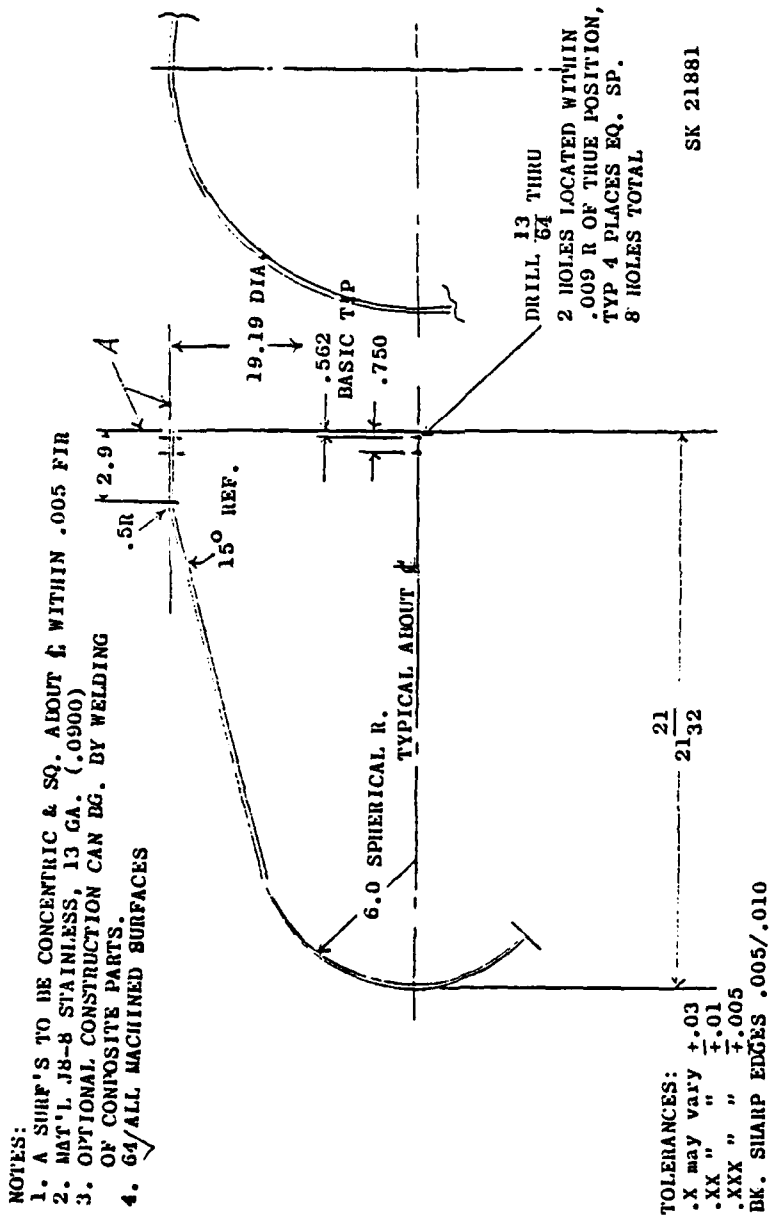


FIG. 6 ENGINE INLET BULLET NOSE

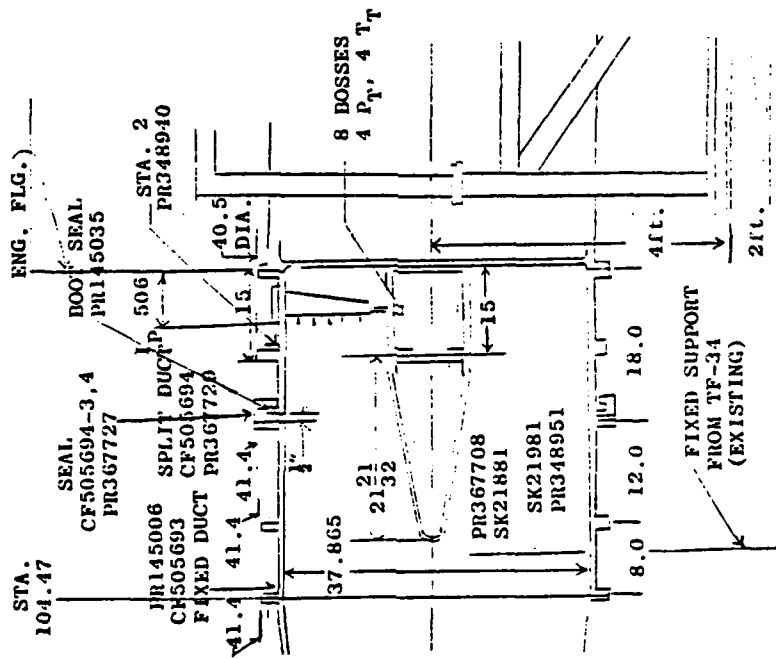


FIG. 7 NASA BULLETNOSSE AND ENGINE INLET INSTRUMENTATION SPOOL PIECE DESIGN.



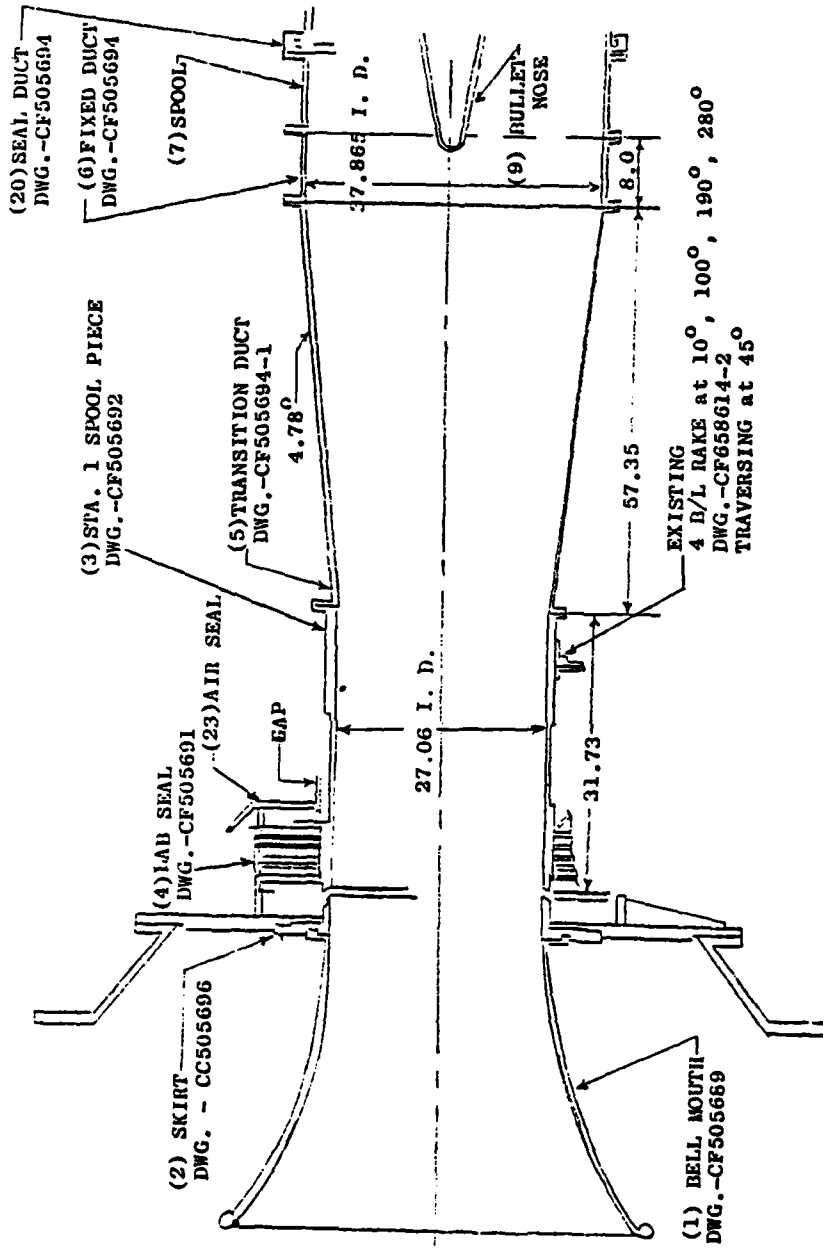
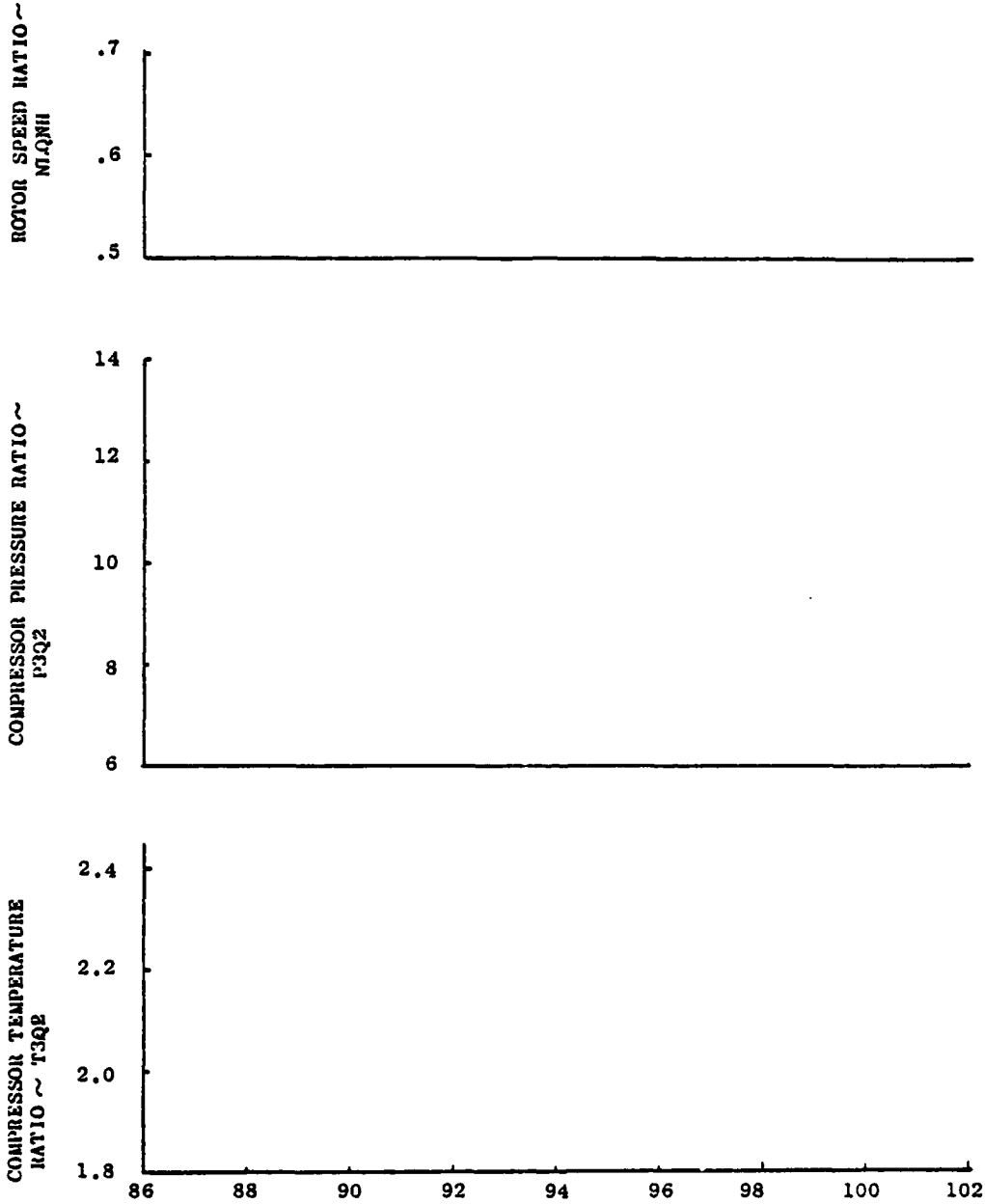


FIG. 9. J57 INSTALLATION AT NASA LeRC

SITE:

ENGINE NO.:

DATE:



a. CORRECTED HIGH ROTOR SPEED ~ NHPERR

Figure 10. Standard ACARD Engine Performance Plots

SITE:

ENGINE NO.:

DATE:

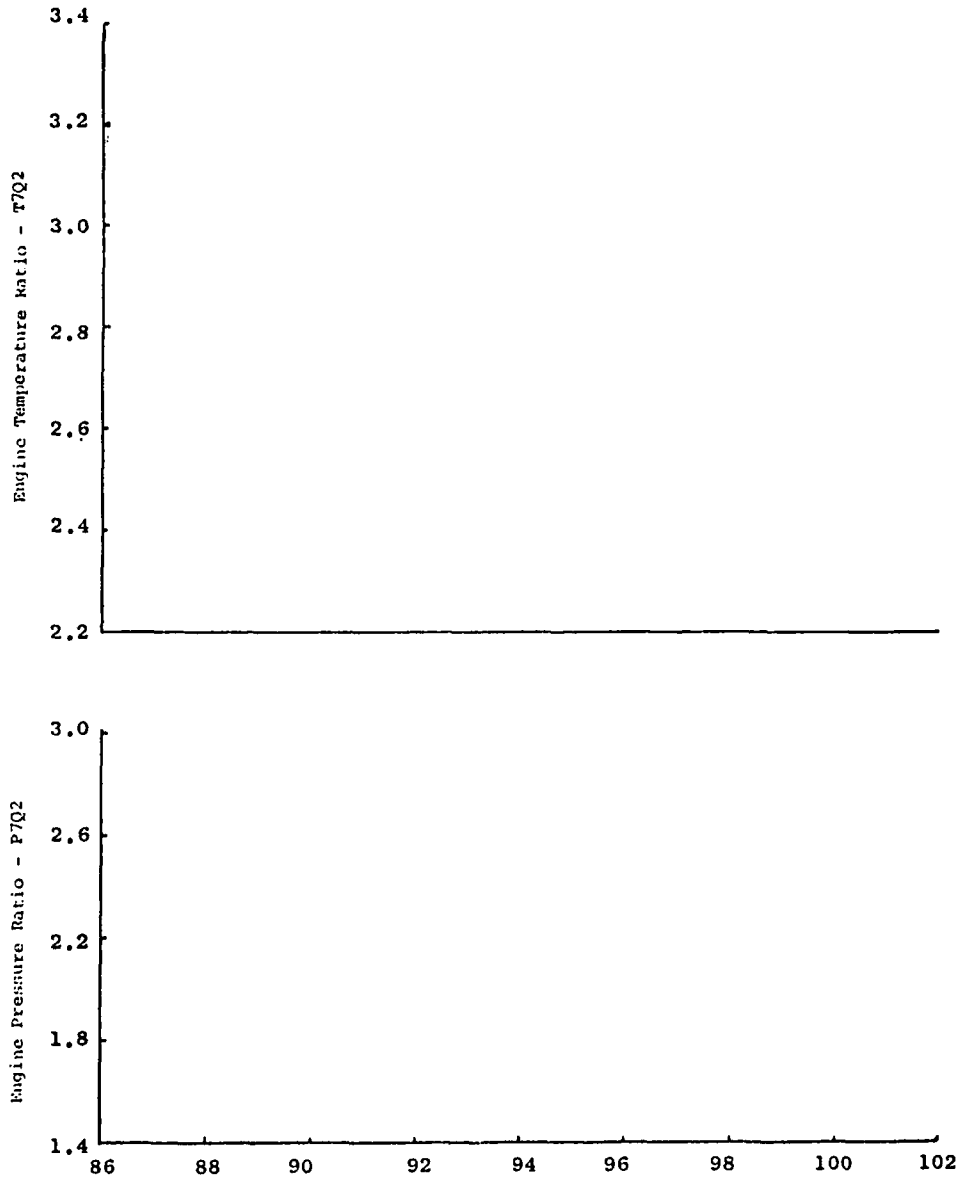


FIGURE 10. (Continued)

SITE:

ENGINE NO.:

DATE:

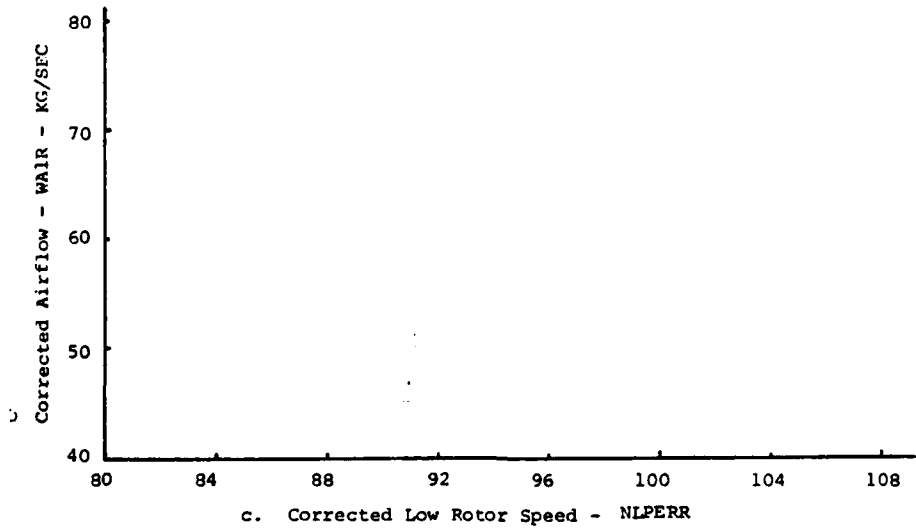
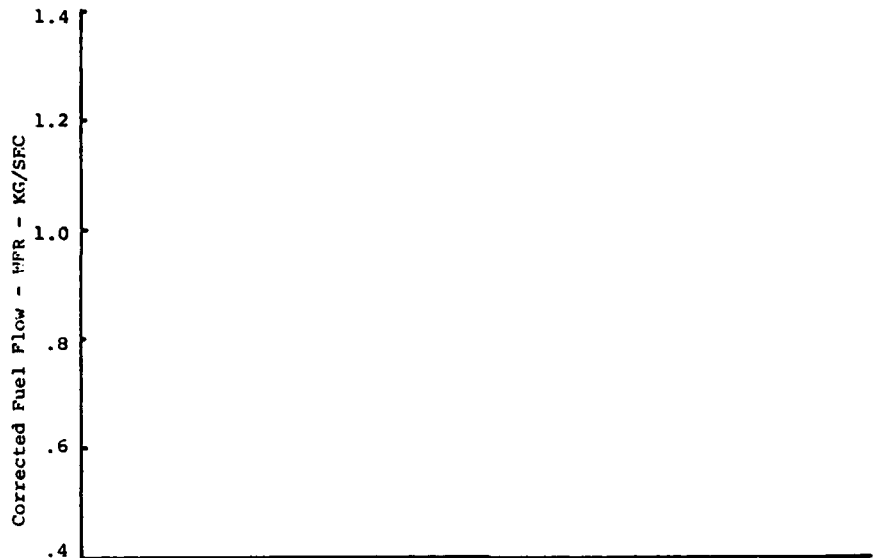


FIGURE 10. (Continued)

SITE:

ENGINE NO.:

DATE:

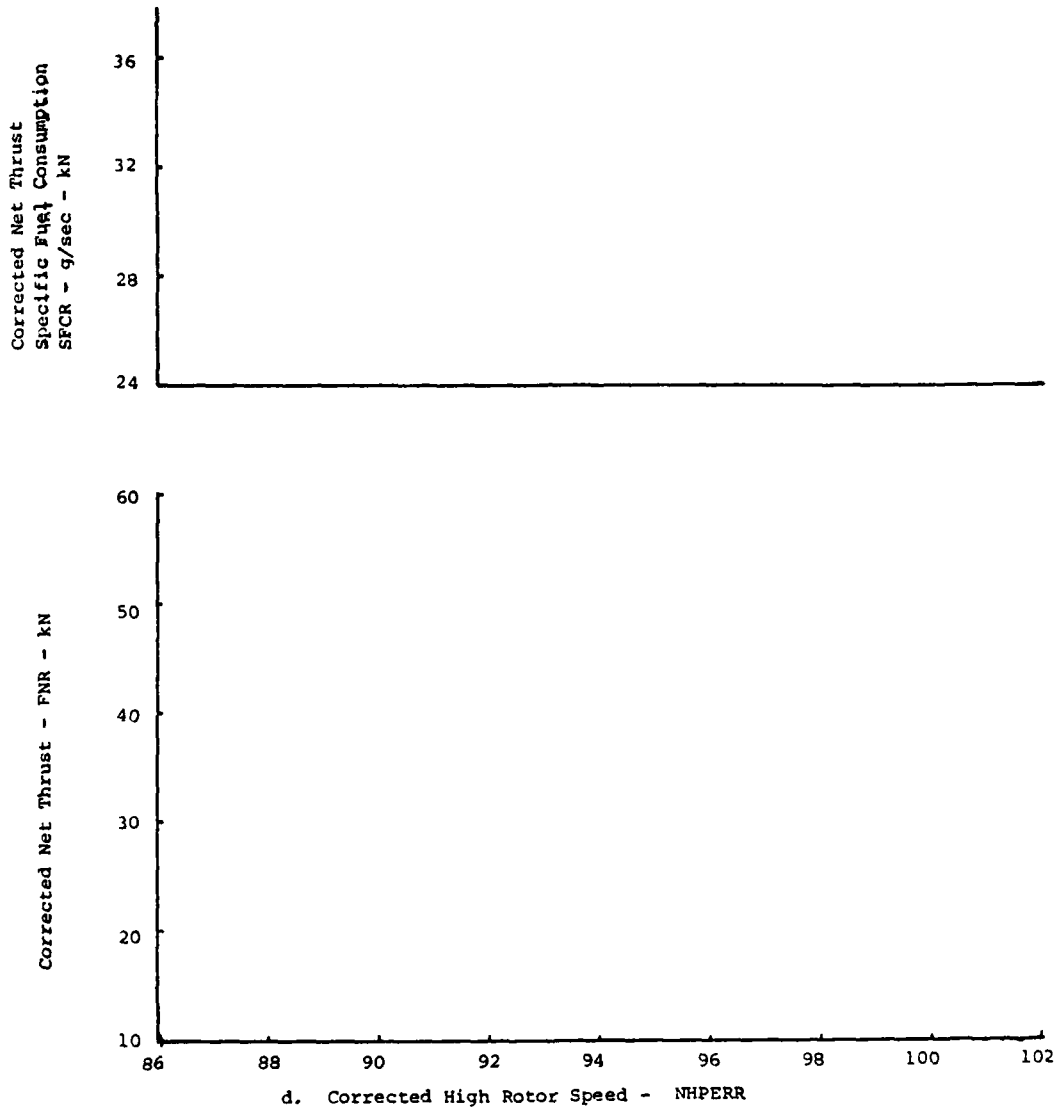


FIGURE 10. (Continued)





A P P E N D I C E S

## APPENDIX I

RECOMMENDED SPARE PARTS FOR J57 UNIFIED ENGINE TEST PROGRAMSMajor Parts

<u>UPE</u>	<u>REQ.</u>	<u>PART NUMBER</u>	<u>DESCRIPTION</u>
1	2	270237	PT7 Probe
4	8	181796	TT7 Probe
1	1	9484-A22	Fuel Pump
1	1	570377L22	Fuel Control
2	2	313093	Igniter
2	2	20300-80	Igniter Leads
2	2	20300-10	Ignition Exciters
<u>EXPENDABLES</u>			
2	4	193837	Gasket, Oil Cooler Tubes
2	8	AS100011	Gasket, Tach Drive
2	8	326239	Gasket, TT4
1	8	254414	Gasket, PT7 Probe
3	40	342433	"o" Ring, Gearbox Drain and Remote Fill
1	20	397741	"o" Ring, Oil Filter
1	20	388064	"o" Ring, N1 Gearbox Drain
1	1	481977	Gasket, Fuel Pump Mount
2	2	385992	"o" ring Fuel Pump
4	4	MS9021-219	"o" Ring, Pump Adapter
1	1	MS9021-221	"o" Ring, Pump Inlet
1	1	202199	Gasket, Fuel Control Mount
4	5	MS9021-217	"o" Ring
1	1	278529	Gasket, Temperature Sensor
4	5	MS9021-011	"o" Ring, Control
1	1	MS9020-04	"o" Ring, Control
2	15	354109	Retainer
2	15	213542	Seal
5	10	MS9021-215	"o" Ring
10	30	354120	Retainer
10	30	213546	Seal
1	2	346648	Moisture Trap Seal

<u>UPE</u>	<u>REQ.</u>	<u>PART NUMBER</u>	<u>DESCRIPTION</u>
1	2	376466	"o" Ring, Oil Tank
2	8	403809	"o" Ring, Oil Tank
2	10	385991	"o" Ring, Cooler Line
1	4	385970	"o" ring, cooler To Tank
2	4	182888	Gasket, Igniter
4	8	182213	Gasket, Anti-Ice Valve

APPENDIX II  
(Refer to T.O. 2J-J57-13 for Official Procedures)

Spectrometric Oil Analysis Program Sample (SOAP) Limits for J57-P-19W  
Engine

Element	Maximum(*)
Fe	11 PPM
Ag	3 PPM
Al	5 PPM
Cr	3 PPM
Cu	3 PPM
Mg	5 PPM
Ni	3 PPM
Ti	3 PPM

(\*) Maximum limits of accumulated wear metal contaminants in parts per million (PPM) concentrations.

NOTE: Notify Working Group 15 Chairman if one or more elements exceed established limits.

APPENDIX III  
(Refer to T.O. 2J-J57-13 for Official Procedures)

ENGINE OPERATING PROCEDURES

Oil Service

1. Service with MIL-L-7808 oil. Total oil tank capacity is 60.6 liters (16 gallons) but 7.57 liters (2 gallons) are sometimes residual in bearing compartments.
2. Run engine for five minutes at idle, accel to 7300 rpm N2 for 30 seconds to scavenge oil from the bearing compartments and shutdown.
3. Hot service oil system within one hour of shutdown.
4. If required, take soap sample.
5. Fill oil tank to full mark.

Engine Depreservation and Fuel/Oil Leak Check (Altitude Facilities)

1. Prior to cell air-on, disconnect pressurizing and dump valve control tube at dump valve. Plug end of tube with suitable fitting and leave dump valve connection open to cell ambient pressure.
2. Altitude test facilities set conditions  $P2 = PAMB = 55.2 \pm 1.4$  kPa ( $8.0 \pm .2$  psia).  $T2 =$  ambient temperature.
3. Ensure engine ignition remains de-energized for this program procedure.
4. Slowly increase P2 to achieve  $N2 = 1500 \pm 100$  rpm. RTD.

---

A. Ensure MOP 330.9 kPa (48 psia) within 15 sec after start windmill.

---

5. Advance PLA to military setting (90 deg) until approximately 7.57 liters (two gallons) of fuel is dumped overboard at dump valve. Check engine for external fuel and/or oil leaks.
6. Retard PLA to cutoff (0 deg).
7. Return test cell to ambient conditions.
8. Reconnect pressurizing and dump valve control tube.

9. Reset conditions in Step 4.
10. With ignition de-energized, advance PLA = 26.5 deg. Observe fogging from engine. Ensure engine fuel flow less than 1259.98 g/sec (1000 lbm/hr). Retard PLA to cutoff (0 deg) and observe engine for proper functioning of fuel dump valves.
11. Windmill engine for two minutes to remove residual fuel. Return to ambient conditions.
12. End of Procedure.

Engine Depreservation and Fuel/Oil Leak Check (Sea-Level Facilities)

1. Prior to initial engine stock, disconnect pressurizing and dump valve control tube at dump valve. Plug end of tube with suitable tilting and leave dump valve connection open to atmosphere.
2. Ensure engine ignition remains de-energized for this program procedure.
3. With ignition OFF, fuel ON, and power lever CLOSED, operate engine by starter at speed sufficiently high enough to ensure that oil system is fully primed and that oil pump maintains pressure indication.
4. Open throttle until approximately two gallons of fuel is dumped overboard at dump valve. Check engine for external oil leaks and check drain valves for proper functioning.
5. Reconnect pressurizing and dump valve control tube.
6. End of procedure.

Engine Starting and Shutdown (Altitude Facilities)

1. Altitude test facilities set conditions  $P_2 = P_{AMB} = 55.2 \pm 1.4$  kPa ( $8.0 \pm .2$  psia) and  $T_2 =$  ambient temperature.
2. Slowly increase  $P_2$  to achieve  $N_2 = 1500 \pm 100$  rpm. Record transient data.

---

CAUTION

- A. Ensure  $N_1$  indication before moving power lever to idle to avoid hung-start and excessive starting temperatures.
  - B. Ensure MOP 330.9 kPa (48 psia) within 15 sec after start windmill.
-

3. Energize ignition and advance PLA = 26.5 deg. Discontinue start if fuel flow is greater than 1259.98 g/sec (1000 lbm/hr).

---

CAUTION

- C. Light-up must occur within 30 sec after PLA is positioned at idle.
  - D. Maximum EGT (average of 4 probes) is 723.15°K (842°F).
- 

4. De-energize ignition system.
5. Obtain steady-state data. Low and high rotor speeds should be approximately 230.4 (2200) and 6000 rpm, respectively.

NOTE: Mild compressor stalls are common with the J57 engine at low rotor speeds. If encountered and does not immediately clear, decel to idle power.

6. To ensure proper engine cooling and maximum oil scavenging, all engines shutdowns shall be made by running the engine at idle for 5 minutes, followed by 30 seconds at N2 = 7450 rpm, and then closing power lever to OFF.
7. Observe engine for proper functioning of fuel drain valve.
8. Altitude test facilities return test cell to ambient conditions.
9. End of Procedure.

Engine Starting and Shutdown (Sea-Level Facilities)

1. Prior to initial start, during engine static condition, energize ignition system and check by listening to ensure that both ignitor are firing.
2. Prior to initial start, accomplish engine depreservation and fuel/oil leak check.
3. Starter air supply to maintain 60 PSIG during start procedure. \*  
Activate starter and ensure N<sub>1</sub> and N<sub>2</sub> indication. Ensure oil pressure (MOP) 48 PSIA within 15 sec.
4. Energize ignition system at 800 -- 1,000 rpm (8.2 -- 10.3 percent) high compressor rotor (N<sub>2</sub>) speed.

5. Open power lever to IDLE position (26 1/2 OPLA) at 1,200 -- 1,500 rpm (12.4 -- 15.5 percent) high compressor rotor (N<sub>2</sub>) speed. Discontinue the start if fuel flow exceeds 1,000 phr. \*
6. Record time to light \_\_\_ from starter initiation to indication in exhaust gas temperature (EGT). \*

Cut off starter at 2500-3000 rpm (26-31%) N<sub>2</sub>.

Allow engine to accelerate to IDLING speed (60% N<sub>2</sub>) and observe maximum EGT. Maximum allowable EGT is 450°C (842°F). Observe oil pressure - min. 40 PSIG.

Record time from starter initiation to IDLE speed (60% N<sub>2</sub>).

---

**CAUTION**

Light-up on NORMAL START shall occur within 30 seconds after power lever is moved to IDLE. If light-up, as evidenced by increase in exhaust gas temperature, does not occur within 45 seconds, return power lever to OFF, de-energize starting and ignition systems, and investigate to find reasons for difficulty. Allow at least one minute for excessive fuel to drain before attempting another start.

---

7. De-energize ignition system.
8. Record steady-state data. To ensure proper engine cooling and maximum oil scavenging, all shutdowns shall be made by running for five minutes at IDLE rpm, followed by 30 seconds at 75 percent rpm, and then closing power lever to OFF position.

---

**CAUTION**

In emergency, shutdown shall be made from any power lever position, however, if emergency shutdown is made, engine shall be rotated by hand to ensure it is free before another start is attempted.

---

9. Immediately following shutdown, inspect front compressor front bearing for oil leakage. Record run down time for both rotors. \*
10. Check oil level and take SOAP sample if applicable. SOAP samples should be taken after approximately 10 running hours. \*
11. End of Procedure. \*

Engine and Fuel Control System Check

1. Conduct engine start per Engine Starting and Shutdown Procedure and stabilize for 5 minutes.
2. Altitude test facilities set conditions  $P2 = PAMB = 82.7 \pm .7$  kPa ( $12 \pm .1$  psia) and  $T2 = 288.15 \pm 1.1^{\circ}K$  ( $59 \pm 2^{\circ}F$ ). Sea-level test-facilities conduct system check at ambient conditions.
3. Slowly advance PLA to determine exact N1 rotor speed at which compressor bleed valves close. Monitor PB for indication. Record Transient Data.
4. Slowly retard PLA to determine exact N1 rotor speed at which compressor bleed valves open. Record Transient Data.

---

 CAUTION

- A. Bleed valve operation must occur within limits shown in Fig. III-1.
- 

5. Set idle power (PLA = 26.5 deg).
6. Observed N2 should be within limits shown in Fig. III-2. Note any discrepancies and continue. If engine is out of trim, terminate testing and consult with AGARD authorities.
7. Advance PLA to engine part power operation (PLA = 70 deg). Observe all engine operating limits in Appendix IV.

NOTE: Mild compressor stalls are common with the J57 engine at low rotor speed. If encountered and does not immediately clear, retard PLA to IDLE.

Normal Operation

1. The J57 engine does not require warmup time at idle before accelerating to military (90° PLA). However, at least enough time should be spent at idle to check engine parameters such as TT5, N1, N2, MOP, PMB, PFO, PFI, WF, PCP, vibs and to visually check engine for fluid leakage.
2. During all excursions to military, check compressor bleeds for proper closing.
3. Mild compressor stalls near idle during transients are not unusual with the J57 engine.
4. The control system does not incorporate inlet pressure compensation, therefore, at some altitude conditions, PLA will have to be modulated to prevent turbine overtemperature.

5. During acceleration from idle to military, temporary overshoot of TT5, N1, N2 and Gn will probably occur. Overshoot will last from 2 to 4 minutes, decreasing during this period. As long as engine transient limits are not exceeded, engine may be allowed to stabilize at military.
6. Engine shutdown should be preceded by 5-minute stabilization at IDLE. If oil level is to be checked, accel to 764.5 Hz (7300 rpm) N2 for 30 sec prior to shutdown to scavenge excess oil from the bearing compartments.
7. Ensure engine performance is comparable to Fig. III-1 through III-5.
8. Slowly advance PLA to military power (PLA = 90 deg).
9. Check turbine cooling air requirements per Fig. IV-3 (Appendix IV).
10. Adjust oil cooler water flowrate to achieve oil temperature out of cooler (TOCO) of  $366.5 \pm 5.6^{\circ}\text{K}$  ( $200 \pm 10^{\circ}\text{F}$ ).
11. Conduct engine shutdown per Engine Starting and Shutdown Procedure.

#### Engine Performance Testing

1. Conduct engine start per Engine Starting and Shutdown Procedure.
2. At idle power, set test condition specified in Test Directive. All test conditions and engine power settings are listed in Section 8. Suggested tolerances for altitude test facilities are: pressure  $\pm .7$  kPa ( $\pm .1$  psia), temperature  $\pm 1.1^{\circ}\text{K}$  ( $\pm 2^{\circ}\text{F}$ ), and ram ratio ( $P2/\overline{P0}$ ) within  $\pm .5\%$  of desired level.

Note that engine trim checks and trim adjustments should not be required for the conduct of the AGARD UETP. The engines were trimmed prior to the initiation of the UETP by NASA. In the event that the desired engine power settings cannot be obtained (due to engine "trim slip" or "engine deterioration"), the chairman of Working Group 15 should be contacted for direction and or authorization of any corrective engine maintenance action.

3. Conduct engine shutdown per Engine Starting and Shutdown Procedure.
4. End of Procedure.

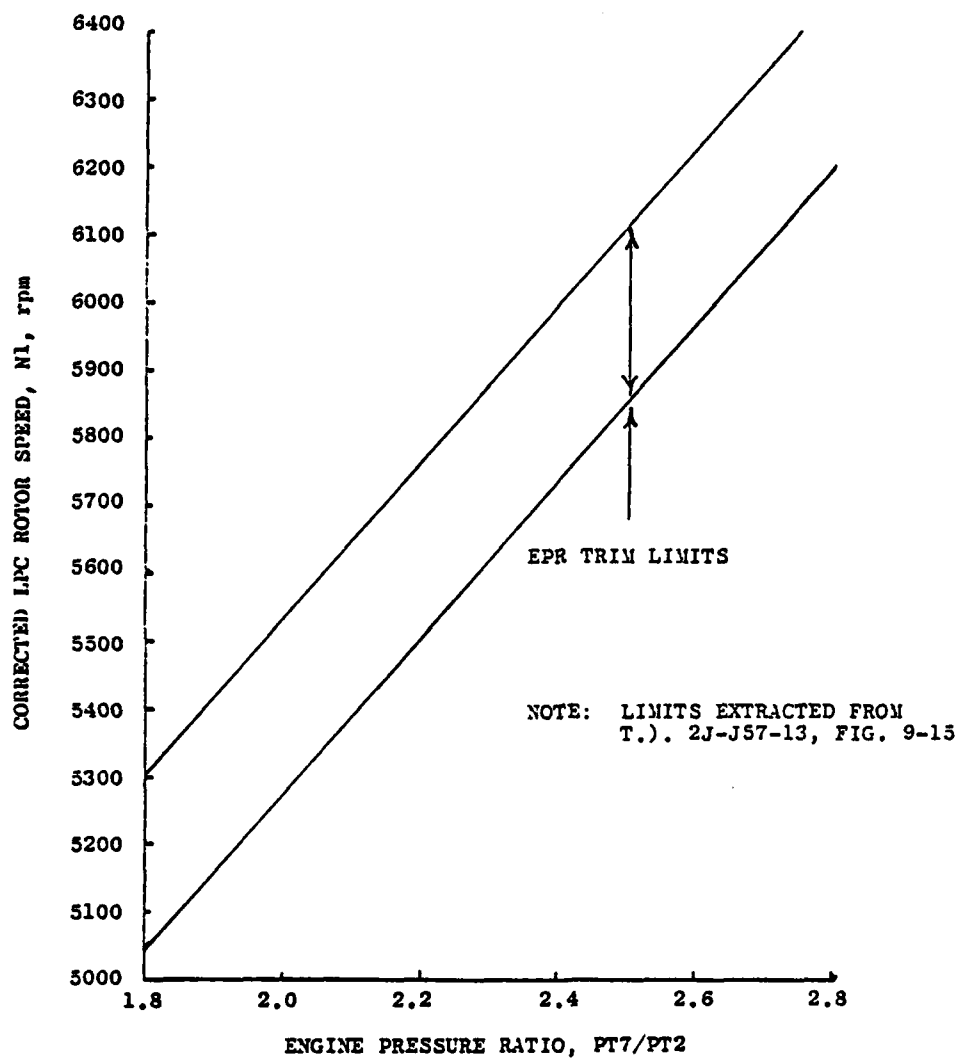


FIG..III-1. CORRECTED LPC ROTOR SPEED AS A FUNCTION OF ENGINE PRESSURE RATIO AT SEA-LEVEL-STATIC CONDITIONS.

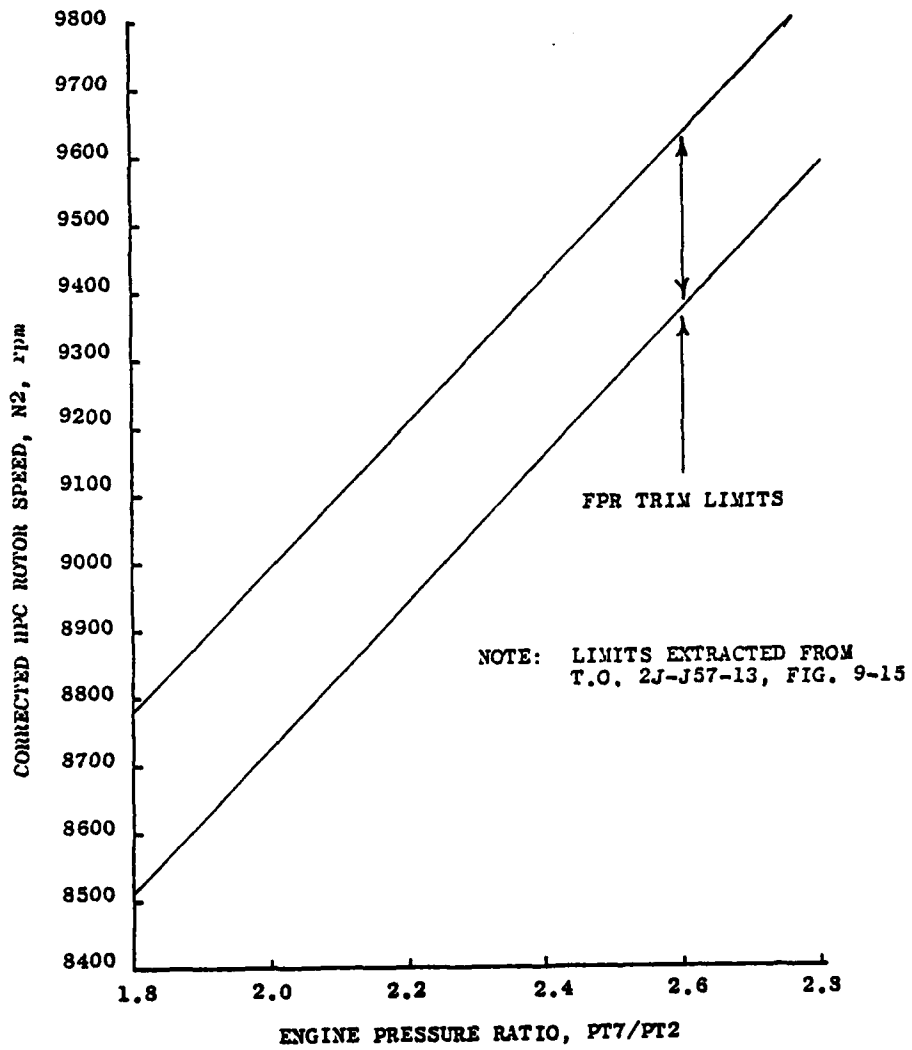


FIG. III-2. CORRECTED HPC ROTOR SPEED AS A FUNCTION OF ENGINE PRESSURE RATIO AT SEA-LEVEL-STATIC CONDITIONS.

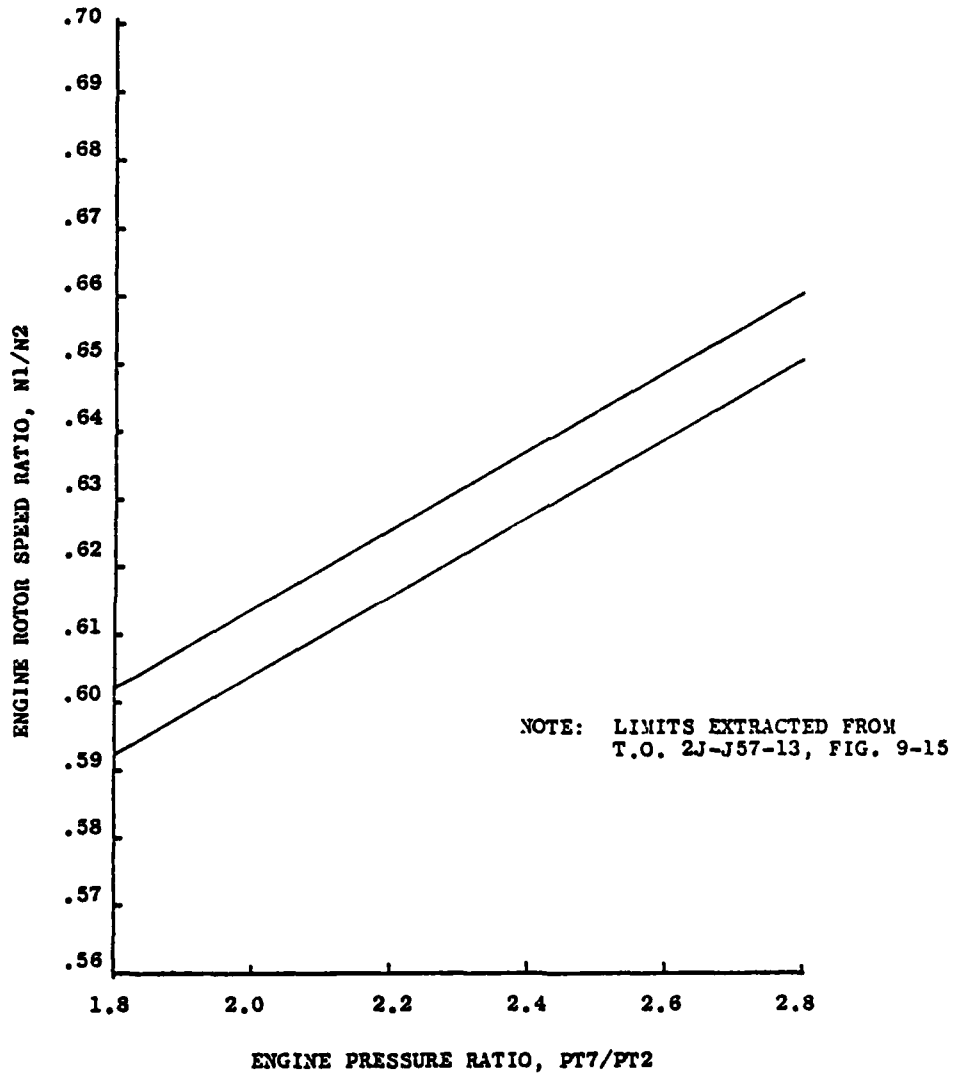


FIG. .1111-3. ENGINE ROTOR SPEED RATIO AS A FUNCTION OF ENGINE PRESSURE RATIO AT SEA-LEVEL-STATIC CONDITIONS.

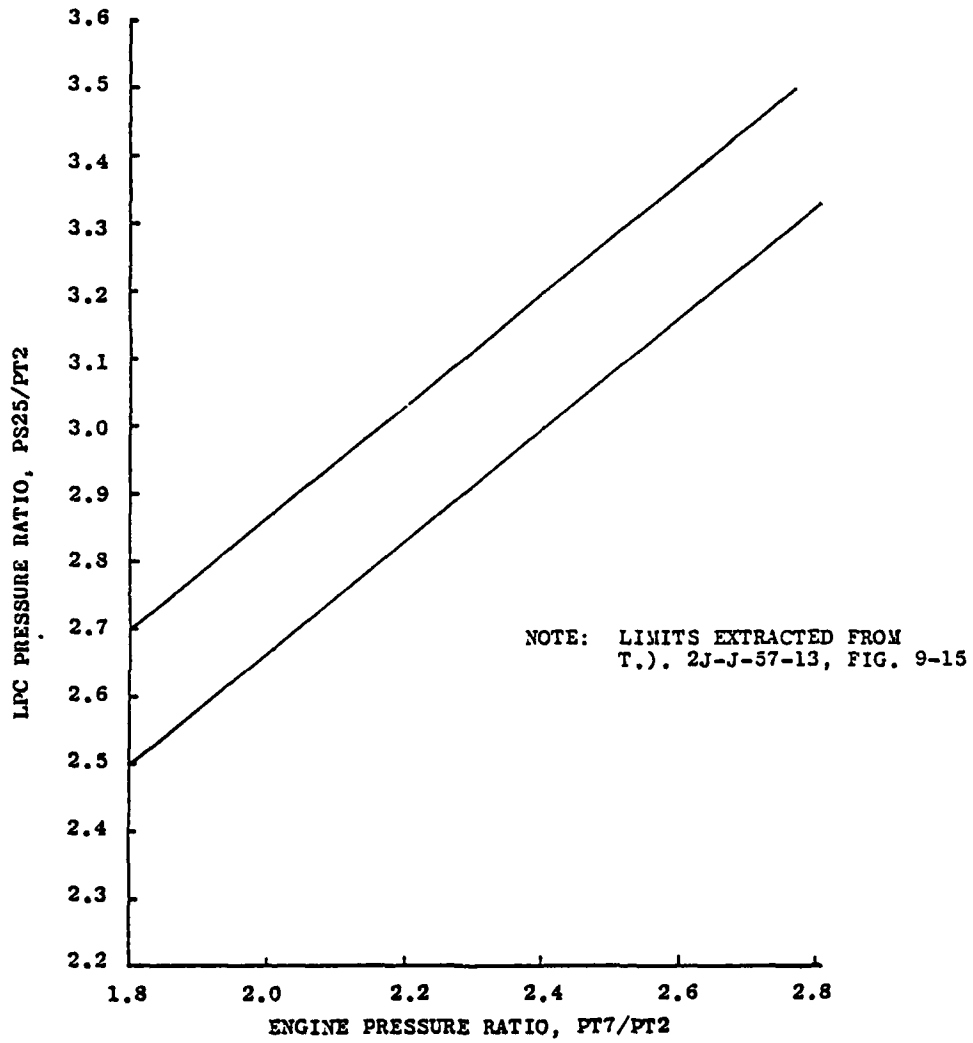


FIG..III-4. LPC PRESSURE RATIO AS A FUNCTION OF ENGINE PRESSURE RATIO AT SEA-LEVEL-STATIC CONDITIONS

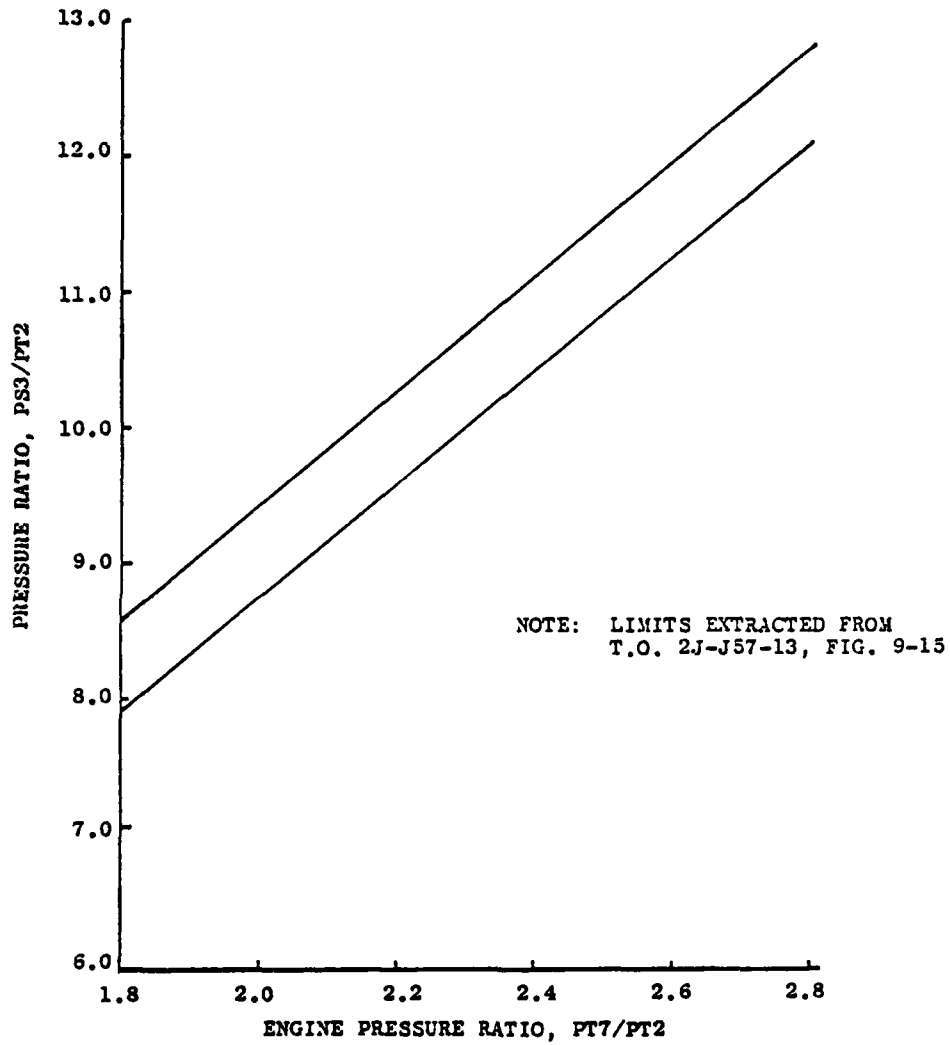


FIG. III-5. PRESSURE RATIO AS A FUNCTION OF ENGINE PRESSURE RATIO AT SEA-LEVEL-STATIC CONDITIONS.

APPENDIX IV  
(Refer to T.O. 2J-J57-13 for Official Limits)

ENGINE OPERATIONAL LIMITS (1)

<u>DESCRIPTION</u>	<u>PARAMETER</u>	<u>LIMITS (2)</u>
Fuel Pressure at Inlet to Engine	PFO	34.5 kPag (5 psig) - Minimum 344.7 kPag (50 psig) - Maximum
Main Oil Pump Discharge Pressure	MOP	241.3 kPag (35 psid) - Minimum at Idle 310.3 (45) $\pm$ 34.5 kPag (5) psid - Minimum at Military
Main Oil Breather Pressure	PMB	13.55 kPa (4 in. Hg) - Maximum Steady-State 37.25 kPa (11 in. Hg) - Maximum Transient
Main Oil Temperature	MOT	394.3 $^{\circ}$ K (250 $^{\circ}$ F) - Maximum Steady-State 405.4 $^{\circ}$ K (270 $^{\circ}$ F) - Maximum Transient
Start Fuel Flow Rate	WFE	1259.98 g/sec (1000) lbm/hr - Maximum
Low Rotor Speed	NL	6460 rpm - Maximum
Low Pressure Compressor Bleed Control Limits		See Fig. IV-1
High Rotor Speed	NH	9925 rpm - Maximum
High Rotor Speed Idle Trim Limits	NH Idle Limit	See Fig. IV-2
Turbine Cooling Air Pressure	PCP	See Fig. IV-3
Exhaust Gas Temperature	T5H	723.15 $^{\circ}$ K (842 $^{\circ}$ F) - Maximum Starting 883.15 $^{\circ}$ K (1130 $^{\circ}$ F) - Maximum Steady-State 910.93 $^{\circ}$ K (1180 $^{\circ}$ F) - Maximum Transient
Exhaust Gas Temperature Individual Probe Limit	T5A01 thru 04	922.04 $^{\circ}$ K (1200 $^{\circ}$ F) - Maximum
Exhaust Gas Temperature Spread (Max-Min)	SPREAD	83 $^{\circ}$ K (150 $^{\circ}$ F) - Maximum *

ENGINE OPERATIONAL LIMITS (1)  
(continued)

<u>DESCRIPTION</u>	<u>PARAMETER</u>	<u>LIMITS (2)</u>
Exhaust Gas Temperature Starting	TT7	722.04°K (840°F) - Maximum Steady-State
Oil Temperature Heat Exchanger Operating Limits	TOCO	366.5 (200) ± 5.6°K (10°F)
Inlet Case Vibration	VIC	5.0 Mils Peak-to-Peak - Maximum
Diffuser Case Vibration	vdc	4.5 Mils Peak-to-Peak - Maximum
Turbine Exhaust Case Vibration	VTC	4.5 Mils Peak-to-Peak - Maximum
Accessory Drive Case Vibration	VAD	7.0 Mils Peak-to-Peak - Maximum
Oil Consumption		.526 ml/sec (4 Pints/Hr) - Maximum
Accessory Fuel Drain Line Leakage	P&D Valve	10 cc/Min - Maximum
	Fuel Cent.	20 cc/Min - Maximum
	Fuel Pump	10 cc/Min - Maximum

- NOTES: (1) Limits extracted from T.O. 2J-J57-13, Section IX.  
(2) Limits are steady-state unless otherwise noted.

NOTE: LIMITS EXTRACTED FROM  
T.O. 2J-J57-13, FIG. 9-5

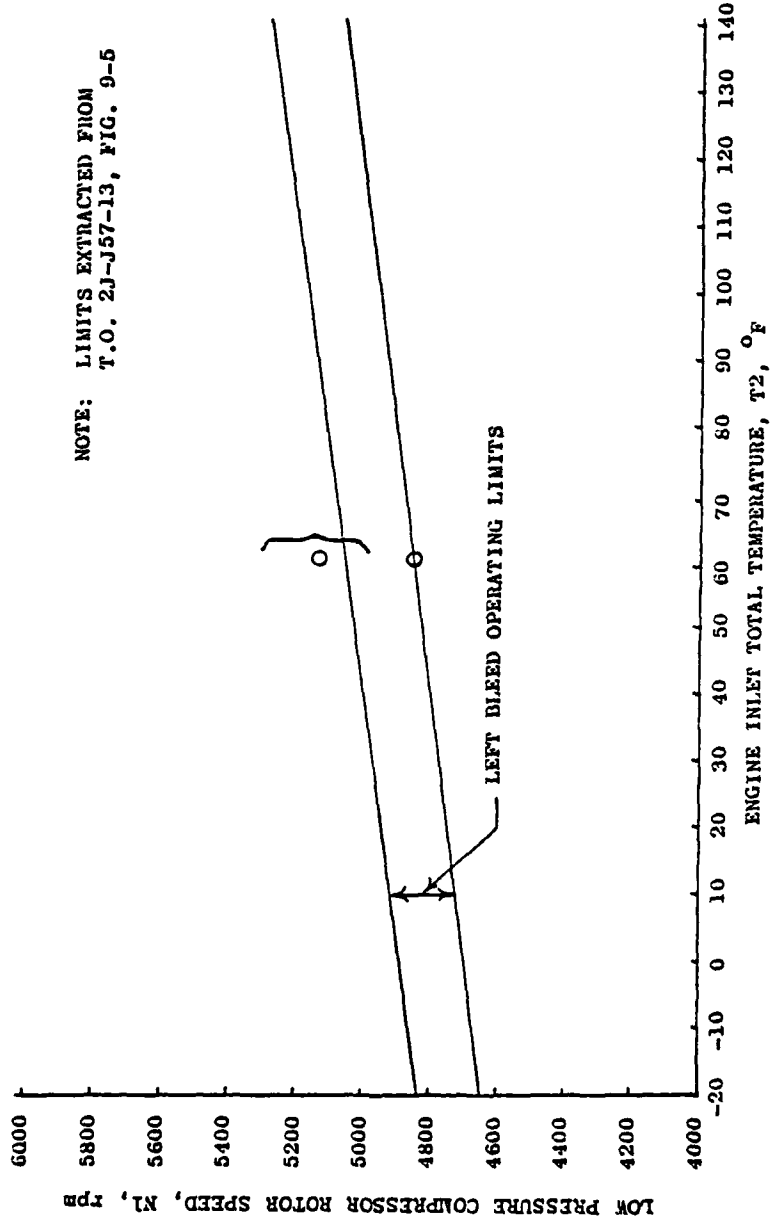


FIG. IV-1. COMPRESSOR BLEED SYSTEM PERMISSIBLE VARIATION OF N1 OPERATING SPEEDS.

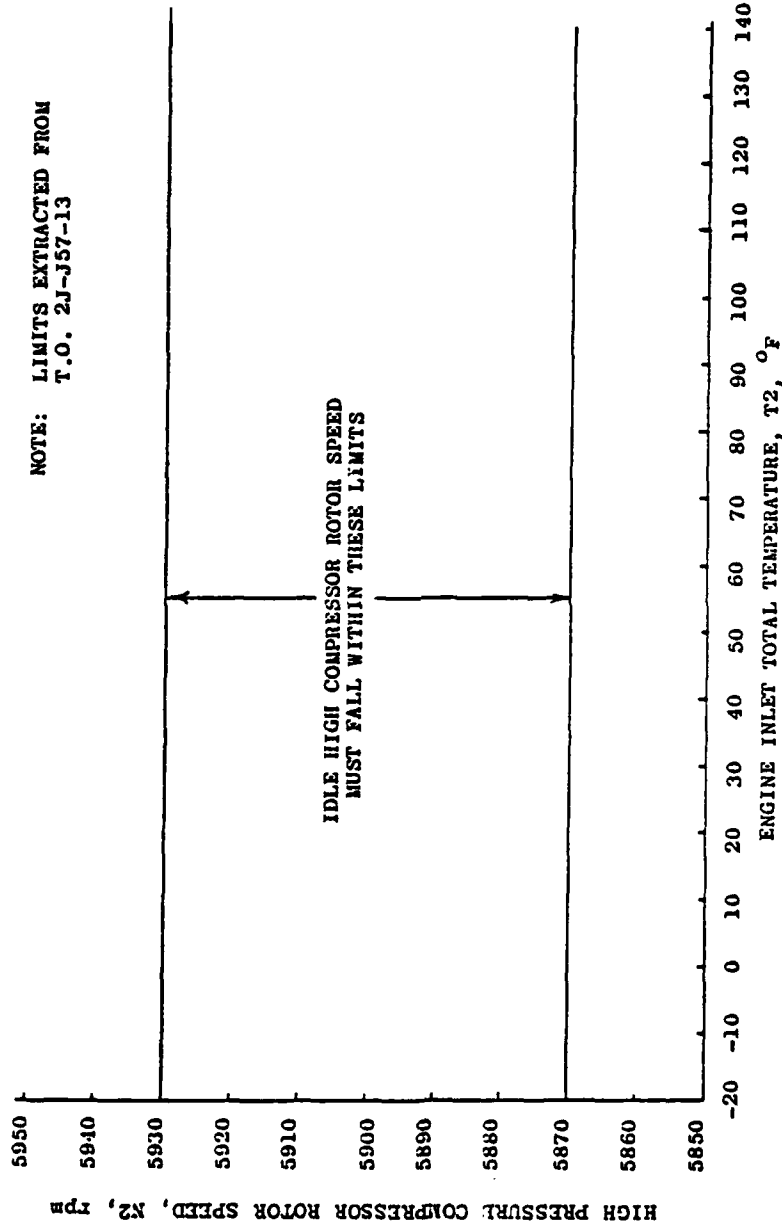


FIG. IV-2. IDLE HIGH COMPRESSOR TRIM LIMITS.

NOTE: LIMITS EXTRACTED FROM  
T.O. 2J-J57-13, FIG. 9-11

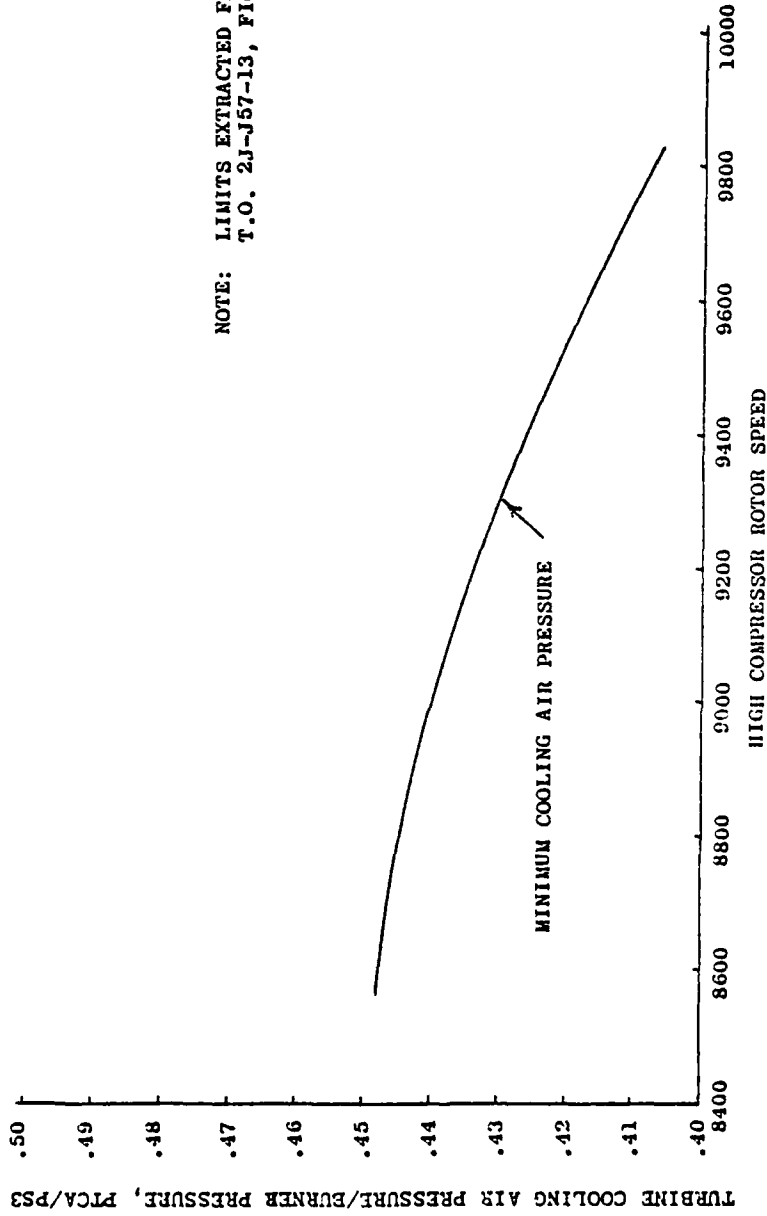


FIG. IV-3. MINIMUM TURBINE COOLING AIR PRESSURE REQUIREMENTS.

## APPENDIX V

## Calculation of Kinematic Viscosity Constants

Each test participant must calculate their own fuel viscosity-temperature characteristics. The method for calculating the constants A and B in the viscosity equation is outlined in part XI.4 of the attached ASTM D341, providing values of viscosity used in the derivation are less than 2.0 cSt. Two experimental points yield two equations with two unknowns that can be solved for A and B. A comparison of the NASA supplied constants and the NRCC constants are shown in Figure IV.1. While differing values of viscosity will not affect the accuracy of turbine flow meters in the linear high-flow flow range, a potential inaccuracy exists in the low flow range.

## ATTACHMENT FOR APPENDIX V

\*

## XI. MATHEMATICAL RELATIONSHIPS

X1.1 The charts were derived<sup>5</sup> with computer assistance to provide linearity over a greater range on the basis of the most reliable of modern data. The general relationship is:

$$\log \log Z = A - B \log T \quad (1)$$

where:

Z	=	( $\nu + 0.7 + C - D + E - F + G - H$ )
log	=	logarithm to base 10
$\nu$	=	kinematic viscosity, cST (or mm <sup>2</sup> /s)
T	=	temperature, K or °R
A and B	=	constants
C	=	$\exp(-1.14883 - 2.65868 \nu)$
D	=	$\exp(-0.0038138 - 12.5645 \nu)$
E	=	$\exp(5.46491 - 37.6289 \nu)$
F	=	$\exp(13.0458 - 74.6851 \nu)$
G	=	$\exp(37.4619 - 192.643 \nu)$
H	=	$\exp(80.4945 - 400.468 \nu)$

X1.1.1 Terms C through H are exponentials on the natural base e since this simplifies computer programming. Equation 1 uses logarithms to the base 10 for general convenience when used in short form.

X1.1.2 The limits of applicability are listed below:

Z = ( $\nu + 0.7$ )	$2 \times 10^7$ to 2.00 cSt
Z = ( $\nu + 0.7 + C$ )	$2 \times 10^7$ to 1.65 cSt
Z = ( $\nu + 0.7 + C - D$ )	$2 \times 10^7$ to 0.90 cSt
Z = ( $\nu + 0.7 + C - D + E$ )	$2 \times 10^7$ to 0.30 cSt
Z = ( $\nu + 0.7 + C - D + E - F + G$ )	$2 \times 10^7$ to 0.24 cSt
Z = ( $\nu + 0.7 + C - D + E - F + G - H$ )	$2 \times 10^7$ to 0.21 cSt

X1.2 It is obvious that Eq. 1 in the simplified form:  $\log \log (\nu + 0.7) = A - B \log T$  will permit kinematic viscosity calculations for a given fluid in the majority of instances required. The constants A and B can be evaluated for a fluid from two data points. Kinematic viscosities or temperatures for other points can then be readily calculated.

X1.3 Older literature refers to a value called the ASTM Slope. It should be noted that this value is not the value of B given in Eq. 1. The ASTM Slope was originally obtained by physically measuring the slope of the kinematic viscosity-temperature data plotted on the older charts given in Method D 341 - 43. The kinematic viscosity and temperature scales were not made to the same ratios in Method D 341 - 43. The improved charts given here utilize even different scale ratios for dimensional convenience and a different constant (0.7) from the older charts; consequently, the original ASTM Slope is not numerically equivalent to B in Eq. 1 from any of the new charts, nor directly convertible from Eq. 1.

X1.4 The complete design equation for the chart as given in X1.1 is not useful for inter-calculations of kinematic viscosity and temperature over the full chart kinematic viscosity range. More convenient equations<sup>6</sup> which agree closely with the chart scale are given below. These are necessary when calculations involve kinematic viscosities smaller than 2.0 cSt.

$$\log \log Z = A - B \log T \quad (2)$$

$$Z = + 0.7 + \exp (-1.47 - 1.84 v - 0.51 v^2) \quad (3)$$

$$v = Z - 0.7 - \exp (-0.7487 - 3.295 Z - 0.7 + 0.6119 Z - 0.7^2 - 0.3193 Z - 0.7^3) \quad (4)$$

The symbols have the same meaning as given previously.

X1.4.1 Inserting Eq. 3 into Eq. 2 will permit solving for the constants A and B for a fluid in which some of the experimental kinematic viscosity data fall below 2.0 cSt. This form can also be used to calculate the temperature associated with a desired kinematic viscosity.

X1.4.2 Conversely, the kinematic viscosity associated with a stated temperature can be found from the equation determined as in X1.4.1 by solving for Z in the substituted Eq. 2, and then subsequently deriving the kinematic viscosity from the value of Z by the use Eq. 4.

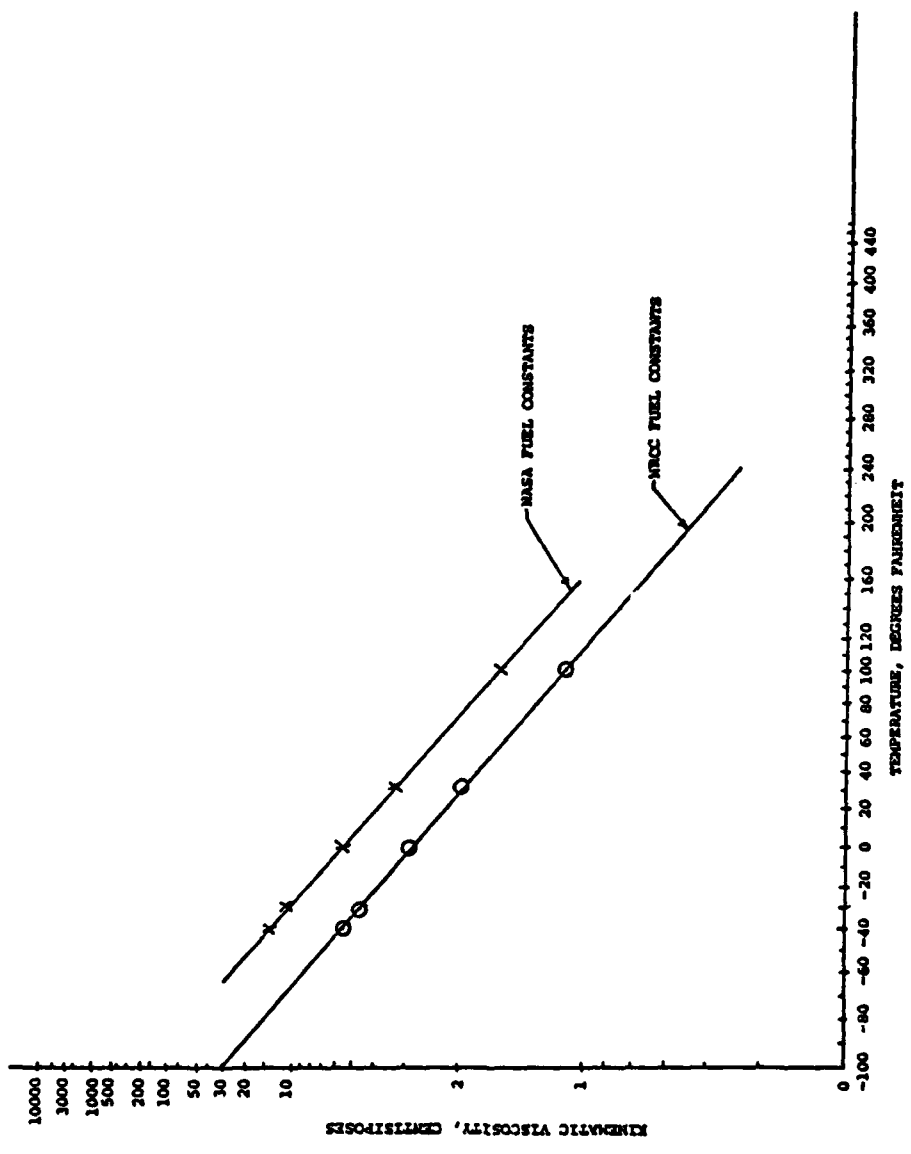
---

<sup>5</sup> Wright, W. A., An Improved Viscosity-Temperature Chart for Hydrocarbons. Journal of Materials. Vol. 4. No. 1. 1969, pp. 19-27.

<sup>6</sup> Manning, R. E., "Computational Aids for Kinematic Viscosity Conversions from 100 and 210°F to 40 and 100°C." Journal of Testing and Evaluation. JTEVA, Vol. 2. No. 6. November 1974.

## X2. OIL BLENDING CALCULATIONS

X2.1 Predicting the volume fractions of two given oils when blending to meet a specified kinematic viscosity at a given temperature is a common problem. A number of blending calculation techniques have been used. The Wright method described here is preferred since it automatically allows for the effects of oil type, molecular weight and viscosity index of component oils. This results in greater accuracy, particularly where component oil kinematic viscosities or types differ significantly.



**SELECTIVE BIBLIOGRAPHY**

This bibliography with abstracts has been prepared to support AGARD Lecture Series No. 169 by the Scientific and Technical Information Division of the U.S. National Aeronautics and Space Administration, Washington, D.C., in consultation with the Lecture Series Director, Dr. James G. Mitchell, Microcraft, Inc., Tullahoma, Tennessee.

UTTL: Compressor blade flutter - An understanding based on wind tunnel tests  
 AUTH: A/SZECHENYI, E.; B/CAFARELLI, I. PAA: B/(ONERA, Châtillon-sous-Bagneux, France) Revue Française de Mécanique (ISSN 0373-6601), no. 1, 1989, p. 73-87. In French.

ABS: The development of modern turbojet engines is tending increasingly toward the use of inlet fans having blades with sharp leading edges and relatively low natural frequencies of vibration. These characteristics increase the propensity of blade flutter. Tests on actual compressors have shown that a variety of blade instabilities can exist. For instance, flutter can occur on one or more blades independent of the neighboring blades of each, or else flutter vibrations can affect all the blades of a rotor which then vibrate according to rotor modes. This paper attempts to give some understanding of the physical causes of these different forms of flutter. The discussion is based on experimental results obtained in a straight cascade wind tunnel.  
 89/00/00 89A49022

UTTL: The investigation of jet engine starting  
 AUTH: A/WANG, HONGMIN PAA: A/(Beijing University of Aeronautics and Astronautics, People's Republic of China) Journal of Propulsion Technology (ISSN 1001-4055), June 1989, p. 70-74. In Chinese, with abstract in English.

ABS: The process of starting a jet engine requires that the engine rotates up to idle reliably and satisfactorily. The starting performance is modified based on the test of a flight evaluation schedule of a sample engine. The measurement and the data acquisition for a small single-spool engine are conducted on a sea-level test bench first. It is shown that, as main fuel is ignited, flame with temperature above 1250 C occurs at blade tips, while the average exhaust gas temperature is 400 to about 500 C. The mechanism and the criteria for overheating turbine blades during starting are presented in this paper. By using heat releasing ratio as the criteria to measure the overheating, the effects of FAR, fuel droplet size, fuel evaporation constant, and air density on it are discussed.  
 89/06/00 89A46025

UTTL: Investigation on thrust measurement of turbojet engine in altitude simulation facility  
 AUTH: A/ZHU, QING; B/TANG, SHIFU PAA: B/(31st Research Institute, People's Republic of China) Journal of Propulsion Technology (ISSN 1001-4055), April 1989, p. 57-61. 76. In Chinese, with abstract in English.

ABS: At present, the thrust of turbojet engines is flight is measured using simulation tests in an altitude chamber. The technology involved in the simulation and measurement, the facility, and the measurement results are discussed here in the context of an actual example. Corrections of

thrust measurements and measurement accuracy are addressed.  
 89/04/00 89A41126

UTTL: Measurements of mean-flow and turbulence characteristics in a turbojet exhaust using a laser velocimeter  
 AUTH: A/SCHAEFER, HANS J. PAA: A/(Saint-Louis, Institut Franco-Allemand de Recherches, France) IN: Symposium on Turbulence, 11th, Rolla, MO, Oct. 17-19, 1988, Preprints (AB9-33402, 13-34), Rolla, MO, University of Missouri-Rolla, 1988, p. A13-1 to A13-9.

ABS: Mean-flow and turbulence characteristics have been measured in a high-temperature axisymmetric jet exhausting from an aero-engine and the effects of exit Mach number and temperature on the jet flow field were studied. A laser Doppler velocimeter was used to map the flow characteristics over a range of Mach numbers from 0.46 to 0.84. Radial distributions of the mean axial velocity and the rms of the corresponding fluctuations were obtained at different axial stations in the flow. The various distributions are found to collapse when plotted in appropriate coordinates and the collapsed data can be approximated by a universal profile. These experimental findings are in good agreement with previous measurements in isothermal jets.  
 88/00/00 89A33410

UTTL: The contribution of wind tunnel tests to the understanding of compressor blade flutter  
 AUTH: A/SZECHENYI, E.; B/CAFARELLI, I. PAA: B/(ONERA, Châtillon-sous-Bagneux, France) (SFM, Journées d'Etude, Paris, France, Oct. 12, 13, 1988) ONERA, TP, no. 1988-144, 1988, 27 p. In French.

ABS: Experimental results were obtained in a straight cascade wind tunnel in order to study the physical causes of various types of flutter experienced by turbojet compressor blades. It is found that flutter is influenced by both the coupling coefficients and the direct coefficients particularly for the case of adjacent blades, and that flutter is not exclusively an effect due to the cascade. It is noted that the effect of interblade coupling depends largely on the blade frequency tuning.  
 RPT#: ONERA, TP NO. 1988-144 88/00/00 89A31805

UTTL: Investigation of aeroacoustic mechanisms by remote thermal imaging  
 AUTH: A/WITTEN, ALAN J.; B/COURVILLE, GEORGE E. PAA: B/(Oak Ridge National Laboratory, TN) IN: Thermal Infrared Sensing for Diagnostics and Control (Thermosense X); Proceedings of the Meeting, Orlando, FL, Apr. 5-8, 1988 (AB9-29508 11-38). Bellingham, WA, Society of Photo-Optical Instrumentation Engineers, 1988, p. 207-214. The thermal structure of the exhaust gas from an aircraft turbojet engine is investigated by means of IR

thermography, in an effort to identify the mechanism producing subaudible acoustic emission observed near engine diagnostic-test facilities (hush houses). The various sources of engine noise are reviewed; the structure of the hush house is characterized; theoretical models of hot turbulent jets are discussed; and images obtained with an IR camera operating at 8-14 microns, equipped with a 45-deg wide-angle lens, and mounted 20-40 ft from the engine are presented and analyzed. Two distinct flow regions are identified: (1) a highly turbulent region at some distance downstream and (2) a near-source laminar region in which the growth of the self-excited instability wave and the transition to turbulence are suppressed by the emission of low-frequency acoustic Cerenkov radiation (as predicted by theory). 88/00/00 89A29511

UTTL: Parallel implementation of real-time control programs

AUTH: A/SHAFFER, PHILLIP L. PAA: A/IGE Control Systems Laboratory, Schenectady, NY IN: IEEE Conference on Decision and Control, 27th, Austin, TX, Dec. 7-9, 1988, Proceedings, Volume 2 (A89-28491 11-63), New York, Institute of Electrical and Electronics Engineers, Inc., 1988, p. 1449-1454.

ABS: Two turbojet engine control programs were analyzed for potential parallelism. Both were subjected to global, hierarchical, large-grain data-flow analysis, using internally developed dataflow analysis tools. Execution times of constituent code segments or procedures were determined, either by graph analysis for maximum execution time, or by accurate measurement. Data dependencies were combined with execution times to determine maximum possible speedup, using the length of the critical path as the shortest possible execution time. The first control program was divided into 199 code segments, and had a maximum speedup of 7.2. The second program consisted of 64 basic control procedures; this program has a maximum possible speedup of 5.3. The amount of data passed between the dependent tasks was small, averaging 1.3 values per dependency. Static, nonpreemptive schedules have been determined using a heuristic algorithm based on the critical path method. For the first control program this allowed a speedup of 6.6 using 7 processors; for the second control program, the maximum possible speedup of 5.3 was achieved using 6 processors. The first program is being implemented in parallel on a shared-memory bus-based multiprocessor. 88/00/00 89A28621

UTTL: The influence on total performance for varying the stator setting angle of multi-stage axial compressor

AUTH: A/KAKEHI, YOH Japan Society for Aeronautical and Space Sciences, Journal (ISSN 0021-4663), vol. 36, no. 418, 1988, p. 505-511. In Japanese, with abstract in English.

ABS: In the development phase of an aircraft gas turbine, the required performances of the gas turbine components are decided after general consideration of the engine total performance. For accomplishing the required performance, the tedious and expensive works of design for modification, production and tests were laboriously repeated. This paper introduces the practical and useful method describing the relation between component performances of the compressor and the combination of the stator setting angle analyzing by statistical methods based on the experimental data. 88/00/00 89A22627

UTTL: Flow measurements in rotating stall in a gas turbine engine compressor

AUTH: A/BEST, R. C.; B/LAFLAMME, J. G. C.; C/MOFFATT, W. C. PAA: C/(Royal Military College of Canada, Kingston) ASME, Gas Turbine and Aeroengine Congress and Exposition, Amsterdam, Netherlands, June 6-9, 1988, 7 p. DND-supported research.

ABS: Hot sensor anemometry has been used to make detailed flow measurements on the first four stages of a 10-stage compressor operating as part of a turbojet engine mounted on a test stand. Results for a number of axial and tangential locations show clear evidence of rotating stall in the front stages during the part-speed operation of the engine. The stall cell configuration and rotating speed as well as details of flow speed and angle at hub, mid and tip radii are discussed. It is concluded that, although rotating stall has its origins in flow instability, it is a highly reproducible phenomenon. ASME PAPER 88-GT-219 88/06/00 88A54304

UTTL: Investigation of measuring and testing techniques for evaluating stable operating margin of twin-spool turbojet engine

AUTH: A/WU, YUEGENG; B/YUN, QISHENG PAA: B/(Liyang Machinery Co., People's Republic of China) Acta Aeronautica et Astronautica Sinica (ISSN 1000-6893), vol. 9, June 1988, p. B248-B256. In Chinese, with abstract in English. ABS: In this paper an experimental technique for forced surge based on water injection into the main combustion chamber is introduced, and a reliable method for testing the actual stable operating margin of the compressor system in the twin-spool turbojet engine is demonstrated. A simple and practical data-treatment method for evaluating the stable operating margin of compressors is recommended. 88/06/00 88A49923

UTTL: 'Flight effect' analysis of turbojet and turbofan nozzle models in the CEPR 19 anechoic wind tunnel at the CEP

AUTH: A/FAVOT, C.; B/SELY, D. PAA: B/(Centre d'Essais de Propulseurs de Saclay, Orsay, France) (Societe Francaise

d'Acoustique, Association Aeronautique et Astronautique de France, and CNRS, Colloque d'Acoustique Aeronautique et Navale, 10th, Marseille, France, Nov. 19-21, 1986) Revue d'Acoustique (ISSN 0557-7713), vol. 20, no. 82, 1987, p. 27-31. In French.

Measurements have been obtained at the Centre d'Essais des Propulseurs CEPRA 19 anechoic wind tunnel using turbojet and turbofan nozzle models in order to study the effect of flight velocity on jet noise. The present results are found to be in good general agreement with both theoretical results and flight test data. It is suggested that noise spectra anomalies noted at frequencies higher than 40 kHz may reflect the passage of sound waves across the mixing zone and/or the turbulent boundary layer which develops along the nozzle fuel line. 87/00/00 88A43304

ABS:

UTTL: A scheme of condition monitoring and main faults  
 AUTH: A/ZHOU, ZONGCAI; B/LI, YINGHONG; C/WANG, ZENGYI PAA: C/(Air Force College of Engineering, People's Republic of China) Journal of Aerospace Power, vol. 2, July 1987, p. 267-269, 287. In Chinese, with abstract in English.

ABS: In order to enhance the ability to diagnose faults and improve maintenance, a condition-monitoring and main-faults diagnosing system for a turbojet engine is developed. The whole system is divided into two subsystems: (1) engine operation monitoring and (2) ground-computer data processing. Subsystem (1) is used for analyzing engine performance and diagnosing some main faults in the engine; i.e., engine-surge, exceeding drop rpm, auto-flameout, and so on. In addition, it can record the parameters at takeoff or before and after a fault occurs. When faults take place in the engine, it can also give pilots warning. Subsystem (2) is used for analyzing the reasons for faults and estimating engine performance. 87/07/00 88A24368

UTTL: Uncertainty of in-flight thrust determination  
 AUTH: A/ABERNETHY, ROBERT B.; B/ADAMS, GARY R.; C/STEURER, JOHN W.; D/ASCOUGH, JOHN C.; E/BAER-RIEDHART, JENNIFER L.; F/BALKCOM, GEORGE H.; G/BIESIADNY, THOMAS PAA: A/(Pratt and Whitney, East Hartford, CT); B/(USAF, Wright-Patterson AFB, OH); C/(McDonnell Douglas Co., Saint Louis, MO); D/(Royal Aircraft Establishment, Farnborough, England); E/(NASA, Flight Research Center, Edwards, CA); F/(General Dynamics Corp., Saint Louis, MO); G/(NASA, Lewis Research Center, Cleveland, OH) CORP.: Pratt and Whitney Aircraft, East Hartford, CT.; McDonnell-Douglas Corp., Saint Louis, MO.; Royal Aircraft Establishment, Farnborough (England); National Aeronautics and Space Administration, Flight Research Center, Edwards, CA.; General Dynamics Corp., Saint Louis, MO.; National Aeronautics and Space Administration, Lewis Research Center, Cleveland, OH.

(SAE Aerospace Information Report, SAE AIR 1678, Aug. 1985) IN: In-flight thrust determination and uncertainty (AB8-15226 04-05), Warrendale, PA, Society of Automotive Engineers, Inc., 1986, p. 243-338.

Methods for estimating the measurement error or uncertainty of in-flight thrust determination in aircraft employing conventional turbofan/turbojet engines are reviewed. While the term 'in-flight thrust determination' is used synonymously with 'in-flight thrust measurement', in-flight thrust is not directly measured but is determined or calculated using mathematical modeling relationships between in-flight thrust and various direct measurements of physical quantities. The in-flight thrust determination process incorporates both ground testing and flight testing. The present text is divided into the following categories: measurement uncertainty methodology and in-flight thrust measurement processes. RPT#: SAE AIR 1678 86/00/00 88A15228

UTTL: An experimental investigation of forced surge by water injection in a twin-spool turbojet engine  
 AUTH: A/ZHANG, JU; B/WU, YUEGENG; C/YUN, QISHENG PAA: C/(Li Yang Machinery Co., People's Republic of China) Journal of Aerospace Power, vol. 2, April 1987, p. 170-172, 191. In Chinese, with abstract in English.

ABS: An experimental investigation of forced surge by water injection in a twin-spool turbojet engine has been performed on a ground thrust bed. It is demonstrated that water injection into the main combustion chamber, coupled with the flow area scale-down of both turbine nozzle and jet nozzle, is satisfactory for the test. An optimum scale-down percentage of both areas was found from a large number of tests. During such a combined forced-surge process, the engine operating condition can approach the surging boundary accurately along the line of the corrected constant rotation speed. Hence, the exact stable operating margin as well as stable operating boundary for the compressor can be obtained. 87/04/00 87A49993

UTTL: Thermal effects on transient process of a turbojet engine  
 AUTH: A/CHEN, DAGUANG; B/PAN, YONGQUAN PAA: B/(Beijing Institute of Aeronautics and Astronautics, People's Republic of China) Journal of Aerospace Power, vol. 2, Jan. 1987, p. 85, 86, 96. In Chinese, with abstract in English.

ABS: A single-shaft turbojet engine has been tested for cold and hot transient processes. The comparative test results show that thermal effects have significant influence on the acceleration time, the changing rate of aerothermodynamic parameters with engine speed, etc. The results also demonstrate that thermal effects must be taken into account in order to establish an accurate mathematical model for the transient process of turbine

engines. 87/01/00 87A37850

UTTL: Methods for monitoring and maintaining military turbojets

AUTH: A/DARGEIN, J. PAA: A/(SNECMA, Evry, France) (Societe Francaise des Mecaniciens, Journee d'Etudes sur les Machines Tournantes, Paris, France, June 10, 1986) Revue Francaise de Mecanique (ISSN 0373-6601), no. 4, 1986, p. 215-217. In French.

ABS: The evolution of military engine monitoring and maintenance practices is traced over the past quarter century. The engines normally experience a series of transitory states due to the nature of military missions, which exacerbate stresses on engines. Engine maintenance and repair is the province of the ground personnel. The job was, for awhile, partly ameliorated by limiting the allowable engine flight hours, after which the engines were pulled. Cost-savings have been realized with modular engine components, so that individual components have programmed lifetimes. Further economies are being gained by identifying inspection techniques which allow assessments of engine parts which are not replaced or repaired until predefined deterioration thresholds are breached. 86/00/00 87A30843

UTTL: Transient operating line indicator and its application

AUTH: A/WANG, ZONGYUAN; B/FANG, JINYAN PAA: B/(Northwestern Polytechnical University, Xian, People's Republic of China) Journal of Aerospace Power, vol. 1, July 1986, p. 41-46. In Chinese, with abstract in English.

ABS: A special instrument is presented for monitoring the transient process in a turbojet engine, which is called a transient operating line indicator. The instrument consists of analog computing circuits. It demonstrates the real-time flow rate and the pressure ratio of the engine, which are calculated from the total pressure and the static pressure at the inlet and the total pressure at the exit of the compressor. By means of this instrument the transient operating line of the engine can be plotted with an x-y recorder. The description, the circuits, and the performance of this instrument are given in this paper. The various transient processes of turbojet engine, such as acceleration, deceleration and surge, have been studied with this instrument. 86/07/00 87A25417

UTTL: Digital simulation of the gas turbine engine performance

AUTH: A/CHAO, YEI-CHIN; B/HO, REN-CHUN PAA: B/(National Cheng Kung University, Tainan, Republic of China) Chinese Society of Mechanical Engineers, Journal (ISSN 0257-9731), vol. 7, Oct. 1986, p. 319-328.

ABS: Digital simulation of gas-turbine engine performance is a

means to estimate all the engine performance parameters at the design point to a more accurate extent. This is an easy approach to simulate the complex gas-turbine engine, and it can also be regarded as a foundation on which the complicated off-design-point analysis is based. The present work is based on numerical analysis by digital computer, assuming a quasi-one-dimensional flow field and the gas mixture obtained from the combustion of air and fuel (CH<sub>4</sub>) as the working fluid. The thermodynamic properties of this gas mixture are assumed to be continuous functions of temperature and fuel-air ratio. Simulation of the turbojet engine, separated-flow turbofan engine, mixed-flow turbofan engine, and turbojet engine and turbofan engine with afterburner is carried out. The application of the computer program developed to determine the important performance parameters (compression ratio, bypass ratio, etc.) of the turbofan engine, and the reason for the improved performance of a turbofan engine with a constant area mixer, are explained by practical examples. 86/10/00 87A23731

UTTL: On the improvement of an expendable turbojet engine flight envelope

AUTH: A/LEVIN, G.; B/ARAD, S.; C/LEVY, A. PAA: C/(Bet Shemesh Engines, Ltd., Israel) IN: Israel Annual Conference on Aviation and Astronautics, 27th, Haifa, Israel, February 27, 28, 1985. Collection of Papers (A87-13635 03-01). Haifa, Israel, Technion - Israel Institute of Technology, 1986, p. 118-124.

ABS: The paper describes how it was found possible to change the maximum allowed flight speed ( $M = 0.9$ ) of the SOREK 4 expendable turbojet to a higher value ( $M = 1.1$ ) at sea level, after an analysis of burst test results of the first compressor stage, its detailed stress calculation, and data about its material. The decision to augment the maximum allowed flight speed has been made possible by a relatively inexpensive procedure as compared with the conventional method of altitude bench testing. 86/00/00 87A13647

UTTL: An overview of USAF engine diagnostic systems

AUTH: A/THORNTON, S. J. PAA: A/(USAF, Aeronautical Systems Div., Wright-Patterson AFB, OH) AIAA, ASME, SAE, and ASEE, Joint Propulsion Conference, 22nd, Huntsville, AL, June 16-18, 1986, 11 p.

ABS: A development history is presented for the U.S. Air Force's engine diagnostic systems, with attention to the automation of diagnostics first introduced in the F100 turbofan engine's Events History Recorder. Other efforts have involved the T-38 trainer's J85 turbojet Engine Health Monitoring System, the A-10 ground support aircraft's TF34 turbofan Turbine Engine Monitoring System, and the F-15 Fighter's F100 turbofan Engine Diagnostics System. State-of-the-art systems are currently installed

in the KC-135, B-1B, and F-16 aircraft. The Integrated Turbine Engine Monitoring System and Joint Advanced Fighter Engine Diagnostic System (for the Advanced Tactical Aircraft), which are undergoing development are also discussed.

RPT#: AIAA PAPER 86-1679 86/06/00 86A42790

UTTL: Experimental investigation on frequency response of a turbojet engine to turbulence-type dynamic distortion  
 AUTH: A/LIU, S.; B/CHEN, F.; C/LI, W.; D/WANG, Z.; E/CONG, M. PAA: E/Northern Polytechnical University, Xian, People's Republic of China) Acta Aeronautica et Astronautica Sinica, vol. 6, Oct. 1985, p. 484-488. In Chinese. With abstract in English.

ABS: The inlet and exit fluctuating pressure signals of a compressor prior to 'drift surge' are investigated by correlation and spectral analyses. It is found that the stochastic process of fluctuating pressure is no longer stationary near the inception of the 'drift surge'. The surge of the tested engine under the dynamic distortion is caused by rotating stall. The whole unsteady operating time for the engine to approach surging is about 5 seconds and the process is characterized by rotating stall cell spreading forward from the rear stage over the whole annular passage of the compressor. It is worth noticing that the tested engine is sensitive to pressure fluctuations with certain frequencies prior to the surge, but a strict conclusion needs further experimental investigation. 85/10/00 86A30740

UTTL: Thrust and drag: Its prediction and verification  
 AUTH: A/COVERT, E. E. PAA: A/(MIT, Cambridge, MA) New York, AIAA (Progress in Astronautics and Aeronautics, Volume 98), 1985, 358 p. No individual items are abstracted in this volume.

ABS: A survey and critical review of the state of the art in prediction and verification of thrust and drag of jet-propelled aircraft is presented. The subjects addressed include: thrust-drag accounting methodology, gas turbine engine performance determination, prediction and verification of aerodynamic drag, throttle-dependent forces, and precision and propagation of errors. A brief historic perspective on the estimation and prediction of drag and on the turbojet engine is also provided. 85/00/00 86A14161

UTTL: Determination of the thrust of a bypass engine under operating conditions

AUTH: A/KOZITSKII, A. D.; B/SHEPEL, V. T. Aviatsionnaia Tekhnika (ISSN 0579-2975), no. 2, 1985, p. 79-81. In Russian.

ABS: A method for determining the thrust of a bypass engine is proposed which uses as the initial data the rotor rpm and

fuel consumption, i.e., parameters that can be easily measured during the operation of the engine, rather than the full gas pressure behind the turbine. The method is simple to implement and sufficiently accurate. For a plus or minus 2-sigma variance, the maximum relative error of thrust determinations is plus or minus 1.7 percent; with a correction for the individual compressor output, the maximum relative error is reduced to plus or minus 1.2 percent. 85/00/00 86A12546

UTTL: Unsteady aerodynamic forces induced by aeroelastic vibrations of a turbojet engine in a nacelle  
 AUTH: A/DESTUYNDER, R.; B/ANGELINI, J. J. PAA: B/(ONERA, Chatillon-sous-Bagneux, France) (Groupe Sectoriel Franco-Sovietique - Aeronautique, Sous-groupe Aerodynamique, Acoustique Aeronautique et Structures, Reunion, 27th, Chatillon-sous-Bagneux, France, Mar. 11-15, 1985) ONERA, TP, no. 1985-56, 1985, 22 p. In French. The results of theoretical and experimental studies of the effects of a wing-mounted engine nacelle on unsteady aerodynamic forces are reported. Trials were run in a transonic wind tunnel using a rigidly mounted wing with and without the nacelle. The wing-nacelle aerodynamic interactions were not significant but the aerodynamic pitching oscillations of the nacelle alone were sufficient to induce flapping. A cylindrical lifting surface model for the oscillations of the nacelle is defined and shown to have good agreement with experimental data, as well as with predictions made using a method of doublets. The experimental data are matched if the effects of internal engine rotations are neglected.

RPT#: ONERA, TP NO. 1985-56 85/00/00 85A47302

UTTL: New functional requirement to aero-engine control system  
 AUTH: A/SUGIYAMA, S. Japan Society for Aeronautical and Space Sciences, Journal (ISSN 0021-4663), vol. 32, no. 371, 1984, p. 701-706. In Japanese.

ABS: Aircraft engine control is reviewed with respect to improvements of performance characteristics of turbojet engines and efficiency in operating airframe/engine system. The electronic supervisory control system, thrust management system, integration of flight and propulsion control system, thrust management system, integration of flight and propulsion control system, FADEC/F-14 system integration for improving operational safety, and the maintenance monitoring system are described. 84/00/00 85A41030

UTTL: Advances in aerospace propulsion; Proceedings of the Aerospace Congress and Exposition, Long Beach, CA, October 15-18, 1984 Congress and Exposition sponsored by the Society of Automotive Engineers, Warrendale, PA, Society

of hub of the blade whose amplitude probability density approximately follows a normal distribution. The distortion causes a drift-mode surge at 100 percent engine speed and at 90 percent when the first stage turbine nozzle area is 12 percent smaller. The inlet distortion generated by the screen produces a classical mode or deep mode surge. The degree of inlet distortion by the screen can change the surge mode, as can a decrease in the turbine nozzle area. The engine speed can affect the unstable behavior of the compressor. 84/06/00 85A12365

UTTL: Correlations of soot formation in turbojet engines and in laboratory flames  
 AUTH: A/GILL, R. J.; B/DLSON, D. B.; C/CALCOTE, H. F. PAA: C/AeroChem Research Laboratories, Inc., Princeton, NJ) American Society of Mechanical Engineers, International Gas Turbine Conference and Exhibit, 29th, Amsterdam, Netherlands, June 4-7, 1984, 8 p.

ABS: Attention is given to the correlation of smoke-related performance in both jet engine and research combustors with several fuel properties, which included percent hydrogen, percent aromatic, percent polycyclic aromatic, smoke point, and the threshold soot index. Smoke-related data encompassed smoke number, liner temperature rise, and radiation flux to the combustor wall. No single fuel property was generally useful in evaluating smoke-related performance, but it is demonstrated that fuel composition plays a dominant role in determining smoke-related engine parameters. It is recommended that fuels used for engine testing programs be chemically analyzed in greater detail.  
 RPT#: ASME PAPER 84-GT-108 84/06/00 84A46945

UTTL: Stress mapping of a low pressure compressor for an advanced turbojet engine  
 AUTH: A/BANKHEAD, H. R.; B/MEECE, C. E. PAA: A/(USAF, Aero Propulsion Laboratory, Wright-Patterson AFB, OH); B/(Pratt and Whitney Aircraft, West Palm Beach, FL) American Society of Mechanical Engineers, International Gas Turbine Conference and Exhibit, 29th, Amsterdam, Netherlands, June 4-7, 1984, 6 p.

ABS: Vibratory stress characteristics of the low pressure compressor in the Pratt & Whitney Aircraft PW120 turbojet engine recently have been evaluated during full-scale engine testing at the United States Air Force's Arnold Engineering Development Center. A description is presented of the approach used to evaluate the vibratory characteristics of the new three stage low pressure compressor. Results are presented showing the effects of simulated altitude conditions, inlet pressure distortion, and off-schedule variable vane operation. Strain gage data is compared to case-mounted light probe data, and the levels of system damping and mistuning are discussed. Predicted vibratory response is compared to test results showing the new compressor to be free of destructive

of Automotive Engineers, Inc. (SAE SP-594), 1984, 163 p.  
 For individual items see 85-39058 to 85-39071.  
 The contributions presented deal with the design and experimental evaluation of propfan, turboprop, turboshaft, and turbojet engine components and systems. The topics include the aerodynamic performance of engine inlets, internal flow passages, inter-nozzle region of a twin-jet nacelle, and wing-mounted turboprop configuration. Moreover, stability and control results for advanced turboprop aft-mount installations are included, as well as a discussion of technology application for added value of in-service support. Finally, consideration is given to reliability assessment for gas turbine engine components, to failure mode analysis of new products, and to repair procedures for commercial aircraft jet nacelle composite structures.  
 RPT# SAE SP-594 84/00/00 85A39057

UTTL: Data acquisition and processing for steady-state inlet pressure distortion at a turbojet engine face  
 AUTH: A/LU, B.; B/WU, Y.; C/ZHANG, N.; D/SUEN, Y.; E/MA, Y. Northwestern Polytechnical University, Journal, vol 2, Oct. 1984, p. 473-478. In Chinese, with abstract in English.

ABS: This paper describes the problem and technique for on-line real time processing of steady-state inlet pressure distortion parameters at a turbojet engine face using the data acquisition and processing system of the 622 computer. When testing steady-state pressure distortion of turbojet engine, about 400 parameters need to be acquired. In computation and processing, there are about 800 output parameters. All programs for testing and processing are programmed in assembly language. By on-line experimenting with an engine, it is proved that both the data acquisition accuracy and the results computed by this system can satisfy the requirements of engine testing. Thus, automatic data acquisition and processing for steady-state inlet pressure distortion of turbojet engine is achieved. 84/10/00 85A19286

UTTL: An experimental investigation on response of turbojet engine to the turbulence-type of dynamic inlet distortion  
 AUTH: A/CHEN, F.; B/LI, W.; C/WANG, Z.; D/CONG, M.; E/LU, B.; F/ZHENG, L. PAA: F/(Northwestern Polytechnical University, Xian, Shaanxi, People's Republic of China) Acta Aeronautica et Astronautica Sinica, vol 5, June 1984, p. 225-232. In Chinese, with abstract in English.  
 ABS: The response of a turbojet engine to turbulence-type dynamic inlet total pressure distortion is discussed. The distortion is generated by a blockage plate with 180 deg circumferential extent and 50 percent blockage ratio in the blade-tip and blade-hub region of the inlet section. Strong pressure fluctuation regions are set up at the tip

1983. 23 p. In German.  
During studies of turbojet engines in altitude-test chambers, the flight conditions have to be reproduced. A description is presented of the equipment employed in the altitude-test chamber of an institute in Stuttgart, West Germany. It was found that the capacity of the altitude-test chamber as established in the first half of the 1960s was not large enough for the testing of the low-pressure turbine of the engine PW 2037 and the entire engine RB 199. The altitude-test chamber was, therefore, rebuilt in 1981 and 1982, and its capacity was considerably enhanced. Attention is also given to a new control station, tests conducted with the PW 2037 low-pressure turbine, the testing of the engine RB 199, and recommendations for further improvements of the altitude-test chamber.

DGLR PAPER 83-099 83/10/00 84429663

UTTL: Finite-element mathematical model of a gas turbine engine in unsteady flow

A/SKVRISOV, I. A. TsAGI, Uchenye Zapiski (ISSN 0321-3429), vol. 13, no. 1, 1982, p. 21-29. In Russian.

The finite-element method is used to construct a mathematical model of a gas turbine engine operating in a one-dimensional unsteady flow. The basic modeling principles are examined using the example of a single-stage turbojet engine. Results obtained with the finite-element method are compared with results obtained by Gourev's difference method for a channel of variable cross section. Finite-element calculations of the unsteady gasdynamic process in an engine with a subsonic inlet channel are compared with experimental data. 82/00/00 83A37252

UTTL: Simulation of advanced engine lubrication and rotor dynamics systems - Rig design and fabrication

A/PEDUZZI, A. PAA: A/United Technologies Corp., Government Products Div., West Palm Beach, FL) AIAA, SAE, and ASME, Joint Propulsion Conference, 19th, Seattle, WA, June 27-29, 1983. 9 p.

Advanced technology dual rotor turbofan and turbojet engines will incorporate rotor support system features to increase rotor speed capability and engine thrust-to-weight ratio while reducing cost. These features may include straddle-mounted rotors, high strain energy low pressure rotors and counter-rotating shafts with a load-carrying intershaft bearing. A 'bladeless engine' rig incorporating the above features has been designed and fabricated, and test plans formulated. The rig will be utilized to evaluate counter rotating intershaft bearing lubrication and breather system operation, low leakage intershaft seals, and dynamic operation of counter-rotating rotors including identification of critical speed modes, shaft deflection and bearing load

82/00/00 84443318

RPT#: ASME PAPER 84-GT-99 84/06/00 84446939

UTTL: Direct measurement of in-flight thrust for aircraft engines

A/FODG, A. PAA: A/(Grumman Aerospace Corp., Calverton, NY) IN: Flight testing technology: A state-of-the-art review: Proceedings of the Thirteenth Annual Symposium, New York, NY, September 19-22, 1982 (A84-44451 21-01). Lancaster, CA, Society of Flight Test Engineers, 1982, p. 33-41.

A review of the accuracies attainable for in-flight engine thrust measurements is presented. The study was limited to turbojet/turbofan engines, with numerical analyses further constrained to the F-14A/TF30 engine. Attention was given to the ease of accessibility of separately podded and internal engines. An analytical model was defined for relating engine mount loads to the net thrust for the internal engine. The only available instruments judged suitable for in situ thrust assessment were resistance-type strain gages, provided compensations are made for temperature changes. Transient responses could be accounted for by numerical analyses or accelerometer data. Test measurements, in comparison with the available data base on the F-14A/TF30, showed that direct measurement is at least as or more accurate than conventional thrust determination techniques. 82/00/00 84444457

UTTL: A study of blockage errors

A/LIU, S.; B/HUANG, Z. Northwestern Polytechnical University, Journal, vol. 1, Oct. 1983, p. 191-199. In Chinese. With abstract in English.

It is shown that placing of probes in the flow passageways of turbojets, gas turbines, and their components during tests to measure aerodynamic parameters causes blockage of the passageways, distortion of the flow fields, and changes in operating conditions. A systematic theoretical analysis of the resulting blockage errors and relevant experimental results are presented. Geometric and aerodynamic blockage are considered. The different characteristics of blockage errors corresponding to different positions of the probe are examined. Experimental curves showing the variation of blockage errors with blockage ratios are given for the compressor, turbine, and exhaust nozzle of a turbojet engine. Some practical methods for reducing blockage errors are presented. 83/10/00 84443318

UTTL: The extension of the Stuttgart altitude-test chamber for an enlarged flow rate

A/BRAIG, W. PAA: A/(Stuttgart, Universitaet, Stuttgart, West Germany) Deutsche Gesellschaft fuer Luft- und Raumfahrt, Jahrestagung, Munich, West Germany, Oct. 17-19, 1983.

The extension of the Stuttgart altitude-test chamber for an enlarged flow rate is described. The chamber was originally designed for a flow rate of 100 kg/s. It is now possible to operate the chamber with a flow rate of 200 kg/s. The chamber is now capable of operating at a pressure ratio of 1.5 and a Mach number of 0.5. The chamber is now capable of operating at a pressure ratio of 1.5 and a Mach number of 0.5. The chamber is now capable of operating at a pressure ratio of 1.5 and a Mach number of 0.5.

82/00/00 84443318

sensitivity to rotor imbalance, as well as oil film damper operation. Pre-test calibrations of damper springrate and high and low rotor resonant frequencies were conducted. System endurance will be evaluated in a 150-hour cyclic endurance test.

RPT#: AIAA PAPER 83-1133 83/06/00 83A36238

ABS:

UTTL: Ground simulation of engine operation at altitude  
AUTH: A/REESE, B. A. PAA: A/(Arnold Engineering Development Center, Arnold Air Force Station, TN) IN: International Symposium on Air Breathing Engines, 6th, Paris, France, June 6-10, 1983, Symposium Papers (A83-35801 16-07). New York, American Institute of Aeronautics and Astronautics, 1983, p. 537-552.

ABS: A discussion is presented concerning the contributions obtainable through ground-simulated high altitude testing of turbojet and turbofan aircraft engine operation, with attention to such criteria for test program success as the early involvement of test personnel in the engine development process, the justification of ground testing over flight testing, and adequate funding of the ground test effort. Development status reports are given for the Aeropropulsion System Test Facility, which will begin its check-out operations in the Fall of 1984, and the Turbine Engine Load Simulator which has not yet received funding. Detailed descriptions are given of the experimental facilities covered. 83/00/00 83A35863

AUTH:

UTTL: A dynamic model of turbojet in starting at high altitude

AUTH: A/YAN, D.-Y., B/MAI, Z.-F. PAA: B/(Beijing Institute of Aeronautics and Astronautics, Beijing, People's Republic of China) IN: International Symposium on Air Breathing Engines, 6th, Paris, France, June 6-10, 1983, Symposium Papers (A83-35801 16-07). New York, American Institute of Aeronautics and Astronautics, 1983, p. 385-393.

ABS: A dynamical model for the starting of a turbojet engine is employed in the computation of the windmilling-to-idling transient process, where the model's establishment required both the definition of steady state mathematical models of components and the construction of a dynamic model for the entire powerplant system. The steady state model presently used for the compressor in the low speed starting region is based on the theory of stage performance for axial compressors, together with the method of functional approximation by means of vectorial transformation. The model is verified in light of the results of both performance tests and digital computations. 83/00/00 83A35846

UTTL: The application of a sub-scale flight demonstrator as a cost effective approach to aircraft development  
AUTH: A/ROSENTHAL, G. PAA: A/(Fairchild Republic Co.,

Farmingdale, NY) (Canadian Symposium on Advanced Technology Light and General Aviation Aircraft, 4th, Ottawa, Canada, Oct. 6, 1982) Canadian Aeronautics and Space Journal (ISSN 0008-2821), vol. 28, Dec. 1982, p. 359-370.

The availability of small and reliable turbojet units, polymer composite primary structures, and compact and powerful flight test instrumentation allows early, low cost flight test programs to be run with a sub-scale demonstrator aircraft. Attention is given to the application of this methodology to a Next Generation Trainer candidate design's evaluation, where it has yielded impressive schedule, cost and test data advantages. It is judged that the overall program required a schedule and expense comparable to that of a wind tunnel test program employing a complex powered model. In addition, comprehensive results were obtained under representative dynamic flight conditions that would not have been accurately simulated in wind tunnel tests. Natural stall warning and excellent stall and post-stall characteristics were exhibited. 82/12/00 83A29395

UTTL: Improved fault detection in the hot section of turbojet engines by individual monitoring procedures  
AUTH: A/TOENSKOETTER, H., B/KURZ, K.-H. PAA: A/(Industrieanlagen-Betriebsgesellschaft mbH, Ottoberbrunn, West Germany); B/(Aachen, Rheinisch-Westfaelische Technische Hochschule, Aachen, West Germany) Zeitschrift fuer Flugwissenschaften und Weltraumforschung, vol. 6, Nov.-Dec. 1982, p. 419-432. In German. Research supported by the Deutsche Forschungsgemeinschaft.

The effects of disturbances and damage in the internal throughflow components of turbojet engines on the behavior of the engines was experimentally studied by simulations of internal and external disturbances. The types of disturbances examined included inflow irregularities, compressor air discharge, compressor contamination, combustion chamber disturbances, and damage to the guide and runner blades. The local and average temperatures and pressures in the individual components were measured and, after a brief summary of the most important measurement results and a comparison with calculated parameter changes, the detectability of the studied disturbances using conventional aerothermodynamic monitoring procedures on the ground and in flight is discussed. Individual fault-specific diagnostic procedures are discussed in regard to improved fault detection in the hot section. 82/12/00 83A19666

UTTL: The nonsynchronous whirls of the turbine rotor in aerjet engines  
AUTH: A/GU, J.-L., B/RFN, P.-Z. PAA: B/(Northwestern Polytechnical University, Xian, Shaanxi, People's Republic of China) In International Council of the Aeronautics

- Sciences, Congress, 13th and AIAA Aircraft Systems and Technology Conference, Seattle, WA, August 22-27, 1982. Proceedings, Volume 1. (AB2-40876 20-01) New York, American Institute of Aeronautics and Astronautics, 1982, p. 665-673.
- ABS:** Several factors involved in the stability analyses of the supercritical overhung-rotor-bearing system of a specific type of aircraft engine are discussed. The phenomenon of 1/2 order subharmonic vibration within aerojet engines and its causes are assessed, and mathematical expressions for destabilizing forces are worked out. The latter include the unbalanced torque force due to circumferential variations of blade tip clearances, the frictional moment within splined coupling, and the aeroelasticity of labyrinth seals. Mathematical expressions for parametric excitation are found for the nonlinear stiffness of single-row deep-grooved ball bearings and for the nonlinear stiffness of the back support. Equations of motion of the high-speed overhung turbine rotor are derived. 82/00/00 82A40944
- UTTL:** Research on the behavior of a turbojet engine during internal and external disturbances with respect to early recognition of damage
- AUTH:** A/TGENSKOETTER, H. Aachen, Rheinisch-Westfaelische Technische Hochschule, Fakultät fuer Maschinenwesen, Dr.-Ing. Dissertation, 1980, 215 p. In German.
- ABS:** The results of a theoretical and experimental study on the behavior of a single-wave turbojet engine during disturbances are presented. The simulated disturbances are categorized as either external or internal. The former influence flow relationships in the engine and vary their behavior, but entail no consequences for the engine parts. Damage and structural changes in the engine components are called internal disturbances. Experimentally obtained thermodynamic parameter changes are presented as volume divisions and average values. A program to calculate the stationary and dynamic operating behavior in turbojet engines is used to determine the extent to which the experimental results coincide with a one-dimensional computational procedure, and whether monitoring of operating behavior can be useful for early detection of damage. 80/00/00 82A40561
- UTTL:** Performance of a 2D-CD nonaxisymmetric exhaust nozzle on a turbojet engine at altitude
- AUTH:** A/STRAIGHT, D. M.; B/CULLOM, R. R. PAA: B/INASA, Lewis Research Center, Cleveland, OH. CORP: National Aeronautics and Space Administration, Lewis Research Center, Cleveland, OH. AIAA, SAE, and ASME, Joint Propulsion Conference, 18th, Cleveland, OH, June 21-23, 1982. AIAA 27 p.
- ABS:** (Previously announced in STAR as N82-26241)
- RPT#:** AIAA PAPER 82-1137 82/06/00 82A40420
- UTTL:** Evaluation of a simplified gross thrust calculation method for a J85-21 afterburning turbojet engine in an altitude facility
- AUTH:** A/BAER-RIEDHART, J. L. PAA: W/INASA, Ames Research Center, Edwards, CA. AIAA, SAE, and ASME, Joint Propulsion Conference, 18th, Cleveland, OH, June 21-23, 1982. AIAA 12 p.
- ABS:** A simplified gross thrust calculation method was evaluated on its ability to predict the gross thrust of a modified J85-21 engine. The method used tailpipe pressure data and ambient pressure data to predict the gross thrust. The method's algorithm is based on a one-dimensional analysis of the flow in the afterburner and nozzle. The test results showed that the method was notably accurate over the engine operating envelope using the altitude facility measured thrust for comparison. A summary of these results, the simplified gross thrust method and requirements, and the test techniques used are discussed in this paper.
- RPT#:** AIAA PAPER 82-1044 82/06/00 82A34978
- UTTL:** Jet noise results from static, wind tunnel, and flight tests of conical and mechanical suppressor nozzles
- AUTH:** A/MCKINNON, R. A.; B/JOHNSON, E. S.; C/ATENCIO, A., JR. PAA: B/Douglas Aircraft Co., Long Beach, CA; C/U.S. Army, Air Mobility Research and Development Laboratory, Moffett Field, CA. CORP: Douglas Aircraft Co., Inc., Long Beach, CA.; Army Air Mobility Research and Development Lab., Moffett Field, CA. American Institute of Aeronautics and Astronautics, Aeroacoustics Conference, 7th, Palo Alto, CA, Oct. 5-7, 1981, 9 p.
- ABS:** Results of jet noise suppression tests conducted on a Rolls-Royce Viper 601 turbojet engine are reported. Seven exhaust nozzle configurations are tested, including two conical nozzles, two suppressor mixers, and three treated ejector configurations with different ejector inlets. Tests are conducted at the NASA Ames outdoor static test facility and the 40- by 80-ft wind tunnel facility at minimum tunnel flow velocity and normal flow velocities of 230 and 290 ft/sec. Near-field multiple sideline noise levels are projected to the far fields to compare far-field fixed microphone outdoor static noise levels, and wind tunnel near-field noise data are projected to the far field and flight distances to compare with noise levels recorded from an Hs-125 aircraft. Near-field outdoor noise data duplicate the far-field data recorded from fixed microphones within 2 PNdB, and the Douglas mechanical jet noise suppressor/treated ejector exhaust system achieves a noise reduction of 12 EPNdB relative to a conic reference nozzle at equal thrust in flight.
- RPT#:** AIAA PAPER 81-1995 81/10/00 81A49733

- UTTL: Excitation of surging type oscillations due to aperiodic external effects  
 A/P/15MENNVI, I. L. Aviasionnaya Tekhnika, no. 1, 1981, p. 34-37. In Russian.
- ABS: Oscillations in multi-shaft turbojet engines caused by aperiodic external effects are investigated analytically with reference to a simplified air-gas duct model. It is shown that aperiodic external effects, such as a decrease in the fuel feed rate, may produce oscillations similar to surging which however are not accompanied by an increase in the turbine temperature and are characterized by higher frequencies. 81/06/00 81A41032
- UTTL: A theoretical and experimental study of combustion chambers with recirculation  
 A/HEBRARD, P.; B/MAGRE, P. PAA: A/(ONERA, Centre d'Etudes et de Recherches de Toulouse, Toulouse, France); B/(ONERA, Châtillon-sous-Bagneux, Hauts-de-Seine, France) (Association Technique Maritime et Aéronautique, Session, 81st, Paris, France, May 18-22, 1981.) ONERA, TP no. 1981-39, 1981, 19 p. In French.
- ABS: Experimental measurements are used to construct a one-dimensional model of the aerodynamics and chemical kinetics of combustion chambers characterized by zones of recirculating flow. Various models of industrial and experimental turbojet engine combustors characterized by different geometries and fuel injection modes were employed in visualization studies of flow distribution in a hydraulic tunnel, hot-wire temperature measurement studies in a wind tunnel, measurements of the residence time distributions of gas in the chamber, and determinations of combustion performance by the analysis of combustion products under various operating conditions. Experimental results, which have shown the presence of vortices forming the recirculation zones in each of the various combustor geometries, are then used to derive a modular model in which the combustion chamber is represented by a series of reactors, the nature, size and connections of which are obtained from experimental data, with combustion modeled by both a global mechanism of kerosene combustion with a pollution reaction and a quasi-global reaction scheme. Predictions of combustion efficiency made on the basis of the model are found to be in satisfactory agreement with measurements made in the primary combustion zone, its exit zone and at the chamber exit as a function of fuel/air ratio.
- RPT #: ONERA, TP NO. 1981-39 81/00/00 81A39242
- UTTL: Tests for inlet distortion in a two-spool turbojet engine on the ground test bed  
 A/JIANG, F. PAA: A/(Shenyang Liming Machinery Co., Shenyang, Communist China) Acta Aeronautica et Astronautica Sinica, vol. 2, Mar. 1981, p. 59-68. In Chinese, with abstract in English.
- UTTL: The measurement and analysis of station parameters of a turbojet engine  
 A/DOONG, Q.; B/ZHAO, J.; C/LIU, S.; D/WU, X.; E/HU, Z.; F/CONG, W.; G/LIN, Q.; H/WANG, Z.; I/YOU, S.; J/ZHENG, L. In: Recent selected papers of Northwestern Polytechnical University, Part 2. (A81-17801 05-01) Xian, Shaanxi, People's Republic of China, Northwestern
- UTTL: Nuclear blast response of airbreathing propulsion systems - Laboratory measurements with an operational J-85-5 turbojet engine  
 A/DUNN, M. G.; B/RAFFERTY, J. M. PAA: A/(Calspan Advanced Technology Center, Buffalo, N.Y.); B/(U.S. Defense Nuclear Agency, Washington, D.C.) American Society of Mechanical Engineers, Gas Turbine Conference and Products Show, Houston, Tex., Mar. 9-12, 1981, 9 p.
- ABS: This paper describes an experimental technique that has been developed for the performance of controlled laboratory measurements of the nuclear blast response of airbreathing propulsion systems. The experiments utilize an available G.E. J-85-5 turbojet engine located in the test section of the Calspan Ludwig-tube facility. Significant modifications, described herein, were made to this facility in order to adapt it to the desired configuration. The J-85 engine had previously been used at Calspan for other purposes and thus came equipped with eight pressure transducers at four axial locations along the compressor section. These transducers have a frequency response on the order of 40 kHz. Pressure histories obtained at several circumferential and axial locations along the compressor are presented for blast-wave equivalent overpressures up to 17.2 kPa (2.5 psi) at corrected engine speeds on the order of 94 percent of maximum speed.
- RPT #: ASME PAPER 81-GT-164 81/03/00 81A30063
- UTTL: The results of tests for inlet total pressure distortion effects on a two-spool turbojet engine's performance and stability are reported. Both the low and high pressure compressors are three-stage, and distortion is generated by metallic mesh screens. Compressor surge was induced by a fuel flow step generator. It was found that when jet nozzle area was increased from 100% to 142%, the operating line of the low pressure compressor falls significantly irrespective of whether the inlet flow is distorted. Surge and operating lines were determined with and without distortion, and test results are given in terms of the relationship of pressure ratio to corrected mass flow and corrected speed. It is concluded that the surge margin and characteristic compressor lines are affected not only by inlet, but also outlet conditions, and that the characteristic lines of independent components could not be used as a substitute for a fully assembled engine's testing. 81/03/00 81A37340

- Polytechnical University, 1979, p. 187-201. In Chinese, with abstract in English.
- ABS:** The flow field parameters at characteristic stations of a turbojet engine were measured under design operating conditions. These data were used to calculate the gasdynamic parameters of the characteristic stations, the main process parameters, the component loss coefficients, and the engine performance. The parameters of the engine under various throttle conditions were recorded for different speeds, different nozzle areas, and with and without compressor bleeding. Attention is also given to the rational selection of probe locations to take due consideration of flow field characteristics, and to the selection of the proper method of data processing for obtaining accurate average station parameters of the engine. 79/00/00 81A17825
- UTTL:** A preliminary experimental investigation of the response of a turbojet engine to inlet pressure distortion
- AUTH:** A/CHEN, F.; B/TANG, D.; C/HU, Z.; D/LI, W.; E/YU, J.; F/WU, X.; G/ZHANG, J.; H/LIN, Q.; I/WANG, Z.; J/LIU, S.
- In: Recent selected papers of Northwestern Polytechnical University, Part 2. (A81-17801 05-01) Xian, Shaanxi, People's Republic of China, Northwestern Polytechnical University, 1979, p. 169-185. In Chinese, with abstract in English.
- ABS:** Preliminary results are presented concerning the influence of inlet pressure distortion on the characteristics and instability of the axial compressor of a turbojet engine. Experiments were performed on the test bed of a turbojet engine with a 9-stage compressor whose first stage is transonic. It is found that the inlet pressure distortion affects not only the stall line but also the shape and position of constant speed lines of the compressor. Inlet pressure distortion shifts the speed lines toward the left and flattens them. The effect of the decrease in the first stage nozzle exit area is similar to that of inlet pressure distortion. 79/00/00 81A17824
- UTTL:** Aerodynamic investigations of a bypass turbofan stage
- AUTH:** A/GERASTIENKO, V. P.; B/KAJKA, S. S.; C/KOVAL, V. A.; D/KONTSEVICH, F. G. Samoletostroenie Tekhnika Vozdushnogo Flota, no. 45, 1979, p. 25-31. In Russian.
- ABS:** The paper deals with an experimental investigation of a bypass turbofan stage with a bypass ratio of unity. The velocity, flow-angle, and pressure distributions over the length of wheel blades and main-flow guide vanes are determined. The measurements correlate well with the results of an aerodynamic analysis. 79/00/00 80A47371
- UTTL:** Tests of an improved rotating stall control system on a J-85 turbojet engine
- AUTH:** A/LUDWIG, G. R.; B/NENNI, J. P. PAA: B/(Caispan Advanced Technology Center, Buffalo, N.Y.) American Society of Mechanical Engineers, Gas Turbine Conference and Products Show, New Orleans, La., Mar. 10-13, 1980, 9 p.
- ABS:** An improved version of a rotating stall control system has been tested successfully on a J-85 turbojet engine. Past tests had pointed out the desirability of increasing the response speed of the control. In this study, the installation of the stall control on the J-85 was modified so as to decrease the response time of the control by a factor of ten over that attained in the past tests. The modified control was tested to see if the decreased response time improved the ability to clear rotating stall once it has started, and also to see if rotating stall could be anticipated and prevented by proper selection of the variables in the stall control detection system. The performance of the stall control was tested by closing the bleed doors on the engine until rotating stall occurred or until the control anticipated stall and held the bleed doors open. The tests showed that the control is capable of anticipating stall before it occurs and keeping the engine completely clear of stall at speeds up to 80 percent of design speed. No tests were performed above 80 percent of design speed because opening the bleed doors at such speeds might aggravate the stall rather than clear it.
- RPT#:** ASME PAPER 80-GT-17 80/03/00 80A42155
- UTTL:** Results from flight noise tests on a Viper turbojet fitted with ejector/suppressor nozzle systems
- AUTH:** A/BRUDOKS, J. R.; B/MCKINNON, R. A.; C/JOHNSON, E. S. PAA: A/(Rollis-Royce, Ltd., Bristol, England); C/(Douglas Aircraft Co., Long Beach, Calif.); D/ROLLIS-ROYCE Ltd., Bristol (England); E/(Douglas Aircraft Co., Inc., Long Beach, CA); F/(American Institute of Aeronautics and Astronautics, Aeroacoustics Conference, 6th, Hartford, Conn., June 4-6, 1980, 18 p.
- ABS:** Noise tests have been performed on a range of advanced exhaust suppressors fitted to a Viper turbojet engine with the objective of evaluating systems potentially suitable for subsonic and supersonic aircraft. A key item in the suppressor systems was an acoustically lined ejector, and tests were made with and without this ejector. Flight tests were made using an HS-125 aircraft in England and were followed by outdoor static tests at NASA Ames Research Center. In addition, acoustic and propulsion measurements were made at static, and in simulated flight conditions, with the engine installed in the Ames 40-by-80-ft wind tunnel. The paper deals mainly with the flight test results. These show that the use of a lined ejector considerably increases the attenuation obtainable using a suppressor nozzle alone and largely confirm predictions made on the basis of previous model and static tests. The maximum measured attenuation adjusted to an altitude of

- 500 ft was 14 EPNGdB at an ideal jet velocity of 2400 ft/sec using the suppressor/ejector design intended for supersonic application. Initial propulsion performance results from the Ames wind tunnel confirm previous smaller scale propulsion results from a Douglas facility.  
RPT#: AIAA PAPER 80-1028 80/06/00 80A38643
- UTTL: Qualification of cooling systems design for high temperature on a turbine facility  
AUTH: A/COURNUT, A. E.; B/LAROCHE, M.; C/LE 80T, Y.; D/MICHARD, P. J.; PAA: B/ISNECMA, Moissy-Cramayel, Seine-et-Marne, France); D/ONERA, Chatillon-sous-Bagneux, Hauts-de-Seine, France) In: Measurement methods in rotating components of turbomachinery; Proceedings of the Joint Fluids Engineering Gas Turbine Conference and Products Show, New Orleans, La., March 10-13, 1980. (ABO-36126 14-35) New York: American Society of Mechanical Engineers, 1980. p.303-317.  
ABS: An advanced turbine test facility for predicting temperature distribution on airfoils and adjacent components is described. The turbine design program including static test rigs, engine tests, and measuring techniques are examined; aerodynamic properties of steam are characterized, including temperature distortion and aerodynamic turbulence, and measurement of heat exchange on blades and vanes. Finally, thermal characteristics of rotor blades and its application to the investigation of film-cooled blade thermal balance are considered.  
RPT#: DNERA, TP NO. 1980-15 80/00/00 80A36156
- UTTL: Status of NASA full-scale engine aeroelasticity research.  
AUTH: A/LUBOMSKI, J. F. PAA: A/(NASA, Lewis Research Center, Cleveland, Ohio) CORP: National Aeronautics and Space Administration, Lewis Research Center, Cleveland, OH. In: Structures, Structural Dynamics, and Materials Conference, 21st, Seattle, Wash., May 12-14, 1980. Technical Papers, Conference sponsored by AIAA, ASME, ASCE, and AHS, New York, American Institute of Aeronautics and Astronautics, Inc., 1980. 18 p.  
ABS: The paper presents data relevant to several types of aeroelastic instabilities which have been obtained using several types of turbojet and turbofan engines. Special attention is given to data relative to separated flow (stall) flutter, choke flutter, and system mode instabilities. The discussion covers the characteristics of these instabilities, and a number of correlations are presented that help identify the nature of the phenomena.  
80/00/00 80A35906
- UTTL: Combustion-gas temperature sensors for turbine and turbojet engines
- AUTH: A/LESIUK, A. Technika Lotnicza i Astronautyczna, vol. 35, Jan. 1980, p. 30-33. In Polish.  
ABS: Some aspects of the application of thermoelectric sensors to in-flight exhaust-gas temperature measurements for turbojet and turbine engines are discussed. The reciprocal action of some metrological parameters is examined with particular reference to the dynamic properties, reliability, and stability of the sensors. 80/01/00 80A34237
- UTTL: Advanced developments in turbo machinery for use in small RPV engines  
AUTH: A/CHEVIS, R. W. PAA: A/(Noel Penny Turbines, Ltd., Coventry, England) In: Remotely piloted vehicles; International Conference, Bristol, England, September 3-5, 1979. Supplementary Papers. (ABO-29651 11-01) Bristol, England, University of Bristol, 1979. p. 17.1-17.10.  
ABS: The paper focuses on outlining recent aerodynamic developments in turbomachinery applicable to small RPV turbojets. The term small is assumed to apply to engines having air mass flows less than about 8 lb/s. Attention is given to the impact of aerodynamic developments on engine performance. The discussion suggests strongly that the application of advanced small compressor and turbine technology can considerably improve performance levels in small RPV turbojets without increase in complexity.  
79/00/00 80A29672
- UTTL: Designing of the test units for aircraft engines  
AUTH: A/PAVLOV, IU. I.; B/SHAIN, IU. IA.; C/ARRAMOV, B. I. Russian. Izdatel'stvo Mashinostroenie, 1979. 152 p. In Russian.  
ABS: The book deals with designing of the test units for aircraft turbojet engines and their parts. Emphasis is placed on test modeling and modern test units which make it possible to imitate high-speed, take-off-landing, weather, and other conditions under which these engines operate. 79/00/00 80A23069
- UTTL: Characteristics and operational conditions of aircraft turbojet engines  
AUTH: A/LITVINOV, IU. A.; B/BOROVIK, V. O. Moscow. Izdatel'stvo Mashinostroenie, 1979. 288 p. In Russian.  
ABS: The operational conditions of gas turbine engines are reviewed and attention is given to the influence of these conditions on the characteristics of engine components. Mathematical models of turbojet engines are described and compared with experimental determinations of operational characteristics. The various operating modes of gas turbine engines are discussed, along with startup and stability considerations. 79/00/00 80A13775

UTTL: Turbine engine altitude chamber and flight testing with liquid hydrogen  
 AUTH: A/CONRAD, E. W. PAA: A/(NASA, Lewis Research Center, Cleveland, Ohio) CORP: National Aeronautics and Space Administration, Lewis Research Center, Cleveland, OH. Deutsche Gesellschaft fuer Luft- und Raumfahrt und Deutsche Forschungs- und Versuchsanstalt fuer Luft- und Raumfahrt, International Symposium on Hydrogen in Air Transportation, Stuttgart, West Germany, Sept. 11-14, 1979, Paper, 20 p.

ABS: In the late fifties the Lewis Research Center evaluated experimentally the use of hydrogen using three different turbojet engines in altitude test chambers. One of these engines was later flown experimentally using liquid hydrogen fuel. This paper is a brief overview of the significant aspects of this exploratory research and gives a few implications of the results to modern turbine engines. A subsequent contract dealing with a positive displacement pump operating on liquid hydrogen is discussed and some aspects of liquid hydrogen propellant systems, reflected by rocket booster experience are treated briefly. Areas requiring further research and technology effort are delineated. 79/09/00 80A10034

UTTL: Parametric method of aircraft engine status diagnostics based on limited information  
 AUTH: A/AKHMEDZIANOV, A. M.; B/TUNAKOV, A. P.; C/GUMEROV, KH. S.; D/DEGTIAREV, I. U. D.: E/MORKOVNIKOVA, E. I. (Aviatsionnaya Tekhnika, vol. 21, no. 3, 1978, p. 12-18.) Soviet Aeronautics, vol. 21, no. 3, 1978, p. 6-11. Translation.  
 ABS: (For abstract see issue 04, p. 542. Accession no. 479-16781) 78/00/00 79A48492

UTTL: CFM56 - An act of cooperation, a new class of engine, a path towards the aeronautics of tomorrow  
 AUTH: A/MALROUX, J.-C. PAA: A/(CFM International, S.A., Paris, France) L'Aeronautique et l'Astronautique, no. 76, 1979, p. 51-61. In French.  
 ABS: The CFM56 aircraft engine is discussed from the viewpoints of its design and development and the cooperation between SNECMA and General Electric which led to the introduction of this new class of engine of from nine to 12 tons of thrust for 100- to 150-seat civil or 50 to 180-ton military transport aircraft. The CFM56 is a twin spool dual flow turbojet engine with high aspect ratio and a variable high pressure compressor stator, designed for subsonic flight and derived from the F101 engine. Engine components are detailed and the division of fabrication, development and testing responsibilities between the two manufacturers is outlined. The engine development program is discussed, noting that the testing program has so far progressed very satisfactorily. Principles guiding the collaboration, the success of which is demonstrated by the ordering of 150

CFM56 engines by a major airline, consist of considerations of mutual long-term interest, a careful allocation of tasks and revenues, program management by a body distinct from both participants, and efforts towards clarity and simplicity. 79/00/00 79A42065

UTTL: Error localization in turbojet engines through determination of the characteristics of structural members  
 AUTH: A/DAHL, G. Braunschweig, Technische Universitaet, Fakultaat fuer Maschinenbau und Elektrotechnik, Dr.-Ing. Dissertation, 1977, 172 p. In German.  
 ABS: In the present thesis, a conventional continuous-process calculation, where the flow parameters are determined from the given component characteristics is inverted in such a way that component characteristics can be determined from the given flow parameters. The ambient pressure and temperature and the pressures and temperatures at the input and output of the compressor and at the turbine output plane, as well as the fuel flow rate, were taken as the flow parameters. The adaptation of this approach to the localization of engine malfunctions is described. 77/00/00 79A41827

UTTL: Effect of shocks on film cooling of a full scale turbojet exhaust nozzle having an external expansion surface  
 AUTH: A/STRAIGHT, D. M. PAA: A/(NASA, Lewis Research Center, Cleveland, Ohio) CORP: National Aeronautics and Space Administration, Lewis Research Center, Cleveland, OH. AIAA, SAE, and ASME, Joint Propulsion Conference, 15th, Las Vegas, Nev., June 18-20, 1979, AIAA 13 p.  
 ABS: Cooling is one of the critical technologies for efficient design of exhaust nozzles, especially for the developing technology of nonaxisymmetric (2D) nozzles for future aircraft applications. Several promising 2D nozzle designs have external expansion surfaces which need to be cooled. Engine data are scarce, however, on nozzle cooling effectiveness in the supersonic flow environment (with shocks) that exists along external expansion surfaces. This paper will present experimental film cooling data obtained during exploratory testing with an axisymmetric plug nozzle having external expansion and installed on an afterburning turbojet engine in an altitude test facility. The data obtained shows that the shocks and local hot gas stream conditions have a marked effect on film cooling effectiveness. An existing film cooling correlation is adequate at some operating conditions but inadequate at other conditions such as in separated flow regions resulting from shock-boundary-layer interactions. RPT#: AIAA PAPER 79-1170 79/06/00 79A38966

UTTL: Engine evaluation of a vibration damping treatment for inlet guide vanes

- AUTH:** A/HENDERSON, J. P.; B/ROGERS, L. C.; C/PAUL, D. B.; D/PARIN, M. L. PAA: A/(USAF, Materials Laboratory, Wright-Patterson AFB, Ohio); C/(USAF, Flight Dynamics Laboratory, Wright-Patterson AFB, Ohio); D/(3M Co., St Paul, Minn.); American Society of Mechanical Engineers, Gas Turbine Conference and Exhibit and Solar Energy Conference, San Diego, Calif., Mar. 12-15, 1979, 9 p.
- ABS:** Welded titanium inlet guide vanes in an Air Force turbojet engine, have been experiencing a high rate of vibration induced cracking after very short service. The cause of this cracking has been identified as resonant vibration excited by pressure fluctuations occurring when the first-stage fan blades pass the inlet guide vanes. A bonded vibration damping wrap has provided a cost effective fix which can be applied on a retrofit basis for major cost savings. The damping wrap, which consists of multiple layers of energy dissipating adhesives separated by constraining layers of aluminum foil, is bonded to the vanes under high temperature and pressure in an autoclave. This paper describes the results of engine test-cell tests and the comparison of these results with actual service experience obtained under operational conditions. Measured effects on engine performance, distortion tolerance, and anti-icing performance are presented along with measured stress reductions, as compared with increases in modal damping.
- RPT#:** ASME PAPER 79-GT-163 79/03/00 79A32425
- UTL:** Characteristics of aeroelastic instabilities in turbomachinery - NASA full scale engine test results
- AUTH:** A/LUBOMSKI, J. F. PAA: A/(NASA, Lewis Research Center, Cleveland, Ohio) CORP: National Aeronautics and Space Administration, Lewis Research Center, Cleveland, OH. In: International Symposium on Air Breathing Engines, 4th, Orlando, Fla., April 1-6, 1979, Proceedings, (A79-25376 11-07) New York, American Institute of Aeronautics and Astronautics, Inc., 1979, p. 91-102.
- ABS:** Several aeromechanical programs have been conducted in the NASA/USAF Joint Engine System Research Programs. The scope of these programs, the instrumentation, data acquisition and reduction, and the test results are discussed. Data pertinent to four different instabilities were acquired: mode instability, stall flutter, choke flutter and a system mode instability. The data indicates that each instability has its own unique characteristics. These characteristics are described.
- RPT#:** AIAA 79-7011 79/00/00 79A29386
- UTL:** Recent General Electric engine development testing for improved service life
- AUTH:** A/TURNBULL, R. C. PAA: A/(General Electric Co., Evendale, Ohio) Society of Automotive Engineers, Aerospace Meeting, San Diego, Calif., Nov. 27-30, 1978, 22 p.
- ABS:** More exact simulation of engine in-service operating conditions by accelerated development test program improvements - T700/F101/F404/CFM56/CF6 - are reviewed for lessons learned towards earlier identification/solution of engine life extension problems. Improved design features, improved analysis and test simulation of mission cycles, improved component test techniques and, in general, increased emphasis on demonstrating required minimum service life prior to production are briefly discussed. Possible future direction of these efforts is indicated for consideration in General Engine Specification revisions.
- RPT#:** SAE PAPER 780990 78/11/00 79A25876
- UTL:** Parametric method for diagnosing the state of aircraft engines on the basis of limited information
- AUTH:** A/AKHMEDZIANOV, A. M.; B/TUNAKOV, A. P.; C/GLIMEROV, KH. S.; D/DEGTIAREV, I. U. D.: E/MORKOVNIKOVA, E. I. Aviatzionnaja Tekhnika, vol. 21, no. 3, 1978, p. 12-18. In Russian.
- ABS:** A diagnostics algorithm is proposed for studying the state of the air-fuel duct on the basis of limited information on the thermodynamic parameters. The mathematical model of the engine is used as the transmitting diagnostic channel. 78/00/00 79A16781
- UTL:** Data handling for a large jet engine test facility
- AUTH:** A/RICKARD, J. R.; B/LAWLEY, M. W. PAA: B/(LARO, Inc., Arnold Engineering Development Center, Arnold Air Force Station, Tenn.) In: SOUTHEASTCON '78: Proceedings of the Southeast Region 3 Conference, Atlanta, Ga., April 10-12, 1978. (A79-16526 04-31) Piscataway, N.J.: Institute of Electrical and Electronics Engineers, Inc., 1978, p. 519, 520.
- ABS:** The Test Instrumentation System (TIS) for a large jet engine test facility is described in terms of its requirements and environment. The system is highly flexible, interactive, adaptive, and reconfigurable in real time. The system will accommodate approximately 4,000 parameters simultaneously, and will incorporate a number of relatively new features such as distributed processing and adaptive data compression. 78/00/00 79A16561
- UTL:** Utilization of high temperature composites in turbojet engines
- AUTH:** A/MESTRE, R. CORP: Centre de Villaroche, Moissy (France). In AGARD, Application of Advanced Material for Turbomachinery and Rocket Propulsion 11 p (SEE N89-22654 16-23)
- ABS:** The design of modern military turbojet engines yields a high performance thrust/weight nozzle of composite materials in the hot section of the engine. Within that context, SNECMA, developed ceramic composites for use as

afterburning nozzles in the turbines, areas of the engine where the temperature of the gas goes above 2000 K, especially after prolonged use. The materials, CERASEP (SiC-SiC) and SEPCARB (C-SiC) provided by the European Society of Propulsion is used for nozzle flaps and other pieces of the structure. Some tests were made on the prototype, in order to validate the fabrication procedures and the design concept. The engine parts were made and tested for endurance, while the engine was in operational use. 89/03/00 89N22667

UTTL: Installed thrust as a predictor of engine health for jet engines

AUTH: A/MACKINTOSH, G. B.; B/HAMER, M. J. CORP: Computing Devices Co., Ottawa (Ontario). In: AGARD, Engine Condition Monitoring: Technology and Experience 10 p (SEE N89-16780 09-06)

ABS: Extensive installed and uninstalled gross thrust measurements were made over one complete maintenance cycle on 19 afterburning turbojet engines. Installed measurements utilized a sensor which can compute the thrust in real time from engine tailpipe pressure measurements. Correlation of installed thrust with maintenance history indicated a maximum degradation below which engines were removed from service. The engines were trimmed uninstalled, using lapse rate charts to produce a specific value of uninstalled thrust, corrected to standard conditions. Significant variations in installed corrected thrust resulted. Higher initial values of installed corrected thrust resulted in more rapid engine degradation and a shorter time before maintenance was required. 88/10/00 89N16806

UTTL: Vibrational impacts of hush house operation

AUTH: A/WITTEN, A. J. CORP: Oak Ridge National Lab., TN. CSS: (Energy Div.)

ABS: United States Air Force (USAF) facilities are required to test turboprop and turbojet engines before or after maintenance or repair and prior to installation on aircraft to ensure that no problems were introduced or remain uncorrected. This requirement prevents the installation of engines in aircraft which require further maintenance. There are a number of facilities in use by USAF for conducting engine diagnostic tests. The most modern of these facilities is the hush house which is a hangar-like structure designed to isolate the noise associated with extended engine operations from the surrounding environment. One type of hush house, the T-10, is of particular concern because of vibrational impacts to surrounding structures induced by subaudible sound (infrasound) emitted during operation. While these facilities fulfill the design requirement of reducing audible noise, serious sitting problems were reported at several installations because of infrasound-induced

vibrations. The worst of these include the abandonment of an avionics laboratory because induced vibrations interfered with this facilities function and structural damage to a concrete block maintenance facility. This paper describes a predictive method for assessing vibration-driven structural impacts. DE88-006983 CONF-880741-2 88/00/00 88N27207

UTTL: Thin film strain gage development program

AUTH: A/GRANT, H. P.; B/PRZYBYSZEWSKI, J. S.; C/ANDERSON, W. L.; D/CLAING, R. G. CORP: Pratt and Whitney Aircraft Group, East Hartford, CT. CSS: (Commercial Engineering Dept.)

ABS: Sputtered thin-film dynamic strain gages of 2 millimeter (0.08 in) gage length and 10 micrometer (0.0004 in) thickness were fabricated on turbojet engine blades and tested in a simulated compressor environment. Four designs were developed, two for service to 600 K (600 F) and two for service to 900 K (1200 F). The program included a detailed study of guidelines for formulating strain-gage alloys to achieve superior dynamic and static gage performance. The tests included gage factor, fatigue, temperature cycling, spin to 100,000 G, and erosion. Since the installations are 30 times thinner than conventional wire strain gage installations, and any alteration of the aerodynamic, thermal, or structural performance of the blade is correspondingly reduced, dynamic strain measurement accuracy higher than that attained with conventional gages is expected. The low profile and good adherence of the thin film elements is expected to result in improved durability over conventional gage elements in engine tests. NASA-CR-174707 NAS 1.26:174707 PWA-5628-69 83/12/00 87N28883

UTTL: Measurement uncertainty for the Uniform Engine Testing Program conducted at NASA Lewis Research Center

AUTH: A/ABDELWAHAB, MAHMOUD; B/BIESIADNY, THOMAS J.; C/SILVER, DEAN PAA. C/(Air Force Systems Command, Cleveland, Ohio.) CORP: National Aeronautics and Space Administration, Lewis Research Center, Cleveland, OH.

ABS: An uncertainty analysis was conducted to determine the bias and precision errors and total uncertainty of measured turbojet engine performance parameters. The engine tests were conducted as part of the Uniform Engine Test Program which was sponsored by the Advisory Group for Aerospace Research and Development (AGARD). With the same engines, support hardware, and instrumentation, performance parameters were measured twice, once during tests conducted in test cell number 3 and again during tests conducted in test cell number 4 of the NASA Lewis Propulsion Systems Laboratory. The analysis covers 15 engine parameters, including engine inlet airflow, engine net thrust, and engine specific fuel consumption measured

at high rotor speed of 8875 rpm. Measurements were taken at three flight conditions defined by the following engine inlet pressure, engine inlet total temperature, and engine ram ratio: (1) 82.7 kPa, 288 K, 1.0, (2) 82.7 kPa, 288 K, 1.3, and (3) 20.7 kPa, 288 K, 1.3. In terms of bias, precision, and uncertainty magnitudes, there were no differences between most measurements made in test cells number 3 and 4. The magnitude of the errors increased for both test cells as engine pressure level decreased. Also, the level of the bias error was two to three times larger than that of the precision error.

RPT#: NASA-TM-88943 E-3234 NAS 1.15:88943 87/05/00 87N28557

UTTL: Development of intake swirl generators for turbo jet engine testing

AUTH: A/GENSSLER, H. P.; B/MEYER, W.; C/FOTTNER, L. PAA: C/Technische Univ., Munich, West Germany), CORP: Messerschmitt-Boelkow-Blom G.m.b.H., Munich (Germany, F.R.G.), CSS: (Helicopter and Military Aircraft Div.), AGARD Engine Response to Distorted Inflow Conditions 21 p (SEE N87-24464 18-07) Sponsored in part by the German Bundesministerium der Verteidigung

ABS: The main objective of this investigation is to assess the influence of different types and magnitudes of swirl on the performance and compatibility of turbojet engines. The generation of intake swirl, typical for many supersonic combat aircraft, is described. Essentially two basic types, i.e., twin swirl and bulk swirl of varying strength and also combinations thereof, were selected in order to simulate these swirl patterns by subscale generators in a model wind tunnel. The swirl patterns measured behind these generators show good agreement with the target patterns selected at the beginning. The small scale swirl generators are being rebuilt at full scale for subsequent testing in front of the Larzac engine under static conditions with a bellmouth inlet at the engine test facility of the Jet Propulsion Institute at the University of the Bundeswehr Muenchen. 87/03/00 87N24480

UTTL: Performance computation of turbofan and turbojet engines in off-design conditions

AUTH: A/BRIDEL, G. CORP: Eidgenossisches Flugzeugwerk, Emmen (Switzerland), CSS: (Research and Testing Dept.)

ABS: A prediction method of underload performance of turbojet and turbofan engines based on gas dynamic relations was developed using mass flow rate, compression ratio, turbine inlet temperature, thrust, and fuel consumption. More precise prediction results can be obtained by incorporating compressor efficiency. A BASIC computer program is described and results are compared with existing data. Up to a throttling coefficient of 50% of the maximum thrust, the deviation with respect to the measured values falls within + or - 20%. The specific fuel

consumption is improved in underload medium range but is increased at high throttling coefficients. Accuracy improvement is achieved with introduction of variable compressor and turbine efficiency.

RPT#: F+W-FD-1746 84/10/11 86N19323

UTTL: Measurement of turbofan-turbojet thrust from tailpipe static pressure

AUTH: A/GIVENS, T. W.; B/LEMOINE, J. A. CORP: Naval Postgraduate School, Monterey, CA. While the most accurate method for measuring turbojet/turbofan thrust is mechanical, a more practical method is often desired since a mechanical device is costly and non-portable. An investigation was conducted to determine whether inferring thrust indirectly from pressure provides sufficient accuracy to justify its use as an alternate technique for determining uninstalled thrust. T41 engine data were provided by the Naval Air Research Facility at Jacksonville, Fla. The data consisted of a variety of engine parameters which had been recorded during routine post-maintenance performance tests plus an additional set of tailpipe static pressure readings that had been obtained from a slave tailpipe used for this project. The engine data were combined and an ensemble plot of tailpipe static pressure versus thrust was produced for analysis. A curve fitting technique was then used to determine how well the parameter correlated with thrust. The results were tested statistically and found to be reasonable. Correlation between thrust and tailpipe static pressure was excellent.

RPT#: AD-A154036 NP567-84-019 84/12/00 85N29967

UTTL: Experimental study of aerodynamic shielding of turbojet engine air intake against exhaust gases

AUTH: A/VYSOKOGRETS, M. M.; B/GILYAZOV, M. S.; C/KOSTERIN, V. A.; D/KHABIBULLIN, M. G. CORP: Joint Publications Research Service, Arlington, VA. In its USSR Rept. Eng. and Equipment (JPRS-UEQ-85-001) p 20 (SEE N85-18200 09-31)

ABS: The use of an aerodynamic shield is a promising method for preventing the entry of high-temperature exhaust gases into the intake of a turbojet engine during the landing of aircraft equipped with reverse-thrust devices. The objective of the study reported here was to investigate experimentally the efficiency of aerodynamic shielding by a single circular jet issuing in the plane of symmetry of the intake at 90 deg to the surface of the runway. The mean temperature at the pair intake is determined as a function of the total air pressure and of the critical flow rate of the shielding air for a turbojet engine intake model. 85/01/10 85N18210

UTTL: Operational and Performance Measurement on Engines

- in Sea Level Test Facilities. CORP., Advisory Group for Aerospace Research and Development, Neuilly-Sur-Seine (France).
- ANN: This Lecture Series considers all the basic features of turbojets and turbofan testing. In the introduction, test cell design is set in historical perspective with brief descriptions of the test arrangement and instrumentation used to test the early jet engines. The way in which these have evolved to modern designs is outlined. Three typical uses for sea level test beds, routine proof testing following overhaul, performance evaluation for type certification and general development testing are described and covered in detail by specialist lectures. One lecture is devoted specifically to turboprop testing. Instrumentation and data handling are dealt with in two lectures, one covering measurement techniques and the other covering data acquisitions and handling. One lecture deals with the test bed measurement performance of the engine from the test bed measurement. For individual titles, see N84-25724 through N84-25731.
- RPT#: AGARD-LS-132 ISBN-92-835-0350-3 AD-A144211 84/03/00 84N25723
- UTTL: Tests for inlet distortion in a two-spool turbojet engine on the ground test bed
- AUTH: A/FENG, J. PAA, A./Shenyang Lining Machinery Co.)  
CORP: Air Force Systems Command, Wright-Patterson AFB, OH.  
CSS: (Foreign Technology Div.) In its Acta Aeron. et Astronautica Sinica (FTD-IDIRS)T-0664-82) p 113-133 (SEE N83-32727 21-01)
- ABS: The effects of the inlet total pressure distortion on the performance and stability of a two spool turbojet engine with a three stage low pressure compressor and three stage high pressure compressor, a medium supercharging ratio and afterburning. The steady state circumferential pressure distortion is created by the 90 deg fan shaped mesh. The relational curve of the mesh with different blockage ratios or distortion amplitude produced by the congruent mesh which follows the engine's inlet rate of flow is determined. 83/03/04 83N32733
- UTTL: Uniform engine testing program. Phase 1: NASA Lewis Research Center participation.
- AUTH: A/BLESTADNY, T.; B/BURKHARDT, L.; C/BRAITHWAITE, W.  
CORP: National Aeronautics and Space Administration, Lewis Research Center, Cleveland, OH.
- ABS: Two jet engines were tested under identical conditions in sea level test beds at two ground level facilities as a means to correlating these facilities. Two J57-19A turbojet engines were tested in an altitude test facility. The test results are summarized.
- RPT#: NASA-TN-82978 E-1407 NAS 1.15-82978 82/10/00 83N14126
- UTTL: Performance of a 2D-CD nonaxisymmetric exhaust nozzle on a turbojet engine at altitude
- AUTH: A/STRAIGHT, D. M.; B/CULLOM, R. R. CORP: National Aeronautics and Space Administration, Lewis Research Center, Cleveland, OH.
- ABS: Baseline thrust and cooling data obtained with a 2D-CD versatile research exhaust nozzle mounted on a turbojet engine in an altitude chamber are presented. The tests covered a range of nozzle pressure ratios, nozzle pressure ratios, nozzle throat areas, and internal expansion area ratios. The thrust data obtained show good agreement with theory and scale model results after correcting the data for leakage and bypass cooling flows. Additional work is needed to improve predictability of cooling performance.
- RPT#: NASA-TN-82881 E-1257 NAS 1.15-82881 82/00/00 82N26241
- UTTL: Optimization of thrust algorithm calibration for Computing System (ICS) for Thrust the NASA Highly Maneuverable Aircraft Technology (HiMAT) vehicle's propulsion system
- AUTH: A/HAMER, M. J.; B/ALEXANDER, R. I. CORP: Computing Devices Co., Ottawa (Ontario)
- ABS: A simplified gross thrust computing technique for the HiMAT J85-GE-21 engine using altitude facility data was evaluated. The results over the full engine envelope for both the standard engine mode and the open nozzle engine mode are presented. Results using afterburner casing static pressure taps are compared to those using liner static pressure taps. It is found that the technique is very accurate for both the standard and open nozzle engine modes. The difference in the algorithm accuracy for a calibration based on data from one test condition was small compared to a calibration based on data from all of the test conditions.
- RPT#: NASA-CR-163121 NAS 1.26-163121 AO11/FR 81/12/00 82N21198
- UTTL: Development tests of an engine with limited life Turbine Engine Testing 7 p (SEE N81-24071 15-07)
- ABS: A propulsion system with short engine life must have mass and surface thrust and a specific consumption while remaining simple in design to assure low production costs. To these qualities are added ease of integration into the airframe (increased coefficient of distortion of the air inlet, concentrated equipment, simple general shape) and firm hold in the face of environmental influences. Development and progress are reported on pilot tests of different engine configurations on pilot aircraft engines. The principal tests conducted on the MFC90-TURBO TR1 60 turbojet engine during four programs for adapting the engine to pilot vehicles are presented. Possible solutions to obtain low production cost are indicated.
- RPT#: NASA-TN-81N24103 81/01/00

in the hot section of an engine is discussed. 81/02/00  
81N23011

UTTL: Some effects of compressor fouling on the behavior of a turbojet engine

AUTH: A/TOENSKOETTER, H. CORP: Technische Hochschule, Aachen (Germany, F.R.). CSS: (Lehrstuhl fuer Strahltriebwerke und Turboarbeitsmaschinen.) In DFLVR On Contrib. to 10th Symp. on Aircraft Integrated Data Systems p 183-218 (SEE N81-20007 11-01)

ABS: Difficulties in the identification of compressor faults by an engine condition monitoring system are discussed. For the example of compressor fouling, simulated on a single spool turbojet engine with a seven stage axial flow compressor, the effects on compressor characteristics (mass flow, pressure ratio, and efficiency) and on additional parameters that are significant for engine condition monitoring are presented. The influence on the behavior of the compressor stages and on the surge line is described. Experimental results are compared with calculated parameter changes showing satisfactory agreement for compressor fouling. Cleaning and surge line determination methods are shown. 80/06/00 81N20015

UTTL: Comparison of thermocouple, gas sampling, and Raman measured temperatures in an afterburning turbojet engine plume

AUTH: A/ROQUEMORE, W. M.; B/YANCY, P. P. CORP: Air Force Aero Propulsion Lab., Wright-Patterson AFB, OH.; Dayton Univ., OH. In APL The 16th JANNAF Combust. Meeting, Vol. 2, p 511-527 (SEE N80-31588 22-28) Prepared in cooperation with Dayton Univ. Research Inst.

ABS: The results of plume temperature measurements made with three different probes, a Pt 13% Rh-Pt thermocouple probe, a gas sampling probe, and a spontaneous Raman scattering optical probe are described. Thermocouple measurements were corrected for radiation and recovery. A combination gas sampling and pressure probe was used to measure carbon dioxide, carbon monoxide, and total hydrocarbon concentrations and total gas stream pressures. Temperatures were calculated from the concentration measurements. Raman scattering measurements were made in a near-backscattering geometry using a pulsed nitrogen gas laser, a computer controlled SPEX double spectrometer, and an 8850 RCA photomultiplier tube with EG&G/ORTEC time gated current integration detection apparatus. Raman temperatures were determined by fitting calculated spectra to the experimental spectra of the nitrogen gas in the plume. The temperatures measured by the Raman, gas-sampling, and thermocouple techniques were in agreement within the experimental error of about 5 percent except at maximum engine power where the thermocouple deviated by about 10 percent. 79/12/00 80N31614

UTTL: Gas turbine engine transient testing

AUTH: A/RUDNITSKI, D. M. CORP: National Research Council of Canada, Ottawa (Ontario). CSS: (Engine Lab.) In AGARD Turbine Engine Testing 15 p (SEE N81-24071 15-07)

ABS: Methods for conducting extensive steady-state and transient-performance tests on J85-CAN-15 turbojet engines are discussed. In particular the instrumentation and techniques developed to monitor and record experimental data rapidly and accurately during rapid-transient engine operation are described. The technique provides repeat-quality time-plots, and compressor operating lines immediately after test, thus permitting rapid assessments of engine performance. 81/01/00 81N24091

UTTL: Specification requirements for fighter engines

AUTH: A/DELL, M. E. CORP: Naval Air Propulsion Test Center, Trenton, NJ. In AGARD Turbine Engine Testing 16 p (SEE N81-24071 15-07)

ABS: Military Specification MIL-E-5007D, a general specification for the development of turbofan/turbojet engines, has been used by the U.S. Government for the procurement of new engines since 1973. This specification was tailored and applied by the U.S. Navy to the F404-GE-400 engine (F-18 aircraft) development program. The military general specification philosophy for the procurement of turbojet/turbofan engines using MIL-E-5007D is discussed. With heavy emphasis on technical requirements and assurance tests related to engine durability, improvements in MIL-E-5007D over previous specifications, experiences in applying MIL-E-5007D to the F404 engine development program, and assurance test approaches being considered for a revision to MIL-E-5007D are described. 81/01/00 81N24073

UTTL: Investigations into local fault detection on turbojet engines

AUTH: A/TOENSKOETTER, H. PAA: A/(Inst. fuer Strahltriebwerke und Turboarbeitsmaschinen Rheinisch-Westfaelische Technische Hochschule Aachen) CORP: European Space Agency, Paris (France). In its Contrib. to the 9th Symp. on Aircraft Integrated Data Systems (ESA-TI-532) p 53-79 (SEE N81-23008 14-01)

ABS: Results of the experimental investigations carried out with simulated faults in a single spool turbojet engine are presented. The effect of small disturbances, such as low compressor air bleed, a single removed turbine guide vane, or one plugged fuel nozzle on local and circumferentially averaged aerodynamic parameters are described. The location of the investigated faults by an engine condition monitoring system is studied and the possibility of including an analysis of circumferential flow nonuniformities at turbine exit for fault detection

x emission levels. Carbon monoxide and HC emissions were very low at these conditions with all of the fuels. At engine idle operating conditions, CO, HC, and NO sub x emission levels were found to be independent of fuel hydrogen content, but a small effect of fuel volatility and/or viscosity was found. At cold day ground start conditions (to 329 K) lightoff was obtained with all fuels, but the required fuel-air ratio increased with the more viscous fuels. At altitude conditions, the current engine relight limits with JP-4/JP-5 fuel were essentially met or exceeded with all of the JP-4 or JP-8 based fuel blends. However, a very significant reduction in altitude relight capability was found when a No. 2 diesel fuel was tested.

RPT#: AD-A078440 R79AEG321 AFAPL-TR-79-2015 CEED0-TR-79-06  
79/06/00 80N19119

UTTL: Tests of an improved rotating stall control system on a J-85 turbojet engine  
AUTH: A/LUDWIG, G. R. CORP: Calspan Advanced Technology Center, Buffalo, NY. CSS: (Aerodynamic Research Dept.)  
ABS: This report presents the results of testing a fast-acting rotating stall control system on a J-85 turbojet engine under sea level static conditions, both with and without inlet distortion. The control is an electronic feedback control system which uses unsteady pressure signals produced by pressure sensors within the compressor to detect incipient rotating stall and provide a correction signal when such a condition occurs. On the J-85 engine, the correction signal is used to drive a fast-response hydraulic actuator which operates intermediate stage compressor bleed doors and inlet guide vane flaps. The performance of the stall control was tested by closing the bleed doors until rotating stall occurred or until the control anticipated stall and held the bleed doors open. The tests showed that the control is capable of anticipating stall before it occurs and keeping the engine completely clear of stall at speeds up to 80 percent of design speed. No tests were performed above 80 percent of design speed because opening the bleed doors at such speeds might aggravate the stall rather than clear it.

RPT#: AD-A077704 CALSPAN-XE-5933-A-104 AFAPL-TR-79-2060  
79/08/00 80N19109

UTTL: Combustion diagnostics using laser spontaneous-Raman scattering  
AUTH: A/YANEY, P. P. CORP: Dayton Univ., OH.  
ABS: An existing computer-controlled Raman spectroscopy system, using a pulsed nitrogen laser and a double spectrometer, was upgraded and used to measure the temperatures in the combustion plume of an afterburning J85-5 turbojet engine. The computer-fitted temperatures had standard deviations between one and three percent. The agreement with simultaneous and sequential gas-sampling probe

UTTL: Turbine flowmeters and their applications at the Naval Air Propulsion Center  
AUTH: A/OBERNDORFER, R. E. CORP: Naval Air Propulsion Test Center, Trenton, NJ. CSS: (Measurement and Information Systems Dept.)  
ABS: At the Naval Air Propulsion Center, it has a specific requirement to make accurate mass flow measurements on the fuel flow of a gas turbine engine to determine the performance characteristics. The problem of acquiring mass flow from the inherent volumetric flow data of a turbine flowmeter is discussed. The development of a universal curve from calibration data is discussed. The unique curve fits for flowmeter, viscosity and specific gravity and their use during on-line data acquisition is described. The accuracy of the final mass flow data and its dependence on the errors associated with viscosity, specific gravity, temperature and frequency measurement is discussed. Some techniques used at NAPC to reduce these errors are described.

RPT#: AD-A084181 NAPC-MS-34 80/04/00 80N27680

UTTL: Investigations on local fault detection at turbojet engines  
AUTH: A/TOENSKOETTER, H. CORP: Technische Hochschule, Aachen (Germany, F.R.). CSS: (Inst. fuer Strahlantriebe und Turboarbeitsmaschinen.) In DFVLR Aircraft Integrated Data Systems p 5:-83 (SEE N80-25275 16-01)  
ABS: Some results of experiments that simulated faults in a single spool turbojet engine are presented. The effect of small disturbances such as low compressor air bleed, a single removed turbine guide vane, or one plugged fuel nozzle are described as a function of local and averaged aerothermodynamic parameters. 79/02/00 80N25278

UTTL: Evaluation of fuel character effects on J79 engine combustion system  
AUTH: A/GLEASON, C. C.; B/OLLER, T. L.; C/SHAYESON, M. W.; D/BAHR, D. W. CORP: General Electric Co., Cincinnati, OH. CSS: (Aircraft Engine Group.)

ABS: Results of a program to determine the effects of broad variations in fuel properties on the performance, emissions, and durability of the J79-17A turbojet engine combustion system are presented. Combustor tests conducted at engine idle, takeoff, subsonic cruise, supersonic dash, cold day ground start, and altitude relight operating conditions with 13 different fuels are described. The test fuels covered a range of hydrogen contents (12.0 to 14.5 percent), aromatic type (monocyclic and bicyclic), initial boiling point (285 to 393 K), final boiling point (552 to 679 K) and viscosity (0.83 to 3.25 mm<sup>2</sup>/s at 300 K). At high power operating conditions, fuel hydrogen content was found to be a very significant fuel property with respect to linear temperature, flame radiation, smoke, and NO sub

TERM: 066

measurements and with sequential thermocouple measurements was within five percent. Upon completion of these studies, the system was extensively modified for use with a 10-inch diameter combustor tunnel. Forty-eight sets of Raman data were taken over a wide range of operating conditions of the tunnel. The temperatures ranged from 1000 to over 2000 K using methane fuel. The turbulent diffusion flame was characterized by an unsteady appearance and was orange-yellow in color. Poisson standard deviations for 21 of the measurements averaged four percent. Measurements of the spectra of the laser-induced and non-laser-induced backgrounds were also obtained and analyzed.

RPT#: AD-A076514 UDR-TR-79-46 AFAPL-TR-79-2035 79/04/00  
80N17165

UTTL: An adaptation and validation of a primitive variable mathematical model for predicting the flows in turbojet test cells and solid fuel ramjets

AUTH: A/STEVENSON, C. A. CORP: Naval Postgraduate School, Monterey, CA

ABS: An adaptation of a primitive variable, finite-difference computer program was accomplished in order to predict the non-reacting flow fields in turbojet test cells and the reacting flow fields in solid fuel ramjets. The study compares the predictions of the primitive variable computer model with an earlier computer model and empirical data. It was found that the new model reasonably predicted the flow fields in both geometries. In addition, the primitive variable model allowed simulation of test cell flows up to full engine throttle conditions and solid fuel ramjet flows which included an aft mixing chamber.

RPT#: AD-A074187 79/06/00 80N14133

UTTL: Turbojet-exhaust-nozzle secondary-airflow pumping as an exit control of an inlet-stability bypass system for a Mach 2.5 axisymmetric mixed-compression inlet

AUTH: A/SANDERS, B. W. CORP: National Aeronautics and Space Administration, Lewis Research Center, Cleveland, OH

ABS: The throat of a Mach 2.5 inlet that was attached to a turbojet engine was fitted with large, porous bleed areas to provide a stability bypass system that would allow a large, stable airflow range. Exhaust-nozzle, secondary-airflow pumping was used as the exit control for the stability bypass airflow. Propulsion system response and stability bypass performance were obtained for several transient airflow disturbances, both internal and external. Internal airflow disturbances included reductions in overboard bypass airflow, power lever angle, and primary-nozzle area, as well as compressor stall. Nozzle secondary pumping as a stability bypass exit control can provide the inlet with a large stability margin with no adverse effects on propulsion system performance.

RPT#: NASA-TP-1532 E-9468 80/01/00 80N14124

UTTL: Parametric method of aircraft engine status diagnostics based on limited information

AUTH: A/AKHMEDZIANOV, A. M.; B/TUNAKOV, A. P.; C/GUMEROV, K. S.; D/DEGTYAREV, Y. D.; E/MORKOVNIKOVA, E. I. CORP: Allerton Press, Inc., New York, NY. In its Soviet Aeronautics Vol. 21, No. 3 p 6-11 (SEE N80-10001 01-01)

ABS: An algorithm was developed for engine flow path diagnostics based on limited information on the thermodynamic parameters. A mathematical model of the engine is used as the diagnostic communication channel.

78/00/00 80N10003

UTTL: Effects of steady-state pressure distortion on the stall margin of a J85-21 turbojet engine

AUTH: A/BOBULA, G. A. CORP: National Aeronautics and Space Administration, Lewis Research Center, Cleveland, OH. Prepared in cooperation with Army Aviation Research and Development Command, Cleveland, St. Louis, Mo.

ABS: The effects of the inlet pressure distortions, induced by five screen patterns, on the performance of a J85-21 turbojet engine was conducted at the NASA Lewis Research Center. Testing was in support of the HiMAT RPRV program at Dryden Flight Research Center. Distortion patterns were chosen based on anticipated application of test results of the HiMAT installation. Tests were conducted at a simulated Mach number and altitude condition of 0.9 and 10 973 meters. Results are presented in terms of distortion levels and standard compressor performance parameters.

RPT#: NASA-TM-79123 E-9958 AVRADCOM-TR-79-12 79/03/00  
79N23968

UTTL: Guide to in-flight thrust measurement of turbojets and fan engines

AUTH: CORP: Advisory Group for Aerospace Research and Development, Paris (France)

ANN: Topics include: fundamentals of thrust measurement in flight; propulsion system thrust and drag book-keeping; thrust expressions, methodology, and options; error assessment and control; and instrumentation. For individual titles, see N79-20128 through N79-20132.

RPT#: AGARD-AG-237 ISBN-92-835-1304-5 AD-A065939 79/01/00  
79N20127

UTTL: Low cost expendable engine

AUTH: A/HUBEN, C. A.; B/METSKER, B. L. CORP: Williams Research Corp., Walled Lake, MI.

ABS: A low cost expendable turbojet engine in the 200 pound thrust class was fabricated and tested. The design, manufacturing, and inspection concepts of the program resulted in the achievement of a projected engine cost of \$2883 each in lots of 1000 engines in terms of 1975 economics. Problems solved during the compressor rig

testing and engine tune-up testing are discussed. The results of the engine demonstration testing both at sea level static conditions and under a simulated Mn O.7 condition are presented.  
RPT#: AD-A062864 AFAPL-TR-78-33 78/03/00 79N20125

UTTL: Parametric performance of a turbojet engine combustor using Jet A and A diesel fuel  
AUTH: A/BUTZE, H. F.; B/HUMENIK, F. M. CORP: National Aeronautics and Space Administration, Lewis Research Center, Cleveland, OH.  
ABS: The performance of a single-can JT8D combustor was evaluated with Jet A and a high-aromatic diesel fuel over a parametric range of combustor-inlet conditions. Performance parameters investigated were combustion efficiency, emissions of CO, unburned hydrocarbons, and NOx, as well as liner temperatures and smoke. At all conditions the use of diesel fuel instead of Jet A resulted in increases in smoke numbers and liner temperatures; gaseous emissions, on the other hand, did not differ significantly between the two fuels.  
RPT#: NASA-TN-79089 E-9913 79/03/00 79N20114

UTTL: Characteristics of aeroelastic instabilities in turbomachinery - NASA full scale engine test results  
AUTH: A/LUBOMSKI, J. F. CORP: National Aeronautics and Space Administration, Lewis Research Center, Cleveland, OH.  
ABS: Several aeromechanical programs were conducted in the NASA/USAF Joint Engine System Research Programs. The scope of these programs, the instrumentation, data acquisition and reduction, and the test results are discussed. Data pertinent to four different instabilities were acquired: two types of stall flutter, choke flutter and a system mode instability. The data indicates that each instability has its own unique characteristics. These characteristics are described.  
RPT#: NASA-TN-79085 E-9908 79/00/00 79N17263

UTTL: Experimental evaluation of the effect of inlet distortion on compressor blade vibrations  
AUTH: A/LUBOMSKI, J. F. CORP: National Aeronautics and Space Administration, Lewis Research Center, Cleveland, OH.  
ABS: Compressor rotor strain gage data from an engine test conducted with an inlet screen distortion were reduced and analyzed. These data are compared to data obtained from the same engine without inlet pressure distortion to determine the net effect of the distortion on the vibratory response of the compressor blades. The results obtained are presented.  
RPT#: NASA-TN-79066 E-9882 79/00/00 79N16300

UTTL: An experimental investigation of turbojet test cell

augmentors  
AUTH: A/SAPP, C. N. JR. CORP: Naval Postgraduate School, Monterey, CA.  
ABS: A one-eighth scale turbojet test cell was used to investigate the effects of various design parameters on augmentor performance. The augmentor inlet design, nozzle-to-augmentor spacing, engine flow rate, nozzle diameter were varied to determine what effect they had on augmentation ratio, total air pumped through the system, and pressure, temperature, and velocity distributions within the augmentor tube. In addition, two augmentor tubes were combined in tandem to investigate the characteristics of a tertiary augmentor configuration.  
RPT#: AD-A057903 78/06/00 79N12101

UTTL: A validation of mathematical models for turbojet test cells  
AUTH: A/WALTERS, J. J. CORP: Naval Postgraduate School, Monterey, CA.  
ABS: Previously developed one-dimensional and two-dimensional computer models for predicting turbojet test cell performance were compared with data obtained from a subscale test cell for the purpose of model validation. Comparisons were made for a variety of configurations and flow rates. A modified one-dimensional model was found to reasonably predict the variation of augmentation ratio with engine flow rate, although predicted magnitudes were consistently too small. The model incorporated excessive drag losses and an inaccurate jet spreading parameter for large engine-augmentor spacings. The two-dimensional model accurately predicted experimental velocity profiles, but over-predicted pressure variations, except for low engine exit Mach numbers.  
RPT#: AD-A056333 78/03/00 79N11045

UTTL: Icing tests on turbojet and turbofan engines using the NGTE engine test facility  
AUTH: A/BALL, R. G. J.; B/PRINCE, A. G. CORP: National Gas Turbine Establishment, Pyestock (England). CSS: (Engine Test Dept.) In AGARD Icing Testing for Aircraft Eng. 15 p (SEE N79-10002 01-01)  
ABS: Tests were made at conditions representing wet icing, that was with the air supply containing a fine dispersion of supercooled water droplets (volumetric mean diameter nominally 20 microns), but facilities also existed for injecting solid ice particles into the airstream thereby enabling a mixed icing environment to be simulated. Wet icing tests were made on the Olympus 593 powerplant (engine intake combination) and on the RB211 high by pass turbofan. 78/08/00 79N10013

REPORT DOCUMENTATION PAGE									
<b>1. Recipient's Reference</b>	<b>2. Originator's Reference</b>	<b>3. Further Reference</b>	<b>4. Security Classification of Document</b>						
	AGARD-LS-169	ISBN 92-835-0565-4	UNCLASSIFIED						
<b>5. Originator</b>	Advisory Group for Aerospace Research and Development North Atlantic Treaty Organization 7 rue Ancelle, 92200 Neuilly sur Seine, France								
<b>6. Title</b>	COMPARATIVE ENGINE PERFORMANCE MEASUREMENTS								
<b>7. Presented at</b>									
<b>8. Author(s)/Editor(s)</b>	Various		<b>9. Date</b> May 1990						
<b>10. Author's/Editor's Address</b>	Various		<b>11. Pages</b> 294						
<b>12. Distribution Statement</b>	This document is distributed in accordance with AGARD policies and regulations, which are outlined on the Outside Back Covers of all AGARD publications.								
<b>13. Keywords/Descriptors</b>	<table> <tr> <td>Turbojet engines</td> <td>Test facilities</td> </tr> <tr> <td>Aircraft engines</td> <td>Comparison</td> </tr> <tr> <td>Performance tests</td> <td>Research projects</td> </tr> </table>			Turbojet engines	Test facilities	Aircraft engines	Comparison	Performance tests	Research projects
Turbojet engines	Test facilities								
Aircraft engines	Comparison								
Performance tests	Research projects								
<b>14. Abstract</b>	<p>The AGARD Propulsion and Energetics Panel has sponsored an international, inter-facility comparison programme for turbine engine test facilities over the past nine years. The effort was driven by the critical nature of engine test measurements and their influence on aircraft performance predictions, as well as the need for a sound understanding of test-related factors which may influence such measurements. The basic idea was that a nominated engine would be tested in several facilities, both ground-level and altitude, the results then compared, and explanations sought for any observed differences. This Lecture Series presents the information obtained from this comprehensive program. Emphasis is given to the definition and explanation of differences in test facility measurements and to the lessons learned from this unique experiment.</p> <p>This Lecture Series, sponsored by the Propulsion and Energetics Panel of AGARD, has been implemented by the Consultant and Exchange Programme.</p>								

<p>AGARD Lecture Series No.169 Advisory Group for Aerospace Research and Development, NATO <b>COMPARATIVE ENGINE PERFORMANCE MEASUREMENTS</b> Published May 1990 294 pages</p> <p>The AGARD Propulsion and Energetics Panel has sponsored an international, inter-facility comparison programme for turbine engine test facilities over the past nine years. The effort was driven by the critical nature of engine test measurements and their influence on aircraft performance predictions, as well as the need for a sound understanding of test-related factors which may influence such measurements. The basic idea was that a nominated</p> <p>P.T.O.</p>	<p>AGARD-LS-169</p> <p>Turbojet engines Aircraft engines Performance tests Test facilities Comparison Research Projects</p>	<p>AGARD Lecture Series No.169 Advisory Group for Aerospace Research and Development, NATO <b>COMPARATIVE ENGINE PERFORMANCE MEASUREMENTS</b> Published May 1990 294 pages</p> <p>The AGARD Propulsion and Energetics Panel has sponsored an international, inter-facility comparison programme for turbine engine test facilities over the past nine years. The effort was driven by the critical nature of engine test measurements and their influence on aircraft performance predictions, as well as the need for a sound understanding of test-related factors which may influence such measurements. The basic idea was that a nominated</p> <p>P.T.O.</p>	<p>AGARD-LS-169</p> <p>Turbojet engines Aircraft engines Performance tests Test facilities Comparison Research Projects</p>
<p>AGARD Lecture Series No.169 Advisory Group for Aerospace Research and Development, NATO <b>COMPARATIVE ENGINE PERFORMANCE MEASUREMENTS</b> Published May 1990 294 pages</p> <p>The AGARD Propulsion and Energetics Panel has sponsored an international, inter-facility comparison programme for turbine engine test facilities over the past nine years. The effort was driven by the critical nature of engine test measurements and their influence on aircraft performance predictions, as well as the need for a sound understanding of test-related factors which may influence such measurements. The basic idea was that a nominated</p> <p>P.T.O.</p>	<p>AGARD-LS-169</p> <p>Turbojet engines Aircraft engines Performance tests Test facilities Comparison Research Projects</p>	<p>AGARD Lecture Series No.169 Advisory Group for Aerospace Research and Development, NATO <b>COMPARATIVE ENGINE PERFORMANCE MEASUREMENTS</b> Published May 1990 294 pages</p> <p>The AGARD Propulsion and Energetics Panel has sponsored an international, inter-facility comparison programme for turbine engine test facilities over the past nine years. The effort was driven by the critical nature of engine test measurements and their influence on aircraft performance predictions, as well as the need for a sound understanding of test-related factors which may influence such measurements. The basic idea was that a nominated</p> <p>P.T.O.</p>	<p>AGARD-LS-169</p> <p>Turbojet engines Aircraft engines Performance tests Test facilities Comparison Research Projects</p>

<p>engine would be tested in several facilities, both ground-level and altitude, the results then compared, and explanations sought for any observed differences. This Lecture Series presents the information obtained from this comprehensive program. Emphasis is given to the definition and explanation of differences in test facility measurements and to the lessons learned from this unique experiment.</p> <p>This Lecture Series, sponsored by the Propulsion and Energetics Panel of AGARD, has been implemented by the Consultant and Exchange Programme.</p> <p>ISBN 92-835-0565-4</p>	<p>engine would be tested in several facilities, both ground-level and altitude, the results then compared, and explanations sought for any observed differences. This Lecture Series presents the information obtained from this comprehensive program. Emphasis is given to the definition and explanation of differences in test facility measurements and to the lessons learned from this unique experiment.</p> <p>This Lecture Series, sponsored by the Propulsion and Energetics Panel of AGARD, has been implemented by the Consultant and Exchange Programme.</p> <p>ISBN 92-835-0565-4</p>
<p>engine would be tested in several facilities, both ground-level and altitude, the results then compared, and explanations sought for any observed differences. This Lecture Series presents the information obtained from this comprehensive program. Emphasis is given to the definition and explanation of differences in test facility measurements and to the lessons learned from this unique experiment.</p> <p>This Lecture Series, sponsored by the Propulsion and Energetics Panel of AGARD, has been implemented by the Consultant and Exchange Programme.</p> <p>ISBN 92-835-0565-4</p>	<p>engine would be tested in several facilities, both ground-level and altitude, the results then compared, and explanations sought for any observed differences. This Lecture Series presents the information obtained from this comprehensive program. Emphasis is given to the definition and explanation of differences in test facility measurements and to the lessons learned from this unique experiment.</p> <p>This Lecture Series, sponsored by the Propulsion and Energetics Panel of AGARD, has been implemented by the Consultant and Exchange Programme.</p> <p>ISBN 92-835-0565-4</p>